PELLEGRINO, FRANCESCO

ENERGY TRANSFER IN THE PRIMARY STAGES OF THE PHOTOSYNTHETIC PROCESS INVESTIGATED BY PICOSECOND TIME-RESOLVED FLUORESCENCE SPECTROSCOPY

City University of New York PH.D. 1981

ENERGY TRANSFER IN THE PRIMARY STAGES OF THE PHOTOSYNTHETIC PROCESS INVESTIGATED BY PICOSECOND TIME RESOLVED FLUORESCENCE SPECTROSCOPY

By

FRANCESCO PELLEGRINO

Picosecond Laser and Spectroscopy Laboratory
Physics Department
The City College of New York
New York, N.Y. 10031

A Dissertation submitted to the Graduate Faculty in Physics in partial fulfillment of the requirements for the degree of Doctor of Philosophy, The City University of New York.

1981

This manuscript has been read and accepted
by the Graduate Faculty in Physics
in satisfaction of the dissertation requirement
for the degree of Doctor of Philosophy.

4/23/81 — Robert R Alfano
date — Chairman of Thesis Examining Committee

4/27/81 — Ehrard Mathieu
date — Executive Officer

Prof. R. Callender — Robert Callender
Dr. D. Auston — David H. Auston
Prof. J. Gersten — Jerome Gersten
Prof. S. Raps — Shirley Raps
Prof. R. Zuzolo — Ralph C. Zuzolo

Supervisory Committee

The City University of New York

Abstract

ENERGY TRANSFER IN THE PRIMARY STAGES OF
THE PHOTOSYNTHETIC PROCESS INVESTIGATED BY
PICOSECOND TIME RESOLVED FLUORESCENCE SPECTROSCOPY

By

Francesco Pellegrino

Adviser: Professor Robert R. Alfano

The aim of this research has been to understand the fate of the absorbed light energy in the primary stages of the photosynthetic process. In particular, the energy transfer in the accessory pigment complex consisting of carotenoids, Chl. a and Chl. b in higher green plants and phycobiliproteins in blue-green algae have been investigated. These accessory pigments are responsible for the highly efficient transfer of the excitation energy to the photochemically active reaction center traps. In this study I have directly measured the risetime, decay time, fluorescence depolarization, temperature and intensity dependence of the fluorescence emission from higher green plant and algal photosystems. Excitation was provided by single picosecond laser pulses, as well as a train of pulses at 530 nm , within an intensity range of 10^{12}-10^{16} photons/ cm^2 per pulse.

The energy transfer in the light harvesting pigment complex of Phycobilisomes from the blue-green alga Nostoc sp. were measured by isolating the phycobiliproteins Phycoerythrin (C-PE), Phycocyanin (C-PC), and Allophycocyanin (APC) forms I,II,III and B. These phycobiliproteins were studied singly, as well as in intact phycobilisomes. A study of the effects of the intensity of a single 6 ps excitation pulse on the decay kinetics and yield of fluorescence in the individual isolated phycobiliproteins at pH 7 and 23^0C has revealed an exponential fluorescence decay for intensities $< 10^{14}$ photons/cm^2 per pulse in all the phycobiliproteins. At higher intensities the fluorescence decay was found to be non-exponential only in C-PE.

The fluorescence risetime and decay kinetics of C-PE and the C-PC+APC emission from intact phycobilisomes of the blue-green alga Nostoc sp. were studied as a function of the intensity of a single 6 ps laser pulse over the range 10^{13} to 10^{15} photons/cm^2 per pulse. A risetime of 34 $\pm$ 13 ps was observed for the C-PC+APC emission in PBS's. Since the fluorescence decay for C-PE in PBS was measured to be 31 $\pm$ 4 ps, energy transfer from C-PE to C-PC is interpreted to occur in this time.

The fluorescence kinetics from the alga Scenedesmus obliquus, Wild Type and Mutants 8 and 11 were measured. Although the Wild Type is known to possess both active PS I and PS II components, Mutant 8 has an inactive PS I

reaction center, while Mutant 11 has an inactive PS II reaction center trap. It was found that while the fluorescence decay kinetics in the Wild Type form is comparable to that observed for other photosynthetic systems, the lifetimes measured in the mutant 8 and 11 forms are considerably longer. This is interpreted in terms of the destroyed cooperation between PS I and PS II, which gives rise to increased fluorescence when one or the other photosystem trap is inactivated.

Depolarization kinetics from the naturally ordered chloroplast arrangement found in the alga Nitella as well as spinach chloroplast and anthocyanin pigments in vivo and in vitro were measured with a novel beam splitter optical delay technique allowing for the simultaneous measurement of both $I_{\parallel}$ and $I_{\perp}$,the fluorescence intensity measured parallel to and perpendicular to the incident polarization direction respectively, in a single shot experiment.

The fluorescence kinetics of Photosynthetic green Norway maple leaves (Acer platenoides), and non-photosynthetic autumnal (yellow) Norway maple leaves at both room temperature and 90^{o} K have been measured. The lifetime at low intensities ($\sim 10^{13}$ photons/ cm^{2} per pulse) has been found to be nearly identical in both cases, though shifted in wavelength. The findings of this study with respect to energy transfer in the carotenoid pigment complex of Norway maple questions the traditional

interpretation of fluorescence kinetics as directly indicative of photosynthetic energy trapping.

Acknowledgements

This thesis is dedicated to my parents Vincent and Antoinette, and to the memory of my dear friend and teacher Dr. William N. Yu.

The patience, encouragement and inspiration of my thesis advisor Dr. Robert Alfano have not only been fundamental to the accomplishment of this work, but have more importantly instilled in me the confidence and perseverance of the scientific quest for knowledge and understanding.

I wish to thank Professors Shirley Raps, Daniel Wong Barbara Zilinskas and Ralph Zuzolo for providing some of the samples used in this work, as well as for constructive insights and criticisms.

The sincere and expert electronic assistance of my good friend and colleague Alexander Kalpaxis in the various electronic and computer interfacing problems which were encountered in this work is greatly appreciated.

The support of the National Science Foundation has made this research possible.

TABLE OF CONTENTS

LIST OF ABBREVIATIONS

APC I	allophycocyanin I
APC II	allophycocyanin II
APC III	allophycocyanin III
APC B	allophycocyanin B
Chl.	chlorophyll
DCMU	3-(3,4-dichlorophenyl)-1,1-dimethylurea
KDP	Pottassium DiHydrogen Phosphate
LHC	Light Harvesting Complex
OMA	Optical Multichannel Analyzer
PBS	Phycobilisome
Pc	Plastocyanin
PC	Phycocyanin
PE	Phycoerythrin
PS I	Photosystem I
PS II	Photosystem II
PSU	Photosynthetic Unit
Sc WT	Scenedesmus obliquus Wild Type
Sc 8	Scenedesmus obliquus mutant 8
Sc 11	Scenedesmus obliquus mutant 11
SHG	Second Harmonic Generation

LIST OF TABLES

LIST OF FIGURES

LIST OF PUBLICATIONS

"Time Resolved Fluorescence Spectroscopy of Spinach Chloroplasts", W. Yu, F. Pellegrino and R.R. Alfano, Biochim. Biophys. Acta 460, 171-181 (1977).

"Subnanosecond Fluorescence Quenching of Dye Molecules in Solution", W. Yu, F. Pellegrino, M. Grant and R.R. Alfano, J. Chem. Phys. 67, 1766-1773 (1977).

"Fluorescence Kinetics of Spinach Chloroplasts Measured with a Picosecond Optical Kerr Gate", F. Pellegrino, W. Yu and R.R. Alfano, Photochem. Photobiol. 28, 1007-1012 (1978).

"Time Resolved Picosecond Laser Spectroscopy", F. Pellegrino, A. Kalpaxis and R.R. Alfano, SPIE 148, 140-148 (1978).

"Video Imaging Systems in Picosecond Laser Spectroscopy", F. Pellegrino and R.R. Alfano, in Multichannel Image Detectors, ed. Y. Talmi, ACS Symposium Series 102, 8, 183-198 (1979).

"Picosecond Absorption and Fluorescence Studies of the Isolated Phycobiliproteins from the Blue-Green Alga Nostoc sp.", A.G.Doukas, F. Pellegrino, D. Wong, V. Stefancic, J. Buchert, R.R. Alfano and B.A. Zilinskas, Proceedings 5 th International Congress in Photosynthesis (1980) (in press).

"Picosecond Fluorescence Absorption and Raman Spectroscopy" F. Pellegrino, A.G. Doukas and R.R. Alfano, (Invited) in Proceedings VII International Conference on Raman Spectroscopy, ed. W.F. Murphy, North-Holland (1980).

"Fluorescence Relaxation Kinetics and Quantum Yield from the Phycobilisomes of the Blue-Green Alga Nostoc sp. Measured as a Function of Single Picosecond Pulse Intensity", F. Pellegrino, D. Wong, R.R. Alfano and B.A. Zilinskas, Photochem. Photobiol. (1981) (accepted for publication).

"Fluorescence Relaxation Kinetics and Quantum Yield from the Isolated Phycobiliproteins of the Blue-Green Alga Nostoc sp. Measured as a Function of Single Picosecond Pulse Intensity", D. Wong, F. Pellegrino R.R. Alfano and B.A. Zilinskas, Photochem. Photobiol. (1981) (accepted for publication).

"Picosecond Fluorescence Polarization Kinetics from Anthocyanin Pigments", F. Pellegrino, P. Sekuler and R.R. Alfano, Photobiochem. Photobiophys. (1981) (accepted for publication).

"Photoluminescent Determination of the Fundamental Gap for the Ferromagnetic Semiconductor $CdCr_2Se_4$", S.S. Yao, F. Pellegrino, R.R. Alfano, W.J. Miniscalco and A. Lempicki, Phys. Rev. Lett. 46, 558 (1981).

"Time Resolved Fluorescence Spectroscopy in Photosynthesis" F. Pellegrino and R.R. Alfano, in Primary Events in Biology Probed by Ultrafast Laser Spectroscopy, ed. R.R. Alfano, Academic Press (1981) (in press).

CHAPTER I. INTRODUCTION

The temporal and spectral evolution of the fluorescence emission from photosynthetic systems has been traditionally interpreted as indicative of energy transfer in the photosynthetic complex consisting of accessory pigments such as carotenoids, Chl. a, Chl. b, and energy trapping reaction centers. In particular the fluorescence lifetime has been readily associated with the time required for the absorbed energy to reach the reaction center "trap" where it may undergo photochemical conversion. By following the energy transfer process to the photochemically active trap it is possible to elucidate the mechanisms which determine the specific pathways and participants as well as the efficiency of the transfers. This is not only important from the point of view of understanding primary photosynthesis itself, but also to provide insight into the underlying construction of highly efficient energy transfer systems which may prove useful in the construction of artificial light harvesting complexes.

The text of this thesis is divided into ten chapters. Chapter 2 presents an overview of the photosynthetic process, placing the research performed in this investigation in its proper perspective in terms of the primary photosynthetic process. In Chapter 3 a review of the various theories which are applicable to the primary

energy transfer process in photosynthesis is presented. An account of the work that has been performed to date in the field of time resolved fluorescence spectroscopy in photosynthetic systems is presented in Chapter 4. The experimental apparatus as well as the characteristics of the laser system used for excitation, and the time resolved fluorescence techniques employed in the picosecond detection systems may be found in Chapter 5. The experimental program and discussion of results has been divided into four chapters and is presented in Chapters 6-9. A summary and review of the important findings is given in Chapter 10.

In order to probe the photosynthetic energy transfer process in photosynthesis, the following avenues of investigation were taken:

1) A study of the role of the accessory pigments and their relationship to the energy transfer kinetics in the accessory pigment complex of phycobilisomes and phycobiliproteins from a blue-green alga (Nostoc sp.).

2) A study of energy transfer in the carotenoid accessory pigment complex of higher green plants (Spinach and Norway maple).

3) A study of the time resolved fluorescence kinetics from spinach chloroplasts and algal photosystem mutants (Sc) probing energy trapping in PS I and PS II.

4) A study of the effect on the fluorescence decay kinetics of non-radiative decay mechanisms in the dye

malachite green, with a parallel study of the fluorescence depolarization kinetics in the same system and in photosynthetic higher green plants (spinach), algal photosystems (Nitella), and non-photosynthetic anthocyanin pigments in vitro and in vivo.

The remainder of this chapter summarizes the important findings of this thesis. In photosynthesis, the transfer of excitation energy from the absorbed photons to the photochemically active reaction center trap must be carried out in an efficient manner. For the blue-green algae, light energy in the spectral region from 500 to 600 nm is first absorbed by the pigment phycoerythrin in the accessory pigment complex known as the phycobilisome, and is then transferred to other accessory pigments also present in the phycobilisome, sequentially, from phycoerythrin to phycocyanin and finally to allophycocyanin. Allophycocyanin in turn transfers this energy to chlorophyll a molecules located on the stromal surface of the lamellae to which the phycobilisomes are attached. This system thus provides an ideal setting for the study of sensitized excitation energy transfer, whose time course can be analyzed by picosecond fluorescence spectroscopy. In this research I have followed the fluorescence from phycobilisomes as well as from isolated phycobiliproteins of the alga Nostoc sp. through the aforementioned energy transfer pathway.

The kinetics of the excitation energy transfer have been analyzed in the exciton annihilation model, and this study is presented in detail in Chapter 6.

A study was conducted in the carotenoid accessory pigment complex of both photosynthetic and non-photosynthetic Norway maple leaves (Acer platenoides) in order to probe the energy transfer kinetics in the non-chlorophyll containing accessory pigment complex of higher plant systems. The observed fluorescence kinetics in this system have led to the formulation of a new model for energy transfer in the primary stages of photosynthesis which is presented in Chapter 7.

The constancy of the fluorescence lifetime under various experimental conditions of excitation and observation that was performed in my early investigations of the fluorescence kinetics from photosynthetic systems was surprising and led to an investigation of the fluorescence kinetics from both photosynthetic and non-photosynthetic accessory pigment systems. The first study in this research was carried out using picosecond pulse train excitation and optical Kerr gate resolution. In this study, the fluorescence kinetics from spinach chloroplasts at 685nm, 690 nm and 730 nm were measured both at room temperature and at low temperature. Since measurements employing picosecond laser pulse train excitation can be complicated by singlet-triplet exciton annihilation effects, or the build up of long lived ionic

species, while high intensity (generally $> 10^{14}$ photons/ cm^2 per pulse) single pulse experiments can be complicated by singlet-singlet exciton annihilation phenomena, an investigation of the intensity dependence of the fluorescence yield and lifetime from spinach chloroplast preparations as well as from a whole spinach leaf was made using single pulse excitation. The results of this study are presented in detail in Chapter 8.

The fluorescence kinetics of PS I and PS II enriched preparations have been previously associated with the two component decay observed in whole chloroplast (Yu et. al., 1975a). The fast component ($\sim$ 56 ps) has been associated with the emission from PS I and the slow component ($\sim$ 200 ps) as the emission from PS II. The alga Scenedesmus obliquus wild type is known to possess both active PS I and PS II components, while the mutant 8 variety has an inactive PS I reaction center and the mutant 11 variety has an inactive PS II reaction center trap. Measurement of the fluorescence kinetics from the alga Scenedesmus obliquus, wild type and mutants 8 and 11 with 530 nm single pulse excitation has been made in order to further probe the association of the fast decay component with the PS I fluorescence and the slower decay component with the PS II emission. The results of this work are also presented in Chapter 8.

Fluorescence polarization studies provide detailed information about non-radiative deexcitation processes as

well as orientational structure of the fluorescing pigment molecules in their local environment. The florescence depolarization of the dye malachite green was investigated as a function of solvent viscosity in order to characterize the picosecond depolarization kinetics in a simple system consisting of randomly aligned dye molecules in solution. Subsequently, measurements were made on the in vivo and in vitro fluorescence kinetics of anthocyanin pigments which are naturally found dissolved in the vacuoles of leaves and the petals of flowers and plants, as well as the skins of fruits. This study has provided a comparison for the kinetics observed from pigments embedded in a membrane (as in the case of the chlorophylls) as opposed to the case of pigments in vacuoles (as in the case of the anthocyanins). These results are presented in detail in Chapter 9.

CHAPTER 2. THE PHOTOSYNTHETIC PROCESS

2.1 Photosynthesis Overview

Photosynthesis is nature's lifesustaining process by which green plants, algae and photosynthetic bacteria convert light energy into chemical energy. The equation which has become synonymous with the photosynthetic process in green plants and algae describes the formation of oxygen and an energy rich compound, a carbohydrate, from constituent water, carbon dioxide and sunlight. The equation that describes this oxidation - reduction reaction between H_2O and CO_2 takes the form:

$$H_2O + CO_2 \xrightarrow{\text{Light}} (CH_2O) + O_2 + 112 \text{ Kcal.}$$

Early attempts to explain photosynthesis described the process as a simple dissociation of CO_2 liberating O_2 and assimilating carbon and water forming a formaldehyde. It was C.B. Van Niel (1935) who first suggested in the late 1930's that the O_2 evolved in the process came from H_2O and not CO_2. Indeed this was demonstrated in the classic ^{18}O radioisotope experiments of Ruben et al., (1941). In the case of photosynthetic bacteria, electron donors other than water take part in the reaction and no O_2 is evolved.

Since Photosynthesis involves energy storage, an uphill transfer of the absorbed light energy must take

place involving transfers between unstable intermediates. It is now known that this uphill transfer takes place between the reductant H_2O at a potential of 0.81 V and the oxidant CO_2 at a potential of -0.4 V, giving rise to a total potential gradient (Govindjee and Govindjee, 1975) of 1.21 V.

Although light is necessary to drive photosynthesis, while at low light intensities the yield curve is nearly proportional to the incident illumination, it can be saturated by excess light. This effect was interpreted by Blackman (1905) as indicative of the presence of a photochemical "dark", or enzymatic mechanism where the saturation of the yield curve indicates the inability of the dark reactions to keep up with the production of the light driven reactions. This light saturation phenomenon can be verified by temperature studies, or by the addition of ions which affect the enzymatic reaction rates and in turn the overall photosynthetic yield.

In 1932 Emerson and Arnold (1932 a,b) using flashes of light of 10^{-5} sec duration performed O_2 evolution experiments in the green alga Chlorella, revealing a maximum yield of one O_2 molecule for every 2500 chlorophyll molecules. They also found that changes in temperature did not affect the maximum yield per flash, although the "dark" recovery time was affected. This experimental evidence subsequently led Gaffron and Whol (1936 a,b) to assign a "Photosynthetic Unit" or PSU as the

site of the primary photochemical energy conversion mechanism and the site of the enzymatic reactions. Since 2 quanta are required for each H atom that is transferred, and 4 H atoms are transferred for each O_2 molecule liberated, in terms of the primary photochemical process the PSU reduces to a cluster of ~ 300 chlorophyll molecules.

Thus the saturation of photosynthetic yield in constant light places an upper limit on the number of chlorophyll molecules that can be serviced by an enzyme in the dark reaction, and measurement of the recovery time of the rate limiting enzymatic step in flashing light experiments has determined the enzyme recovery (Rabinowitch and Govindjee, 1969) rate at ~ 50 sec^{-1}, giving rise to a total production of one O_2 molecule each 50 seconds. Photosynthetic liberation of O_2 was shown to also take place extracellularly in suspended leaf material in the presence of iron salts by Robert Hill in 1937. This process, now referred to as the Hill reaction, forms one of the basic tests for photosynthetic activity, and many oxidants (e.g. ferricyanide, quinone, $NADP^+$) are capable of sustaining the Hill reaction.

Since Chl. *a* is a basic element of all photosynthesizing cells, the question naturally arises as to what role it plays in the photochemical stage. We have seen that in photosynthesis light drives an oxidation reduction reaction against an electrochemical potential

gradient of 1.2 V. Before the excitation energy can be transferred along this uphill gradient, an energy acceptor capable of stabilizing and temporarily storing this energy in an energy rich bond capable of driving a subsequent chemical reaction, is needed. This is the role envisioned for the Chl. a molecules. Indeed indication of this energy transfer and storage role was found in 1948 by A.A. Krasnovsky who observed that in vitro Chl. a dissolved in pyridine could be reversibly reduced in the presence of light by ascorbic acid (Rabinowitch and Govindjee, 1969). Krasnovsky was thus able to postulate that chlorophyll molecules in vivo are reduced by H_2O.

2.2 The Photosynthetic Unit: Structure and Function

The concept of a photosynthetic unit (PSU) evolved naturally from the oxygen evolution experiments of Emerson and Arnold. The assumption that 8 light quanta are required for the evolution of one oxygen molecule from a set of 2500 chlorophyll molecules can be directly coupled to the condition that photosynthesis involves the splitting of water where 4 units of (H) reduce one molecule of CO_2, and 4 units of (OH) yield one O_2 molecule. Thus 2 light quanta can be connected with the primary dissociative act,

$$H_2O \xrightarrow{2\ h\nu} (H) + (OH) \ .$$

The PSU thus reduces to a structural unit of 2500/4 = 625 chlorophyll molecules for a 2 quanta reaction, and a single photochemical event would therefore appear to involve 2500/2x4 = 313 molecules. It is important to realize that these deductions are intuitive and no direct evidence for such a relationship between structure and photochemical function can easily be found.

Other factors which contribute to the PSU concept include (Clayton, 1965); the presence of one cytochrome molecule and one specialized chlorophyll molecule for every 300 chlorophyll molecules; Inhibition by herbicides, such as DCMU, of the photosynthetic activity at a concentration of one DCMU molecule for every 200 chlorophyll molecules and the abrupt decline in the Hill reaction when chloroplast fragments are broken into particles containing fewer than 200 chlorophyll molecules. Similar findings in the case of photosynthetic bacteria lead to a bacterial photosynthetic light harvesting unit of 30 - 60 Bacteriochlorophyll (BChl.) molecules.

In the case of green plants and most algae the PSU is located in the chloroplast. The chloroplast is the organelle found in living cells which contains chlorophyll as well as other accessory pigments. The chloroplast structure is delineated by a filamental or lamellar substructure consisting of sacs or thylakoid vesicles which at certain regions of the chloroplast can become

clustered into disc-shaped stacks called grana. Surrounding these thylakoid vesicles is the stroma which makes up the general chloroplast matrix. From electron micrographs (Arntzen, 1975), the lamellar structure is found to contain hemispherical "bumps" capable of containing the requisite number of chlorophyll molecules which comprise the PSU. R.B. Park and J. Biggers (1964) called these granular bumps "quantasomes", denoting the sites of the primary quantum energy conversion in photosynthesis. Typical chloroplast size may range from 5 - 10 u across for an ellipsoidal shaped body, while the grana are about 0.5 um in diameter and 0.3 um thick. In the red and blue green algae, the lamellae structure is present without the chloroplast.

The chloroplast lamellae reveals an estimated quantasome unit size of (Rabinowitch and Govindjee, 1969) 18x16x10 nm. Assuming 300 chlorophyll molecules per unit and a molecular dimension for the porphyrin head (Campillo and Shapiro, 1977) of 15.5 x 15.6 x 3.7 A, this would give rise to a 0.16 M chlorophyll concentration in vivo. Although grana are not absolutely essential for photosynthetic activity of chloroplasts, stacking of the lamellae into grana may serve to bind pigment layers into closer aggregates which can give rise to more efficient

energy transfer as well as a locked-in site for the enzymes and substrates (e.g. cytochromes, plastocyanin, plastoquinone, etc.) which are necessary for the photochemical conversion process.

2.3 Spectroscopic Properties of Photosynthetic Pigments

For Photosynthetic pigments to be biologically useful in capturing energy from sunlight, they must absorb strongly in that emission region of the solar spectrum that actually reaches the earth, typically from 300 - 1100 nm. Ultraviolet light below 300 nm is effectively used in the conversion of O_2 to ozone in the upper atmosphere, (which in turn absorbs light up to 350 nm reforming O_2) and is thus not present in the spectrum of sunlight which reaches the earth.

With such a wide solar spectrum reaching the earth it is natural to inquire as to why plants are green, absorbing in the blue and yellow to red region of the solar spectrum. Part of the answer may lie in the fact that although their green color precludes absorption of a good portion of the solar spectrum, there are many more yellow to red photons in the solar spectrum than there are green ones. From the point of view of energy transfer it is the absorption band of the final reaction center molecule or trap which must determine the upper absorption limit of the antenna pigment system. To have an accessory pigment molecule absorbing beyond this region would indeed be

detrimental to the plant as the captured light energy would then be channeled past the intended destination and would thus be useless for photochemical conversion, requiring a highly improbable uphill transfer of the excitation energy in order to reach the trap. In addition, to place the final acceptor pigment molecule in the infrared region of the spectrum would have been catastrophic for photosynthetic life forms existing more than a few cm below water, as infrared radiation beyond 1100 nm is strongly absorbed by water (Clayton, 1971).

In order for a photochemical change to take place, the absorbed light energy must be comparable to chemical bond energies. Molecular structures consisting of conjugated double bonds generally have strong absorption in the visible to near ultraviolet region of the spectrum, while single bonded structures generally possess far ultraviolet absorption. Thus the region from 300 to 1100 nm is a suitable photochemically active region for photosynthesis, and indeed the absorption of pigment molecules in green plants, algae and photosynthetic bacteria span this spectral region.

The three major types of photosynthetic pigments consist of the chlorophylls, the carotenoids and the phycobilins. Chlorophyll a (Chl. a) present in green plants, brown, red, and blue-green algae or Bacteriochlorophyll (BChl.) present in photosynthetic bacteria is an indispensible component of photosynthesis.

As many as seven different forms of Chl. a are believed to be present in vivo (Rabinowitch and Govindjee, 1969). The characteristic absorption peaks for Chl. a in vivo lie at 420 - 435 nm and 670 - 680 nm, with peak emission at 685 nm and a minor emission band at 740 nm. (A detailed account of the physical and structural properties of the chlorophylls may be found in The Chlorophylls by Vernon and Seely). Pigments other than Chl. a (or BChl.), although not strictly essential for photosynthesis, are generally found in all photosynthesizing cells acting mainly as light harvesting accessory pigments.

The most closely related accessory pigment is Chl. b, with a peak absorption at 480 and 650 nm, found in higher green plants and green algae. Other accessory pigments, as well as the bacteriochlorophyll forms are listed in Table 2.1. Chlorophyll c (Chl. c) with characteristic absorption at 645 nm is found in diatoms and brown algae, while Chl. d with peak absorption at 740 nm occurs in red algae. Chlorophyll forms in bacteria include; BChl. a, with absorption bands at 800, 850 and 890 nm, fluorescing at 920 nm, found in purple and green bacteria; Bacteriochlorophyll b (BChl. b) with absorption band at 1017 nm, and Bacterioviridin, also known as chlorobium chlorophyll, with absorption at 750 nm found in green bacteria.

Were it not for the fact that certain bacteria (e.g. R-26, a mutant of Rhodopseudomonas spheroides)

can undergo photosynthesis although lacking carotenoids, carotenoids too would be, like chlorophyll, an indispensable component of photosynthesizing cells. Mostly all photosynthetic cells possess some carotenoid pigments. In the chloroplast carotenoids are interleaved among the chlorophylls which spectrally mask their presence. Carotenoids are composed of a linear, alternating, conjugated double bond structure with ionone (C_9H_{15}) rings at either end. As they are hydrophobic, they are found in the lipid layer of the thylakoid membrane. Oxygen containing carotenoids are classified as carotenols or Xanthophylls, while the hydrocarbon forms are known as carotenes.

In autumn when the chlorophyll in leaves begins to disintegrate, the natural yellow - orange color of the carotenoids becomes apparent. In vivo absorption and fluorescence spectra of carotenoids are difficult to obtain as their absorption bands overlap the chlorophyll absorption bands, making their energy transfer efficiencies high (20 - 40 %) so that the in vivo fluorescence emission is practically undetectable. Carotenes exist in three major forms as the stereoisomers α, β and γ carotene. The characteristic absorption in organic solvents for both the carotenes and carotenols range from 420 - 524 nm.

The next major accessory pigment system consists of the water soluble phycobilins found in the red

Table 2.1 Photosynthetic Pigments

Chlorophylls:	Absorption
Chl. a	435, 670
Chl. b	480, 650
Chl. c	645
Chl. d	740
Chlorobium chlorophyll (Bacterioviridin)	
BChl. a	800, 850, 890
Bchl. b	1017

Carotenoids:	
α-carotene	
β-carotene	(Carotenes)
γ-carotene	
Luteol	
Violaxanthol	
Fucoxanthol	(Carotenols)
Spirilloxanthol	

Phycobilins:	
Phycoerythrin	565
Phycocyanin	620
Allophycocyanin	650-671

(Rhodophyceae) and blue-green (Cyanophyceae) algae. These phycobiliproteins are contained in structures called phycobilisomes (PBS) which are attached to the lamellae within the algae . Phycobilisomes are composed of the pigment containing phycobilin units phycoerythrin (PE) absorbing at 565 nm and fluorescing at 577 nm, phycocyanin (PC) absorbing at 620 nm and fluorescing at 648 nm, and various allophycocyanin (APC) forms absorbing at 650-671 nm and fluorescing at 660-678 nm.

The structures of the accessory pigment molecules basic to photosynthesis are easily obtainable from common chemical bases. The simplest building block consists of the conjugated bond ring structure of benzene, C_6H_6, consisting of two resonating ring structures as shown in Fig. 2.3.1 a. Pyridine , C_5H_5N, is formed when trivalent Nitrogen replaces a carbon atom in the ring structure of benzene, forming a single bond with a carbon atom on one side and a conjugated double bond with a carbon atom on the other side (Fig. 2.3.1 b).

The structures of the various pigment molecules are integrally related to the basic porphyrin structure, shown in Fig. 2.3.2. Chl. a whose structure is shown in Fig. 2.3.3, is characterized by the presence of a magnesium atom at the center of the porphyrin ring. The basic differences between the structure of Chl. a and that of basic porphyrin are the missing double bond in the fourth pyrrole ring and the presence of the Mg atom in the

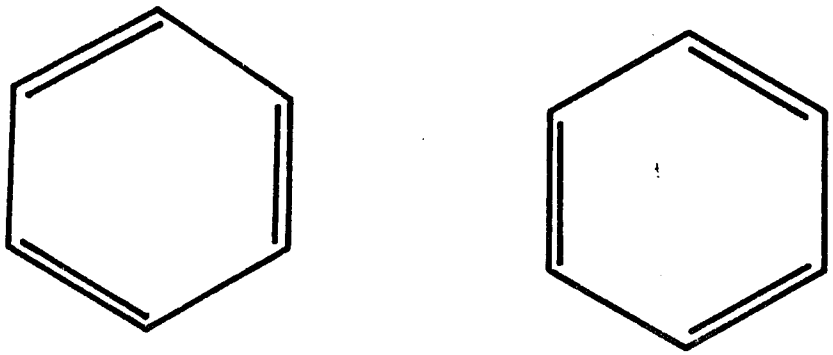

Fig. 2.3.1a Structure of Benzene.

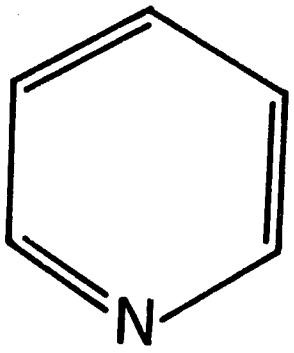

Fig. 2.3.1b Structure of Pyridine.

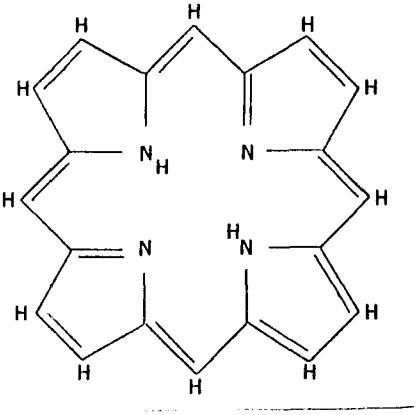

Fig. 2.3.2 Structure of Porphyrin.

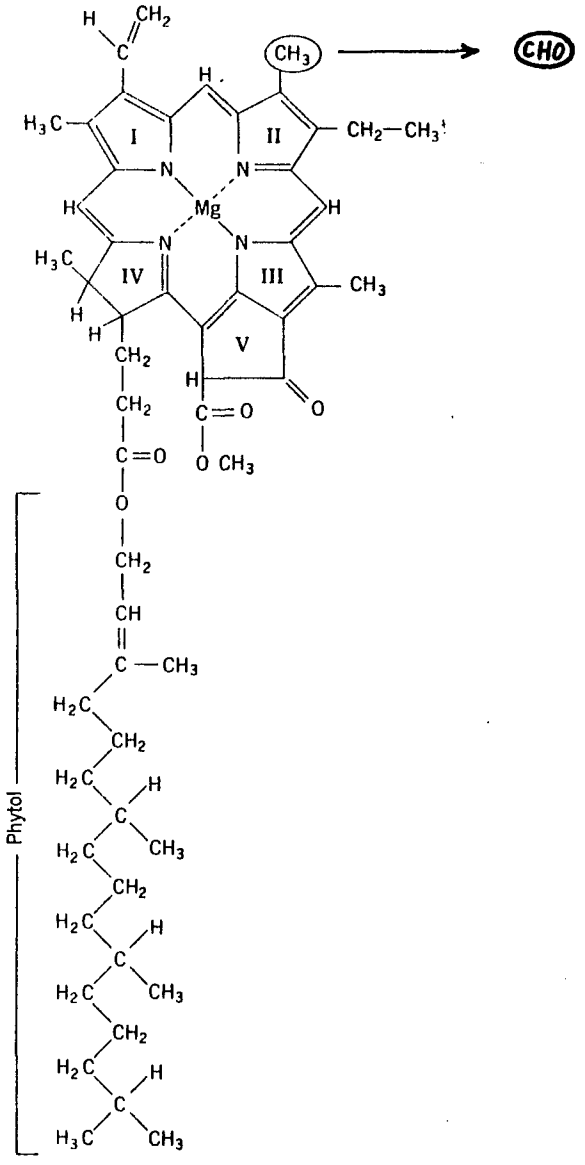

Fig. 2.3.3 Structure of Chlorophyll a and b.

tetrapyrrole head. The Mg atom and the nearly saturated phytol tail give the molecule its characteristic polar properties, making the porphyrin head polar and thus hydrophilic, while the phytol tail is hydrophobic. Replacement of the CH_3 group in the second pyrrole ring with CHO obtains Chl. b (see Fig. 2.3.3). It is interesting to note that simple replacement of the Mg atom with an atom of Fe in porphyrin determines the basic heme structure of hemoglobin, the red pigment constituent of blood.

The basic structure of the carotenoid forms is shown in Fig. 2.3.4. The distinguishing features here consist of a polyene conjugated double bond linear structure with ionone rings at each end.

The basic structure of bilan can also be obtained from porphyrin by stretching out the ring and removing the central Mg atom, as shown in Fig. 2.3.5 a. The structures of phycoerythrobilin, phycocyanobilin, and the unit structures for phycoerythryn, phycocyanin and allophycocyanin are shown in Fig. 2.3.5 b, c and d respectively.

The composite absorption spectra for the various photosynthetic pigments are shown in Fig. 2.3.6 a and the in vivo emission spectra is shown in Fig. 2.3.6 b.

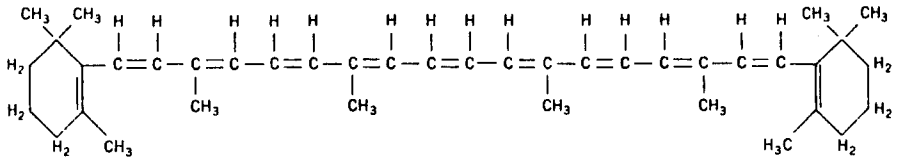

Fig. 2.3.4 Structure of carotenoid forms.

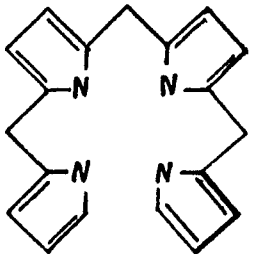

Fig. 2.3.5a Bilan Structure.

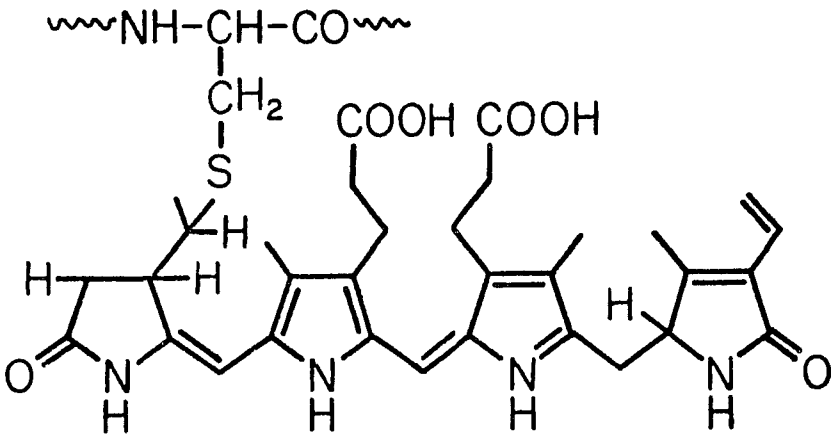

Phycoerythrobilin (PEB)

Fig. 2.3.5b Structure of phycoerythrobilin.

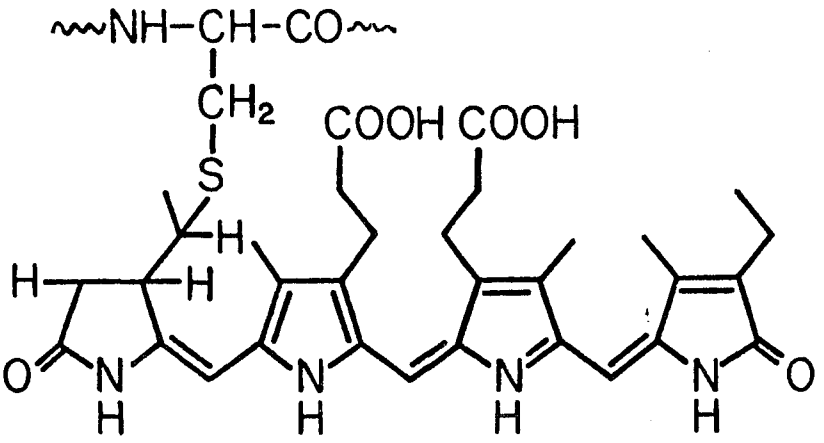

Phycocyanobilin (PCB)

Fig. 2.3.5c Structure of phycocyanobilin.

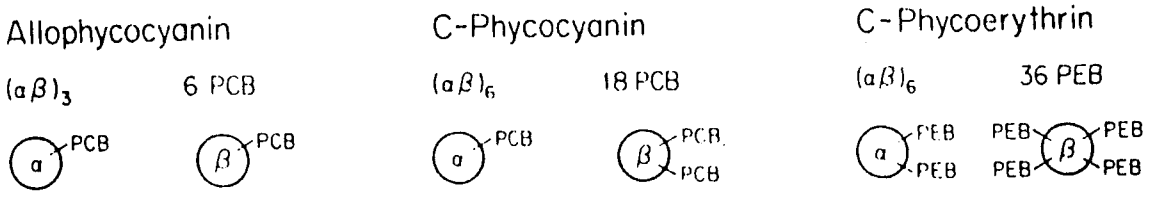

Fig. 2.3.5d Phycobiliprotein Unit Structures.

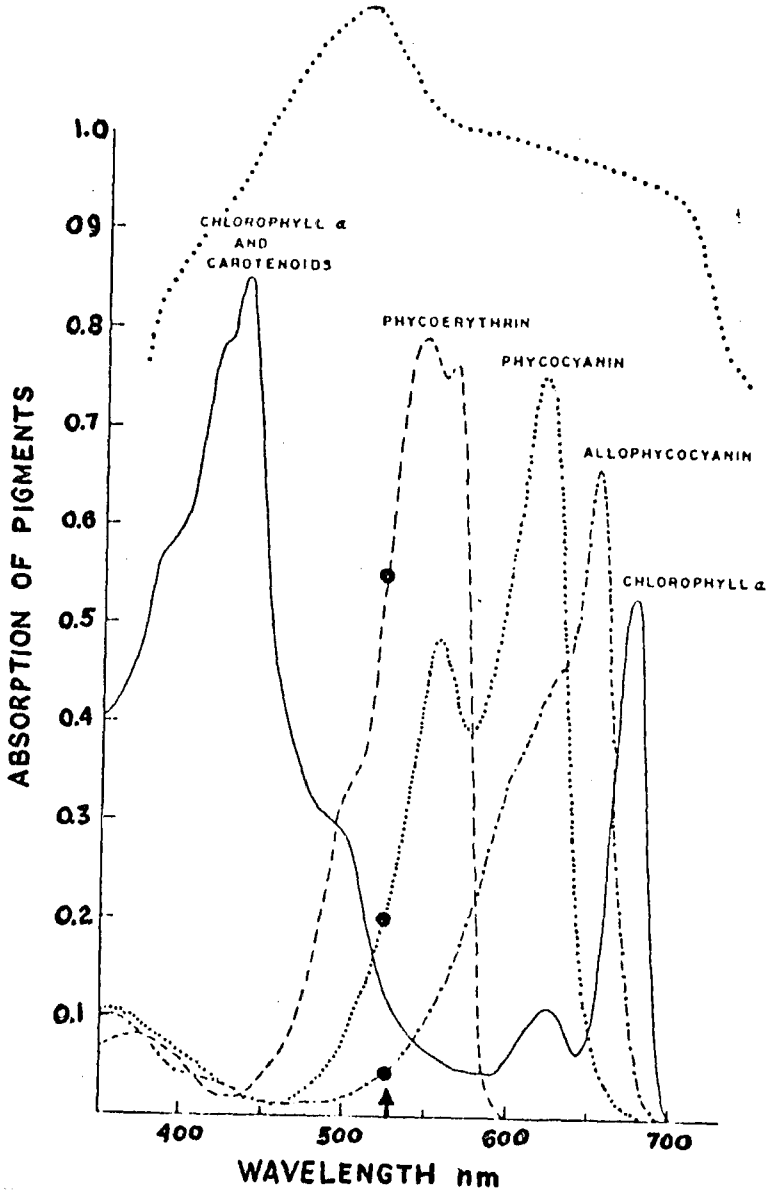

Fig. 2.3.6a Absorption Spectra of photosynthetic pigments.

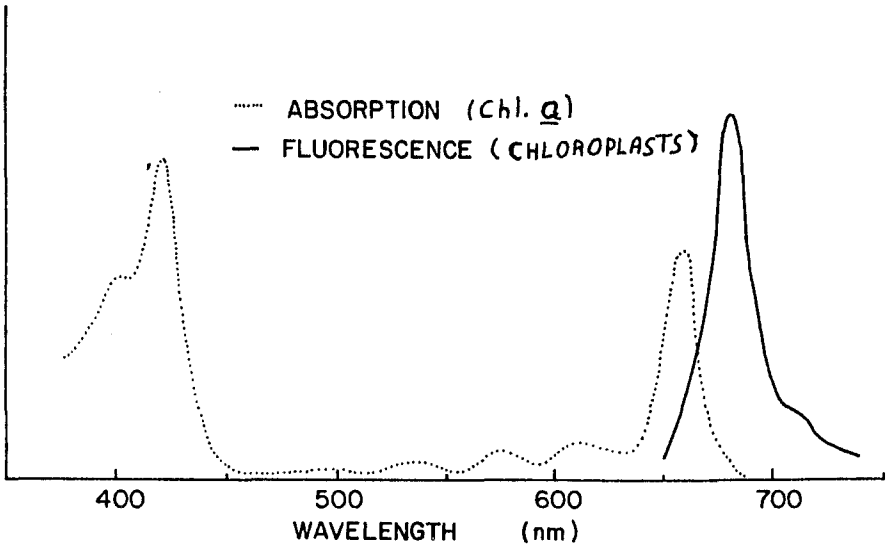

Fig. 2.3.6b Emission spectra of photosynthetic pigments.

2.4 The Primary Process

The primary process in photosynthesis consists in the absorption of light energy by the assembly of pigment molecules in a PSU and its subsequent transfer to a specialized reaction center molecule capable of undergoing charge separation resulting in the reduction of some primary electron acceptor. The initial absorption occurs within the accessory pigment complex or a Chl. *a* molecule and takes place within 10^{-15} sec. Thereafter, unless the energy is absorbed by the reaction center molecule itself, the excitation energy must find its way to the reaction center in order for the energy to become photochemically useful. The energy may also be dissipated through non-radiative internal conversion in the vibrational-rotational manifold of either the initial absorbing molecule or some latter acceptor in the energy transfer chain, or through inter-system crossing, where it may later be emitted as phosphorescence.

These energy transfers may be followed through time resolved fluorescence spectroscopy. A picosecond excitation pulse at 530 nm directly excites the carotenoid or phycobiliprotein accessory pigment system in higher green plants and algae , respectively. By measuring the risetime of the fluorescence emission of chlorophyll *a*, a direct measurement of the energy transfer time can be obtained. Time resolved spectral measurements can also be

used to follow the excitation energy in the accessory pigment complex, while temperature studies may be used to probe the effect on the photosystem fluorescence of closing specific energy decay routes or providing an energy barrier to up-hill energy transfer by increasing the activation energy required for transfer. In addition, time resolved fluorescence polarization studies can provide detailed information on the diffusion of excitations in the photosystem. The various possible energy transfer mechanisms are described in Chapter 3.

The presence of efficient energy decay paths *in vivo* is evidenced by the fact that while the *in vivo* fluorescence yield of Chl. *a*, is approximately 3 %, the *in vitro* yield is approximately 10 times higher. The currently held view of primary energy transfer involves a fast efficient transfer of the excitation energy from the accessory pigment pool directly to chlorophyll *a*. The excitation energy then migrates in the Chl. *a* lattice until it encounters the specialized reaction center. Some convincing arguments for this view include the following:

1. *In vivo* accessory pigment fluorescence (with the exception of the Chl. *b* fluorescence observed by Govindjee and Briantais (1972)) has not been observed to date.

2. The risetime of the Chl. *a* fluorescence emission is $\lesssim 10$ ps, (generally resolution limited) indicating a fast energy transfer.

3. Excitation energy transfer from carotenoids to Chl. a occurs with a 10 - 50 % efficiency (Dutton et al., 1943; Duysens, 1952; Goedheer, 1972).

Excitation energy transfer from Chl. b to Chl. a is extremely efficient (~ 95 - 99 %) (Cho and Govindjee, 1970).

Excitation energy transfer from phycobilin accessory pigments to Chl. a is 80 - 90 % efficient (French and Young, 1952; Duysens 1952; Govindjee and Mohanty, 1972)

4. Closing of the reaction center traps through the addition of poisons (e.g. DCMU), saturating light intensity, or lowering the temperature increases the fluorescence yield (Breton and Geacintov,1976; Searle et al., 1977).

While heterogeneous energy transfer is directly evidenced by Chl. a emission at 685 nm regardless of which accessory pigment is excited (sensitized fluorescence), homogeneous energy transfer is indicated by the complete depolarization of Chl. a fluorescence in vivo (Arnold and Meek, 1956; Mar and Govindjee, 1972). The process by which the transfer of the excitation energy takes place can occur either through the migration of an excited electron - hole pair throughout the lattice (exciton migration), or through the actual motion of electrons and holes in the conduction band of the molecular system, leading the electrons to a reduction site and the holes to

an oxidation site (mass motion). The maximum time that a molecule can remain in the excited state is determined by its natural radiative lifetime, $\tilde{\tau}_o$, and other avenues of escape for the excitation energy reduce this time to the observed fluorescence lifetime, $\tilde{\tau}$.

At the reaction center, excitation of the electron to the first excited singlet state leaves the reaction center oxidized, while reducing the primary electron acceptor. The reaction center is then reduced by the primary electron donor allowing it to undergo further excitations. Spectral isolation of reaction center molecules is made difficult by the fact that in order for transfer to be efficient their emission must necessarily be close to that of the bulk pigment. Moreover as efficient traps for the excitation energy their concentration is smaller by at least 2 orders of magnitude from that of the bulk pigment, and they therefore possess very low quantum yields.

Reaction center molecules have been identified by measurement of light induced absorption changes. A specialized Chl. a molecule with absorption at 700 nm (P 700) was identified by Kok (1956) as the reaction center for PS I, while Doring et al. (1967,1968,1969) and Doring and Witt (1972) have attributed absorption changes at 682-690 nm to a specialized Chl. a molecule (P 680) as the reaction center for PS II. These reaction center

molecules are believed to consist of two Chl. a or BChl. molecules joined by water molecules (Shipman et al., 1976).

Photochemical charge separation from the reaction center molecule to the primary acceptor can be followed through changes in the prompt fluorescence from Chl. a. The initial rise in the fluorescence yield indicates a decrease in the primary electron acceptor and/or donor pool (Duysens and Sweers, 1963; Mauzerall, 1972; Butler, 1972). When the electron acceptors and donors are returned to the pool, through the action of secondary acceptors and donors, the fluorescence yield begins to decrease (Malkin and Kok, 1966). Addition of DCMU acts to block the reoxidation of the primary electron acceptor by secondary acceptors and can thus increase the fluorescence yield. Measurement of the fluorescence lifetime under "open" (dark adapted) or "closed" (DCMU + illumination) trap conditions provides a means of investigating the photoactivity of PS II, as well as exciton transfer in the Light Harvesting Complex (LHC) under conditions where the PSII traps are closed.

2.5 The Two Photosystems

A Photosystem is the term that is used to describe an assembly of molecules which can cooperatively carry out a primary photochemical conversion. There are three such photosystems which can be isolated in nature; Photosystem I (PS I) and Photosystem II (PS II) in green plants and algae and the photosystem of photosynthetic bacteria.

To each of the series coupled PS I and PS II there is an associated light reaction. PS II governs the reduction of plastoquinones and the evolution of O_2, while PS I reduces $NADP^+$ and oxidizes plastoquinones. Charge separation in each pigment system occurs in less than 20 ns, while the reoxidation of plastoquinone requires $\sim$20 ms thus becoming the "bottleneck" for electron flow (Govindjee, 1978).

A possible energy transfer reaction scheme between the accessory pigments A, the reaction center of PS II (P-680) and the primary acceptor, Q, is given by (Wong et al., 1978),

$$\text{A P680 Q} \xrightarrow{h\nu} \text{A}^* \text{ P680 Q} \xrightarrow{\sim 300 \text{ ps}} \text{A P680* Q} \xrightarrow{< 20 \text{ ns}}$$

$$\text{A P680}^+\text{Q}^- \xrightarrow{30 \text{ ns}} \text{A P680Q}^- \xrightarrow{100\text{-}600 \text{ us}} \text{A P680Q}$$

$$\text{Z} \rightarrow \text{Z}^+ \qquad \text{R} \rightarrow \text{R}^-$$

with Z a secondary electron donor and R a secondary electron acceptor. The oxidation of water with evolution of O_2 results from the accumulation of four positive charges from Z^+ to some other complex.

A possible energy transfer reaction scheme between the accessory pigments A, the reaction center of PS I (P-700), the charge transfer complexes A_1, A_2, a bound ferrodoxin form P-430, identified as the primary acceptor in PS I by Hiyama and Ke (1971), and the plastocyanin pc is given by (Sauer et al., 1977),

$$A\ P700\ A_1A_2\ P430 \xrightarrow{h\nu} A^*\ P700\ A_1A_2\ P430$$

$$A^*\ P700\ A_1A_2P430 \xrightarrow{-100ps} A\ P700^*\ A_1A_2P430 \xrightarrow{<20ns}$$

$$A\ P700^+\ A_1^-A_2\ P430 \rightarrow A\ P700^+\ A_1A_2^-\ P430 \longrightarrow$$

$$A\ P700^+\ A_1A_2\ P430^- \xrightarrow{20us} A\ P700\ A_1A_2\ P430^- \longrightarrow$$

$$Pc \curvearrowright Pc^+$$

$$\xrightarrow{5\ ms} A\ P700\ A_1A_2\ P430$$

$$Fd \curvearrowright Fd^-$$

where reduced ferrodoxin (Fd) in turn reduces $NADP^+$ to NADPH. ATP synthesis can take place in the presence of the H^+ released during the flow of electrons from H_2O to $NADP^+$.

Series coupling between the two photosystems, or "Z

scheme" was first proposed by Hill and Bendall (1960) to explain electron flow in photosynthesis. The "Z scheme", outlined in Fig. 2.5.1 describes the uphill electron transport from H_2O to $NADP^+$ through the PS II and PS I electron transfer mechanisms outlined above.

The primary acceptor Q in PS II was identified with C-550 by Arnon et al. (1971) and Erixon and Butler (1971) through absorbance change measurements. Similarly, Hiyama and Ke (1971) associated the primary acceptor of PS I with P 430.

The electron transport chain consisting of cytochrome b 559 (Cyt. b559), Plastoquinone (PQ), cytochrome f (Cyt. f) and Plastocyanin (PC) reduce P 700 as they simultaneously drive the non-cyclic photophosphorylation converting ADP to ATP. However, cyclic photophosphorylation can also occur in PS I by electron flow from the primary acceptor back to plastocyanin or plastoquinone.

In order to obtain efficient photosynthetic conversion this series formulation requires either that the two photosystems be driven at the same rate (equivalent absorption properties), or that excitation energy be transferred from PS II to PS I when the latter receives fewer excitations. Overdriving of PS II can therefore cause excitation energy to "spillover" into PS I when the reaction centers of PS II are predominantly closed over those of PS I.

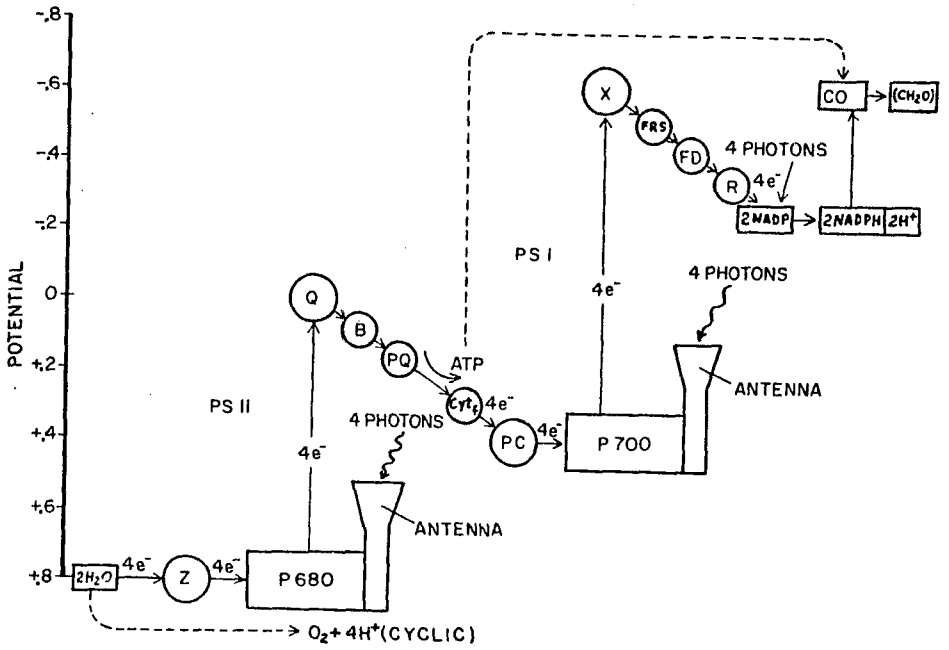

Fig. 2.5.1 "Z" scheme of Photosynthesis.

2.6 Models for Energy Transfer in the PSU

The transfer of excitation energy within and among PS II and PSI has been the subject of numerous investigations. These studies have resulted in the formulation of various models which describe the interaction or coupling between pigment molecules in the photosystems.

Three possibilities are available for excitation energy transfer: 1) the excitation energy can migrate to any pigment molecule and reaction center in the light harvesting complex composed of many photosystems; 2) it can be limited to the local domain of pigment molecules and reaction center of its own photosystem; or 3) an admixture of both. These models have been called the "lake", "puddle" (Robinson, 1967), and "connected" (Lavorel and Joliot, 1972) model, respectively. All of the above models must take into consideration the fact that although excitation energy not used in PS II may spillover into PS I, the reverse cannot occur as it would involve an uphill energy transfer process. For the case where spillover is not allowed, the photosystems are essentially physically isolated and this latter model is referred to as the "separate package model". The spillover rate can be affected by the presence of salts such as Mg^{2+} or Ca^{2+}, which are known to affect grana stacking (Izawa and Good, 1966; Murakami and Packer, 1971).

Picosecond fluorescence kinetic measurements and intensity dependence of the fluorescence quantum yield not only give direct information on the trapping rate, but provide a probe of the interactions among the various photosystem components as well.

CHAPTER 3. THEORIES OF ENERGY TRANSFER IN PHOTOSYNTHESIS

Subsequent to excitation, the major role of accessory pigment molecules is to efficiently transfer the excitation energy to the site of primary photochemical conversion, namely the reaction center or trap. The excitation energy can be transferred homogeneously between like molecules or heterogeneously between unlike molecules. Homogeneous energy transfer involves the exchange of excitations of equal strengths or magnitude among molecules with identical absorption and emission spectra, so that the process can be a pure first order process with no intermediate states taking part. Heterogeneous energy transfer on the other hand generally involves some vibrational energy deexcitation in the excited state manifold of the donor molecule before coupling to a parallel state in the acceptor molecule.

Possible energy transfer mechanisms which allow interaction between two molecules involve either mass motion, such as in electron transfer or collision, or electromagnetic coupling, as in radiative or resonance transfer.

Experiments conducted by Arnold (1965) showed that dried leaf material obeys the same resistance versus temperature relationships as that observed for semiconductors (see also Szent-Gyorgyi, 1941; Arnold, 1977). However a conduction state in photosynthesis is

inconsistent with the observed fluorescence properties. In order to be efficiently populated, the conduction state would necessarily have to be lower in energy than the first excited singlet state. Fluorescence would then require the matching of an electron hole pair with a quantum of energy capable of transfering the electron to the singlet state. The low probability for this simultaneous occurrence would thus appear to rule out energy transfer by mass motion.

3.1 Forster Theory

A quantum mechanical theory for the electromagnetic coupling and transfer of excitation energy between similar molecules was proposed by Theodor Forster in 1948 in an attempt to describe the depolarization properties of dye molecules in solution.

We first consider the Forster theory from a classical point of view (Hoch and Knox, 1968). Starting with a classical point dipole located at the origin of a cartesian coordinate system and oriented along the z axis with dipole moment,

$$\vec{P} = M \cos wt \, \hat{e}_z .$$

We obtain the electric field components at a distance (r,θ) by solving Maxwell's equations for a dipole in polar

coordinates obtaining;

$$E_r = \frac{2 \cos \theta}{\epsilon(w)\, r^3} M \left(\cos wt' - r/\lambda\!\!\!^{-} \sin wt' \right)$$

$$E_0 = \frac{\sin \theta}{\epsilon(w)\, r^3} M \left((1 - r^2/\lambda\!\!\!^{-2}) \cos wt' - r/\lambda\!\!\!^{-} \sin wt' \right)$$

where $\lambda\!\!\!^{-} = \lambda/2\pi = c/nw$ and $t' = t - nr/c$. For completeness we note that the field at (r,θ,t) is actually a "retarded" field due to radiation which originated at a time nr/c earlier and thus make use of the retarded time t'.

For the case where $r >> \lambda\!\!\!^{-}$ (radiation zone), neglecting terms falling off as $1/r^2$ or faster we obtain

$$E_r \longrightarrow 0$$

$$E_\theta \longrightarrow -\frac{\sin\theta\, M \cos wt'}{\epsilon(w)\, \lambda\!\!\!^{-2}\, r}$$

Thus the radiated field is transverse, falling off as $1/r$, and power can be radiated to the acceptor molecule.

For the case where $r << \lambda\!\!\!^{-}$, (static zone) we have, omitting the harmonic time dependent term,

$$E_r \longrightarrow \frac{2\, M \cos \theta}{\epsilon(w)\, r^3}$$

$$E_\theta \longrightarrow \frac{M \sin \theta}{\epsilon(\omega)\, r^3}$$

Thus in the static zone both a longitudinal and a transverse component of the electric field are present.

If we assume that the acceptor molecule itself reacts as a dipole in the external field set up by the donor molecule, we may then use the Lorentz model to describe the reaction of an acceptor molecule A in the presence of the radiated field from donor molecule D. In this model we take A to be a charge e of mass m oscillating along the z axis about a fixed charge -e to which it is bound by spring constant k and damping constant γ (The width of the absorption line of A). Assuming that molecule B does not reradiate energy back to A (If $w_A = w_B$ both A and B must be considered simultaneously) and the wavefunctions of the two molecules do not overlap then, under the applied force $F_o \cos wt$, the molecular dipole A will respond according to the classical damped oscillator equation,

$$m\ddot{z} + m\gamma\dot{z} + k\,z = F_o \cos wt$$

with steady state solution given by:

$$z = \left(\frac{F_o}{m}\right) \frac{(w_A^2 - w^2)\cos wt + w\gamma \sin wt}{(w_A^2 - w^2)^2 + (w\gamma)^2}$$

where $w_A^2 = k/m$.

If we place the dipole of molecule A along the z axis ($\theta = 0$) within the static zone we obtain the static dipole, or "near zone" case, where:

$$F_o = eE_r(\theta = 0)$$

$$F_o = \frac{2 M_D e}{\epsilon(w) r^3}$$

and $$\ddot{z} = \left(\frac{w F_o}{m}\right) \frac{(w_A^2 - w^2)(-\sin wt) + w\delta \cos wt}{(w_A^2 - w^2)^2 + (w\delta)^2}$$

The power radiated can be expressed as,

$$P(w) = m\delta \ddot{z}^2$$

$$= \frac{\delta w^2 F_0^2}{m} \frac{(w_A^2 - w^2)^2 \sin^2 wt + w^2\delta^2 \cos^2 wt - K}{((w_A^2 - w^2)^2 + (w\delta)^2)^2}$$

with $$K = 2w\delta(w_A^2 - w^2) \sin wt \cos wt .$$

Averaging over one time period and using

$$\int_{-T/2}^{T/2} \sin^2 wt \, dt = \int_{-T/2}^{T/2} \cos^2 wt \, dt = T/2$$

$$\int_{-T/2}^{T/2} \sin wt \cos wt \, dt = 0$$

We obtain,

$$P(w) = \frac{\gamma w^2 F_o^2}{2m} \quad \frac{((w_A^2-w^2)^2 + w^2\gamma^2)}{((w_A^2-w^2)^2 + (w\gamma)^2)^2}$$

$$P(w) = \frac{F_o^2}{2m} \quad \frac{\gamma w^2}{(w_A^2 - w^2)^2 + (w\gamma)^2}$$

Thus the power transferred from A to B is given by

$$P(w) = \frac{1}{2m}\left(\frac{2M_D e}{\epsilon(w) r^3}\right)^2 \quad \frac{\gamma w^2}{(w_A^2 - w^2)^2 + (w\gamma)^2}$$

$$P(w) = \frac{2M_D^2 e^2}{m\epsilon^2(w) r^6} \quad \frac{w^2}{(w_A^2 - w^2)^2 + (w\gamma)^2}$$

One of the most important consequences of this equation is that the radiated power is inversely proportional to the sixth power of the distance between the donor A and the acceptor B (R^{-6}), and is thus critically dependent on the separation between the molecules. The power is also proportional to the square of the dipole moment of the donor (M_D^2) and inversely proportional to the square of the dielectric constant ($\epsilon^{-2}(w)$). We also note that as $\gamma \rightarrow 0$ (corresponding

to the lack of vibrational coupling between the states), no energy transfer can take place unless $w = w_A$.

Since the oscillator will not radiate sharply at w_D, but rather in a band of frequencies centered at w_D, we may define an effective dipole moment $\mathcal{M}_D(w)$, obtaining:

$$P(w) = \frac{2e^2}{m\, r^6} \int \frac{1}{\epsilon^2(w)} \quad \frac{\mathcal{M}_D^2(w)\, \gamma_w^2}{(w_A^2 - w^2)^2 + (w\gamma)^2}\, dw \quad .$$

This can in turn be further separated into an oscillator and source contribution. Defining the absorption cross section of the acceptor as,

$$\sigma_A(w) \equiv \frac{4\pi e^2}{n(w)\quad mc} \quad \frac{\gamma_w^2}{(w_A^2 - w^2)^2 + (w\gamma)^2}$$

and the intensity distribution of the source as,

$$I_D(w) = \frac{n(w)\quad w^4 \mathcal{M}_D^2(w)}{3\, c^3} \quad .$$

One obtains a simplified expression for the power radiated from molecule A to molecule B:

$$P_{D\rightarrow A} = \frac{3\ c^4}{2\pi r^6} \int \frac{I_D(w)\ \sigma_A(w)\ dw}{\epsilon^2(w)\ w^4} .$$

This equation has been obtained for the special case where the acceptor dipole is located along the z axis, with the radiated field in the static zone. If we were to place the dipoles at an arbitrary orientation with respect to one another we would then obtain the angular factor (Knox, 1975),

$$K = \hat{e}_D \cdot \hat{e}_A - 3\ (\hat{e}_D \cdot \vec{r})\ (\hat{e}_A \cdot \vec{r})$$

where r is the position vector of molecule A with respect to molecule D, $(\vec{r}_A - \vec{r}_D)$ (Averaging this factor over all directions obtains $K^2 = 2/3$). The radiated power for molecules that have a particular orientation is therefore given by,

$$P_{D\rightarrow A} = \frac{3c^4\ K^2}{8\pi r^6} \int \frac{I_D(w)\ \sigma_A(w)\ dw}{\epsilon^2(w)\ w^4}$$

This is the famous equation obtained by Forster which lies at the foundation of the resonance transfer mechanism.

Since the transfer times are inversely related to their respective rates,

$$\frac{\tilde{\tau}_t^{-1}}{\tilde{\tau}_o^{-1}} = \frac{P_{D\rightarrow A}}{P_o}$$

where:

P_o = $I_D(w)\, dw$ = Radiative power of the donor,

$\tilde{\tau}_o$ = the natural radiative lifetime, and

$\tilde{\tau}_t$ = the energy transfer time from donor to acceptor.

The transfer rate thus becomes:

$$\frac{1}{\tilde{\tau}_t} = \frac{1}{\tilde{\tau}_o}\, r^{-6}\left(\frac{3c^4\, K^2}{8\pi}\right)\int \frac{I_D(w)\, \sigma_A(w)\, dw}{\epsilon^2(w)\, w^4}$$

with $k_t = 1/\tilde{\tau}_t = 1/\tilde{\tau}_o\, (R_o/r)^6$.

From the above equation we see that R_o thus signifies the distance at which the transfer rate becomes equal to the natural radiative rate. The transfer rate can therefore be obtained independently, from the intensity distribution of the donor and the absorption cross section of the acceptor, and is thus sensitive to the overlap between the emission band of the donor and the absorption band of the acceptor. If no nonlinear processes are present in the de-excitation of the donor, the observed lifetime is related to the natural radiative lifetime through the quantum yield as,

$$\tilde{\tau} = \tilde{\tau}_o\, \phi .$$

The transfer rate can then be related to the observed

lifetime directly as,

$$k_t = \frac{1}{\tilde{\tau}} \phi \left(\frac{R_o}{r}\right)^6 .$$

We can thus define a more useful parameter, $\bar{R}_o$, as $\bar{R}_o = \phi^{1/6} R_o$, as the distance from donor to acceptor at which the transfer rate is equal to the actual de-excitation rate of the donor, which includes all linear deexcitation processes and not merely radiative decay.

We now describe the Forster theory from a quantum mechanical point of view. We begin with the wave function for the system of acceptor and donor molecules,

$$\Psi = c(t)\psi_A^* \psi_D + c'(t)\psi_A \psi_D^*$$

with the interaction energy given by

$$u(E_D E_A) = \langle \psi_{D'A}(E_D, E_A) | V | \psi_{DA'}(E_D E_A') \rangle$$

Use of time dependent perturbation theory allows the calculation of the probability coefficients,

$$|c(E_D, E_A, , t)|^2 = \frac{4\, u^2(E_D E_A,)}{(\Delta E)^2} \sin^2\left(\frac{\Delta E t}{2\hbar}\right)$$

with the excitation transfer probability given by,

$$p_{DA'}(t) = \iint |c(E_D, E_{A'}, t)|^2 \, dE_D \, dE_{A'} \, .$$

We now obtain 3 special cases:

1. The Strong Coupling Case:

The strong coupling case exists when the interaction energy, $|u|$, is so large that the vibrational levels of the donor molecule are all in resonance with the vibrational levels of the acceptor molecule. The interaction energy thus allows the transferred energy to excite any of the vibrational levels of the acceptor. In this case the vibrational quantization condition may be relaxed as the energy oscillates between both molecules and is not localized.

Under the restriction that $p_{DA'}(t) \ll 1$, and $\Delta E t/2\hbar \ll 1$ (needed to replace the sine term by its argument in the above expression), where ΔE is the energy difference between the initial and final states, the probability that the acceptor molecule is excited is given by:

$$p_{DA'}(t) \sim U^2 t^2/\hbar^2 \, .$$

For interaction energies $|u| \sim \hbar/t$ we obtain, $2|u| \gg \Delta E$, which gives the strong coupling criterion that the energy of interaction be much greater than the energy difference between the energy levels of the donor and acceptor. If we define the energy difference between the equilibrium

configurations of ground and excited state (the Franck Condon energy) as $\Delta\varepsilon$, with $\Delta\varepsilon'$ the energy of a vibrational quantum, then this condition can be expressed as,

$$|u| >> \Delta\varepsilon >> \Delta\varepsilon'$$

For the case of strong coupling, resonance between the vibronic levels of the donor and acceptor give the resonance transfer rate as (Forster, 1965),

$$N_{D\rightarrow A} = 4\ |u|/h \quad ,$$

describing resonance at fixed nuclear levels.

2. The Weak Coupling Case:

The weak coupling case, originally termed the medium coupling case by Forster, is identified by the criterion that the interaction occurs between similar vibrational levels, so that

$$\Delta\varepsilon >> |u| >> \Delta\varepsilon'$$

The transfer probability is again restricted by the condition $\Delta E t / 2\hbar << 1$, however the transfer now occurs between distinct vibronic levels involving a slower exchange as the excited donor molecule may undergo several vibrations before transfer occurs. The resonance transfer

takes place between specific vibrational levels of both molecules, and is now denoted by,

$$p_{D(w).A'(v)}\ (t) \approx u_{vw}^2 t^2/\hbar^2.$$

In this case the transfer rate is modified by the vibrational overlap integral between the vibrational levels of the donor (v) and acceptor (w),

$$N_{D\to A}^{vw} = \frac{4\,|u|}{h} S_{v,w}^2 \quad .$$

3. Very Weak Coupling Case:

The very weak coupling case, originally termed by Forster as the weak coupling case, occurs when

$$|u| << \Delta\mathcal{E}' << \Delta\mathcal{E}$$

In this case resonance between acceptor and donor levels is limited to very small regions, since the increase in the interaction time ($\Delta t = \hbar/\Delta u$, where Δu is very small) allows the excitation to relax to the lowest vibronic state of the donor before transfer occurs, so that the condition $\Delta E t/2\hbar << 1$ no longer holds. The excitation transfer probability must now be evaluated in the limit of large t yielding (Forster, 1965):

$$p_{DA'}(t) = 2\pi t/\hbar \iint u^2(E, \Delta E)\, \delta(\Delta E)\, dE\, d(\Delta E) \quad .$$

For such very weak interactions $\Delta E \sim 0$, and the transfer rate is easily obtained as,

$$N_{D\rightarrow A}^{vw} = \frac{2\pi}{h} \int u^2(E,0)\, dE$$

Since the integration is over a restricted energy region, $\Delta\varepsilon$, the integrand may be replaced by an average energy density,

$$u^2(E,0) = \frac{u_{vw}^2}{(\Delta\varepsilon)^2}$$

and we obtain:

$$N_{D\rightarrow A}^{vw} = \frac{2\pi}{h} \frac{u_{vw}^2}{\Delta\varepsilon} .$$

As opposed to the strong and weak coupling case, the transfer rate is now proportional to the square of the interaction energy. For the case of dipole-dipole interaction this energy is given by,

$$U = \frac{1}{n^2 R^3} \left[\vec{M}_D \cdot \vec{M}_A - \frac{3}{R^5} (\vec{M}_D \cdot \vec{R})(\vec{M}_A \cdot \vec{R}) \right]$$

so that,

$$U^2 = \frac{K^2 M_D^2 M_A^2}{n^4 R^6} .$$

The transfer rate now becomes,

$$N_{D\rightarrow A} = \frac{K^2}{n^4 h^2 r^6} \iint M_D^2 S_D^2 (E'_D, E'_D - h\nu) \quad X$$

$$M_A^2 S_A^2 (E_A, E_A + h\nu)\, d\nu$$

Finally, by integrating over the initial excited states of the donor and the final states of the acceptor we obtain the well known Forster transfer rate representing the overlap between the fluorescence band of the donor and the absorption band of the acceptor,

$$N_{D\rightarrow A} = \frac{9K^2 (\ln 10) c^4}{128 \pi^5 n^4 N' \tilde{\tau}_{e,D}} \frac{1}{R^6} \int f_D(\nu) \epsilon_A(\nu) \frac{d\nu}{\nu^4}$$

where n is the refractive index of the medium, N' is the number of molecules per millimole, $\tilde{\tau}_{e,D}$ is the radiative lifetime of the donor, $f_D(\nu)$ the fluorescence spectrum of the donor and (v) is the molar extinction coefficient of the acceptor.

The cases of strong, weak and very weak coupling are therefore determined by the strength of the interaction energy. They may be identified spectroscopically by changes in the absorption spectra resulting from changes in the localization of the electronic excitation.

In the strong coupling case since the excitation is shared by the donor and acceptor molecules, major changes in the absorption spectra are found. In addition the

transfer rate is temperature independent since the interaction energy is larger than kT. The transfer rate is also directly proportional to the interaction energy and can be as high as (Barber, 1977) 10^{15} sec^{-1}.

In the weak coupling case minor changes in the absorption spectra characterize the fact that the excitations are localized to the individual molecules, generally maintaining the vibrational energy band structure of the individual molecules. Since the wavelength of the exciting light determines the vibrational level of the donor molecule that will be involved in the transfer, the transfer rate should be dependent on the wavelength of excitation, and can range from 10^{11} - 10^{13} sec^{-1}.

In the very weak coupling case the excitation is completely localized to the individual molecules and no changes in the absorption spectra are found since the de-excitation of the donor is from the lowest vibrational state and thus determines the transfer energy exactly. The rate here is proportional to u^2 and is about 10^{11} sec^{-1}. The strong dependence of the transfer rate on the interaction energy for the three cases outlined above can be clearly seen in Fig. 3.1.

With specific reference to photosynthesis, since the absorption spectrum of Chl. a does not differ significantly in the in vivo and in vitro state, the strong interaction case may be ruled out. In addition

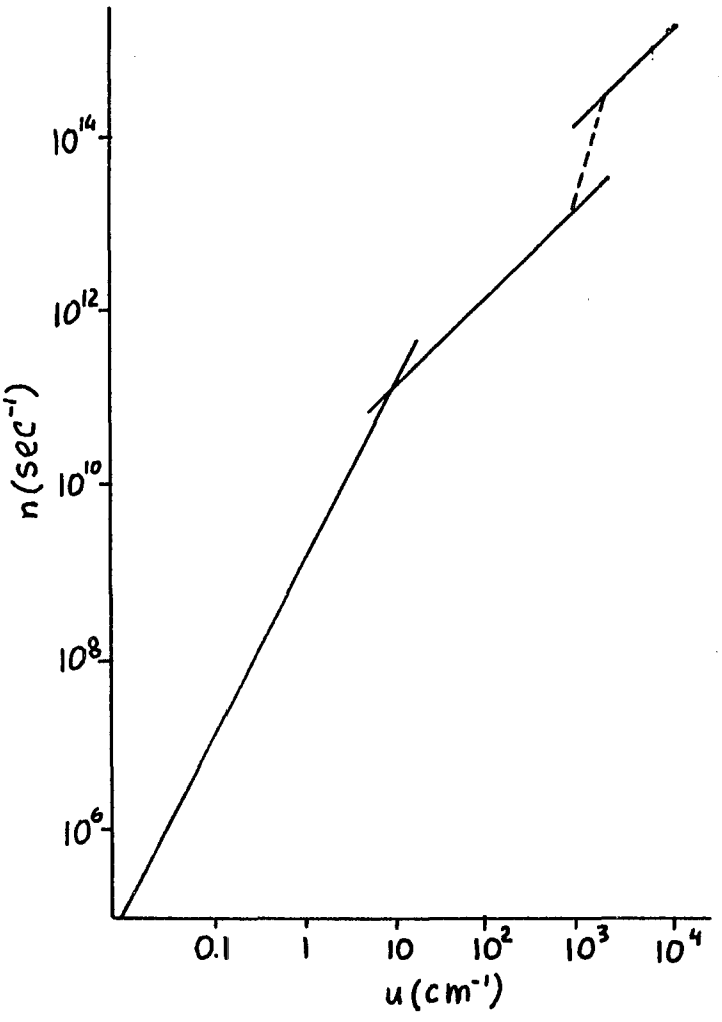

Fig. 3.1 Dependence of Forster transfer rate on the interaction energy.

Rabinowitch (1959) has pointed out that the existence of strongly coupled crystalline states *in vivo* is doubtful since an *in vivo* crystalline type spectra for Chl. *a* is not observed.

Further insight as to which case is applicable to the photosynthetic system can be inferred by calculating the upper limits for the interaction distance as a function of the interaction energy by considering the Robinson calculation for the momentum in a molecular crystal lattice (Robinson, 1967). With this method upper limits of 55 A and 175 A can be obtained for the lattice spacing of a PSU from interaction energies of 10 cm^{-1} and 1 cm^{-1} respectively. Similarly by considering the dipole-dipole interaction energy and relating the transition moment to the Einstein coefficient for spontaneous emission and the natural radiative lifetime, Forster obtained 31 A and 67 A for interaction energies of 10 cm^{-1} and 1 cm^{-1} respectively. Thus intermolecular distances $<$ 31 A would imply the applicability of the weak coupling case. It is interesting to compare these results with the estimates of actual intermolecular distances based on structural arguments which give an upper limit (Barber, 1978) of 17 A . Thus the weak coupling case would appear to be favored in photosynthesis.

Although small inter-chlorophyll distances can lead to efficient energy transfer, distances that are too small can give rise to the formation of coupled molecules or

excimers which can interfere with efficient transfer. Barber has pointed out that little energy transfer occurs at Chl. a concentrations comparable to those that exist in the PSU, whether the molecules are in liquid solution, solid monolayers, or lipid vesicles (Barber et al., 1977). In light of this evidence the efficient energy transfer occurring in the PSU at these high concentrations cannot be easily explained, and further studies such as on the orientational depolarization from adjacent pigment molecules are needed to more fully understand the primary energy transfer process.

3.2 Random Walk, Diffusion and the Master Equation Approach

Exciton energy transfer in the Forster theory can be equivalently analyzed by either a random walk, exciton diffusion or master equation formalism which can be shown to be interchangeable in the description for exciton energy migration on a lattice.

3.2.1 Random Walk

Montroll (1969) formulated the random walk problem for the PSU by considering a unit cell of N elements with (N-1) elements consisting of chlorophyll molecules and the remaining element acting as a trap. The problem was then formulated by the question, "how many steps must be taken by the exciton in a random walk before it is trapped." Considering only nearest neighbor interactions he obtained the average number of steps required for trapping on a

square lattice of N molecules as,

$$\langle n \rangle = \frac{1}{\pi} N \ln N + 0.1951 N .$$

Using a similar expression derived by Knox (1968), Barber (1977) calculated a trapping time of 344 ps for a PSU consisting of 300 randomly aligned chlorophyll molecules separated by 15 A in the very weak Forster coupling case. However Knox (1975) has pointed out that the trapping time can vary by a factor of 24 depending on the orientation assumed for the Chl. a dipole moments, and by a factor of 96 if monopole coupling is present. Therefore the assumption of random alignment of chlorophyll molecules is a rather strong one and must be carefully considered in light of the high chlorophyll concentrations present in the photosystems.

The specific location of the trap with respect to bulk pigments is not critical to the energy transfer rate. Trap locations at the center of the ensemble of chlorophyll molecules constituting the unit cell give rise to a trapping rate that is only half as large as the trapping rate obtained if the trap is located on the periphery of the unit cell (Bay and Pearlstein, 1963). If instead of a square lattice we consider a linear chain arrangement, then the number of steps that are involved in the random walk from the initially excited molecule to the trap (Montroll, 1969; Pearlstein, 1967; Knox, 1968) is

proportional to N^2 and for a cubic lattice it is proportional to N.

3.2.2. Exciton Diffusion

In 1963 Bay and Pearlstein (1963) formulated a theory of energy transfer in the photosynthetic unit which gave rise to an equation for energy migration formally identical to the classical diffusion equation. Using the Forster theory for the case of weak coupling and considering only nearest neighbor interactions they obtained,

$$\left(\frac{\partial}{\partial t} + \frac{1}{\tilde{\tau}} \right) p(r,t) = D \nabla^2 p(r,t)$$

where p is an excitation probability density, $\tilde{\tau}$, is the excitation decay time constant and D is the diffusion constant (For completeness both a source term and a trapping term can be included). The probability of excitation of the molecule at time t is given by,

$$P(t) = \int p(r,t)\, dV$$

and the de-excitation time of the ensemble of molecules in Volume V is,

$$\bar{t} = \int_0^\infty P(t)\, dt \ .$$

Using this model Bay and Pearlstein found that the number

of jumps, n, before the energy is trapped depends on the number of dimensions and the number of nearest neighbors. Thus the trapping time can be related to the random walk model through,

$$\bar{t}_t = nt_1/B$$

where t_1 is the pair-wise transfer time, B the number of nearest neighbors and n the number of jumps required to reach the trap. The diffusion constant obtained for a 3- dimensional spherical model with central trap is,

$$D = R^2/t_1$$

with R the mean separation of adjacent Chl. a molecules. Since t_1 is obtained in the Forster theory as

$$t_1 = \tilde{\tau}_o \left(\frac{R}{R_o}\right)^6 ,$$

by measuring the fluorescence decay time ($t_f = t_t$) one can estimate the number of jumps to the trap and the energy of interaction ($n = B \quad t_f / t_1$).

According to the Bay Pearlstein model, the quantasome unit contains 400 chlorophyll molecules, assumed to be spaced on a square or cubic lattice with a spacing of 11 A or 17 A respectively. Under conditions of irreversible traps, reversible transfer among the pigment molecules,

uniform excitation of the unit, and random alignment of the molecules ($k^2 = 2/3$), by using a set of master equations with Forster pairwise jump times of 0.3 ps for the 2-D square lattice and 4 ps for the 3-D cubic lattice, they obtained an average trapping time of 40 ps and 90 ps for the two and three dimensional case, respectively.

Similarly, by using a value of R_o of 60 - 70 A, (obtained from concentration quenching experiments), a nearest neighbor number B = 6 (for the hexagonal porphyrin structure of chlorophyll), and a nearest neighbor distance of 18 A for PS I and 23 A for PS II, a trapping time of 60 ps for PS I and 200 ps for PS II is obtained from the Bay Pearlstein model.

Picosecond fluorescence kinetic measurements can be used to obtain an estimate of the pairwise transfer time or the number of transfers required for trapping in a photosynthetic unit when an appropriate model is assumed from which the nearest neighbor number can be obtained. Measurement of the fluorescence risetime of the acceptor can in addition provide for the direct measurement of the energy transfer time from donor to acceptor in a sensitized fluorescence kinetic measurement. The time resolved spectra at t = 0 (i.e. within the resolution time of the experimental detection apparatus) can give information on the initial excited state distribution, while the time resolved fluorescence spectra directly probes the decay and build up of the participating

components in the energy transfer process.

3.2.3 Master Equation

The master equation approach extends the simple diffusion theory to a more generalized formulation which takes into account all molecular decay transfer pathways in determining the time dependence of the de-excitation. In a matrix formulation where intermolecular transfers are represented by off diagonal matrix elements, G_{ij} $i \neq j$, while the diagonal elements represent unimolecular decay rates, the equations take the form:

$$\frac{\partial p_i}{\partial t} = - \sum_{j=1}^{N} G_{ij} p_j + E_i$$

where E_i is a source excitation term for molecule i and p_i is the probability that molecule i is excited (Knox, 1975; Pearlstein, 1972; Hemenger et al., 1972).

A solution for the quantum yield using this approach is given by (Campillo and Shapiro, 1977)

$$\phi_f = \sum_{j=1}^{N} \sum_{k=1}^{N} \frac{1}{\tau_{oj}} (G^{-1})_{jk} f_k \quad ,$$

where f_k is the fraction of light absorbed by molecule k, and τ_{oj} is the natural radiative lifetime of molecule j. Swenberg et al., (1976) have shown that this fluorescence yield can vary by a factor of 10 as the Chl. b concentration increases from 0% to 50% (assuming a nearest neighbor transfer rate of 10^{12} sec^{-1}).

3.3 Exciton Percolation Theory

The efficient directed migration of excitons among molecules in a mixed disordered crystal is called exciton percolation (Kopelman, 1976a; Shante and Kirkpatrick, 1971). An exciton consists of an excited electron and a positively charged hole which move together from one molecule to another as a directed energy package without actual charge separation. The components of the disordered molecular crystal which make up the roadway for the traveling exciton consist of an exciton conducting lattice, A, called the guest lattice, an exciton insulating lattice, B, called the host lattice and some traps. The singlet energy level S_1 of the insulating lattice B is assumed to be much higher than the singlet energy level of the conducting lattice A. The trap level however is lower in energy than the conducting lattice, and the exciton energy can be readily transferred to the trap molecules with finite trapping efficiency. The exciton travels along the guest lattice, with the host molecules acting as obstacles to the exciton exchange, possibly even caging the exciton, while the trap acts as a sink. The exciton thus rapidly visits various sites during its lifetime which results in its eventually being trapped. Since the host molecules act as obstacles to the exciton pairwise transfer, random diffusional transfer is not truly active. In addition, at high exciton densities, exciton-exciton interactions such as annihilation

processes can also occur.

Kopelman proposed exciton percolation as a model for energy transfer in photosynthesis by considering the accessory pigment molecules consisting of the carotenoids and Chl. b to act as the insulating lattice for the lower lying energy levels of Chl. a molecules in the conducting lattice. The excited state energy difference between Chl. b and Chl. a is 0.07 eV, giving a Chl. b to Chl. a transfer approximately 20 times more probable than a Chl. a to Chl. b transfer (Knox, 1977). The excitation energy can thus migrate in the Chl. a lattice directed by Chl. b insulating molecules until it is trapped by the specialized reaction center or trap. The transfer is therefore not indescriminate but must proceed by homogeneous transfer from Chl. a molecule to Chl. a molecule.

Exciton percolation or efficient migration requires an effectively connected conducting lattice. The problem of the dynamic percolation of energy among the conductors, insulators and traps can be formulated in terms of the static properties of the conducting lattice alone. In particular, the probability, p, that any site of the conducting lattice belongs to an infinite conductive cluster can be described in terms of an order parameter of that cluster, such as the concentration. Although this probability is apparently zero when the conducting lattice concentration is zero, and unity when the conducting

lattice concentration is unity, Kopelman (1976b) has found that the probability is also nearly unity for an infinite lattice whose guest concentration is 0.59, for a square lattice, and 0.31 for a simple cubic lattice. At these critical concentrations the guest lattice is effectively connected and there is a sudden increase in the probability of exciton migration, and consequently trapping on the guest lattice through the formation of directed as opposed to random pathways to the trap.

In photosynthesis the guest or chlorophyll a concentration in a two dimensional case must therefore be greater than 0.6 in order to achieve efficient trapping. Since the guest and host concentration must necessarily sum to 1.0 , the trap concentration being negligible (of the order of 0.01 or smaller), we find that the guest to host ratio or equivalently the Chl. a/ Chl. b ratio for efficient trapping must be greater than 0.6/0.4 = 1.5. This is consistent with the concentrations present in photosynthetic systems outlined in Table 3.1.

Table 3.1

System	Chl.a	Chl.b	Chl. a / Chl. b
PS I	85 uM	15 uM	5.7
PS II	67	33	2
chloroplast	70	30	2.3

Ref. "In vivo chlorophyll concentrations", J. P. Thornber Ann. Rev. Plant Physiol. 26, 127-58 (1975))

As the guest to host concentration is higher in PS I than in PS II, one would expect that exciton migration is more efficient in PS I. This may partially account for the fact that the quantum yield of PS I is smaller than that of PS II by a factor of $\sim$ 5 at room temperature.

The advantage to green plants in the use of percolation transfer as opposed to a "funnel" transfer (through Chl. b - Chl. a layers), lies in the random substitution requirement of the former as opposed to the perfect structure requirement of the latter. Since the random substitution model of percolation is not seriously affected by the presence of impurities, it may have been consequently favored on an evolutionary basis. In addition the process of exciton energy spillover can more easily be accomodated in the random substitution model as opposed to the funnel model (Kopelman, 1976c), as the latter requires two separately directed funneling networks for PS I and PS II.

CHAPTER 4. History of Time Resolved Fluorescence Spectroscopy in Photosynthesis

The history of time resolved fluorescence spectroscopy in photosynthesis has been integrally related to the history of technological advances in the field of light pulse generation and temporal resolution techniques. This intrinsic relationship between discovery and technological advancement arises from the fundamental nature of the scientific process which demands that the experimental conditions of excitation and measurement be always more accurately defined. The development in the late 1960's of mode locked lasers capable of generating ultrashort pulses of picosecond (10^{-12} sec) duration at well defined regions of the spectrum, and the subsequent introduction of comparable time resolution techniques ushered in a new era of scientific discovery. At last a means for exciting and probing a system on a time scale of physical interest comparable to molecular vibrational and rotational deexcitation was available. Picosecond time resolved fluorescence spectroscopy can be used to follow energy transfer from donor to acceptor in sensitized fluorescence kinetic measurements by directly measuring the decay time of the donor and the rise time of the acceptor. In addition, picosecond fluorescence polarization measurements can give information on the orientational order of the pigment molecules with respect to each other.

If scientific investigation were not limited by quantum mechanical restrictions, the quest for understanding nature's basic processes would someday be rewarded by the ability to observe physical processes in detail in their natural state. In photosynthesis the scenario for this event would begin with the observation of the absorption of a single quantum of light, as it strikes the outer surface of a leaf at a typical radiant flux density of 10^{16}-10^{17} visible quanta per sec per cm^2, the incident solar flux at the earth's surface at noontime. The initial absorption would most likely take place in the accessory pigment complex composed of carotenoids, chlorophyll b (Chl. b) and chlorophyll a (Chl. a) in green plants or phycobiliprotein pigment complexes in the red or blue green algaes. The molecular structure of the excited pigment complex would subsequently search out modes of deexcitation leading to molecular stability consistent with the structural and energy gradients present in the immediate domain of exciton interaction.

Molecular deexcitation can either proceed through nonradiative internal decay in the vibrational rotational manifold, or be transferred by inter system crossing from the lowest excited singlet state to a triplet state. Other processes contributing to the relaxation might involve second order processes of excited state annihilation between two singlet excitations or

singlet-triplet exciton annihilation. Inter-molecular energy transfer between the singlet states of like molecules (homogeneous transfer) or the singlet states of unlike molecules (heterogeneous transfer) could also contribute to this relaxation.

In the crowded accessory pigment system the exciton might very well visit many molecular sites during its lifetime before becoming hopelessly trapped in a low lying state of a reaction center molecule where the energy might be photochemically converted or diverted to a radiationless trapping site where it may undergo a biologically wasteful deexcitation. Throughout its migration the exciton is also subject to a radiative decay probability in the form of fluorescence, again a wasteful process from the biological point of view.

Possible energy transfer mechanisms which consider interaction between two molecules involve either a mass motion mechanism, such as in electron transfer or collision, or electromagnetic coupling, as in the radiative or resonance transfer process. Studies of Chl. a in solution at the concentrations present in the photosynthetic unit (PSU), where the inter-chromophore separation is estimated at 11-17 Å (Thomas et al., 1956; Colbow, 1973; Bay and Pearlstein, 1963) have shown that little energy transfer occurs at these high concentrations (Beddard and Porter, 1976). Chlorophyll excimer formations apparently act as strong quenchers of the

excitation at these high concentrations, allowing the energy to be transferred among chromophore molecules only at lower inter-chromophore separations (Trosper et al., 1968). The fate of the absorbed photon must therefore necessarily depend on such factors as the excited state population of the donor, the spacing between molecules, the relative angles between the absorption and emission dipole of the acceptor and donor molecules respectively, as well as the overlap between the absorption spectra of the acceptor and the emission spectra of the donor (Forster, 1948).

Exciton energy migration in the photosynthetic pigment complex has been described by a variety of physical models which have taken the theoretical constructs of random walk theory (Montroll, 1969; Robinson, 1967), diffusion (Bay and Pearlstein, 1963), and exciton percolation (Kopelman, 1976 a,b,c). These models have recently been applied to the physical structures present in photosynthetic systems.

From the very first experimental observation of the role of sunlight in photosynthesis by Jon Ingenhousz (Rabinowitch and Govindjee, 1969), that very component which forms the driving force of photosynthesis, light, has been of invaluable assistance in probing the physical nature of the process. Ingenhousz published his findings on "the influence of the light of the sun upon the plant" in 1779, three years after Joseph Priestley's treatise on the "improvement of air by plants", which formed the

foundation for the understanding of the photosynthetic process. Since then countless experiments have sought to unravel the energy transfer kinetics which occur in this all important process.

The overall temporal evolution of the fluorescence emission from photosynthetic systems posesses an interesting characteristic behavior. The range of the emission spans a time scale which begins with the ultrafast absorption process (10^{-15} sec) to the slow decay of delayed emission which lasts for many minutes subsequent to excitation (Strehler and Arnold, 1951; Lavorel, 1975; Malkin, 1977).

To place the fluorescence kinetics from the primary process in its proper time perspective relative to the total fluorescent emission from the photosynthetic system, it is important to keep in mind that the fluorescence emission is a measure of the total depletion of the first excited singlet state population and is influenced by the state of the reaction center traps and the aggregation and orientational relationship of the pigment molecules in the photosystem.

The overall temporal behavior of the relative fluorescence intensity in green plants and algae subsequent to excitation follows an initial Onset (O), followed by a steep Increase (I), then a slight Dip (D) appears in the fluorescence emission and is subsequently followed by a slower increase to the Peak (P) of the

emission, which occurs approximately 0.4 sec subsequent to excitation. A gradual decline of the fluorescence to the Steady (S) state level occurs, and the emission rises to a Maximum (M) before decaying to a final Terminal (T) steady state level. (Murakami et al., 1975). These events are depicted in Fig. 4.1.

Primary photochemistry is reflected only in the initial fluorescence emission, (i.e. the "O" level in Fig. 4.1). The maximal limiting time for the primary photosynthetic process must necessarily be that time at which the excitation energy has been completely dissipated in the structural framework of the photosystem, which we can take to be the time associated with the natural radiative lifetime that measures the unimolecular fluorescence decay in the absence of all other excitation decay mechanisms. For the primary pigment, chlorophyll a, the natural radiative lifetime was calculated by Brody and Rabinowitch (1957) from the area under the absorption curve to be 15.2 ns. The measured fluorescence lifetime of Chl. a however is $\sim$ 5 ns, indicative of a fluorescence quantum yield of $\sim$ 33% ($\phi = \tilde{\tau} / \tilde{\tau}_o$). Thus in primary photosynthesis we shall be concerned only with the time regime from initial absorption (10^{-15} sec) of the excitation energy to the time at which it has finally decayed by the slowest process available to it, ($\sim 10^{-8}$ sec), the natural radiative lifetime. However, the fluorescence yield of chlorophyll a in vivo is only about

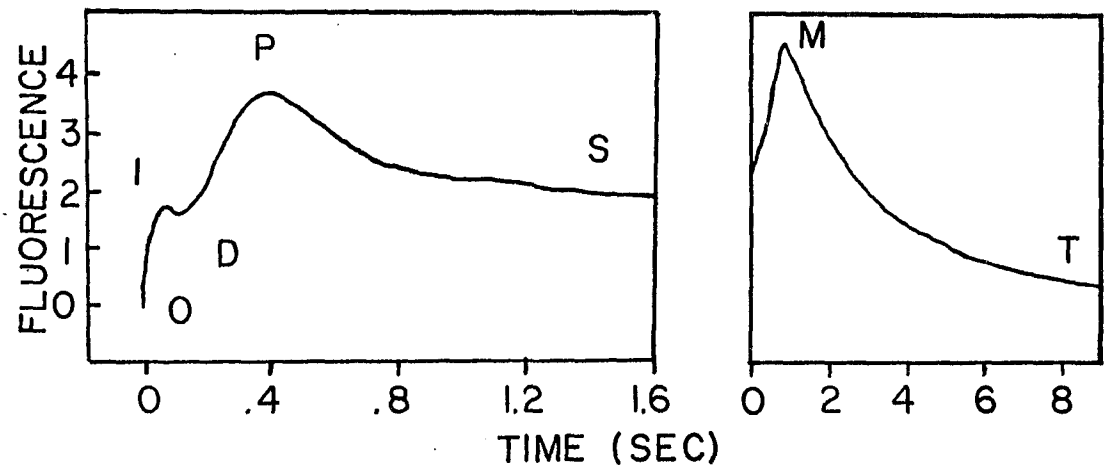

Fig. 4.1 Temporal dependence of photosynthetic fluorescence emission.

3 %, which indicates an efficient transfer of the excitation energy for photosynthetic use.

Time resolved Fluorescence Spectroscopy Techniques:

The myriad of experiments that have been performed in the primary temporal regime offer a variety of information which, like the pieces of a giant jigsaw puzzle, must be carefully mated in order to obtain an enlightening and cohesive picture of primary photosynthesis. However, the pieces that we must deal with are not privileged to sharp and well defined interpretations which give rise to a precise solution of the puzzle. On the other hand, our pieces are complicated by the fact that we are often forced to compare information which differs in such basic characteristics as sample specie investigated, sample homogeneity and cross-sectional thickness, wavelength of excitation, wavelength of observation, preparation and state of the sample, intensity of excitation, temperature etc. Thus we must be very careful in deriving our conclusions from the apparent agreement, or lack thereof, of experimental observations.

In order to fully appreciate the progress of research on primary photosynthetic fluorescence kinetics a brief description of the various experimental techniques covering the excitation and detection methods used in these investigations is presented to acquaint the reader

with some of the advantages and disadvantages of each technique. A detailed account of some picosecond experimental systems is presented in Chapter 5.

Various excitation sources are available for studying photosynthetic as well as other photobiological systems such as the visual process and DNA synthesis. These excitation sources include: the hydrogen flash lamp; gas lasers such as the He-Ne, Krypton ion, Argon and Nitrogen laser; solid state lasers such as the Nd:glass, Nd:Yag and ruby laser; and dye lasers which offer the advantage of wavelength tunability, high repetition rate and short pulse duration. The excitation source can be characterized by a description of the wavelength and spectral bandwidth of the source, the energy, pulse width (generally FWHM) and pulse intensity profile. These characteristics are generally quite different for the excitation sources cited above and generally cannot be duplicated by any two such sources. Therefore each experiment is distinguished unequivocably by the excitation source used.

For purposes of biological investigation, it is important to consider the effective photobiological cross section that is active during the time period of observation. Some of the factors which must be considered include: 1)The photorecovery of the system at the photon flux of the excitation source. 2) The effective local absorption of the fluorescing specie at the wavelength of

excitation. 3) The possibility of multi-photon processes occurring during absorption. 4) The formation of triplet excitations. 5) The formation of ionic species with localized conduction states, and 6) Excitonic interactions among excited state molecules.

To measure the temporal evolution of the response of the systems subsequent to excitation various techniques are currently available. In order to measure decay times on an ultrafast time scale, of the order of picoseconds, a clocking mechanism with a picosecond "gear" is needed. If it were possible to spatially sweep the fluorescent emission perpendicular to its direction of travel, we would obtain a temporal profile of the light emitting event. In terms of simple classical spatial dispersion of the emitted light we would find that in order to obtain a 10 ps resolution over a 0.001" detector resolution array located 1" away from a classical dispersing device such as a rotating mirror, the mirror would need to rotate at approximately 1.6×10^7 rev/sec, a practically unattainable, and relativistic angular rotation frequency. Thus we are naturally led to consider other techniques which either directly or indirectly map the time axis into a spatial one.

Fast photodetectors and large bandwidth oscilloscopes form by far the simplest tools capable of temporally resolving the time course of fluorescence emission. However, the temporal resolution obtainable with such

conventional devices is approximately 300 ps. Sampling oscilloscopes coupled with fast photodetectors ($\leq$50 ps risetime) can give rise to temporal resolution of a few tens of picoseconds in experiments with repetitive signals.

The earliest time resolved fluorescence techniques made use of controlled flashing light excitation, phase fluorometry and photon counting. The flash excitation method makes use of conventional photodetection temporal resolution techniques (e.g. photomultiplier and oscilloscope) and is thus limited by the response time of this equipment, typically 0.3 ns. The phase modulation technique (Bailey and Rollefson, 1953; Muller et al., 1965; Borisov and Godik, 1972a) involves exciting the sample with a light source that is modulated at a specific frequency and measuring the lag or phase delay between the excitation light and the emitted fluorescence light. The fluorescence signal is collected from the sample and compared with a reference beam from the excitation source. The phase difference between these two signals is determined by comparison with calibrated phase shifts that are electronically generated. The signal to noise ratio is enhanced by the fact that only the fluorescence signal at the modulated frequency is discriminated by the detection apparatus, thereby significantly reducing background light. Measurement of the phase angle determines the lifetime of the excited state, since the phase is related to the frequency of modulation and the

lifetime by the relationship $\tan\varphi = w\tau$.

Photon counting makes use of pulse amplitude descrimination and pulse amplification devices to detect weak photomultiplier signals. The discriminated pulses are counted electronically, and thereby constitute a measure of the emission from the sample investigated. Since photon counting makes use of photomultiplier detection directly, it is privileged to the high sensitivities available to photomultiplier detectors, and thus forms one of the most sensitive steady state detection techniques (Alfano and Ockman, 1968).

The direct measurement of fluorescence emission on a picosecond time scale can also be accomplished with a picosecond optical Kerr gate or streak camera. The picosecond optical Kerr gate operates like an ultrafast shuttering device actuated by the intense electric field of the laser pulse. This technique is described in detail in Chapter 5. When activated by intense optical pulses of picosecond duration, such as from a Nd:glass laser ($\sim$ 8 ps pulse width) a 10 ps resolution element can be selected from the fluorescent emission of the sample. The optical Kerr technique (Duguay and Hansen, 1969) allows for the sequential sampling of the decay profile from a light emitting event, which is achieved by merely delaying the arrival of the gate opening pulse relative to the portion of the decay being sampled. Since the intensity of the transmitted light is proportional to the square of the

intensity of the gate activating pulse, and since in addition laser pulse stability is not easily obtainable in high power, short pulsed lasers, extensive signal averaging and normalization is required in order to obtain a complete temporal decay profile in a Kerr gate measurement.

A streak camera with picosecond resolution provides an ideal device for the measurement of subnanosecond fluorescence kinetics. The streak camera provides a continuous and direct measurement of the temporal profile of a light emitting event ranging from a few picoseconds to several nanoseconds (Yu et al., 1977b; Pellegrino and Alfano, 1979; Shapiro et al., 1975; Harris et al., 1976).

In the streak camera, photoelectrons emitted by light striking the photocathode are deflected by an applied voltage ramp which causes the electrons to be transversely streaked across a phosphorescent screen. Photoelectrons released at a certain function of time from the photocathode will strike the phosphorescent screen at a corresponding function of position, causing a track representative of the incident fluorescence intensity temporal decay profile to be produced. The use of the streak camera in fluorescence kinetic measurements is described in Chapter 5.

The streak camera provides certain distinct advantages over the Kerr gate. In particular, the streak camera is able to obtain the entire decay in a single shot, as

opposed to the Kerr technique which provides only one point of the decay profile for a single laser shot. In addition, since the delay time in the Kerr gate is obtained by changing the optical path length of the gate activating pulse by moving a prism over a linear translation stage, the time range which can be investigated with a Kerr gate is generally limited to a few nanoseconds.

Streak cameras are also generally plagued by "jitter" which causes the sweep deflection ramp to be initiated anywhere in a window which can be as wide as 100 to 200 ps, thus hindering signal averaging of the fluorescence signal from shot to shot. Morou and Knox, (1980) have greatly reduced the jitter time by using direct optical triggering of a silicon semiconductor junction with the laser pulse itself.

Among the various other techniques which are available for displaying events as a function of time are the echelon multi-step array which utilizes a stack of glass plates with spatial steps that are separated by a few millimeters in space (or equivalently by a few ps in time). In this technique, a picosecond continuum pulse generated by self phase modulation is imaged onto an echelon array (e.g. a set of stacked plates) and the sequentially reflected or transmitted pulses form a series of interrogation pulses separated in time by the echelon step unit which is now used to probe the absorption

changes in the sample as a function of time. This technique is useful mainly in absorption measurements.

The oblique wave front scattering technique(also known as the single shot optical Kerr gate) consists of passing a picosecond laser pulse through a scattering solution. As the pulse propagates it creates scattering centers throughout its path which act as secondary sources of picosecond emission at the same wavelength. These secondary pulses are delayed relative to one another by the amount of time that is required for the generating pulse to travel from one scattering site to the next. Therefore a sequence of closely spaced pulses can be obtained which can be used to probe absorption in a sample.

Unlike the optical Kerr gate or streak camera however, the latter techniques suffer from a shorter overall temporal display range, generally greater background noise, optical distortion problems, non-uniformity of the radial beam profile in the overlap region of the pump and probe pulse, low sensitivity and the need for extensive data averaging and analysis.

Time Resolved Fluorescence Kinetic Measurements in Photosynthesis:

The picosecond fluorescence emission from photosynthetic systems is generally interpreted as indicative of the energy migration and trapping that takes

place in the photosynthetic unit (Sauer, 1975). The parameters of fluorescence emission in primary photosynthesis are therefore precisely those variables which influence the fluorescence state, the first excited singlet, both prior to and during the trapping process.

The first measurement of the fluorescence lifetime from Chl. a was obtained by Brody and Rabinowitch (1957) using nanosecond flash lamp excitation pulses and direct detection methods. Dimitrievsky et al., (1957) made indirect measurements through the use of phase fluorometry, obtaining a value of $\sim$ 1.5 ns. Subsequent measurement of the in vivo fluorescence lifetimes by Muller et al., (1969) indicated that the in vivo fluorescence lifetime was excitation intensity dependent, and the fluorescence lifetime was even shown to be dependent on photosynthetic activity (Tumerman et al., 1961). This intensity dependence of the fluorescence lifetime was later found to also occur in direct picosecond fluorescence measurements by Campillo et al., (1976b) and Mauzerall (1976).

Early measurements of fluorescence lifetimes using the phase technique developed by Bailey and Rollefson (1953) were undertaken by Murty and Rabinowitch (1965), Nicholson and Fortoul (1967), Muller et al., (1969) Tumerman and Sorokin (1967), Borisov and Godik (1972 a,b), and recently by Moya et al., 1977, where the fluorescence lifetime, measured at low light intensities, in the range

$0.001\text{-}1 J/m^2$ sec, was found to vary from 0.35 to 0.8 ns. In these measurements, the necessary assumptions of the experimental dependence of the fluorescence decay necessarily limit the interpretation of the fluorescence kinetics. Indeed, the assumption of a single exponential decay law for the in vivo fluorescence from photosynthetic systems cannot be justified in light of the possible effects from concentration quenching, different unimolecular decay rates for the various pigment components present in the photosynthetic system, and characteristic fluorescence emission from PSII and PSI as well as from the light harvesting complex (LHC). Fluorescence from non-photosynthetically active specie as well as characteristic PSU structural influences on the fluorescence lifetime must also be considered.

Merkelo et al., (1969) first introduced the use of mode-locked gas lasers to study fluorescence from photosynthetic systems by using a 0.8 ns pulse from a He:Ne laser. Both direct (photomultiplier and oscilloscope) and indirect (phase) measurement of the fluorescence emission from in vitro and in vivo samples were made. In vitro measurements of chlorophyll b (3.87 ± 0.05 ns) and phycocyanin (1.14 ± 0.01 ns) and in vivo measurements of Chl. a fluorescence from Chlorella pyrenoidosa (1.4 ± 0.05 ns) were obtained. Seibert et al., (1973) used a picosecond mode-locked solid state laser (Nd:glass) to obtain a train of $\sim$ 100 pulses at 1.06 um

which were frequency doubled to 0.53 um by the process of second harmonic generation in a potassium dihydrogen phosphate crystal (KDP) to measure the decay kinetics from escarole chloroplasts. A Duguay Hansen optical Kerr gate was used for the time resolved measurements and a lifetime of 320±50 ps for the *in vivo* Chl. *a* fluorescence from escarole chloroplasts was obtained. The experiment was later repeated in spinach chloroplasts by Seibert and Alfano in 1974, yielding a two component decay with a characteristic "dip" in the fluorescence occurring at 50 ps into the emission. This "dip" was later attributed to statistical fluctuations of the laser output as well as a possible insufficient number of data points in that region, and did not show up in later measurements. Two maxima were observed in the fluorescence emission, one at 15 ps and the other at 90 ps. From their measurements Seibert and Alfano (1974) attributed a lifetime of 10 ps to the PS I emission component and a lifetime of 210 ps to the PS II emission component. The 90 ps delay in the appearance of the second peak was attributed to possible energy transfer from carotenoids to PS II.

Subsequent experiments by the same group (Yu et al., 1975a) in isolated PSI and PSII enriched preparations of spinach chloroplast confirmed the dual exponential nature of the decay and in particular identified the fast emission component (60 ps) with emission from PSI and the slow (200 ps) emission as arising from PSII. These

results were repeated in intact chloroplast preparation from spinach (Yu et al., 1977a) and again verified the presence of a two component fluorescence decay at room temperature and 685 nm, of 56 ps and 220 ps nearly identical in value to their previously reported results in enriched PSI and PSII preparation of spinach chloroplast (Yu et al., 1975a). At room temperature the 730 nm fluorescence was found to decay as a single exponential with a lifetime of 100 ps. The risetime of the 730 nm emission at 90 ^{o} K was measured to be 13 ps. These experiments were carried out at an intensity of $2x10^{14}$ photons/cm^2 per pulse, with 530 nm pulse train excitation and Kerr gate time resolution apparatus. The spectral and temperature characteristics of the t=0 emission from spinach chloroplasts was reported by Yu et al., (1977a) and Pellegrino et al., (1978), and is discussed later on in this chapter.

The streak camera detection technique, with its simplicity of operation, and capability of obtaining the complete fluorescence decay measurement in a single shot, facilitated the investigation of fluorescence measurements from photosynthetic systems. Paschenko et al., (1975) measured the fluorescence emission from one pulse in a train of exciting pulses at an intensity of $3x10^{14}$ photons/cm^2 per pulse using a streak camera and ruby laser excitation and reported the observation of a three component decay for green pea chloroplasts with lifetimes

of 80 ps (wavelength of observation greater than 730 nm) which was attributed to PSI fluorescence, 300 ps (wavelength of observation greater than 650 nm) which was attributed to PSII fluorescence and a very long component of 4500 ps attributed to fluorescence from chlorophyll pigments not involved in photosynthesis. Borisov and Il'ina (1973) had estimated the lifetime for PSI from pea subchloroplast particles to be $\leq$ 30 ps by use of phase fluorometry.

For PS II fluorescence, Muller et al., (1969) initially reported lifetimes of 380 ps through phase fluorometry measurements while a value of 700 $\pm$ 200 ps using the nanosecond flash lamp method had been reported by Singhal and Rabinowitch (1969). Kollman et al. (1975) and Shapiro et al., (1975) have used streak camera detection and picosecond pulse train excitation from a Nd:glass laser to measure Chl. a fluorescence from Chlorella pyrenoidosa and Anacystis nidulans, reporting lifetimes as short as 75 ps (for wavelength of observation greater than 640 nm) for Anacystis nidulans and 41 ps (for wavelength of observation greater than 640 nm) for Chlorella pyrenoidosa. These low values of fluorescence lifetime were attributed to concentration quenching, since comparable lifetimes were obtained in concentrated solutions of Chl. a and Chl. b in chloroform. A similar experiment performed by Beddard et al., (1975) again using picosecond pulse train excitation with an intensity of

$5x10^{14}$ photons/pulse reported short lifetime of 134 ps (wavelength of observation greater than 580 nm) for Chl. a fluorescence from spinach chloroplasts and 108 ps for Chlorella and 92 ps for Porphyridium cruentum, in general agreement with the lifetimes reported by Kollman et al., (1975). However, even though Beddard et al., (1975) varied the excitation intensity by a factor of ten in their measurement of the fluorescence lifetime from Porphyridium cruentum they did not observe a change in the lifetime. Indeed most experiments using picosecond pulse train excitation performed during this period appeared to result in anomolously fast lifetimes, and the picosecond fluorescence lifetime measurements generally seemed to result in faster values than those obtained earlier with the use of conventional techniques. These fast lifetimes were later attributed to annihilation effects.

For dark adapted Chlorella, Harris et al., (1976) measured a double component decay of 32 ps and 90 ps at room temperature and with pulse train excitation of 10^{15} photons/cm^2 per pulse. At low intensity ($\sim 10^{14}$ photons/cm^2 per pulse) and also under various experimental conditions , it was found that the decay could be well described by a $t^{1/2}$ time dependence. Recent measurements by Beddard et al., (1979) however have characterized the fluorescence decay from spinach chloroplasts at room temperature as a double exponential, a short component of 410 ps and a long component of

1.4 ns were reported. These measurements were obtained with mode locked dye laser excitation and the use of a photon counting apparatus. Searle et al., (1979) have also recently analyzed their results in terms of a dual exponential component. It is interesting to compare the findings of Beddard et al., (1979) with the results of Moya (1974) and Moya et al., (1979) who reported a lifetime change from 0.4 to 1.4 ns upon addition of DCMU to chloroplasts in order to close the reaction center traps of PS II. It would appear that by simple analogy one could associate the short component measured by Beddard et al., (1979) with photochemical trapping, and the long component as representing general exciton diffusion in the photosynthetic membrane.

The question as to whether photosynthetic fluorescence emission can be interpreted in terms of a double exponential or in terms of a $t^{1/2}$ dependence is a subject of some controversy. Generally speaking, although an exponential decay, a $t^{1/2}$ and a $t^{1/3}$ time dependence can be easily distinguished theoretically, (see Fig. 4.2), in practice fluorescence kinetic data obtained at low excitation intensity appears to be most readily described by a simple exponential decay. A random diffusion of the excitation energy in a three dimensional system via Forster energy transfer mechanism does indeed predict a $t^{1/2}$ time behaviour, however it is generally agreed that the photosynthetic apparatus is best described

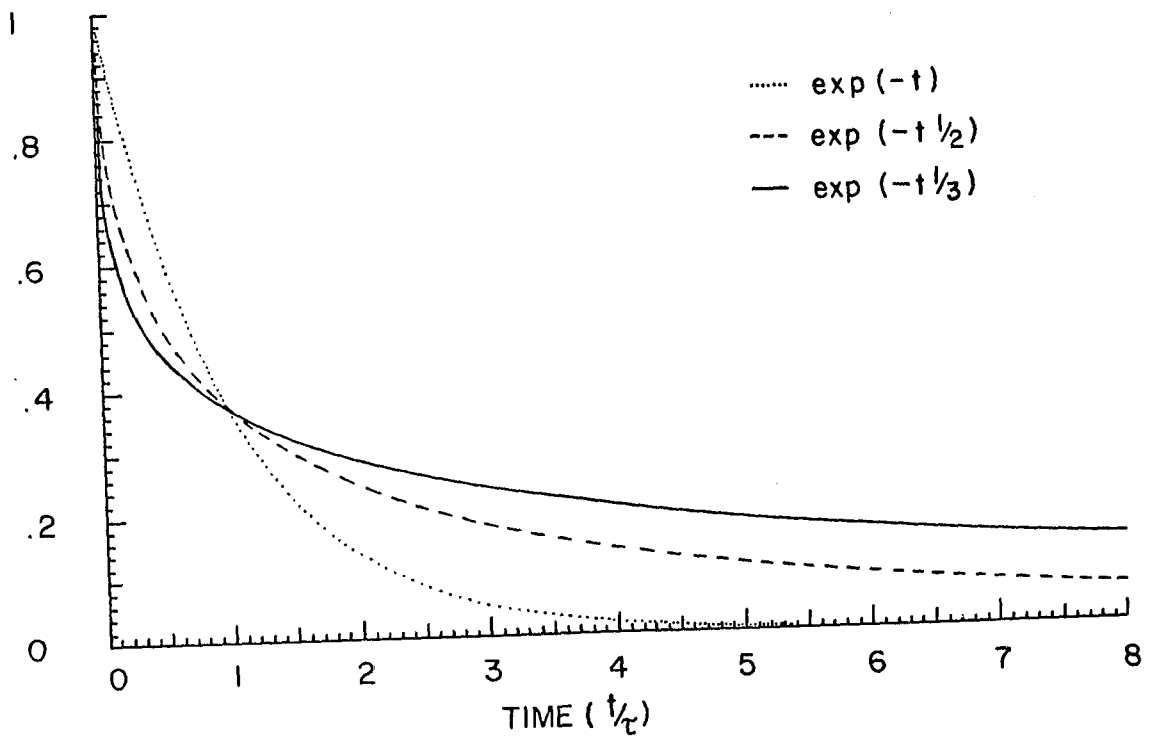

Fig. 4.2 Exponential: (t/τ), $(t/\tau)^{1/2}$ and $(t/\tau)^{1/3}$ dependence.

by a two dimensional model (Paillotin et al., 1979), and in this case a $t^{1/3}$ dependence holds for Forster energy transfer (Nakashima and Yoshihara, 1980).

The experiments of Mauzerall (1976) and Campillo et al., (1976b) gave a first clue to the possible reason for the observed short lifetimes by presenting a clear indication of the effect of excitation pulse intensity on the fluorescence yield and lifetime in photosynthetic systems. These observations led to a greater awareness of the multiple excitation problem and exciton interactions arising from both picosecond pulse train excitation and high intensity single picosecond pulse excitation. The possibility of creating long-lived triplet states or ionic species from laser pulse train excitation was now clearly recognized as affecting the results of measurements of the prompt fluorescence.

Mauzerall's (1976) observed decrease in the fluorescence quantum yield of Chlorella with increasing excitation intensity from a 7 ns pump pulse was interpreted in terms of a Poisson statistical theory governing the distribution of excitations in the PSU. However, for the case of closed reaction center traps, 20 % of the fluorescence quantum yield appeared to be unaffected by quenching. These results were verified for single picosecond pulse excitations by Campillo et al., (1976a) who showed the onset of a similar decrease in the fluorescence quantum yield of Chlorella at an excitation

intensity of approximately 10^{13} photons/cm^2 per pulse. This quenching of the fluorescence from multiple excitations reflects the inability of the photosynthetic domain to appropriately make use of or efficiently transfer excitations above a certain threshold value.

The fluorescence quenching of the quantum yield under single pulse excitation probing singlet-singlet interactions and microsecond pulse excitation probing singlet-triplet interactions was investigated by Geacintov et al., (1977 a,b). In addition, Breton and Geacintov (1976) and Geacintov and Breton (1977) made a thorough investigation of the effect of excitation intensity on the fluorescence yield in spinach chloroplasts, at both room temperature and 100K. A decrease in both the 685 nm and 735 nm fluorescence yield at 100K was observed subsequent to exposure to an increasing number of 10 ps pulses spaced 5 ns apart from a dye laser with output wavelength of 610 nm. When a whole train of pulses ($\sim$300) was used for excitation, it was found that the low temperature (100K) 735 nm fluorescence begins to quench at an intensity of 10^{15} photons/cm^2 for the whole pulse train, while the 685 nm fluorescence quenches at an intensity which is at least a factor of ten higher. For single pulse excitation however, both wavelength component emissions were found to quench in a similar manner, and the quenching of the room temperature fluorescence at 685 nm subsequent to exposure to multiple excitation pulses at 610 nm was found to be

less pronounced than at low temperature. Geacintov et al., (1977) also observed quenching of the fluorescence lifetime from spinach chloroplast at low temperature (77K). Although the lifetime shortening for the 690 nm component qualitatively followed their observed quantum yield decrease , the lifetime of the 735 nm component appeared to be intensity independent (for the two excitation intensities used) even though the 735 nm yield curve showed a marked decrease over this range of intensities. Since annhilation was found to commence subsequent to excitation by the sixth pulse in their pulse train of 610 nm picosecond laser pulses, and since the fluorescence quenching was attributed to the presence of triplets, they additionally were able to deduce that the triplet diffusion time in PS I was on the order of 50 ns. Porter et al., (1977) also have observed singlet-triplet quenching of fluorescence from Chlorella subsequent to excitation from multiple picosecond laser pulses.

Recently Breton et al., (1980) have shown that for pulse train excitation, the creation of ionic species is negligible, and in addition the fluorescence quenching is sensitive to the presence of oxygen. From these observations they have attributed the quenching effects to the formation of triplet excitations from prior pulses in the pulse train. Mathis et al., (1979) have also recently shown that carotenoid triplets can act as fluorescence quenchers in both whole chloroplasts and PS I, PS II and

LHC preparations of spinach chloroplasts. Breton et al., (1980) also measured the onset of triplet fluorescence quenching in spinach chloroplasts and a light harvesting chlorophyll protein complex (LHCP) containing 3 Chl. a, 3 Chl. b and one carotenoid molecule, isolated by SDS solubilization and polyacrilamide gel electrophoresis. A Poisson statistical behaviour of the fluorescence intensity as a function of excitation intensity was observed consistent with the smaller domain size present in the complex particle. As expected from the the smaller number of accessory pigment molecules present in the complex particle as opposed to whole chloroplasts, quenching in whole chloroplasts was found to occur at an excitation energy a factor of 100 lower than the complex particle.

Singlet-singlet annihilation and its effect on the fluorescence lifetime was directly demonstrated by Campillo et al., (1976b), who measured 1/e point lifetimes at a wavelength of 700 nm for Chlorella pyrenoidosa of 50 ps, 175 ps and 375 ps for single (20 ps) pulse excitation intensities of $3x10^{15}$, $3x10^{14}$ and 10^{14} photons/cm^2 per pulse respectively.

Searle et al., (1977) have measured the fluorescence lifetime in PSI and PSII preparations of spinach chloroplasts with single picosecond pulse excitation. The PSI fluorescence was found to be intensity independent over the range from $5x10^{13}$ to 10^{16} photons/cm^2 at

room temperature, with a 1/e time of 100 ps ($\lambda \geq 650$ nm). The PSII fluorescence however was found to be intensity dependent with a 1/e time of 500 ps ($\lambda \geq 650$ nm), for measurements in the range 5×10^{13} to 10^{14} photons/cm^2 per pulse, decreasing to 150 ps at the higher intensities of 5×10^{15} to 10^{16} photons/cm^2 per pulse. An increase in the PSI fluorescence to 1.90 ns at 77K and 5×10^{13} photons/cm^2 excitation was measured for wavelengths greater than 700 nm. The PSII low temperature lifetime was measured to be 2.47 ns ($\lambda \geq 650$ nm).

The interpretation of the fluorescence quenching in terms of exciton annihilation introduces a mechanism which is independent of the photosynthetic activity state of the system but is dependent on the existence of closely spaced excitations. A theoretical study of singlet-singlet and singlet-triplet annihilation has been made by Breton et al., (1980). Swenberg et al., (1976) have obtained an expression for the fluorescence quantum yield dependence on the intensity given by,

$$\phi = (2k/\Gamma I) \quad \log (1 + I (\Gamma /2k))$$

where k is the inverse of the fluorescence lifetime, I is the intensity of excitation and Γ is the singlet-singlet annihilation parameter related to the singlet-singlet annihilation coefficient γ_{ss}. This equation has been used to fit the fluorescence quantum yield measurements both in spinach chloroplasts (Geacintov et al., 1977) and

phycobilisomes (Pellegrino et al., 1981) as well as isolated phycobiliproteins from Nostoc sp. (Wong et al., 1981). Paillotin et al., (1979 a,b) have considered a more general approach and have developed a model for exciton annihilation which encompasses the descriptions proposed by Mauzerall (1976) and Swenberg et al., (1976) as special cases. This model is found to be supportive of the "lake" description of energy migration in photosynthetic systems.

Exciton annihilation has also been investigated in organic and inorganic systems. Excitons in organic molecular crystals may undergo similar interactions as excitons in the photosynthetic unit (Knox, 1975). An extraordinary variety of excitonic interactions have been measured in aromatic hydrocarbons such as tetracene (Arnold et al., 1976; Swenberg and Stack, 1968; Geacintov et al., 1969). Indeed a theory describing the efficient directed migration or "percolation" of excitons among molecules in a mixed crystal has been proposed by Kopelman (1976a, b), and indeed it may prove interesting to probe energy transfer in photosynthetic systems by modeling energy transfer in parallel artificial systems.

The exciton annihilation phenomenon can be divided into two basic categories when applied to photosynthetic systems, namely singlet-singlet and singlet-triplet annihilation, which can contribute to a decrease of the excited state population, and shorten the fluorescence

lifetime and fluorescence quantum yield. Since the build up of a sufficient triplet population usually requires several nanoseconds, singlet-triplet annihilation is expected to occur only during multiple pulse excitation with pulse spacing of several nanoseconds. Singlet-singlet annihilation on the other hand depends solely on the singlet state population and is thus dependent on the intensity of the excitation pulse. The role of triplets in quenching of the fluorescence was first noted by Breton and Roux (1975).

Although the exciton annihilation phenomenon can be a hinderance in measurements of true in vivo kinetics, it can prove useful in revealing the structural configuration of the system investigated as well as energy transfer within the photosynthetic unit. Singlet-singlet annihilation and singlet-triplet annihilation processes reflect the density of both singlet and triplet state excitations. Systems with different structural arrangements, whether in terms of different inter-chomophore spacing or presence or absence of traps, will affect the singlet and triplet excited state population numbers and density which subsequently become reflected in the fluorescence kinetics and quantum yield measurements. Campillo et al., (1977) have used the singlet-singlet exciton annihilation process to measure topological differences in the photosynthetic units of the mutants PM-8 dpl, wild type strain 2.4.1 and a carotenoid

altered Ga mutant specie of Rhodopseudomonas spheroides. Measurement of the relative fluorescence quantum yield as a function of the intensity of excitation of a single 20 ps pulse at 530 nm revealed different quenching curves for each of these mutants. In this case the lack of reaction centers for the mutant PM-8 dpl was attributed as responsible for the earlier and stronger quenching observed for this mutant with respect to the reaction center containing wild type strain 2.4.1 and Ga mutant species. This conclusion is also supported by their measurement of a longer lifetime for the PM-8 dpl mutant (1100 $\pm$ 200 ps) than for the Ga or wild type 2.4.1 mutant (100 $\pm$ 25 ps) specie, as well as a carotenoidless strain of Rhodopseudomonas spheroides, R-26. Most recently exciton annihilation effects in intact phycobilisomes and isolated phycobiliproteins from the blue-green alga Nostoc sp. have been investigated by Pellegrino et al., (1981) and Wong et al., (1981) respectively.

Environmental Effects on the Fluorescence from Photosynthetic systems:

Various physical factors which influence the photosynthetic activity of the system being measured can significantly affect the measurement of fluorescence kinetics. Among such factors are the prescence of background illumination or the presence of poisons which act to block trap recovery by preventing electron transfer

from the primary acceptor to the electron transport chain.

Phase fluorescence measurements (Muller et al., 1969; Briantais et al., 1972; Moya et al., 1977) have shown the fluorescence lifetime from higher green plants to increase from 0.35 to 1.92 ns as the reaction centers become closed by illumination from intensities ranging from 0.1 to 100 J/m^2 sec. An increase in the PS I fluorescence from 80 ps to 200 ps, and in PS II fluorescence from 300 ps to 600 ps with use of saturating background illumination, was reported by Paschenko et al., (1975) with a similar increase in the lifetime of the PS II fluorescence with the addition of DCMU. It is known that the in vivo chlorophyll fluorescence lifetimes increase by a factor of 3 when the reaction centers are closed (Harris et al., 1976). However since the in-vivo chlorophyll fluorescence yield is approximately 1-3%, this corresponds to a total increase of the fluorescence yield to only about 9%, which is still about a factor of 3 lower than the measured in vitro fluorescence yield. Therefore either other decay mechanisms are present in vivo or equivalently not all of the in vivo chlorophyll gives rise to fluorescence (Duysens, 1952). Sauer and Brewington (1978) have measured a lifetime change from 0.2 to 0.48 ns in chloroplasts as the PS II reaction center traps are closed by addition of DCMU. Hervo et al., (1975) measured a similar change from 750 ps to 1.15 ns in the

fluorescence lifetime under addition of DCMU, while Beddard et al., (1979) have recently reported only minor changes in lifetime under similar conditions. Along with the increase in the fluorescence yield, a corresponding increase of the fluorescence lifetime under conditions which act to close the reaction center traps has also been observed by Briantais et al., (1972), Tumerman and Sorokin, (1967), and Yu et al., (1977). When DCMU is added, a much longer fluorescence lifetime should be observed since normal electron transfer to the traps is inhibited by the non-recovery of closed traps. If indeed primary photochemistry is an efficient process, the closing of the reaction center traps should then make available to the fluorescent emission process all photons normally used for photoconversion, but this does not appear to be the case. Emerson has also shown an opposite effect on the fluorescence quantum yield when multiple excitation wavelengths are used on the sample. A significant drop in the fluorescence quantum yield, accompanied by an increase in the photosynthetic activity is obtained upon providing additional excitation in the wavelength region lying in the active spectrum of PS I. This phenomenon is known as the Emerson enhancement effect, and clearly demonstrates the pressure of a second active photosystem (PS I) present in the overall process.

Interactions between the LHC and antenna components of PS I and PS II can affect the intensity dependence of the

yield and lifetime. Moreover millimolar concentrations of monovalent cations (e.g. Na^+) can enhance the LHC to PS I interaction relative to the interaction between LHC and PSII, (Barber, 1976; Williams, 1977) while divalent cations (e.g. Mg^{2+}) can produce the reverse effect (Arntzen and Ditto, 1976; Butler and Strasser, 1978). Barber et al., (1978) have observed that Mg^{2+} affects the energy transfer rate from PS II to PS I in DCMU treated chloroplasts. However, the effects of DCMU on the lengthening of the fluorescence lifetime and on the increase of the fluorescence quantum yield appear to be rather inconclusive. Beddard et al., (1979) and Searle et al., (1979) have observed only quantum yield changes, without changes in the lifetimes in similar experiments with DCMU treated chloroplasts. The relative amount of coupling between these antenna components may be investigated by using the Tripartite model proposed by Butler and Kitajima (1975), and Butler, (1978) which describes interactions within and among PS I, PS II and the LHC. It appears that conformational changes of the stromal thylakoid membrane lies at the heart of this coupling dynamics (Butler, 1977).

Picosecond Fluorescence Temperature Studies:

Time resolved fluorescence measurements at low temperatures indicate that the fluorescence from green plants or algae at 77K possesses two emission maxima, one at 735 nm and another at 685 nm, attributed to the

emission from PS I and PS II respectively (Yu et al., 1977). Recently Moya et al., (1979) have observed four emission components from chloroplasts at low temperatures in the 680 to 760 nm region. A decrease in the temperature to near liquid Nitrogen values, acts to immobilize the electron transport from the primary acceptor to the electron transport chain and thus affects an increase in the population density of closed traps. Yu et al., (1977) measured the fluorescence kinetics from spinach chloroplast preparations both at room temperature and $90^{o}K$. A six-fold change was observed in the lifetime of the 730 nm fluorescence from 100 ps to 600 ps as the temperature was lowered to 90K, while the fluorescence kinetics of the 685 nm component was found to be temperature independent. In addition, a risetime of 13 ps was measured for the 730 nm component at 90K, although all other risetimes, both at room temperature and 90K, were resolution limited ($\leq$ 10 ps).

The measured temperature dependent change in the fluorescence kinetics at 730 nm was also supported by measurement of the time resolved spectra at room temperature and 90K, measured relative to the 685 nm emission. At room temperature, the spectra (for wavelengths greater than 700 nm) was found to be larger within 10 ps of excitation than the time integrated spectra. This is indicative of the presence of a faster component at wavelengths greater than 700 nm relative to

the lifetime of the component at 685 nm. In addition, as expected from the low temperature kinetic measurement of the increased fluorescence lifetime of the 730 nm component at 90K, the 90K time-integrated spectra was found to be greater (for wavelengths greater than 700 nm) than the spectrum obtained within 10 ps of excitation, indicating the prescence of a longer lived decay at low temperature measured relative to the 685 nm emission. The ratio of the 730 nm fluorescence intenstiy measured relative to the 685 nm emission was found to be 1/9 at room temperature and 1/2 at 90K. Govindjee and Yang (1966) placed this ratio at a value of 1/11 at room temperature and 1.4 at 77 K .

Geacintov et al., (1977b) and Campillo et al., (1976a) have shown that the 735 nm fluorescence kinetics at 77K under single pulse excitation is intensity independent while the emission at 685 nm is intensity dependent. Campillo et al., (1977) have measured the rise of the 735 nm fluorescence at 77 K and low intensity ($\sim 10^{14}$ photons/cm^2 per pulse) to be 140 ps. The slow rise of the PS I emission at low temperatures followed the decay of the LHC fluorescence in this intensity region and is supportive of the idea of energy transfer from PS II or LHC to PS I. Butler et al., (1979) have reported an increase in both the lifetime and quantum yield of the 735 nm emission as the temperature was lowered from 213 K to 77 K. This emission component was attributed to a

chlorophyll form C-705 which was interpreted as being an efficient trap for PS I excitations at higher temperatures, channeling the energy to the photochemical trap of PS I, P-700. The observed change in the fluorescence characteristics were attributed to the dynamic quenching of the fluorescence from singlet-singlet exciton annihilation in the chlorophyll a light harvesting complex (LHC).

Energy Transfer in the Accessory Pigment Complex of Red and Blue Green Algae:

The transfer of energy in the accessory pigment complex of photosynthetic systems is most easily followed in the phycobilisomes, which form a regularly structured arrangement of chromophores in organized units. The measurements obtained for energy transfer kinetics in the phycobilisomes and isolated phycobiliproteins of the blue-green alga Nostoc sp., which represent a major portion of this thesis are presented in Ch. 6. The measured fluorescence kinetics were found to be consistent with the interpretation of Grabowski and Gantt (1978) who suggested that energy transfer is more efficient among the accessory pigments of phycobilisomes from blue-green algae than from those of red algae.

Searle et al., (1978) have measured the rise and decay times of B-phycoerythrin (B-PE) and allophycocyanin (APC) from the phycobilisomes of the red alga Porphyridium

cruentum. Their measurements revealed that B-PE possesses a fast fluorescence risetime (rising within the duration of the excitation pulse) with a 1/e decay time of 70 ps. The decay time of B-PE was observed to be excitation intensity independent from 10^{13} to 10^{15} photons/cm^2. The APC fluorescence risetime was measured to be 120 ps with a single exponential decay behavior for excitation pulse intensities within the range of $2x10^{13}$ to $4x10^{14}$ photons/cm^2. However, the relaxation time of APC decreased from 4 ns to 2 ns over this intensity range, with a more complex exponential behavior occurring at higher intensities. However, the decay time for APC in solution has been reported to be 2.6 $\pm$ 0.1 ns by Grabowski and Gantt (1978) with use of the photon counting technique. As there are likely to be more decay mechanisms active for the APC fluorescence decay in PBS as opposed to in solution, an even shorter lifetime than 2.6 ns is therefore expected for the APC fluorescence emission from PBS, and this has been verified by the measurements reported in Ch. 6.

Time resolved fluorescence spectroscopy with picosecond time resolution techniques has allowed for the direct probing of energy transfer in the primary photosynthetic apparatus. The investigations of the last decade have provided a solid foundation upon which further studies can be made. The future direction appears to lie in the area of model systems made up from naturally

occurring photosynthetic components or artificial analogs. In recent studies, attempts have been made to duplicate the properties of chlorophyll a in the photochemical reaction centers of green plants (Boxer and Closs, 1976; Shipman et al. 1976; Wasielewski et al., 1976; Fong and Koester, 1976; Galloway et al., 1979). Interest in such artificial duplication of reaction center chlorophylls arises from the fact that these forms possess the capacity to dissociate water (Fong and Galloway, 1978) which may prove instrumental in developing a means to generate H_2 fuel from the dissociation of water in photosynthetic systems (Porter and Archer, 1976; Hall, 1977). Fluorescence studies of these chlorophyll a - water aggregate systems have recently been reported (Fong and Koester, 1976; Galloway et al., 1979). Galloway et al., (1979) have recently measured the fluorescence lifetime of the chlorophyll dihydrate polycrystal (Chl. a $2H_2O)_n$ with emission peak at 760 nm. The fluorescence decay at 780 nm was found to be biphasic and temperature dependent, with the fast component lifetime decreasing to less than 50 ps at 294 K. The development of new laser excitation sources with wavelength tunability, sub-picosecond pulse widths and low intensity excitation, combined with streak cameras with comparable time resolution and high repetition rates will provide a means to investigate the details of energy transfer more fully. This will eventually lead to a complete

description of the mechanisms responsible for the primary process in photosynthesis.

CHAPTER 5. Experimental Techniques

5.1 Experimental Apparatus

The advent of time-resolved picosecond laser spectroscopy has enabled the investigation of physical processes on the all important time scale of molecular vibrations, rotations, and intermolecular energy transfers. The fluorescence decay rate is an experimentally accessible parameter from which the various modes of energy transfers within a molecule, or among like or unlike molecules may be investigated. Since molecular vibrational levels are generally on the order of 10 cm^{-1}, while rotational levels are on the order of 1 cm^{-1}, the clocking interval required to probe molecular vibrational or rotational decay is on the order of a few picoseconds.

Photoselection with spectrally narrow pulses of a few picosecond duration was first made possible by the development of the mode-locked laser. Picosecond pulses scanning the spectral range from 0.3-3.0 u can presently be obtained through the use of mode-locked, pulsed or continuous wave lasers.

The availability of such short-lived pulses and the interest in observing physical processes on an ultra-short time scale have made necessary the development of sophisticated temporal resolution techniques, such as the

optical Kerr gate (Duguay and Hansen, 1969; Shimizu and Stoicheff, 1969), the single-shot optical Kerr technique (Duguay and Mittick, 1972; Ho and Alfano, 1977) and the streak camera (Zavoiski and Fanchenko, 1956; Bradley et al., 1970; Bradley et al., 1971, Shelev et al., 1971). These techniques allow for measurement of the time evolution of a light emitting event by transposing the time axis onto a spatial one. In this research, we have made use of both the Optical Kerr gate technique and the streak camera to measure the fluorescence kinetics photoexcited by a 6 ps laser pulse generated from a mode locked Nd^{+3}:glass laser.

5.2 The Mode-Locked Laser

The Nd^{+3}:glass laser used in our experiments consists of an optical resonator cavity formed by two mirrors aligned parallel to each other, and perpendicular to the axis of the resonator, as shown in Fig. 5.2.1. A mode-locked and Q-switched Nd^{3+}: glass laser emits a train of 1.06 um pulses of a few picosecond duration (typically 8 ps). A 1/2 " diameter glass rod, 7 1/2 " in length can give rise to a beam of light $\sim$ 1 cm in diameter with a typical power density of 10^9 watts. The pulses in the train which forms the output of the mode locked laser are separated by the round trip time of the laser cavity, generally on the order of a few nanoseconds. The

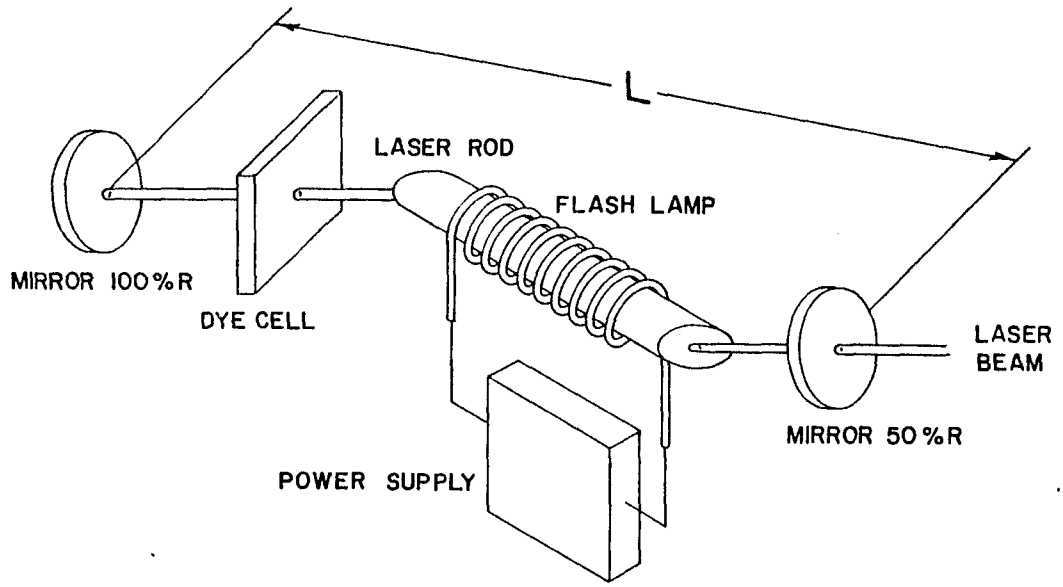

Fig. 5.2.1 Optical Resonator Cavity Configuration

total energy in one laser shot is typically 1 joule and about 6 millijoule is contained in each pulse. A single pulse is readily extracted from the pulse train by employing a Pockels cell shutter.

In order to obtain a stable resonator configuration, the rear mirror is curved, and is 100% reflecting at 1.06 u, while the output mirror is flat with 50% reflection at 1.06u. The optical path length of the cavity is 84 cm., which determines the pulse spacing of the output train (2L/c) to be 5.54 ns. The dielectric coated mirrors, obtained from the Laser Energy Co., are mounted in Lansing mounts with micrometer positioning controls. The front or output mirror was wedged $1/2^0$ in order to eliminate multiple cavity modes. The laser medium situated between the two mirrors is an Owens-Illinois (Owens-Illinois, Toledo, Ohio) ED-2, Nd^{+3}:glass rod 7.5 inches long and 0.5 inches in diameter. The center of the laser rod faces from the rear and output mirror are 18 and 45 cm, respectively. The ends of the rod are optically polished and cut at Brewster's angle, again to reduce multi-cavity resonances. The rod is housed in a Korad K-1 series laser head (Korad Division, Union Carbide Corp., Santa Monica, Calif.) consisting of a water cooled enclosure surrounding a 5 inch Xenon flash lamp. The flash lamp is fired by discharging a 400 uf capacitor, through the triggering circuit of the Korad K-1, 5 KV power supply. A Korad KWC-3 temperature controlled cooler provides cooling for

the laser rod, flashlamp, and housing at a rate of 2 gal/min and a pressure of 7 psi at 22^0C. Distilled, de-ionized water is used in the cooling system with a de-ionizer in the KWC-3 cooler maintaining the low ionic concentration required to prevent shorting of the electrodes at the flash lamp contacts.

Picosecond pulses of high power were generated by Q-switching and mode-locking the laser through the use of the dye Kodak 9860 (Eastman Co.) dissolved in 1,2-dichloroethane (Eastman Co.). The dye transmission ranged from 69%-72% at 1.06 u, and was measured in a photometer at normal incidence through a 1 cm optical path, 2" diameter cell with optical quality pyrex windows. The photometer used for this measurement was constructed by imaging light from a battery powered 6V lamp through the dye cell and a Corning 1.06 u 3-cavity filter (10 A bandwidth). The transmitted light at 1.06 u was detected by a selenium photodetector monitored by a Keithley 150B microvolt-ammeter.

Positioning of the dye cell in the laser cavity is important in order to avoid the creation of satellite pulses. Satellite pulses can arise when a weak pulse oscillating in the cavity, and not strong enough by itself to bleach the dye, passes through the dye cell coincident with a strong bleaching pulse traveling in the opposite direction. To avoid the formation of satellite pulses the dye cell may be placed in contact with the rear mirror or

is made long enough to allow for the complete absorption of the weaker pulse as it passes through it. A 1 cm long dye cell with Kodak 9860 dye dissolved in dichloroethane provides a 50 ps travel path which can allow the dye cell to completely absorb a weak 10 ps pulse. The dye cell is placed at Brewster's angle with respect to the cavity axis in order to avoid reflection losses.

It was found that a reproducibly mode-locked train of laser pulses is critically dependent on various factors, including:

1. The transmission of the Q-switching and mode-locking dye (typically 69-72% transmission at 1.06u).

2. The voltage applied to the flashlamp (typically 10-40 volts above the threshold lasing voltage).

3. Alignment of the laser cavity; A Davidson Optronics (Davidson Optronics, West Covina, California) autocollimator was used to align the two end mirrors and the rod center by superpositioning the rod image onto reflections from the rear and output mirrors.

4. The temperature of the laser rod and cavity enclosure ($\sim 25^{o}$C).

5. The humidity in the cavity (air-conditioning was used to remove excess humidity and maintain room temperature to 24^{0} C).

The 1.06 um fundamental of the Nd^{+3}:glass laser is not very useful in experiments which probe biophysical

processes whose absorption spectrum is by far mostly weighted to the visible and U.V. portions of the spectrum. The production of picosecond laser excitation pulses in this region can be achieved through the use of non-linear optical processes such as harmonic generation and self phase modulation (Alfano, 1972; Alfano and Shapiro, 1973). Second harmonic generation (SHG) can be achieved by passing the 1.06 um beam through a KDP (Potassium DiHydrogen Phosphate) crystal. When properly phase matched, a $\sim$ 10% conversion to green 0.53 um light can be obtained from a 10^9 watt fundamental 1.06 um pulse. The pulse width at the second harmonic is typically $\sim$ 4 ps. Further frequency doubling of the 0.53 um beam by use of a KDP or ADP crystal allows the possibility of obtaining a 256 nm UV beam. This conversion efficiency, however, is about $\sim$ 0.1%. The third harmonic at 353 nm can also be generated.

Pulses at 530 nm were obtained by the process of Second Harmonic Generation (SHG) (Franken et al., 1961; Giordmaine, 1962). Second Harmonic Generation is a special case of the phenomenon of 3-wave mixing whereby a photon at twice the fundamental frequency is generated from two photons at the fundamental. The power conversion efficiency for this effect is given by (Yariv, 1975),

$$\frac{P^{2w}}{P^{w}} = 2(u/\xi)^{3/2} \frac{w^2}{n^3} d_{ijk}^2 L^2 \frac{P^{w}}{A} \frac{\sin^2 \Delta kL/2}{(\Delta kL/2)^2} .$$

Efficient SHG thus requires that $\Delta k=0$, where

$$\Delta k = k_3^j - k_1^i - k_1^k$$

is the momentum mismatch between the waves k_1^i and k_1^k propagating in the i,k directions respectively, with momentum $k=n^{(w)}w/c$ ($n^{(w)}$ denotes the index of refraction for the wave at frequency w in the dispersive medium) and the second harmonic wave k_3^j propagating in the j direction with momentum $k=n^{(2w)}(2w)/c$.

$$k = n^{(2w)}(2w/c) - 2n^{(w)}(w/c)$$

$$= 2w/c(n^{(2w)} - n^{(w)})$$

In general, for either ordinary or extraordinary rays, this condition will not be satisfied in normally dispersive media since the refractive index, n, is an increasing function of w. However, it is possible to satisfy this condition by propagating the fundamental beam as an ordinary wave in a negative uniaxial crystal where $n_e^{(2w)}$ is a function of the angle between the

propagation direction and the optic axis:

$$1/n_e^2(\Theta) = (\cos^2 \Theta)/n_o^2 + (\sin^2 \Theta)/n_e^2$$

where n_o, n_e are the indices of refraction for the ordinary and extraordinary ray respectively.

Thus it is possible to find an angle, Θ^*, such that,

$$n_e^{(2w)}(\Theta^*) = n_o^{(w)}$$

$$\sin^2(\Theta^*) = \frac{(n_o^w)^{-2} - (n_o^{2w})^{-2}}{(n^{2w}{}_e)^{-2} - (n^{2w}{}_o)^{-2}}$$

For the Nd^{+3}:glass laser the fundamental wavelength is at 1.06 u, and the phase matching angle is $41^o12'$. We have used a 1" long Potassium Di-hydrogen Phosphate (KDP) crystal from Lasermetrics Co. (Teaneck, N.J.), housed in index matching solution and phase matched to generate the second harmonic of the laser at 530 nm. The power conversion was measured with a Laser Precision Co. RKP-335 probe and RK-3230 readout system to be 10 % . The pulse width was measured to be 6 $\pm$ 2 ps at 0.53 u by use of the Two Photon Fluorescence (TPF) technique (Giordmaine et al., 1967) in a super saturable solution of 7 diethylamimo 4-methyl coumarin dissolved in ethanol.

The TPF technique utilizes the non-linear dependence of the two photon fluorescence process on the intensity of the excitation pulse. If the laser beam passes through a liquid which has a two photon absorption at the laser frequency, and if further the pulse propagating in one direction is superimposed on its own reflection, then the fluorescence density measured as a function of time can be written as (Klauder et al., 1968)

$$f(t) = 1 + 2\, G^{(2)}\ (\tilde{\tau}\ )$$

where,

$$G^{(2)}(\tilde{\tau}) = \frac{\int I(t)\ I(t+\tilde{\tau})\,dt}{\int I^2(t)\ \ dt}$$

is the second order autocorrelation function. In an ideally mode locked laser, for regions of the cell where the laser pulse is not superimposed on its reflection, the background fluorescence density, f_B (t) = 1. At those positions where the pulse is superimposed on its reflection, f_p (t)= 3. This results in a contrast ratio of,

$$\frac{f_p\ (t)}{f_B\ (t)} = 3$$

for the regions where the pulse is superimposed on itself, as compared to the background fluorescence track. For an ideally mode-locked multi-transverse mode laser this ratio is 2. The contrast ratio may easily be measured on photographic film, and the pulse time duration determined by correlating the spatial extent of the overlap region with the speed of light in the dye solution ($ct_p/2n$).

5.3 Generation of High Power Picosecond Laser Pulses

The laser consists of an amplifying medium situated inside of an optical resonator cavity (Maiman, 1960; Schalow, 1961; Javan, 1961). Stable solutions for the electromagnetic field inside such a resonator consist of electromagnetic waves whose frequencies allow for an integral number of half wavelengths to be accomodated inside of the cavity, and are thus an integral multiple of c/2L, where L is the optical path length of the resonator. In addition, frequencies which lie within the gain bandwidth of the amplifying medium (fluorescence linewidth 260 A FWHM for Nd^{+3}:glass) will not only experience the losses intrinsically present in all non-ideal resonating cavites, but will receive gain upon passing through the amplifying medium. For these particular modes, the gain will eventually exceed the losses, and pulse amplification will be achieved.

However, the oscillation of these modes occurs with a random phase relationship, resulting in a noise-like laser output. If the phases and amplitudes of these randomly oscillating modes are made to possess a fixed relationship with respect to one another (i.e. are mode-locked), then bandwidth limited pulse sharpening will take place as the oscillating pulse acquires more and more spectral content on further "mode-locking" oscillations in the cavity.

In order to increase the power content of the pulse a large population inversion is necessary. Depletion of this inversion through spontaneous lasing action can be prevented by dramatically increasing the losses in the cavity (i.e. degrading the Quality factor, Q, of the resonator) thereby preventing oscillations from taking place until the inversion has achieved a maximum value. This phenomenon is known as Q-switching the laser, and can be achieved through the use of various techniques. Active modulation techniques include the use of a rotating prism or cavity end mirror (Fowler and Schlafer, 1966), the electrooptic crystal (White and Enderby, 1963), and the liquid Kerr cell (Hellwarth, 1966), while the saturable absorber provides a passive modulation technique.

The power of the output pulse can also be increased by mode-locking, which compresses the Q-switched pulse of nanosecond duration into an ultra-short pulse of a few picoseconds. The various active techniques which are available for the Q-switching and mode-locking of lasers

are well discussed in the literature. We have used the passive technique employing a saturable dye solution (De Maria, 1968; Smith, 1970; De Maria et al., 1969) of Kodak 9860 dye dissolved in 1,2-dichloroethane. Passive mode-locking by use of a saturable absorber establishes a phase relationship between the oscillating modes in the laser cavity by acting as an intensity selective gate. The saturable absorber linearly absorbs light up to a certain threshold level, thereafter the absorption decreases non-linearly with increasing light intensity. This property also makes the saturable absorber suitable as a Q-switcher.

Kodak 9860 dye has a peak absorption close to the fundamental wavelength of the Nd^{+3}:glass laser, with an absorption bandwidth of $\sim$200 A, and an absorption recovery time of $\sim$10 ps. These properties allow the dye cell to act as an optical shutter actuated by the oscillating pulse in the laser cavity. While low intensity pulses are absorbed, high intensity pulses are allowed to oscillate and build up freely as they are modulated at the shuttering frequency c/2L , which, not by coincidence, is the inter-mode separation frequency. Thus each mode is modulated at the inter-mode frequency and acquires side bands which eventually extend to both the preceding and subsequent mode position in frequency space, thereby coupling the electric fields of all of the oscillating modes in the cavity together. In addition, as the intense

bleaching pulse passes through the dye cell, its low intensity "wings" are preferentially absorbed, further sharpening the pulse.

Thus the randomly phased laser pulses which oscillate in the cavity subsequent to Q-switching are locked in phase and amplified on subsequent round-trip passes. A typical mode-locked laser output is shown in Fig. 5.3.1 . A train of approximately 100 pulses of 8 ps. duration each, separated by the round trip time of the laser cavity (5.4 ns) is displayed.

The laser pulse train was monitored with a Hadron 105 C (Hadron Division of ITT) photodiode with S-1 photodetector surface operated at 2.0 KV. The output of the photodiode was displayed on a Tektronix 519 (Tektronix Beaverton, Oregon)oscilloscope with 1 GHz bandwidth. Typical risetime for the photodetector is 0.3 ns, so that the pulse train with 5.4 ns, spacing between pulses can easily be resolved. The energy content of a typical output train from the laser is 177 mJ, providing approximately 1.77 mJ per pulse with a corresponding power of 2.2×10^8 watts.

A schematic diagram of the experimental apparatus is shown in Fig. 5.3.2. A single pulse was extracted from the train of pulses by rotating its polarization vector with respect to that of the rest of the pulses in the train. This was accomplished by applying a 5 ns (inter-pulse separation = 5.4 ns), 8.5 KV pulse to a

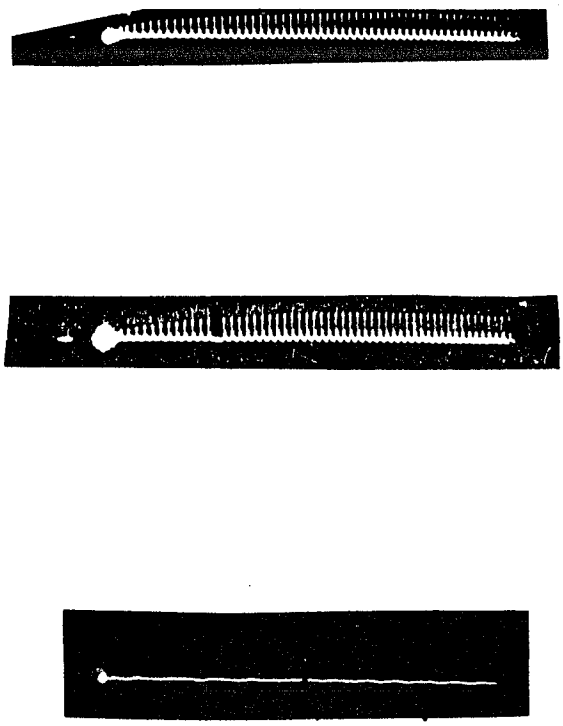

Fig. 5.3.1 Mode locked laser pulse train, single pulse selection and single pulse.

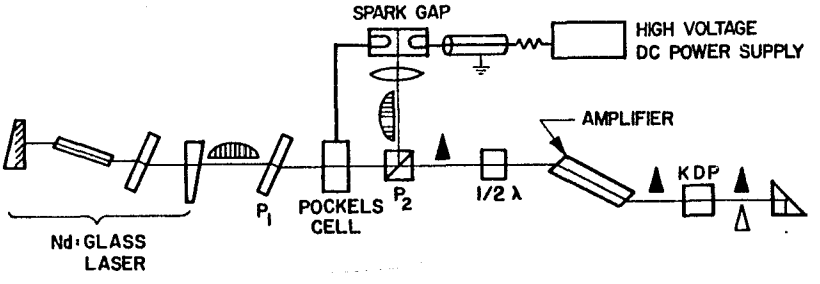

Fig. 5.3.2 Nd:glass laser with SHG and Amplifier

Pockels cell (Lasermetrics Co., Teaneck, N.J.) situated between two crossed polarizers. The first polarizer is polarized along the output polarization direction of the laser fundamental and is used only as a precaution to avoid reflections from the Pockels cell surface or other components in the setup from returning to the oscillator cavity. The second polarizer is a Glan-Air polarizing prism which acts to reject the polarization vector of the laser output. Thus only the pulse rotated by the Pockels cell is allowed to pass the Glan-Air prism polarizer. The rejected pulse train is focussed between the electrodes of a Nitrogen pressurized spark gap cell. Ionization of the Nitrogen atoms in the spark gap by the first few pulses in the rejected laser train provides the necessary carriers needed to cause avalanche breakdown across the electrodes, thereby providing a conductive path for the voltage pulse. A 17 KV pulse is preformed on a transmission line connected to the input electrode of the spark gap (the spark gap housing provides continuity of the transmission line ground, while the central electrodes are connected to the central leads of the transmission lines both in and out of the spark gap cell). Standard 125Ω doubly sheathed cable was used to form the transmission line, with a 10 MΩ resistor providing current limiting for the 3.3 ft length of cable which formed the 17 KV, 5 ns pulse. The output of the Pockels cell transmission line was dumped into a 50Ω resistor after passing through 15 ft

of cable in order to eliminate pulse reflections from returning to the Pockels cell. A pressure of 59 psi at a voltage of 17 KV, for an electrode spacing of 2 mm, provided reliable pulse selections. Complete pulse selection was obtained with a reliability of 50 - 90 %.

The second harmonic generated by the selected single pulse was monitored by a Hadron ITT-105 C ,S-20 photodiode and Tektronix 519 oscilloscope. The homogeneity of the pulse intensity profile was measured by monitoring exposures of Polaroid 3000 speed film at the sample site. By use of calibrated neutral density filters the attenuation characteristics of the beam were found to be uniform from an intensity range of 10^{13} to 10^{15} photons/cm^2. This measurement also provided direct evidence of beam spot size at the sample site. A collimating lens pair was used for all of the experiments utilizing the streak camera detection system, and the beam spot size was measured to be 1.54×10^{-2} cm^2. A "clean-up" dye cell filled with 4-5 % transmission, Kodak 9860 dye dissolved in 1,2-dichloroethane was used to absorb the smaller noise pulses leaking through the single pulse selector. A signal to noise ratio of 574:1 was measured for the single pulse at 530 nm relative to the noise leakage through the single pulse selection apparatus.

The intensity of the excitation pulse was calibrated

by beam splitting a 4% portion of the excitation pulse into a Hadron 105-C, S- 1 photodiode. The pulse height was monitored on a Tektronix 519 oscilloscope with a sweep speed of 10 ns/cm. A Laser Precision RKP-335 energy probe and RK-3230 readout meter (Laser Precision, Yorkville, New York) were used to directly measure the energy of the transmitted pulse. The energy readings at the sample site were correlated to pulse heights as measured on the oscilloscope. A calibration factor of 1.02×10^{15} photons/cm^2 per millimeter pulse height on the 519 oscilloscope trace and with Corning 4-96, 1-75, Hoya ND 13, ND 25 at the photodiode, was used to determine the excitation pulse intensity in the experiments. The intensity of the 0.53 u pulses were found to fluctuate typically 20% from shot to shot. Neutral density filters from Hoya Co. were used to attenuate the excitation pulse along the pump path in the intensity dependence studies.

5.4 Optical Kerr Gate Time Resolution Technique

In the initial stage of this research time resolved fluorescence kinetic measurements were obtained using picosecond laser pulse train excitation and the optical Kerr gate time resolution technique. The Kerr gate basically consists of a birefringent material situated between two crossed polarizers. An intense linearly polarized pulse of light can induce a temporary birefringence in an otherwise optically isotropic medium

by disturbing the equilibrium distribution and distorting the electronic cloud structure of the molecules of the medium. This is achieved by coupling of the intense electric field of the laser to the polarizability of the medium.

The polarization may be expanded in powers of the electric field (Bloembergen, 1964; Yariv, 1975) as,

$$P_i = X^1_{ij} E_j + X^2_{ijk} E_j E_k + X^3_{ijkm} E_j E_k E_m + \ldots$$

with $E_j(t)$ the component of the electric field along the j-axis. X^1_{ij} is the linear susceptibility tensor responsible for the processes of refraction and attenuation, while the higher order tensor terms give rise to non-linear optical phenomena.

For an isotropic medium, inversion symmetry requires that the even ordered terms of the susceptibility tensor vanish. Thus the lowest ordered non-linear term of the induced polarization for a particular frequency w_1 propagating in the medium is given by (Owyoung, 1972)

$$P^3_i(w_1) = \delta X_{ij}(w_1) E_j(w_1)$$

where $\delta X_{ij}(w_1)$ is the change in the susceptibility tensor of the medium at w_1. The processes which

contribute to the change in the susceptibility tensor are electronic cloud distortion, molecular libration, molecular redistribution and molecular reorientation. Although the first three processes are ultrafast (Hellwarth, 1967), and for the case of picosecond pulse excitation can be assumed to respond almost instantaneously to the applied field, the molecular reorientational motion generally lasts longer than the excitation pulse (Ho and Alfano, 1977).

Using

$$n = n_0 + \delta n$$
$$X = X_0 + \delta X$$
$$n^2 = 1 + 4\pi X$$

We may write,

$$n_0^2 + 2n_0 \delta n + (\delta n)^2 = 1 + 4\pi X_0 + 4\pi \delta X$$

Where for small index changes, $(\delta n)^2$ may be neglected and we obtain

$$\delta X = (n_0/2\pi)\ \delta n$$

A circularly polarized optical pulse travelling through such a medium experiences a phase retardation between the parallel and perpendicular components of the electric field at wavelength λ, given by

$$\delta\phi(t) = 2\pi L/\lambda \quad \delta n(t)$$

where L is the length of the birefringent medium traversed.

It is easily seen from Fig. 5.4.2, that for a Kerr gate consisting of two crossed polarizers, where the incident pulse is parallel to the first polarizer, the intensity of the transmitted signal is given by

$$I_t = I_o \sin^2 \frac{\delta\phi}{2}$$

where,

$$\delta\phi = \frac{2\pi L}{\lambda} n_2 E^2$$

where n_2 is the Kerr coefficient for the material, L is the length of the cell, λ is the wavelength of the transmitted light, and E is the electric field intensity of the gate opening pulse. Since the transmitted signal is proportional to the square of the intensity of the laser fundamental, fluctuations in laser power from shot to shot, necessitate signal averaging.

A diagram of the optical Kerr gate used in the experiments is shown in Fig. 5.4.3. After passing through a KDP crystal, the fundamental is separated from the second harmonic by use of a dielectric coated mirror which transmits 80 % at 0.53 u and reflects 99 % at 1.06 u. The 0.53 u pulses were optically delayed in order to compensate for the additional path length traversed by the

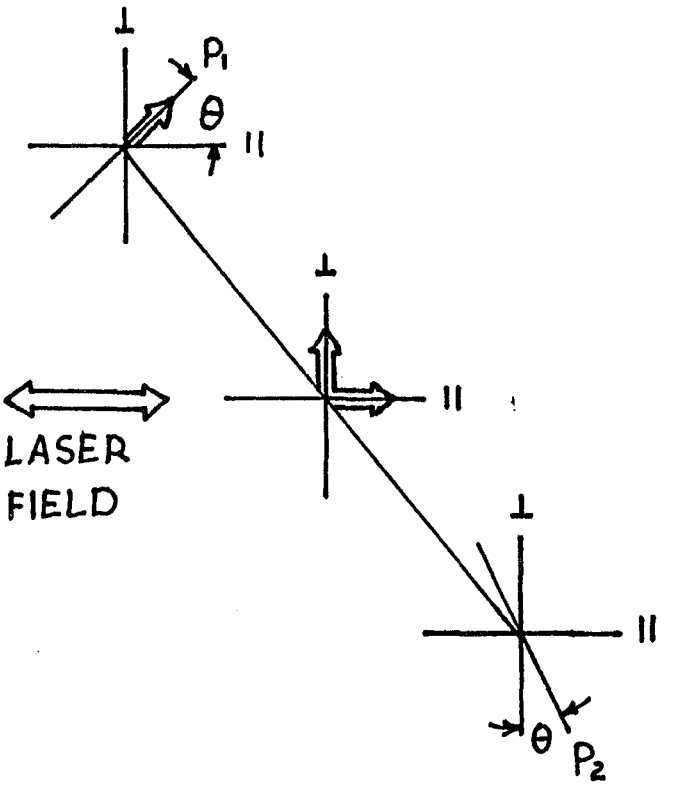

LIGHT PASSING THROUGH POLARIZER P_1:

$$E_{P_1} = E_0 \cos\omega t \,(\cos\theta\, \hat{X}_{\parallel} + \sin\theta\, \hat{X}_{\perp})$$

AFTER PASSING THROUGH KERR CELL OF LENGTH L:

$$E = E_0 \,(\cos\theta\cos(\omega t + \delta\varphi)\, \hat{X}_{\parallel} + \sin\theta\cos\omega t\, \hat{X}_{\perp})$$

$$\delta\varphi = \frac{2\pi L}{\lambda} n_2 E_L^2$$

$$E_{P_2} = E_0 \cos\theta\sin\theta\,(\cos\omega t\, \hat{X}_{\perp} - \cos(\omega t + \delta\varphi)\, \hat{X}_{\parallel})$$

$$I_t \propto \langle E_{P_2}^2 \rangle \propto E_0^2 \sin^2 2\theta \sin^2\frac{\delta\varphi}{2}$$

$$\text{FOR } \theta = 45^\circ, \quad I_t \propto E_0^2 \sin^2\frac{\delta\varphi}{2}$$

Fig. 5.4.2 Optical Kerr Gate Schematic

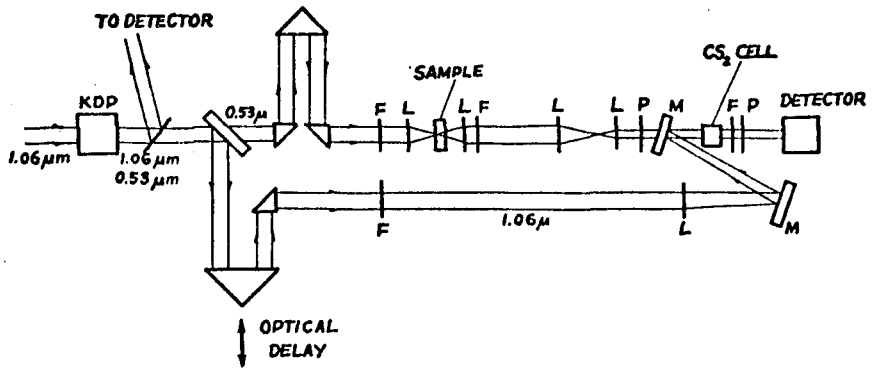

Fig. 5.4.3 Optical Kerr Gate Setup

1.06 u beam, so as to insure arrival of both the fluorescence signal and the 1.06 u pulse at the Kerr cell within the delay range of a prism set on a linear translation stage providing optical delay for the 1.06 u gate opening pulses. The 0.53 u pulses are passed through a Corning 1-75 filter to insure rejection of the laser fundamental, and are focussed to a 5mm diameter spot at the sample site. The fluorescence is collected and the 0.53 u pump light is filtered by a Corning 3-67 filter. A collimating lens pair was used to obtain a uniform fluorescence beam which fills up an aperture of 5 mm diameter at the Carbon Disulfide (CS_2) cell. Prior to entering the CS_2 cell the fluorescence signal is passed through a polarizer P_1 (Polaroid HN 22), which polarizes the flourescence emission 45° with respect to the plane of the table. Flourescence passing through the Kerr cell is filtered (Corning 1-75 filter) for the gate opening 1.06 u light pulses which are made to travel collinearly with the fluorescence signal through the Kerr cell. The 1.06 u laser pulses, polarized parallel to the plane of the table, were reflected from a dielectric mirror with front surface coating of 99 % reflection at 1.06 u, situated between P_1 and the Kerr cell, thereby providing collinear alignment with the fluorescence signal. A polarizer P_2 (Polaroid HN 22), analyzes the fluorescence signal so that no fluorescence reaches the detector when the Kerr cell is not activated by the intense 1.06 u

pulses.

Although a null ratio of 5×10^{-6} can be achieved for Polaroid HN 22 polarizers, the natural birefringence of the optical cell, mirror and filters placed between the polarizer and analyzer allowed an extinction ratio of 3×10^{-5} to be obtained. The fluorescence signal passing through the second polarizer (P_2) was filtered for 1.06 u light and imaged into the entrance slit of a 1/4 m Jarrell-Ash monochromator.

The gated signal was detected with an RCA 7265 (RCA Electron Tube Div., Harrison, N.J.) S-20 photomultiplier. For 530 nm light, a transmitted signal I(t=0) to noise, $I(t \gg 0)$, ratio of $\sim 10^3$ can be obtained through the Kerr gate. Coincidence in time and space of the 1.06 u gate opening pulse and the sample excitaion pulse (530 nm) at the Kerr cell, (when the sample cell is filled with solvent only) defines the zero time of the gate. The resolution time of the Kerr gate is obtained by convoluting the pulse width of the 1.06 u laser pulse and the response time of the birefringent material. The response time for CS_2 has been measured to be $\sim$ 1.8 ps (Shapiro and Broida, 1967). Thus the resolution time of the Kerr gate is $\sim$ 10 ps.

Kerr gate experiments require extensive data normalization since light transmission through the gate depends nonlinearly on the intensity of the gate activating pulse. Thus the signal through the Kerr gate

was normalized to the intensity of the excitation pulse train at 0.53 u , the square of the 1.06 u laser pulse train intensity, and the total fluorescence signal at the wavelength of investigation. The four signals were recorded on a Tektronix 556 dual beam oscilloscope with Polaroid camera recording system, and a LeCroy Research Systems integrator with quad A/D converters and descriminators. Typically 300 to 500 laser shots are required in a Kerr gate experiment to obtain a complete decay profile.

The measured signals thus consisted of the fluorescence signal for a given wavelength and time resolution element $I(\lambda,t)d\lambda\,dt$, the total fluorescence intensity $\int I(\lambda,t)d\lambda\,dt$, the intensity of the 0.53 um excitation light, and the intensity of the 1.06 um laser fundamental. The intensity of excitation for both the 1.06 u and 0.53 u light were measured with an RCA 7102 S-1, and an RCA 7265 S-20 photomultiplier respectively.

The total fluorescence signal at the wavelength of interest was collected from the sample at 90^{o} to the direction of the 530 nm excitation pulses, and imaged onto the surface of an RCA 7265, S-20 photomultiplier (after appropriate filtering of 530 nm pump light, and wavelength selection with appropriate narrow band filters with 100 A typical bandwidth).

5.5 Streak Camera - Optical Multichannel Analyzer System

In order to follow the time course of the fluorescence signal from the picosecond to the nanosecond time regime using single pulse laser excitation, a streak camera optical multi-channel analyzer detection system was used for the latter investigations of this research. A streak camera with picosecond resolution provides an ideal device for the measurement of subnanosecond fluorescence kinetics. The streak camera provides a continuous and direct measurement of the temporal profile of a light emitting event ranging from a few picoseconds to several nanoseconds (Yu et al., 1977; Pellegrino and Alfano, 1979).

A diagrammatic representation of the streak camera is shown in Fig. 5.5.1. Photoelectrons emitted by light striking the photocathode are deflected by an applied voltage ramp which causes the electrons to be transversely streaked across a phosphorescent screen, at the same time that they are accelerated through an anode. Photoelectrons released at a certain function of time from the photocathode will strike the phosphorescent screen at a corresponding function of position, causing a track representative of the incident fluorescence intensity temporal decay profile to be produced. The spatial intensity profile of this track is directly proportional to the incident temporal intensity profile of the light

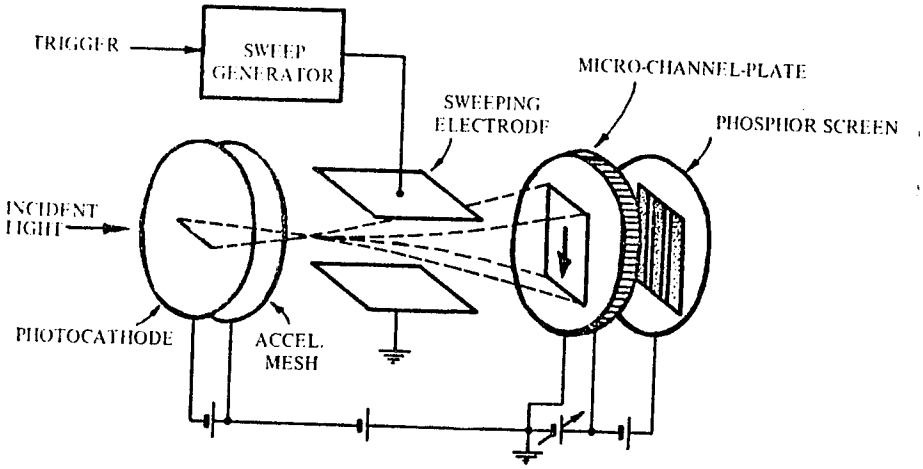

Fig. 5.5.1 Streak Camera Schematic

emitting event. The spatial intensity distribution may be recorded on photographic film and subsequently analyzed with a densitometer, or it may be captured and stored through the use of a video system or photodiode array coupled to a data storage device.

The streak camera provides certain distinct advantages over the Kerr gate. In particular, the streak camera is able to obtain the entire decay in a single shot, as opposed to the Kerr technique which provides only one point of the decay profile for a single laser shot. In addition since the delay time in the Kerr gate is obtained by changing the optical path length of the gate activating pulse by moving a prism over a linear translation stage, the time range which can be investigated is generally limited to a few nanoseconds.

The streak camera used in the measurements conducted in this research was a prototype manufactured by the Hamamatsu Corporation (Middlesex, N.J.). This camera incorporates a microchannel plate image intensifier within the streak tube (N895). The microchannel plate acts as a multiplier for the photoelectrons emitted by the photocathode through secondary emission processes in the microchannel walls. The four stages of channel plate gain were measured to give amplification factors of 12, 50, 205, 700, and 1960 respectively, giving a maximum gain of 2×10^3. The streak camera sensitivity was measured to be 5×10^5 photons/cm^2 for a 530 nm pulse incident on

the entrance slit of the camera. This makes the streak camera approximately 1/200 as sensitive as an S-20 photomultiplier.

The streak camera must be calibrated for streak rate linearity, which affects both time base and intensity calibration (Yu et al., 1977). This calibration is easily achieved by using laser pulses which are separated by a known time interval. An etalon formed by placing two 92 % R (8 % T) dielectric coated mirrors at 5300 A, with reflective coated surfaces facing one another, and separated with a cylindrical aluminum spacer machined to 10^{-3} inch accuracy was used to obtain a series of pulses of geometrically decreasing intensity, separated by 2D/c where D is the length of the aluminum spacer. Since the intensity of each succeding pulse decreases by $(1-T)^2$ (a constant), an exponentially decreasing pulse train envelope is obtained. The intensities of the output sequence of pulses is thus,

$$I_o,..I_o(1-T)^2,..I_o(1-T)^4,.....$$

This exponentially decreasing sequence may be expressed as (Schiller et al., 1980),

$$I = I_o \, \mathrm{Exp}(\, t/\Delta\tilde{\tau} \, \ln(1-T)^2 \,) \quad .$$

The average streak rate as a function of position on

the output slit of the streak camera is recorded by this method and stored in a computer file where it can be easily retrieved for calibration in the data analysis program. The quantity which is obtained on the output slit of the streak camera is the fluorescence intensity i(x) as a function of position on the OMA detector surface. For a particular resolution element on the detector surface, the product of the fluorescence intensity and the average streak rate for that position ($\Delta x/\Delta t$) yields the fluorescence intensity as a function of time, I(t).

$$I(t) = i(x) \quad (\Delta x/\Delta t)$$

Four streak rates were available on the Hamamatsu camera, providing for nominal sweep ranges of 10, 5, 2, and 1 nanoseconds over the 15 mm length of the output slit. The streak rate variations were found to be less than $\pm$ 5 % for the nominal 1 and 2 ns scales, $\pm$ 10 % for the 5 ns scale, and $\pm$ 40 % for the 10 ns scale. With this calibration the actual ranges covered were determined to be 5.2, 2.1, 0.96, and 0.40 ns over the 12.5 mm active length of the OMA detector, for the nominal 10, 5, 2, and 1 ns scales respectively.

The static (non-sweep) resolution of the streak camera measured with a 30 u input slit was obtained as the full-width at half maximum (FWHM) for a He-Ne laser

scattered from a frosted glass scatter plate at the sample site. The static resolution was found to be 1/40 of the 12.5 mm detector length of the OMA, giving a time resolution of 10, 24, 53 and 130 ps for the nominal 1, 2, 5, and 10 ns sweep ranges. The dynamic resolution of 12 ps was measured as the FWHM for the 6 ps, 530 nm calibration pulse with a 30 u input slit on the fastest time scale. This measurement represents the convolution of the laser pulsewidth, Δt_p, with the response time of the streak camera-OMA system, Δt_r, so that the observed resolution pulsewidth is

$$\Delta t_o^2 = \Delta t_p^2 + \Delta t_r^2$$

Thus the measurement of 12 ps for the FWHM of the laser pulsewidth (6 ps) is consistent with a streak camera response time of 10 ps.

Operation of the streak camera requires proper electronic triggering of the deflection voltage prior to arrival of signal on the streak tube detector surface. The streak camera was triggered by beam splitting a portion of the output laser pulse into a pin diode (Hamamatsu Corp., Middlesex, N.J.) which provides a 2-10 volt trigger signal into the 50Ω trigger input of the camera. Prior triggering is required by the fact that the streak camera uses avalanche transistors (which possess an inherent delay of ~25 ns) to generate the sweep deflection

voltage ramp. Thus the camera must be triggered as soon as possible subsequent to the obtaining of the single pulse, and the excitation pulse optically delayed in order to ensure the simultaneous occurrence of the arrival of the fluorescence signal and actual sweeping of the voltage at the streak tube.

The Optical Multi-channel Analyzer (OMA) used to record the output streak image of the camera consists of a model 1205 D detector head with S-20 photodetector surface and 1205 A console. The peak spectral response of this surface is close to the peak spectral output of the streak camera P-11 phosphor (4650 A), so that efficient transfer of the streak output is achieved. The OMA detector surface consists of a 1" diameter photocathode with a 2.5 mm x 12.5 mm active area. Photoelectrons emitted from the photocathode are electronically focussed onto a thin layer of silicon which is internally scanned by an electron beam. This active photosensitive area is divided into 500 regions (diodes), or channels of resolution, which are scanned at the rate of 64 us per channel, or 32 ms for the entire 500 channel array. The amount of charge deposited by the beam is proportional to the amount of charge depleted by the photoelectric effect induced by light striking the outer surface of the detector head. The output signal of the diode array is obtained by capacitative coupling to the scanning electron beam.

The scanning of the tube target in vidicon

photodetectors is sensitive to lag problems. Lag is defined as the residual signal charge left on the tube target face after three scans of the active area. Since lag is a non-linear function of the incident intensity and may vary by as much as 400 % for a ten-fold change in incident illumination (RCA Sit Camera tube 4804 and Vidicon specification manual), it is essential that most, if not all, the charge be read from the tube target face in order to obtain an accurate recording of the signal data. The signal from 5 scans of the tube target face was accumulated in all the measurements using the OMA. This ensures reading of at least (97 %) of the signal charge.

It is also essential that the scan be triggered so as to commence after the arrival of the fluorescence signal on the tube target face and be initialized to the beginning of the detector active area, in order to eliminate the possibility of overrepresenting certain regions of the detector surface. The internal clocking frequency of the OMA 1205 A readout console was used to first blank the target face for two scans, and to send a 5 V signal to the Korad power supply triggering circuit to activate the laser firing mechanism.

Since triggering of the streak camera sweep is subject to an inherent jitter (uncertainty) of $\sim$50 ps, a time reference marker is required in order to correctly average corresponding elements of different data sets. This is

achieved by beam splitting the excitation pulse to provide a 530 nm calibration pulse which enters the streak camera input slit prior to the arrival of fluorescence light from the sample. Since the laser pulse duration is comparable to the resolution time of the streak camera system, signal averaging data starting from the peak of the calibration pulse allows different data sets to be superimposed with an uncertainty of only 2-3 resolution channels. In the experiments employing the streak camera-OMA system, front surface excitation and optically thin (1-2 mm) samples were used in order to minimize self-absorption and time resolution losses.

5.6 Computer Interface and Analysis of Time Dependent Data

Signal averaging of data is required in order to observe fluorescence signals at very low excitation intensities. By signal averaging it is often possible to enhance the signal to noise ratio by averaging the random noise fluctuations present in the streak tube and microchannel plate of the streak camera and the Silicon Intensifier Target (SIT) tube of the OMA. These fluctuations generally arise from thermionic emission (Melissinos, 1966) or shot noise (Harnwell and Livingood, 1961).

A PDP 11/03 minicomputer (Digital Equipment Corp., Maynard Mass.) with 28 Kb MOS memory and dual floppy disk

storage system with 256 K Bytes storage per disk, A/D converter, D/A converter and graphics VT-55 terminal was used to store and analyze the data. A program coded in Fortran was used to synchronize data transmission between the OMA 1205 A console and the computer. The program provided for background subtraction, streak rate calibration, signal scaling, pump pulse intensity calibration, and curve fitting to both single and double exponential decays.

The data was analyzed by plotting the logarithm of the 500 data points and visually selecting the limits for a linear least squares fit to the log plot. For the case of double exponential decays, the starting point for the long component fit was selected beyond the point at which the extrapolated fast component would have decayed into background, in order to eliminate data from the overlap regions of the two components. The long component fit was then subtracted from the data and the log of the result displayed. Nearly all the decays obtained could be well fitted to either a single or double exponential. Moreover, the limited temporal range of the data (the decay generally covered less than three 1/e time intervals) and the low intensity of the signals obtained made curve fitting to more than a double exponential decay unwarranted. In some cases the fitted curves were optimized by a variation of parameters scheme (generally limited to variations of 0.5 standard deviations of both

the short and long components within a range of 1.5 standard deviations of each, thus giving 49 different attempted fits for each decay curve). The components giving rise to the least deviation between the data and computer fit curve were taken as the best fit components.

Quantum yields were calculated by multiplying the t=0 height of the fluorescence signal obtained from the streak camera output by the corresponding lifetime. For double exponential decays the component quantum yields were individually calculated and summed.

5.7 Sample Preparation

Preparations of spinach (Spinacia oleracea) chloroplasts were obtained by a modification of the method of Avron (1961) and Cramer and Butler (1967). In a darkened sample preparation room, 50 g of market fresh spinach leaves were washed under cold water, de-veined and cut into pieces approximately 1 inch square. The leaves were placed in an ice cold Waring blender along with 150 ml ice cold buffer solution consisting of 0.4 M sucrose, 0.05 M Tris-HCl, 0.01 M NaCl, and 0.01 M ascorbic acid titrated to pH 7.6 with 0.2 M HCl. The blender was operated at low speed for two 10 sec intervals. A filter consisting of 8 single layers of cheese cloth was used to separate the resultant suspension from the spinach leaf fragments. The suspension was centrifuged at 0° C in a

Sorvall RC2-B (DuPont Instruments,Newtown,Ct.) ultracentrifuge for 90 sec at 500 g. The supernatant was centrifuged for 7 min at 1,000 g and the resulting pellet resuspended in 40 ml ice cold buffer solution and centrifuged for 10 min at 2,000 g. The resultant pellet was suspended in 5 ml ice cold buffer and chilled to use.

Samples of whole spinach leaf (Spinacia oleracea), Norway maple leaf (Acer platenoides), Streptocarpus holstii, and Anthurium andreanum were placed on a flat piece of aluminum and the ends of the leaf lightly stretched to provide a flat, homogeneous layer for excitation.

Nitella (Chara) cells were obtained from Prof. Ralph Zuzolo of the Biology Department of The City College of New York. The cells were collected from their natural (pond water) growth media, screened according to size (which is related to cell age) and were cut from the cell chain, taking special care not to damage or rupture the cell wall. Typically four cells were aligned side by side with the long axis of the cells vertical, along the inner surface of a 2 mm optical cell. Surface tension between the Nitella cell wall and the inner surface of the optical cell provided the necessary adhesion which maintained the cells in an upright position. The cell walls of the Nitella were aligned side by side and a central region of the cell bodies excited by the 530 nm pulse.

Samples of Scenedesmus obliquus (Sc), Wild type,

Mutant 8, and Mutant 11 were obtained from Prof. Shirley Raps of the Biology Department of Hunter College of the C.U.N.Y. The samples were suspended in growth media consisting of 0.809g KNO_3, 0.468g NaCl, 0.178g $Na_2H_1PO_4$, 0.468g NaH_2PO_4, 0.022g $CaCl_2$, 0.247g $MgSO_4 7H_2O$, 0.020g EDTA, 0.01g $FeSO_4$, 0.2 ml MnCl, 0.1 ml $ZnSO_4$, 0.5g dextrose, 0.25g yeast extract dissolved in 1 liter of H_2O. Fluorescence measurements were obtained by placing the suspensions in 2 mm optical cells. The suspensions were maintained as homogeneous as possible throughout the experiments by inverting the cells at two minute intervals.

Phycobilisomes and isolated phycobiliproteins from the alga Nostoc sp. were obtained from Prof. Barbara Zilinskas of the Botany Department of Cook College, Rutgers University, N.J.. The phycobiliproteins were separated by gel electrophoresis on brushite columns. In the experiments, the samples were suspended in 100 mM phosphate buffer at pH 7. A detailed account of the phycobiliprotein sample preparation methods is given in chapter 6.

Experimental Results and Discussion

The experimental results of this thesis are reported in the following chapters.

Chapter 6. Energy transfer kinetics in the accessory pigment complex of phycobilisomes and isolated phycobiliproteins.

Chapter 7. Energy transfer kinetics in the carotenoid accessory pigment complex of photosynthetic systems.

Chapter 8. Energy transfer kinetics in the chlorophyll light harvesting complex in primary photosynthesis.

Chapter 9. Fluorescence kinetics and polarization anisotropy from dyes and photosynthetic systems.

Chapter 6. Energy transfer kinetics in the accessory pigment complex of phycobilisomes and isolated phycobiliproteins.

The pathway of energy transfer in the light harvesting pigment complexes of oxygen evolving photosynthetic organisms is most readily followed in the phycobilisomes (PBS's) (Gantt, 1975) which occurr naturally in red and blue-green algae. Phycobilisomes consist of an aggregation of the phycobiliproteins; phycoerythrin, phycocyanin and allophycocyanin. Energy transfer in PBS's is generally believed to take place by the Forster inductive resonance energy transfer mechanism from the shorter to the longer wavelength absorbing elementary pigments: phycoerthryn (PE) $\longrightarrow$ phycocyanin (PC) $\longrightarrow$ allophycocyanin (APC) (Gantt and Lipshultz,1973; Grabowski and Gantt, 1978; Duysens, 1952; Dale and Teale, 1970; Searle et al., 1978) followed by transfer to chlorophyll *a* in the thylakoid membrane. Tomita and Rabinowitch (1962) reported energy transfer times from B-phycoerythrin to R-phycocyanin of 300 $\pm$ 200 ps and from APC to chlorophyll *a* of 500 $\pm$ 200 ps. Estimates of the Forster critical distances and the inter-chromophore distances by Dale and Teale (1970), when combined with the intrinsic fluorescence lifetime of the bilin prosthetic group, yield a Forster pair-wise transfer time of 10 ps. More recently, Grabowski and Gantt (1978) have used a

hemispherical model consisting of layered concentric shells for the phycobilisomes and have estimated the mean energy transfer time from the PE layer to the PC layer to be 280 $\pm$ 40 ps. Searle et al., (1978) have shown that energy transfer in PBS's isolated from the red alga Porphyridium cruentum can be followed through fluorescence kinetic measurements. They have found that quenching of the red fluorescence occurs with single pulse excitation intensity of 10^{14} photons/cm^2 per pulse. They have also measured a risetime of 120 ps for the APC fluorescence, indicative of the energy transfer time from B-PE to APC.

Grabowski and Gantt (1978) have suggested that the efficiency of energy transfer in PBS's isolated from blue-green algae is greater than that from red algae. In addition, there exists at present an apparent anomoly in the fluorescence properties of APC. Measurements on isolated APC have given lifetimes of $<$ 3 ns (Grabowski and Gantt, 1978; Wong et al., 1981) while it has been suggested by Searle et al., (1978) that the lifetime is 4 ns in the isolated PBS's of P. cruentum. However, since the PBS's are an aggregate of biliproteins, they should be more susceptible to exciton annihilation effects and presumably show a shorter lifetime for the APC component than can be observed in solution. This has indeed been verified in the experiments reported here.

In order to better understand the energy transfer

kinetics as well as the fluorescence quenching in PBS's, it is necessary to study the fluorescence kinetics from isolated phycobiliproteins. The isolated phycobiliproteins C-PE, C-PC, and APC each contain different amounts of bilin chromophores. For example, C-PE contains 18 chromophores in the trimer form, while C-PC contains 18 chromophores in the hexamer form, and APC contains 6 chromophores in the trimer form. The bilin chromophores are covalently attached to the apo-proteins which are 120 A in diameter by 30 A thick in the basic trimer unit. Due to this chromophore packing arrangement, one should expect to observe fluorescence quenching due to singlet-singlet exciton annihilation within each phycobiliprotein. In intact phycobilisomes a lesser amount of quenching is expected in PE and PC as energy transfer from PE $\rightarrow$ PC $\rightarrow$ APC is also present in this case. However there also exists a tendency for increased quenching in intact phycobilisomes due to the higher effective local absorption and the closer packing arrangement of the phycobiliprotein units. The results obtained in the isolated phycobiliproteins are consistent with the occurrence of singlet-singlet exciton annihilation among the bilin prosthetic chromophores in the phycoerythrin and phycocyanin units. In the allophycocyanins only a slight fluorescence quenching was observed over the range of 10^{13} to 10^{15} photons/cm^2.

This section reports the first application of direct

picosecond fluorescence techniques to the study of PBS's and isolated phycobiliproteins from a blue-green alga, Nostoc sp. The fluorescence rise and decay kinetics and fluorescence quantum yield from the isolated phycobiliproteins C-PE, C-PC and APC forms I, II, III, and B as well as the C-PE and C-PC+APC emission from intact phycobilisomes were studied as a function of the intensity of a single 530 nm, 6 ps excitation pulse over the intensity range 10^{13} - 10^{15} photons/cm^2.

Phycobilisome samples were obtained by the following method. Nostoc sp. was grown in a fermentor on medium CG-10 (Ingram and Van Baolen, 1970) according to the method described by Ruscowski and Zilinskas (1980). Phycobilisomes were isolated as described by Zilinskas et al., (1978), by a modification of the procedure of Gray and Gantt (1975), and stored in pellet form at 4^{o} C until used. Experimental samples were prepared from pellets within a week of isolation by resuspension in 0.75 M phosphate buffer, pH 7 at 23^{o} C. The optical density of the suspension was 0.5 at 530 nm in a 2 mm cuvette. Precautions were taken to ensure sample homogeneity and to minimize settling effects by mixing the suspension every 10 minutes. In measurements using intact phycobilisomes, the phycoerythrin fluorescence was spectrally isolated by using a combination of a Corning 3-67 glass filter and an Optical Coatings Laboratories Cyan Dichroic filter; (600 - 800 nm cut-off region). The allophycocyanin fluorescence

was observed by replacing the Cyan dichroic filter with a Magenta dichroic filter (500 - 600 nm cut-off region).

The phycobiliproteins C-PE, C-PC and APC forms I, II, III, and B were obtained as follows. Phycobilisomes from several isolations which had been stored at $4^{o}C$ in pelleted form were suspended in a minimal volume of 0.75 M potassium phosphate buffer, pH 7.0, and dialyzed against multiple changes of 0.01 M potassium phosphate buffer, pH 7.0, over a 3 hr period. After dialysis, these partially dissociated phycobilisomes were centrifuged at 40,000 xg for 30 min to remove any contaminating membrane material. The resulting supernatant was applied to 2.5 x 30 cm brushite column which had been equilibrated with 0.01 M potassium phosphate buffer, pH 7.0, containing 0.1 M NaCl and 0.02% NaN_3 (brushite equilibration buffer). Brushite was prepared according to the procedure of Siegelman and Firer (1964). A mixture of C-PE and C-PC was eluted from this column with 500 ml of brushite equilibrating buffer. The APC fraction from the dissociated phycobilisomes remained adsorbed at the top of the brushite column. Allophycocyanin I, II, III and B were separated from this allophycocyanin pool according to the method of Zilinskas et al., (1978) with modifications described by Troxler et al., (1980).

The mixture of C-PE and C-PC described above was concentrated on an Amicon ultrafilter cell (PM-10 filter), dialyzed exhaustively against water, and lyophilized.

This mixture (equal absorbance at 620 nm (PC) and 570 nm (PE)) was suspended in a minimal volume of 1mM potassium phosphate buffer, pH 7.0, and layered on a 2.5 x 60 cm brushite column equilibrated with the same buffer, containing 100 mM NaCl and 0.02% NaN_3. The column was developed with a linear gradient of potassium phosphate from 1 mM to 20 mM, containing 100 mM NaCl and 0.02% NaCl (700 ml total volume). Fractions with a 560 nm/620 nm absorbance ratio $\geq$ 1.5 were pooled as PE-enriched; fractions with a 620 nm/560 nm ratio $\geq$ 1.85 were pooled as PC-enriched.

The PE-enriched pool was brought to 35% saturation with $(NH_4)_2SO_4$ at 20°C according to the procedure of Bennett and Bogorad (1971). The pellet, greatly enriched in PE, was resuspended in 10 ml of 10 mM potassium phosphate buffer, pH 7.0, and was brought to 35% saturation with $(NH_4)_2SO_4$. This was repeated once more, and the final pellet suspended in 100 mM potassium phosphate, pH 7.0, showed no absorbance beyond 600 nm and is considered pure C-PE.

The PC-enriched pool was similarly brought to 35% saturation with $(NH_4)_2SO_4$. The pellet was considerably enriched in PC (A620/A560 = 2.5) and the supernatant was enriched in PE (A620/A560 = 1.6). After three such repeated fractionations in 35% saturated $(NH_4)_2SO_4$, the final pellet was resuspended in 100 mM potassium phosphate, pH 7.0. Absorption and

fluorescence spectra indicated that the sample was free of all PE. The PE-PC lyophilized mixture was suspended in a small volume of 100 ml potassium phosphate buffer, pH 7.0, and was layered on a 2.5 x 60 cm Sephacryl S-200 gel filtration column equilibrated with the same buffer. PC-enriched fractions eluted slightly ahead of the PE-enriched fractions. The PC-enriched fractions were pooled, concentrated on a Amicon PM-10 ultrafilter and reapplied to the Sephacryl S-200 column and PC-enriched fractions again collected. This was repeated once more and the resultant PC was applied to a 1.5 x 30 cm brushite column equilibrated with 1 mM potassium phosphate buffer, pH 7.0, containing 100 mM NaCl and 0.02% NaN_3. The column was developed with a linear gradient of potassium phosphate buffer, pH 7.0, from 1 mM-20 mM, containing 100 mM NaCl and 0.02% NaN_3. Phycocyanin fractions which were free of all phycoerythrin as determined by absorption and fluorescence spectra were pooled and concentrated.

All biliprotein samples were stored at $4^{o}C$ in 100 mM potassium phosphate buffer, pH 7.0, containing 0.02% NaN_3. In most cases, picosecond measurements were made within a week of isolation. Lyophilized biliproteins were also used on occasion and no differences were detected in measurements of these lyophilized samples and fresh samples.

Sedimentation constants (S20,w) were determined by centrifugation in a Beckman SW40 rotor at 40,000 rpm for

16 h using a linear sucrose gradient of 0.15 - 0.8 M sucrose in 0.1 M potassium phosphate, pH 7.0 total volume 13 ml. The approximate S20,w values reported here were calculated by the numerical integration of the centrifuge equation and also by estimation according to McEwen (1967). Two hundred microliters of sample, 0.5 - 2 mg protein/ml, were layered on each gradient.

Absorption spectra were recorded at room temperature in a Cary 17 D recording spectrophotometer. Fluorescence spectra were measured in an Aminco-Bowman spectrofluorimeter equipped with a R446S (Hamamatsu TV photomultiplier tube). The band pass on the excitation and emission sides were 1.1 nm and 2.8 nm, respectively, for excitation spectra and the reverse for emission spectra. The spectra were uncorrected for lamp output and the emission grating and phototube efficiency. The relative quantum yields of fluorescence of the samples were measured on and standards adjusted to an absorption at the excitation wavelength of 0.1 (540 nm for rhodamine B and PE and 600 nm for cresyl fast violet and PC) with fluorescence yields for rhodamine B and cresyl fast violet in ethanol of 0.94 and 0.98 respectively (Dale and Teale, 1970).

The decay kinetics and the fluorescence yield in phyibilisomes as well as individual isolated phycobiliprotein were measured at pH 7 and 23^{o}C. The samples were excited by a single pulse at 530 nm at

intensities ranging from 10^{13}-10^{15} photons/cm^2. The fluorescence was detected by the Streak camera-OMA system described in detail in Chapter 5. The limiting resolutions of the apparatus was ~ 12 ps.

The measured picosecond fluorescence kinetics for the isolated phycobiliprotein pigments C-PE, C-PC and APC are presented first followed by their respective emission components in the intact phycobilisomes.

Isolated Phycobiliproteins: Results

Phycoerythrin (C-PE)

The absorption and fluorescence emission and excitation spectra of c-phycoerythrin in 0.1 M potassium phosphate buffer, pH 7.0, are shown in Fig. 6.1. Ultracentrifugation experiments indicated that under these conditions, at a protein concentration of 0.5 - 2 mg/ml, the phycoerythrin exists as a trimer (5.3s). The relative quantum yield of fluorescence of c-phycoerythrin from Nostoc sp. compared with rhodamine B in ethanol as standard was 0.62 ± 0.05. Recent work on aggregations is discussed by Glazer (1976, 1979).

The risetime of phycoerythrin fluorescence subsequent to a single 6 ps, 530 nm pulse excitation was found to be within the instrument resolution time of $\leq$ 12 ps. The decay kinetics of the fluorescence were found to be dependent on the excitation intensity. At low pulse intensities ($I < 10^{14}$ photons/cm^2), the fluorescence relaxation was exponential with a 1/e time of 1552 $\pm$ 31ps (average of 12 single-shots, each with I between 2×10^{13} and 8×10^{13} photons/cm^2). A typical low and high intensity fluorescence decay are displayed in Fig. 6.2a and Fig. 6.2b respectively. At higher excitation intensities, the relaxation kinetics were non-exponential, but could be approximated by the sum of two exponentials with a 1/e time of 130 $\pm$ 23ps for the fast component

(average of 26 single-shots) and 1417±29 ps for the slow component. The ratio of the relative initial amplitude of the "fast" component to that of the "slow" component of the decay varied from 0.6 at $I \sim 2 \times 10^{14}$ to 1.0 at $I \sim 2 \times 10^{15}$ photons/cm^2. While the overall 1/e times for the fluorescence decay of PE decreased to 0.3 of its initial value (Fig. 6.3a), the individual fast and slow components decreased to only 0.75 over the intensity range of 3×10^{13} to 2×10^{15} photons/cm^2 (Fig. 6.3b). The normalized fluorescence yield, , defined as the ratio of the relative quantum yield at intensity I to the relative quantum yield at low intensities, declined significantly at I 10^{14} photons/cm^2 (Fig. 6.4).

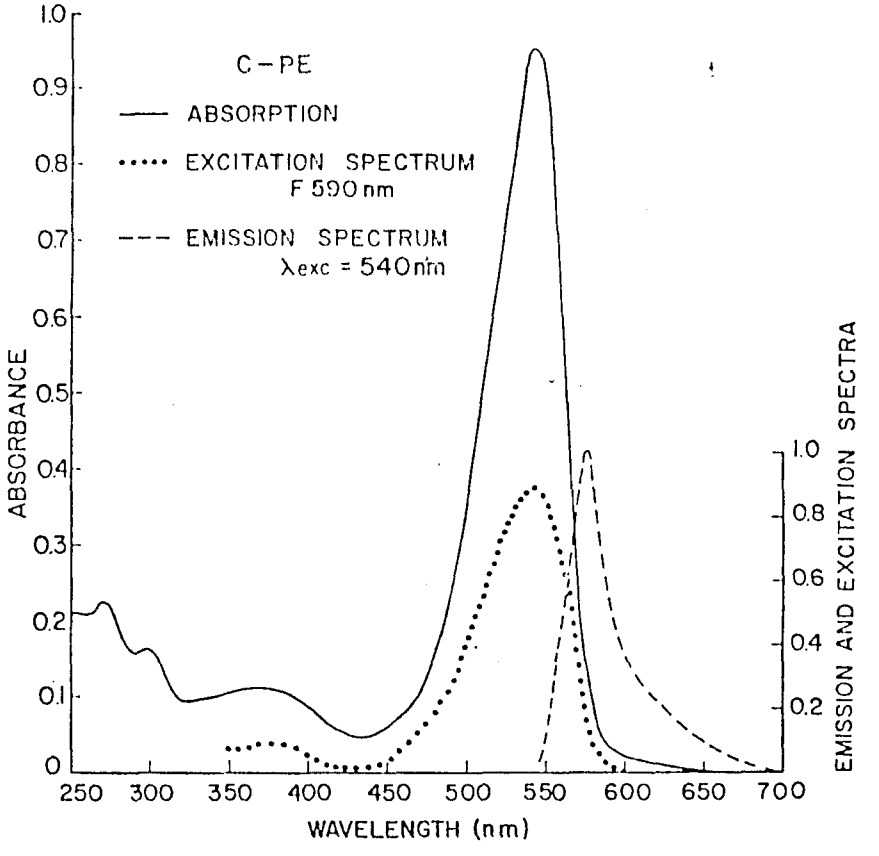

Fig. 6.1 Absorption, Emission and Excitation specra of C-PE.

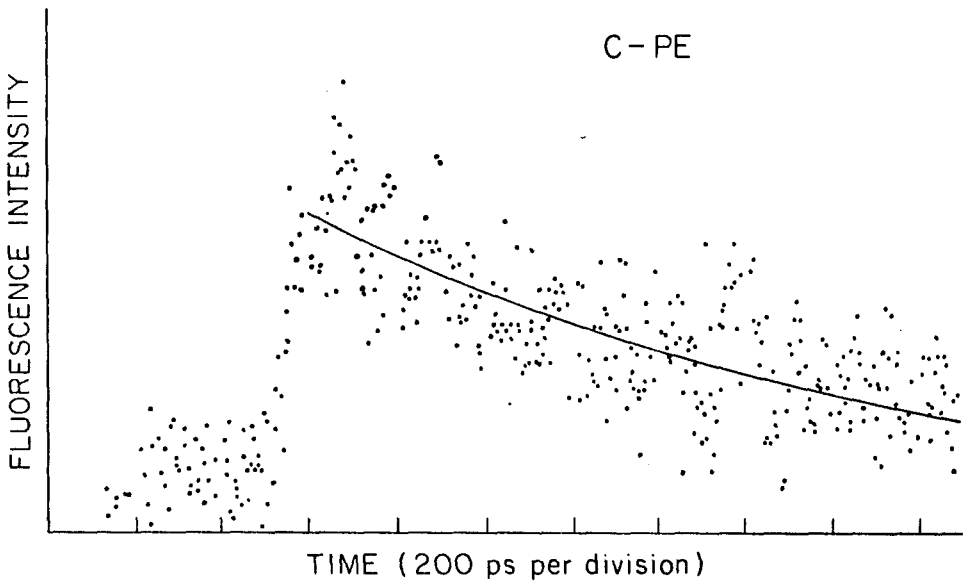

Fig. 6.2a Low Intensity Decay of C-PE.

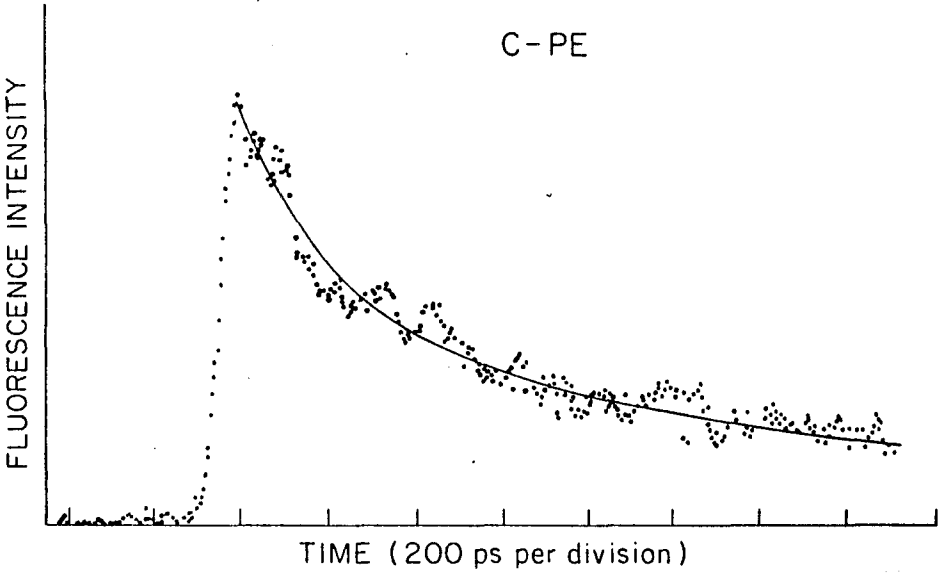

Fig. 6.2b High Intensity Decay of C-PE.

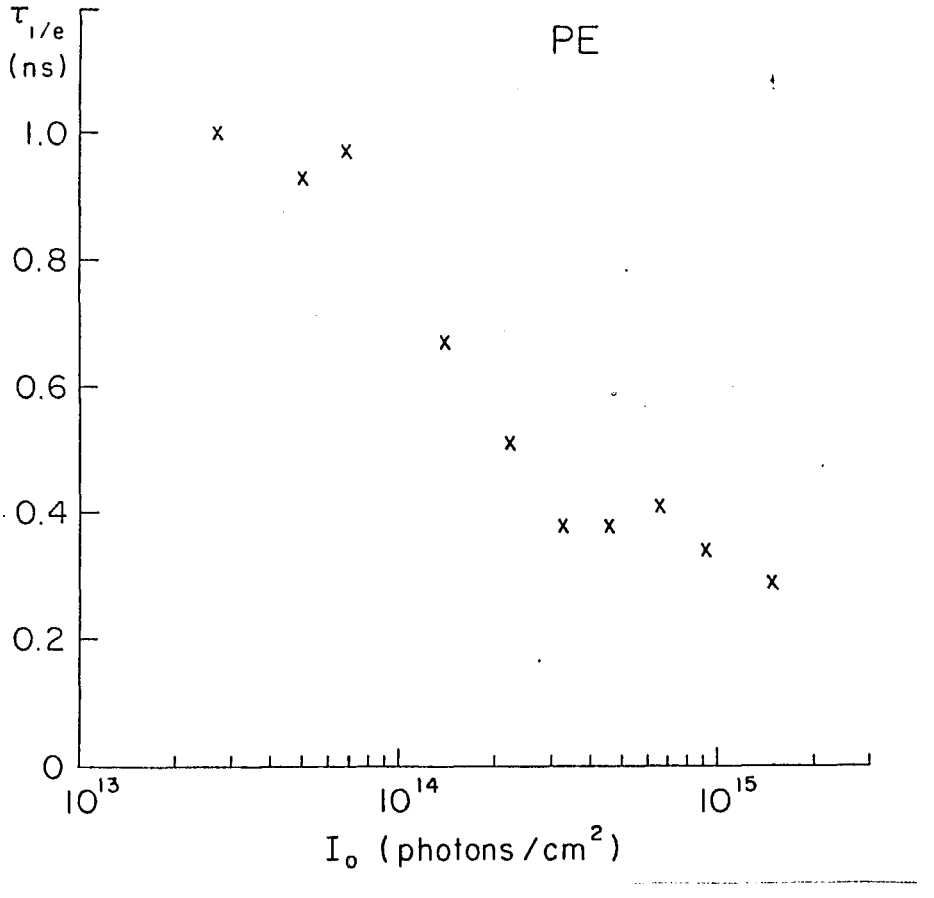

Fig. 6.3a Intensity Dependence of C-PE Relaxation Times.

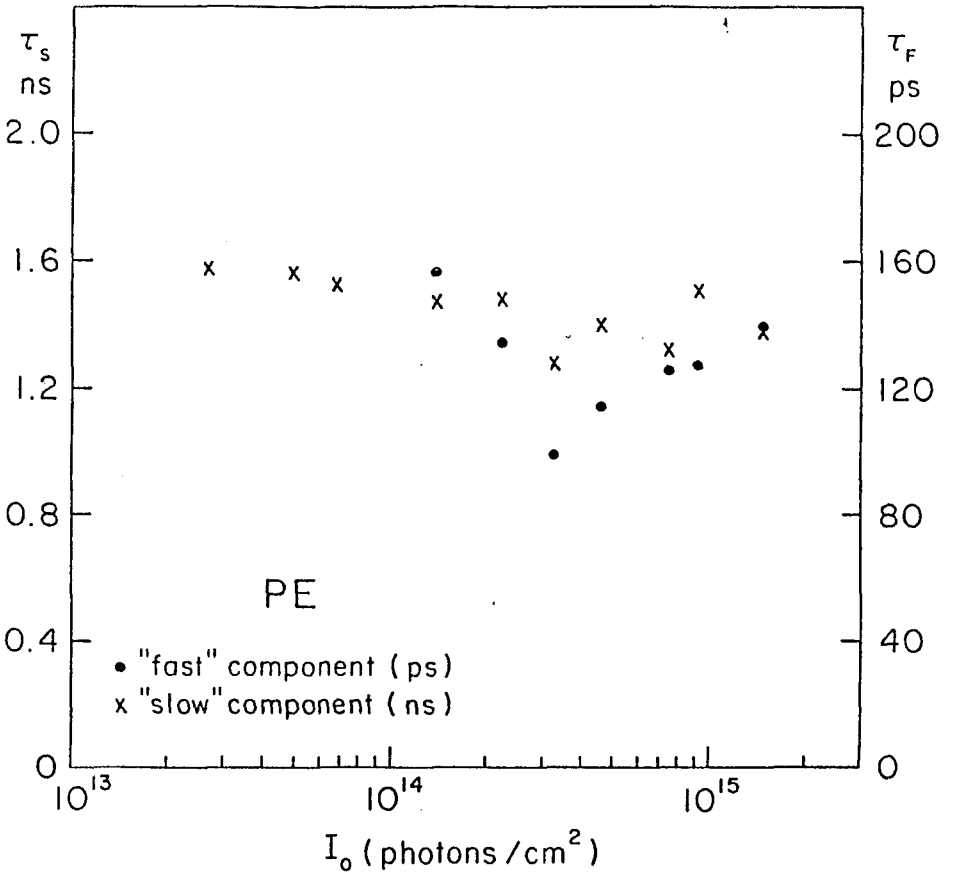

Fig. 6.3b Intensity Dependence of Fast and Slow Component of C-PE.

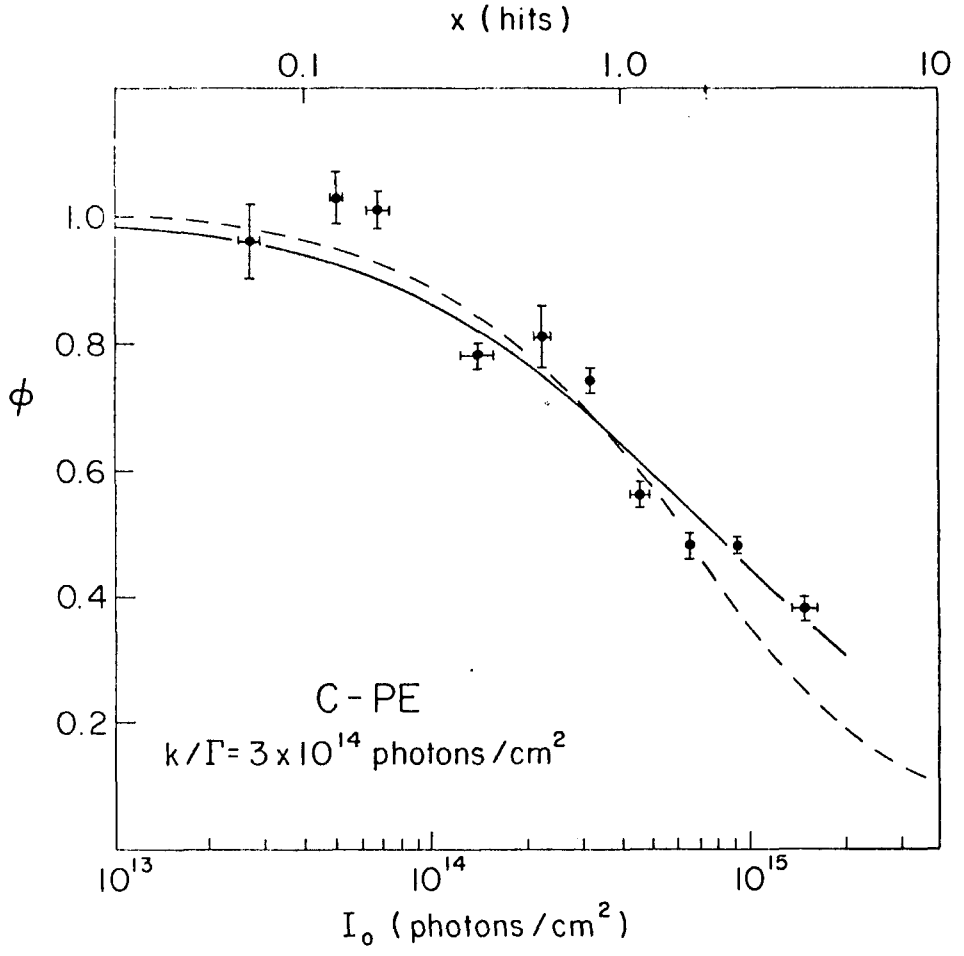

Fig. 6.4 Relative Fluorescence Yield of C-PE Versus Intensity.

Phycocyanin (C-PC)

The absorption and fluorescence emission and excitation spectra of c-phycocyanin in 0.1 M potassium phosphate at pH 7.0 are shown in Fig. 6.5. Excitation of C-phycocyanin at either 540 nm or 600 nm resulted in identical fluorescence emission spectra with no detectable fluorescence at 575 nm, characteristic of phycoerythrin contamination. Ultracentrifugation studies of C-PC at pH 7.0 in 100 mM phosphate at a protein concentration of 0.5 - 2 mg/ml showed the phycocyanin to exist predominantly as the trimer (5.7s) with approximately 25% in the hexameric (10.5s) aggregation state. The existence of these aggregation states of phycocyanin is well documented in the literature (Berns, 1971; Glazer, 1976, 1979; Bryant et al., 1979). The relative quantum yield of fluorescence measured relative to cresyl fast violet in ethanol was 0.75 ± 0.06.

In Fig. 6.6 the risetime of the C-PC fluorescence at pH5 and pH8 subsequent to single pulse excitation is compared with that from Rhodamine 6G. All of the risetimes were found to be within the temporal solution of the experimental system, $\leq$ 12 ps.

The decay kinetics of C-PC fluorescence, unlike that for C-PE, were found to be exponential (see Fig. 6.7a,b) for excitation intensities in the range 10^{13} to 10^{15} photons/cm^2. In Fig. 6.8 the intensity dependence of the relaxation time is shown. For a single pulse of I $\sim$ 3

x 10^{13} photons/cm^2, the fluorescence lifetime, $\tilde{\tau}$, was 2111 $\pm$ 83ps (10 single-shots). The lifetime declined with increasing excitation intensity giving $\tilde{\tau}$ = 1376 $\pm$ 24 ps (6 single-shots) at I = 1.3 $\pm$ 0.2 x 10^{15} photons/cm^2. As in the case of C-PE, the quantum yield for C-PC decreases with intensity as shown in Fig. 6.9. Measurements on C-PC obtained by the two different purification procedures gave similar results. No significant difference was observed in the fluorescence kinetics between C-PC samples at pH5 and at pH8.

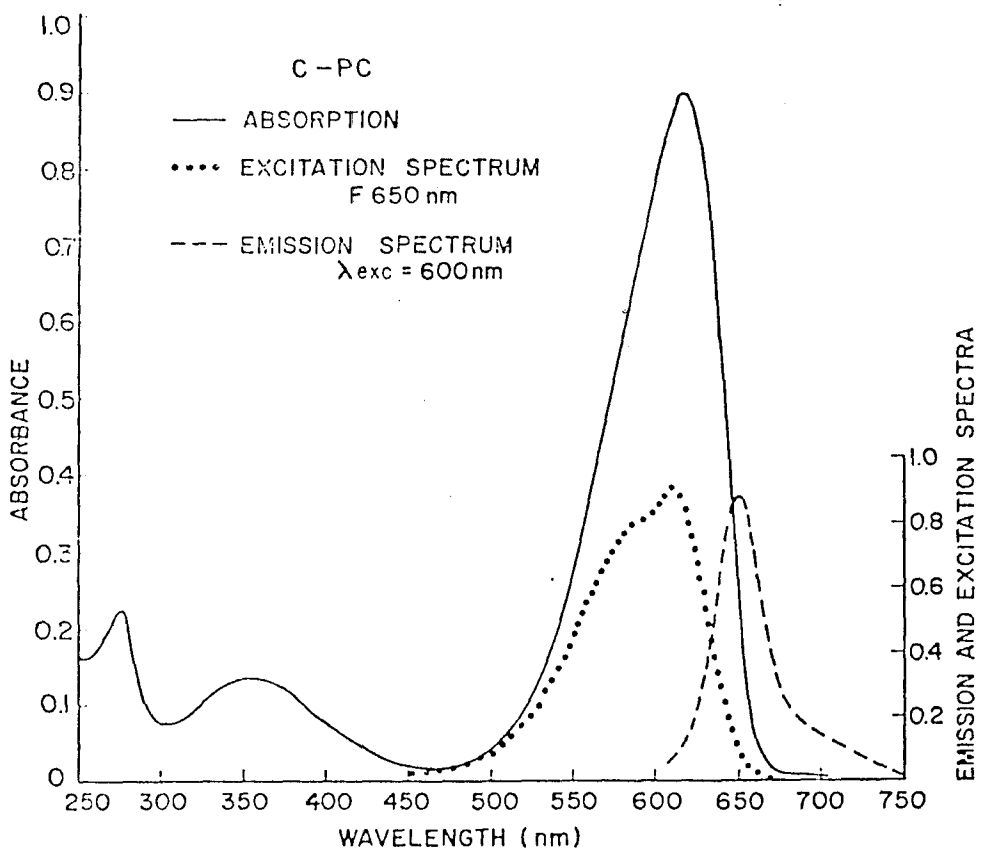

Fig. 6.5 Absorption, Emission and Excitation Spectra of C-PC.

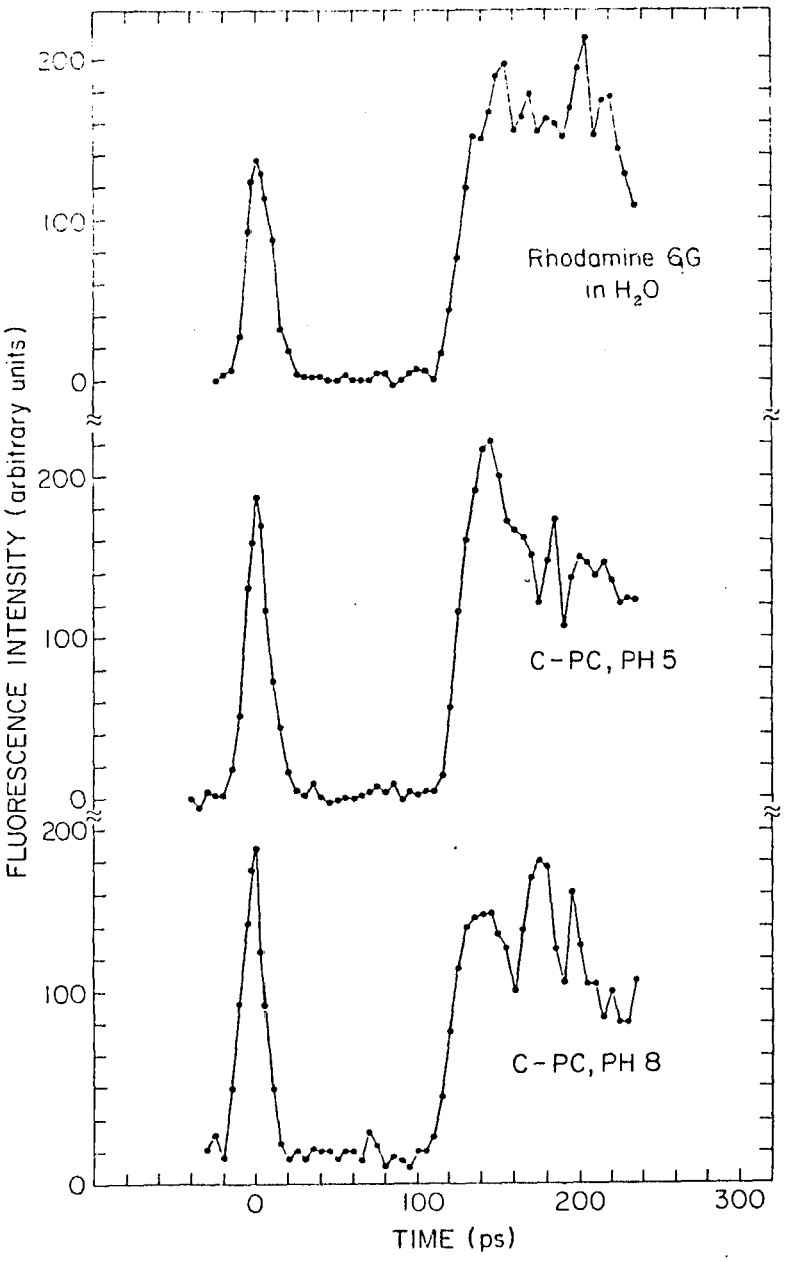

Fig. 6.6 Risetime of C-PC and Rhodamine 6G.

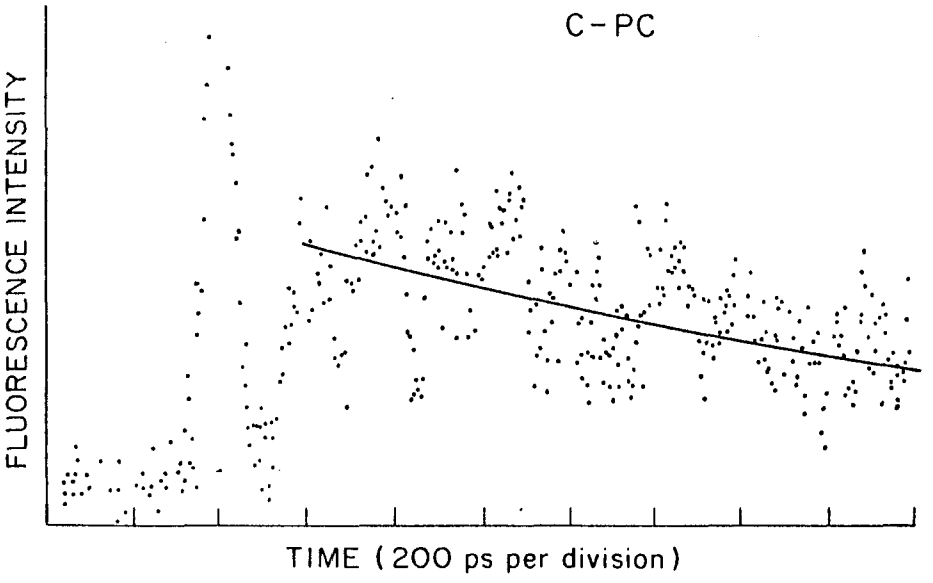

Fig. 6.7a Low Intensity Decay of C-PC.

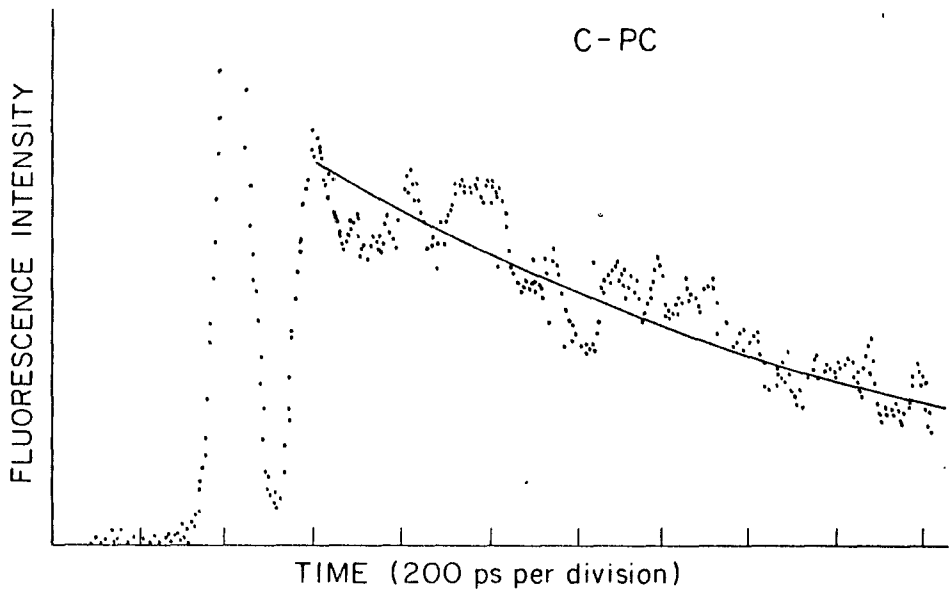

Fig. 6.7b High Intensity Decay of C-PC.

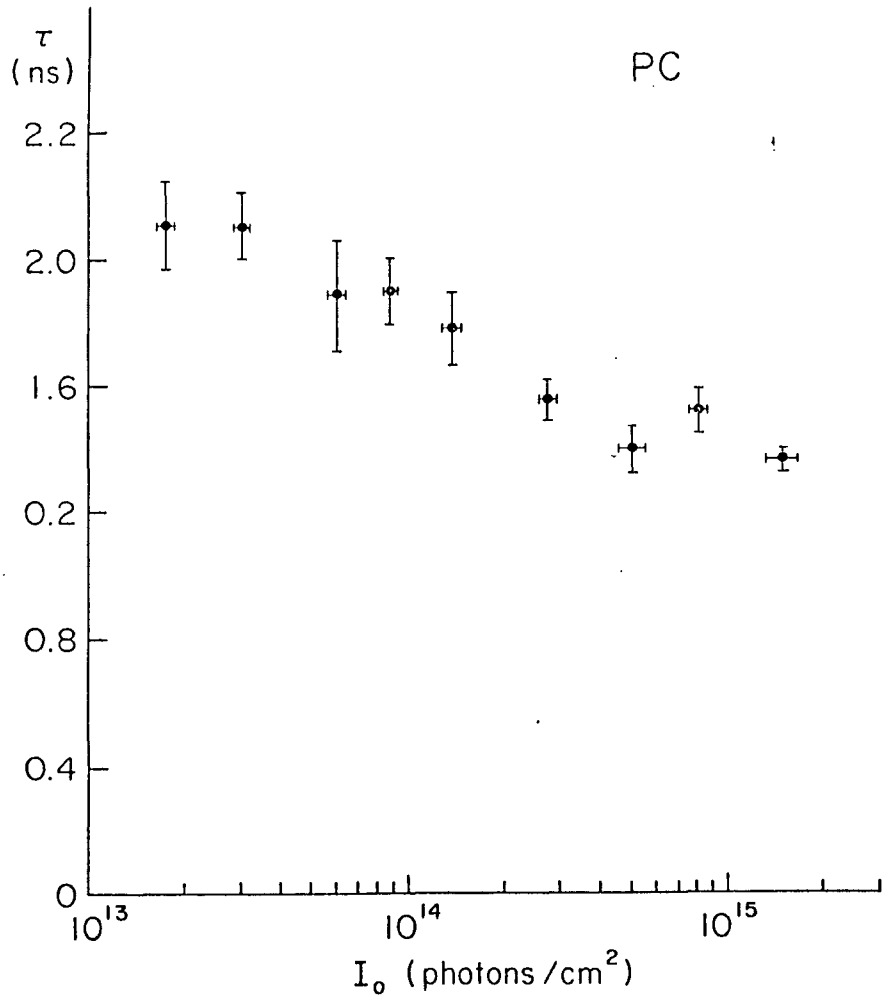

Fig. 6.8 C-PC Relaxation Time Versus Intensity.

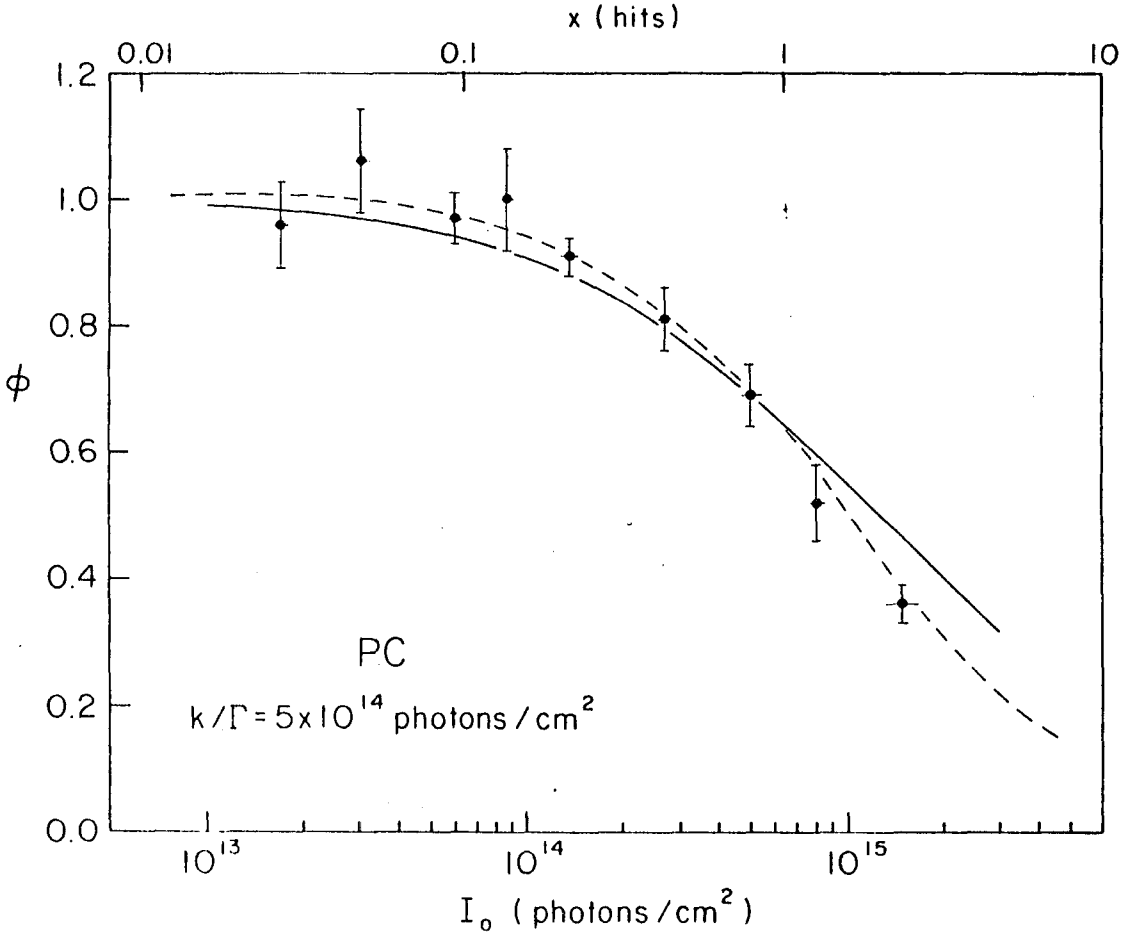

Fig. 6.9 Relative Fluorescence Yield of C-PC Versus Intensity.

Allophycocyanin (APC)

The sedimentation and spectral properties of allophycocyanin I, II, III and B are described in detail in Zilinskas et al., 1978; Zilinskas et al., 1980, and Troxler et al., 1980.

The individual fluorescence kinetics of the APC forms I, II, III, and B were measured separately. The fluorescence rise was within the instrument resolution time. The fluorescence decay curve in each sample was readily fitted with a single exponential at single pulse excitation intensities of 10^{13} to 10^{15} photons/cm^2 (see Fig. 6.10a,b). The relative fluorescence yield and lifetime for APC I, II, III and B are displayed in Figures 6.11a,b,c, and d, respectively. For I between 10^{13} and 10^{14} photons/cm^2, the fluorescence lifetime was 1932 $\pm$ 165 ps for APC I (average of 11 single shots), 1870 $\pm$ 90 ps for APC II (average of 17 single shots) and 1816 $\pm$ 88 ps for APC III (average of 14 single shots). The average of APC forms I, II, and III, was 1869 $\pm$ 62 ps (27 single-shots) and for APC B 2577 $\pm$ 121 ps (average 20 single-shots). Although the lifetimes were found to be 20% shorter at the higher excitation intensities, the fluorescence quantum yield remained constant throughout the intensity range investigated.

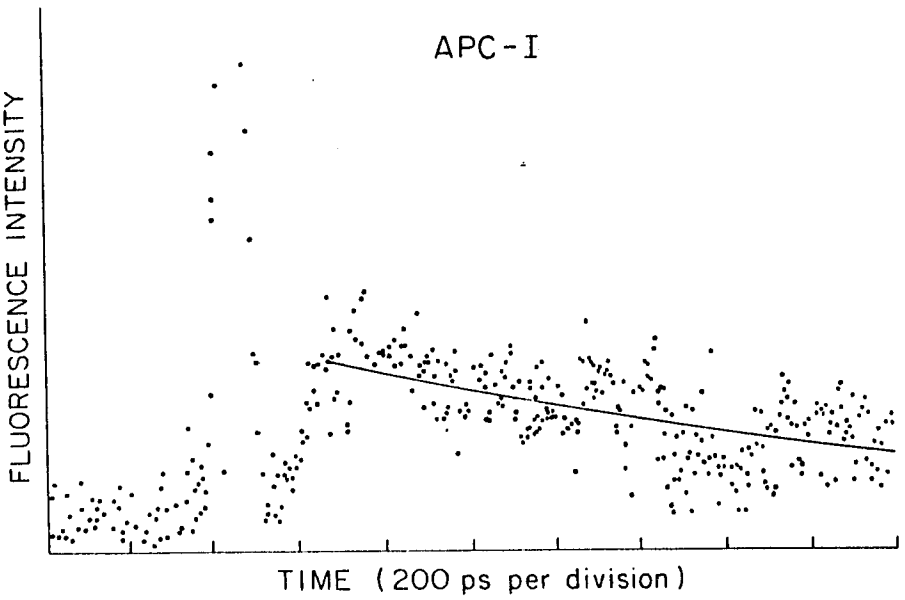

Fig. 6.10a Low Intensity Decay of APC.

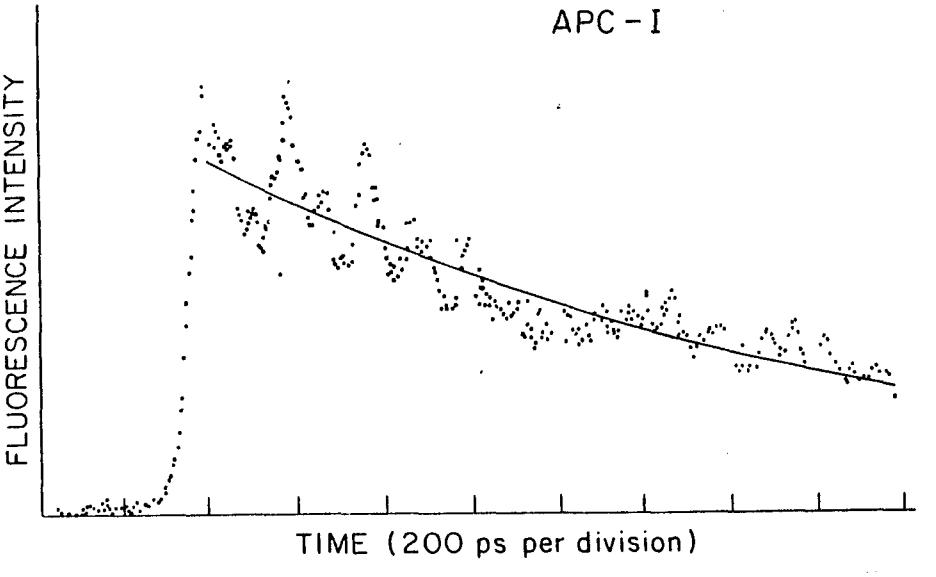

Fig. 6.10b High Intensity Decay of APC.

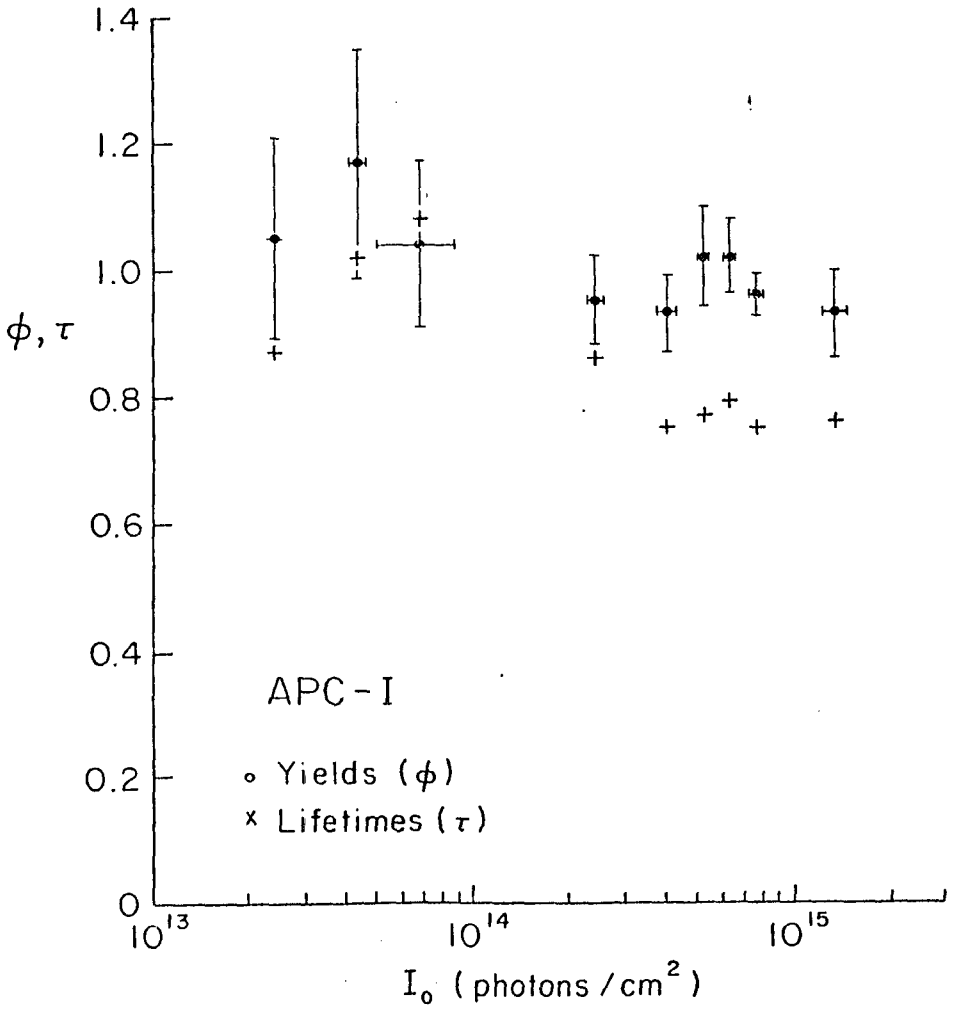

Fig. 6.11a Relative Fluorescence Yield and Lifetime of APC I.

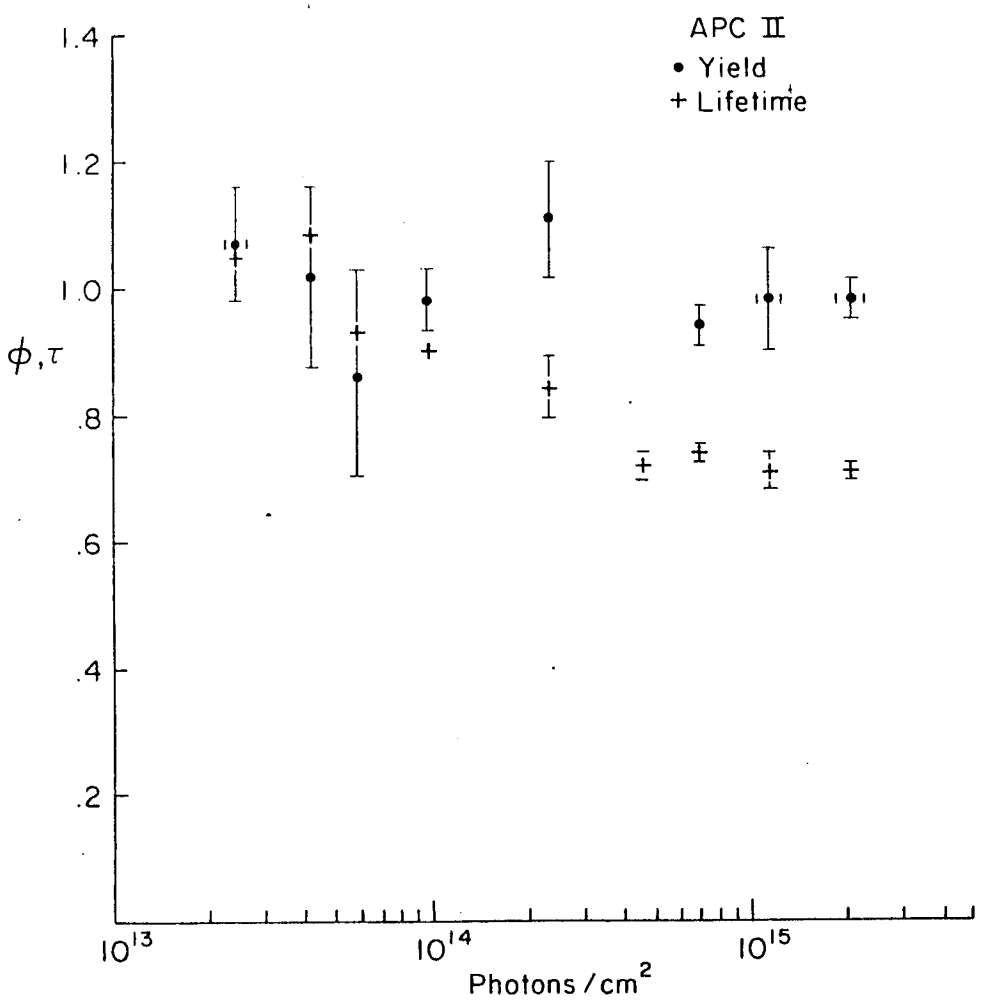

Fig. 6.11b Relative Fluorescence Yield and Lifetime of APC II.

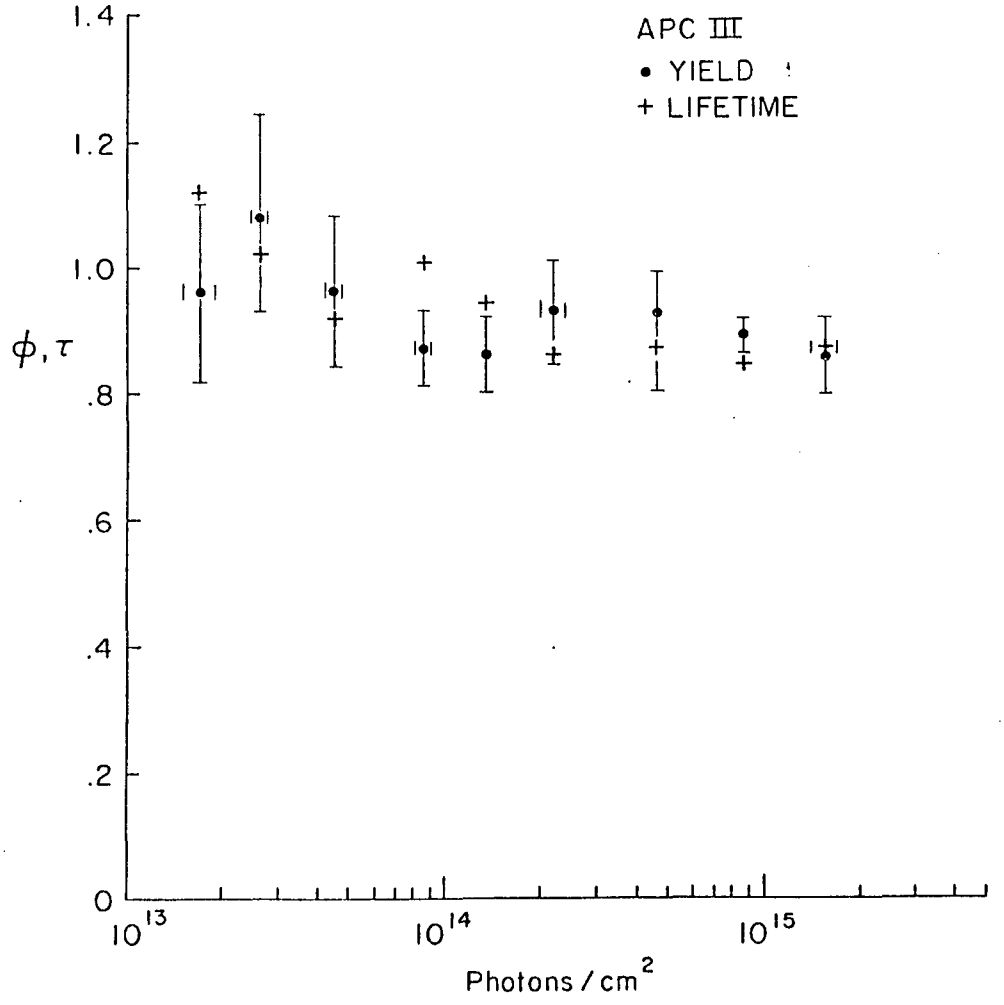

Fig. 6.11c Relative Fluorescence Yield and Lifetime of APC III.

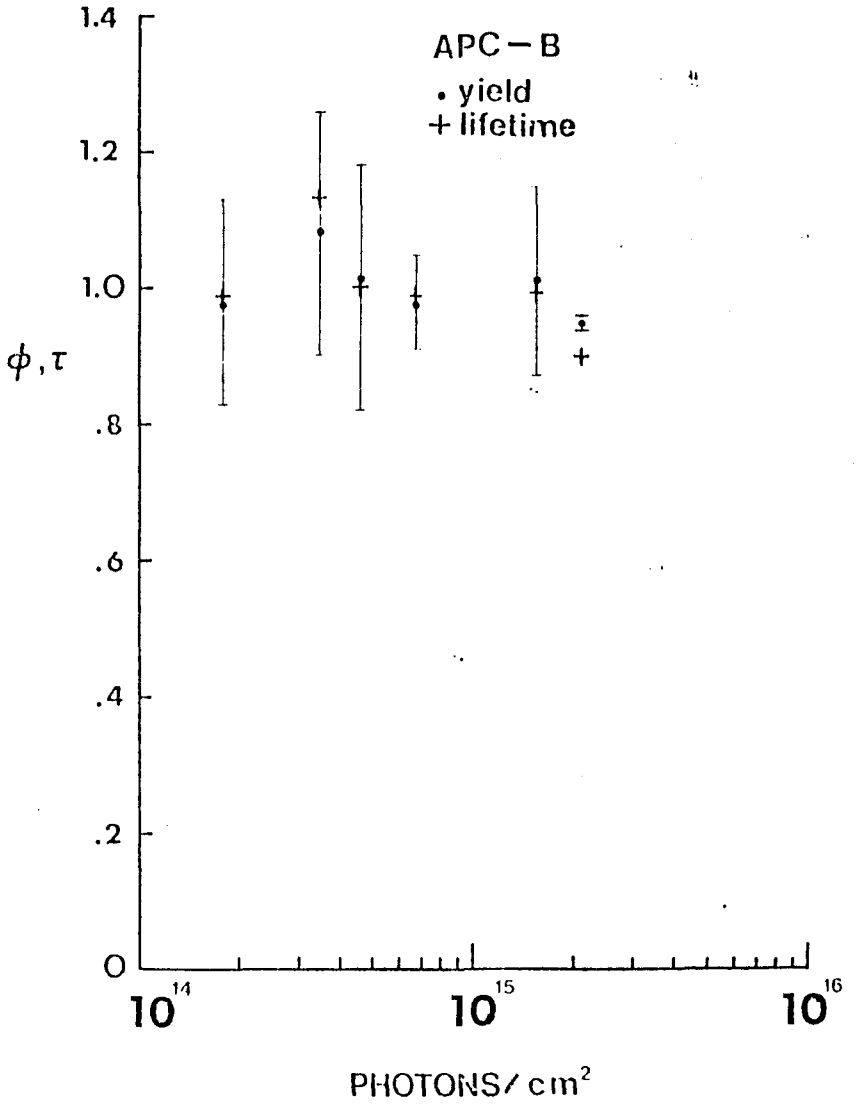

Fig. 6.11d Relative Fluorescence Yield and Lifetime of APC B.

Isolated Phycobiliproteins: Discussion

For the isolated phycobiliproteins exciton annihilation must occur within the chromophore pool of the individual phycobiliprotein units rather than between the isolated separate phycobiliprotein units in solution (i.e. the 18 phycocyanobilin chromophores in a C-PC hexamer and not between separate C-PC and C-PC hexamers in solution). In order to calculate the singlet-singlet annihilation coefficient, it is necessary to know the local absorption coefficient of the phycobiliproteins. This local absorption coefficient can be obtained by using the molar extinction coefficients of the individual biliproteins (Glazer and Hixson, 1975; Cohen-Bazire et al., 1977), the number of chromophores in each phycobiliprotein and the protein volumes (Glazer, 1976, 1979). Thus we obtain the local absorption coefficient at 530 nm for the phycobiliprotein units: $\alpha_{PE} \sim 2988\ cm^{-1}$, $\alpha_{PC} \sim 298\ cm^{-1}$ and $\alpha_{APC} \sim 86\ cm^{-1}$. Alternatively, these values can be calculated from the multiple excitation theory of Mauzerall (1978) based on a Poisson distribution of "hits" per phycobiliprotein units, which is presented below. The difference between the values calculated by these two methods, which can be as much as a factor of 4, can arise from uncertainties in the values used for the reported extinction coefficients in the literature, and the exact state of aggregation used in the experiment

(Glazer, 1976, 1979). Since the applicability of the multiple excitation theory is not well established, the values of α were obtained by using the extinction coefficient (Glazer and Hixson, 1975) and the molarity (Glazer, 1979) (for example see Geacintov et al., 1977; Campillo and Shapiro, 1978).

For the phycobiliproteins C-PE, C-PC, and APC I the singlet-singlet exciton annihilation coefficient, γ_{ss} can be calculated from the Γ's obtained from the fluorescence quenching curves of Fig. 6.4, Fig. 6.9 and Fig. 6.11a respectively. By using the measured low intensity fluorescence decay rates and k/Γ from quenching data we obtain:

$$\Gamma_{\text{C-PE}} = 2.15 \times 10^{-6} \text{cm}^2\text{sec}^{-1},$$

$$\Gamma_{\text{C-PC}} = 9.47 \times 10^{-7} \text{cm}^2\text{sec}^{-1}, \text{ and}$$

$$\Gamma_{\text{APC I}} \quad 6.7 \times 10^{-8} \text{cm}^2\text{sec}^{-1}.$$

Thus the threshold for the onset of exciton annihilation, which depends on the value of the local absorption coefficient and the singlet-singlet exciton annihilation rate, is different in the different phycobiliproteins. The calculated values for γ_{ss} are of comparable magnitude.

$$\gamma_{ss}\ (\text{C-PE}) \sim 1.44 \times 10^{-9} \text{cm}^3\text{sec}^{-1}$$
$$\gamma_{ss}\ (\text{C-PC}) \sim 6.3 \times 10^{-9} \text{cm}^3\text{sec}^{-1}, \text{ and}$$
$$\gamma_{ss}\ (\text{APC I}) \lesssim 1.6 \times 10^{-9} \text{cm}^3\text{sec}^{-1}.$$

These values are similar to the value measured for chlorophyll in chloroplast (Mauzerall, 1978; Geacintov et al., 1977). Although these singlet-singlet annihilation coefficients indicate a higher annihilation rate in C-PC over C-PE and APC, it is the higher local absorption of C-PE at the wavelength of excitation which allows exciton annihilation to manifest itself earlier in that phycobiliprotein.

Mauzerall (1978) has shown that for excitons confined to a localized domain the fluorescence yield can be described in terms of the number of excitations per domain by the equation:

$$\frac{\phi}{\phi(0)} = \frac{1 - e^{-x}}{x}$$

where X is the number of hits per domain. This equation also provides a satisfactory fit to the measured fluorescence quantum yield data as shown by the dashed lines displayed in Figs. 6.4 and 6.9. From these fits the following effective optical cross sections are estimated:

$\sigma_{PE} = 2.5 \times 10^{-15} cm^2$, $\sigma_{PC} = 1.7 \times 10^{-15} cm^2$ and $\sigma_{APC} < 1.2 \times 10^{-16} cm^2$.

The important aspect of the present work is the simultaneous evaluation of fluorescence lifetime and relative yield as a function of the excitation pulse intensity. An analysis of this data shows clear differences in the three groups of biliproteins. First, the APC's showed small intensity dependence of both the lifetime or relative yield. Second, C-phycocyanin showed a slight dependence of the lifetime, but a strong dependence of the relative yield on excitation intensity. Thus for PC the lifetime decreased 10-30% as the intensity of the excitation pulse increased from 10^{13} to 10^{15} photons/cm^2. Although the fluorescence decay remained exponential in this region, the relative fluorescence yield corresponded well with a model of exciton annihilation in the isolated C-PC, presumably in the monomers and trimers (Glazer, 1976; 1979). The fluorescence yield results for PC appear contradictory to those recently published by Kobayashi et al., (1979), where no intensity dependence of the yield was observed. However, a proper comparison between these two studies is not possible without knowledge of the beam cross-sectional area or equivalently the intensity region investigated by Kobayashi et al., (1979). C-PE showed a strong dependence of the fluorescence decay and relative yield on the excitation intensity. The change of the decay curve from

exponential to non-exponential with increasing intensity and the relative yield versus intensity followed the exciton annihilation quenching relation and is consistent with the occurrence of exciton-exciton annihilation in C-PE and C-PC. In conclusion, therefore, exciton annihilation appears to be the predominant mechanism which explains the fluorescence kinetics measurements for PE, PC and APC.

The observation that the fluorescence from the isolated biliproteins, in particular PC at pH 5 and pH 8, rise as fast as from rhodamine 6 G (Fig. 6.6) suggests that the fluorescent chromophores were excited in less than 12 ps. If one assumes that energy transfer from 's' to 'f' occurs in 32 to 85 ps (Kobayashi et al., 1979), then this result argues against the concept of energy transfer from the 's' to 'f' chromophores. But, if the 's' to 'f' energy transfer (Teale and Dale, 1970) does take place, it must occur in $<$ 12 ps. From these results, it appears that the fast absorption component in C-PC measured by Kobayashi et al., (1979), arises from singlet-singlet annihilation and not from the 's' to 'f' transfer.

Phycobilisomes: Results

Phycoerythrin Fluorescence in Phycobilisomes

The spectral region 560-600 nm was isolated for measurement on phycoerythrin fluorescence (emission peak at 575 nm). The rise of the C-PE fluorescence in PPS's was within the resolution time of the instrument $\sim$ 12 ps. A typical fluorescence decay curve for the C-PE emission component in PBS is shown in Fig. 6.12. The fluorescence relaxation kinetics for C-PE in the phycobilisomes were found to be exponential and intensity independent over the excitation intensity range 10^{13}-10^{15} photons/cm^2 (Fig. 6.13). The relaxation lifetime of C-PE fluorescence for intensities $< 10^{14}$ photons/cm^2 was 31 $\pm$ 4 ps, which is shorter than that reported by Searle et al., (1978) for PBS's isolated from Porphyridium cruentum and much shorter than that of isolated PE in solution.

The normalized fluorescence yield, defined as the ratio of the quantum yield at intensity I to the quantum yield at low intensities, is shown in Fig. 6.14. The fluorescence yield can be seen to decrease at an intensity $> 10^{14}$ photons/cm^2 per pulse. This decline occurs at a higher intensity than in the isolated phycobiliprotein C-PE. In addition, the decline takes place more slowly for the C-PE emission in PBS's than in the isolated pigment case.

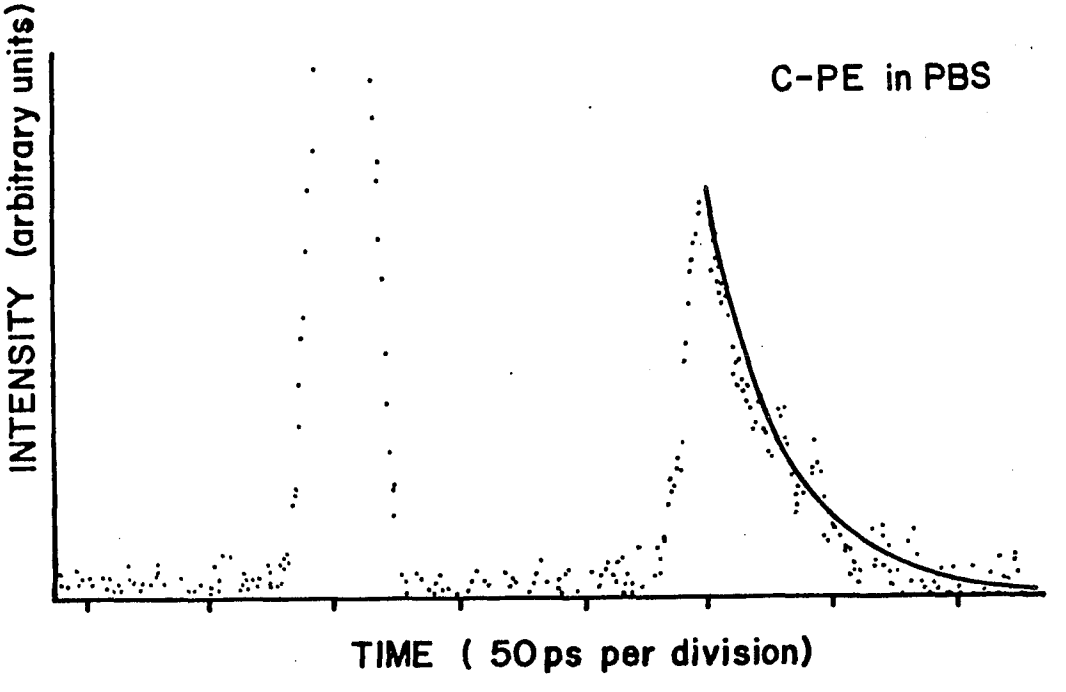

Fig. 6.12 Fluorescence Decay of C-PE in PBS.

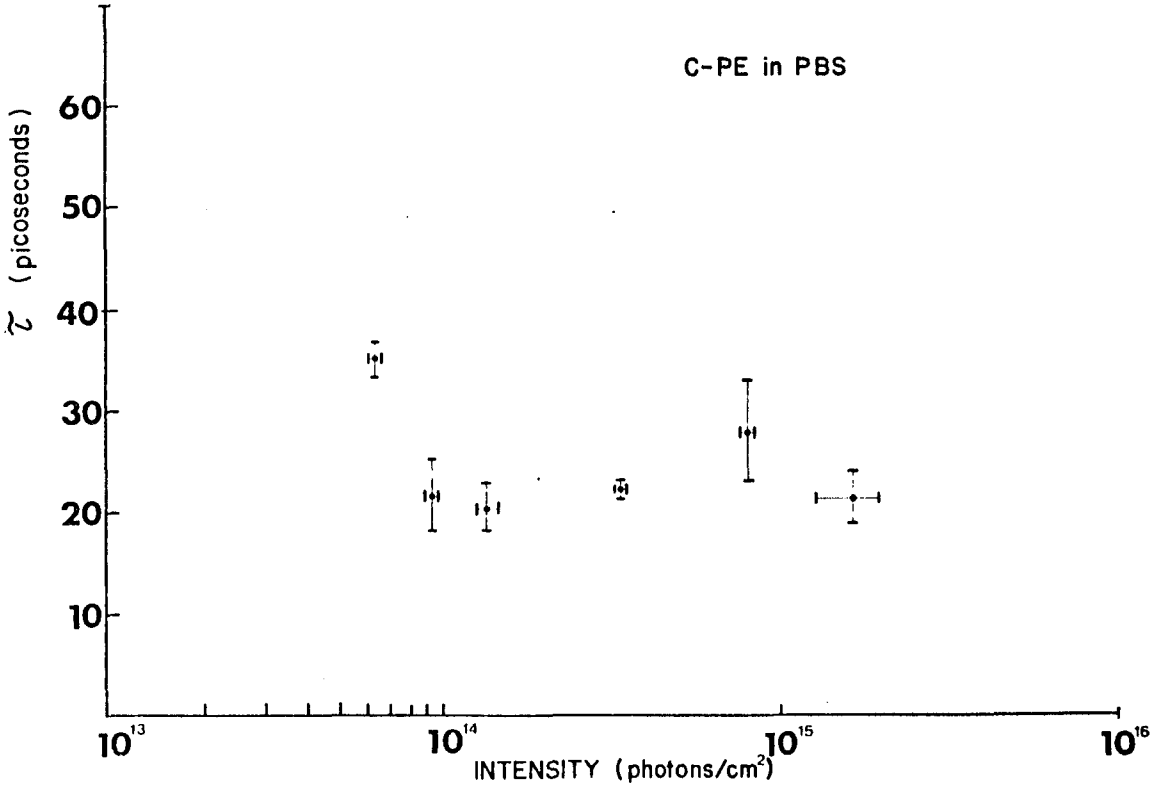

Fig. 6.13 Intensity Dependence of Relaxation Time for C-PE in PBS.

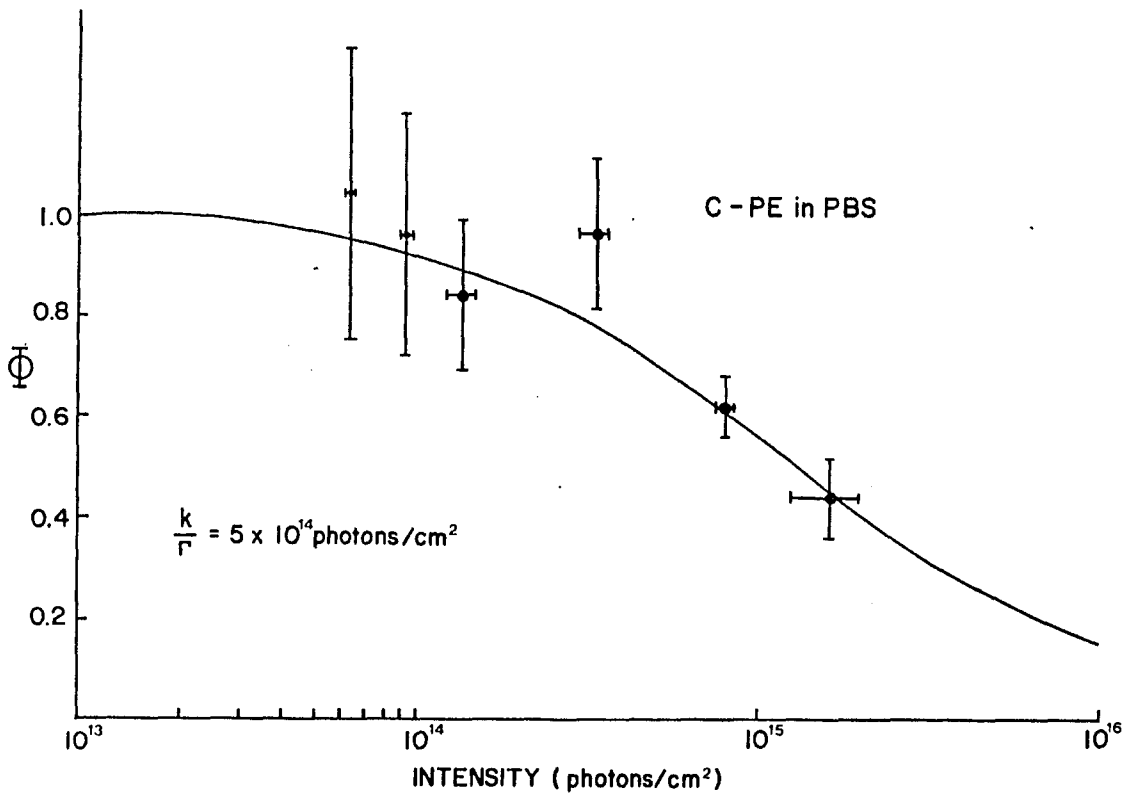

Fig 6.14 Relative Fluorescence Yield of C-PE in PBS Versus Intensity.

C-Phycocyanin + Allophycocyanin Fluorescence in Phycobilisomes

The spectral region > 600 nm was isolated for measurement of the C-PC+APC emission component from PBS's. A typical fluorescence rise curve for the C-PC+APC emission is shown in Fig. 6.15 and is compared with the resolution limited risetime for a 2×10^{-4}M solution of erythrosin in water. At low pulse intensities ($I < 6 \times 10^{13}$ photons/cm^2), the time for the C-PC+APC fluorescence to rise from 10% to 90% of the maximum level was 34 ± 13 ps (14 measurements). The decay kinetics showed a marked dependence on the excitation intensity (Fig. 6.16a,b).

The decay kinetics were found to be non-exponential, but could be adequately fitted with a sum of two exponentials. In Fig. 6.17 a plot of the 1/e decay times as a function of the intensity of the excitation pulse is displayed. The relative amplitudes and lifetimes for the low and high intensity regions may be summarized as follows: at a pulse intensity of 2.7×10^{13} photons/cm^2 the decay was $F = 1.2 \exp(-t/212) + \exp(-t/1174)$ and at 2.7×10^{15} photons/cm^2 the decay could be described by $F = 6.2 \exp(-t/83) + \exp(-t/716)$, with t in picoseconds. The calculated fluorescence yield dropped by a factor of ~ 13 over the intensity range investigated (Fig. 6.18).

This large decrease in the fluorescence quantum yield

for APC in PBS's does not follow the yield dependence observed in the isolated phycobiliprotein APC, where the fluorescence quantum yield varied by less than 20% over the intensity range 10^{13}-10^{15} photons/cm^2 per pulse.

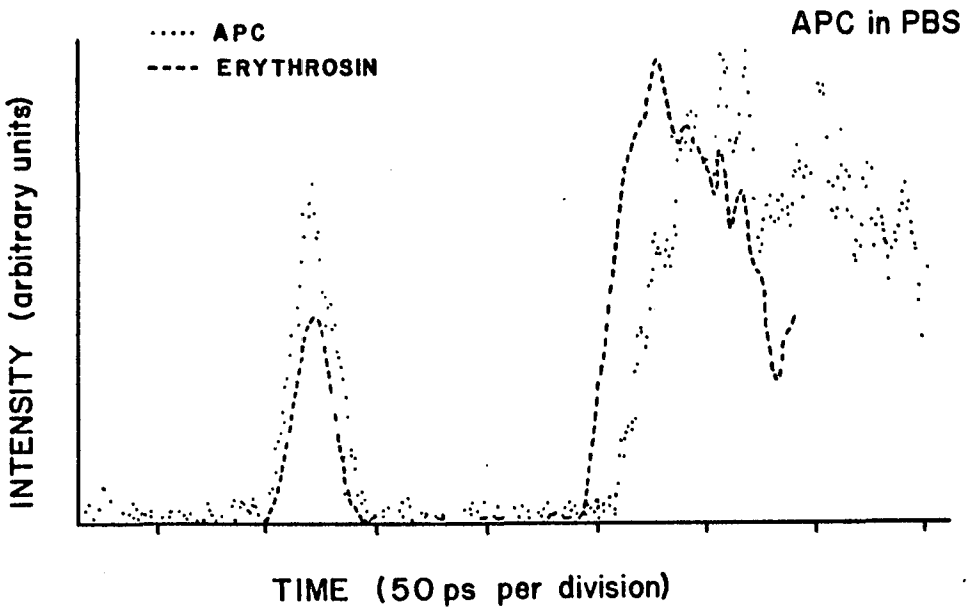

Fig. 6.15 Risetime of Erythrosin and C-PC+APC emission in PBS.

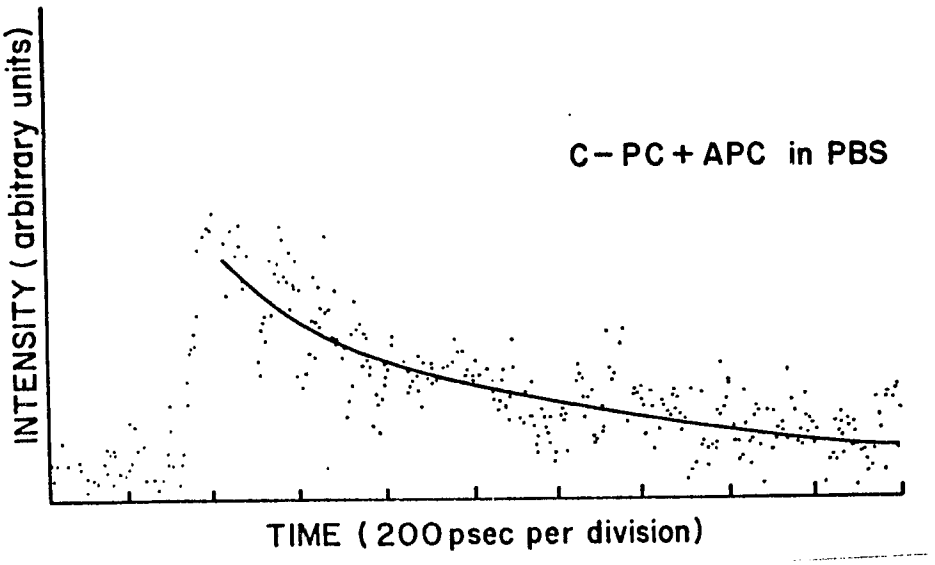

Fig. 6.16a Low Intensity Decay of C-PC+APC emission in PBS.

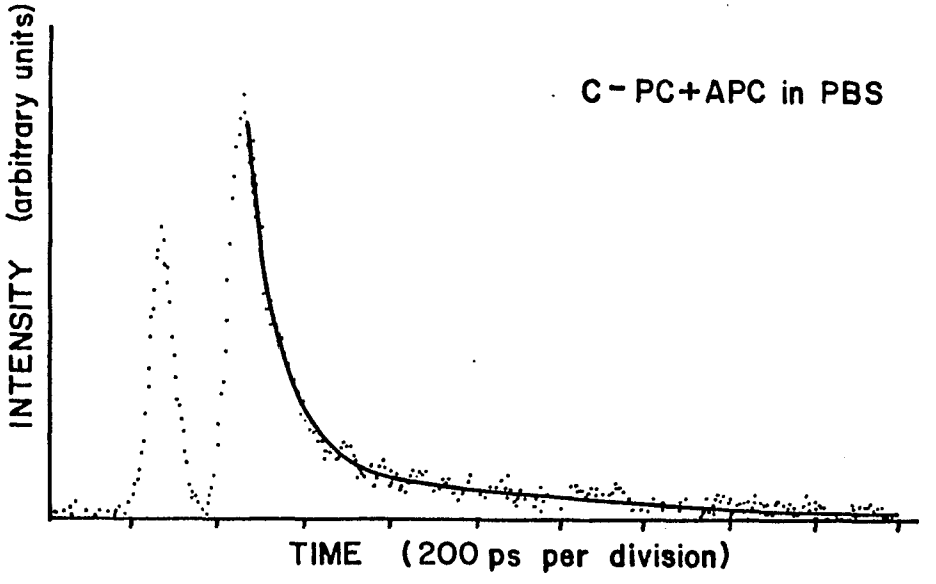

Fig. 6.16b High Intensity Decay of C-PC+APC emission in PBS.

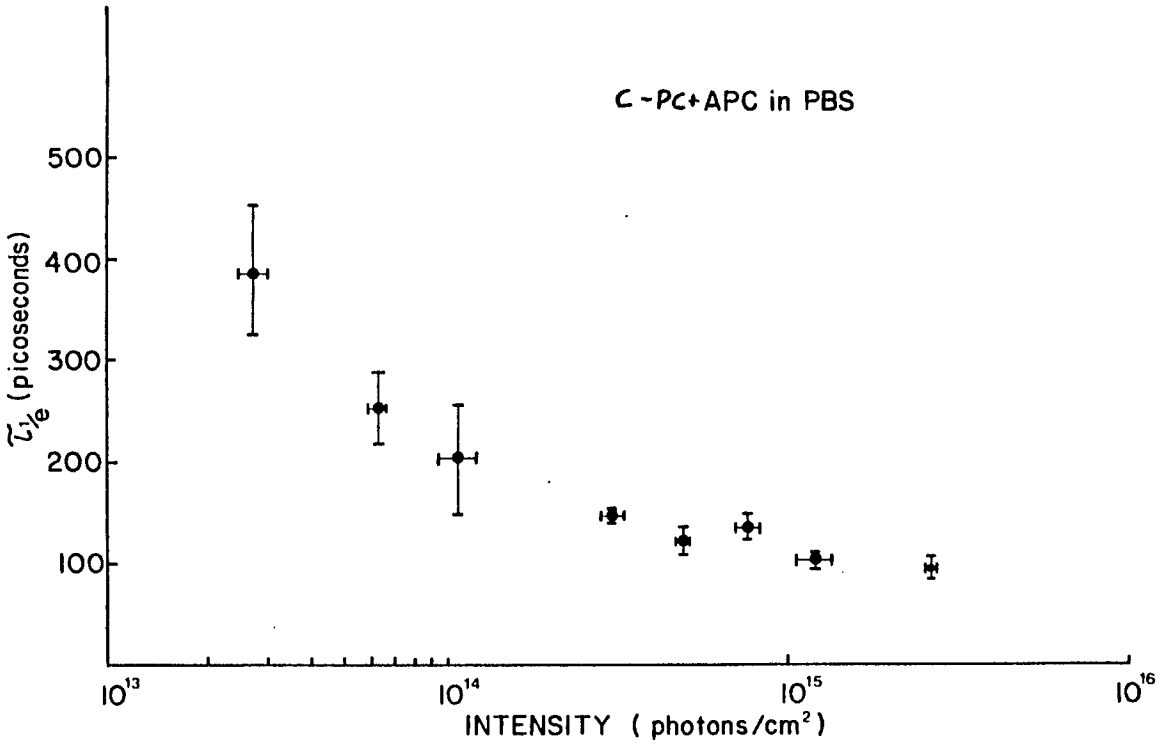

Fig. 6.17 Intensity Dependence of Relaxation Time of C-PC+APC emission in PBS.

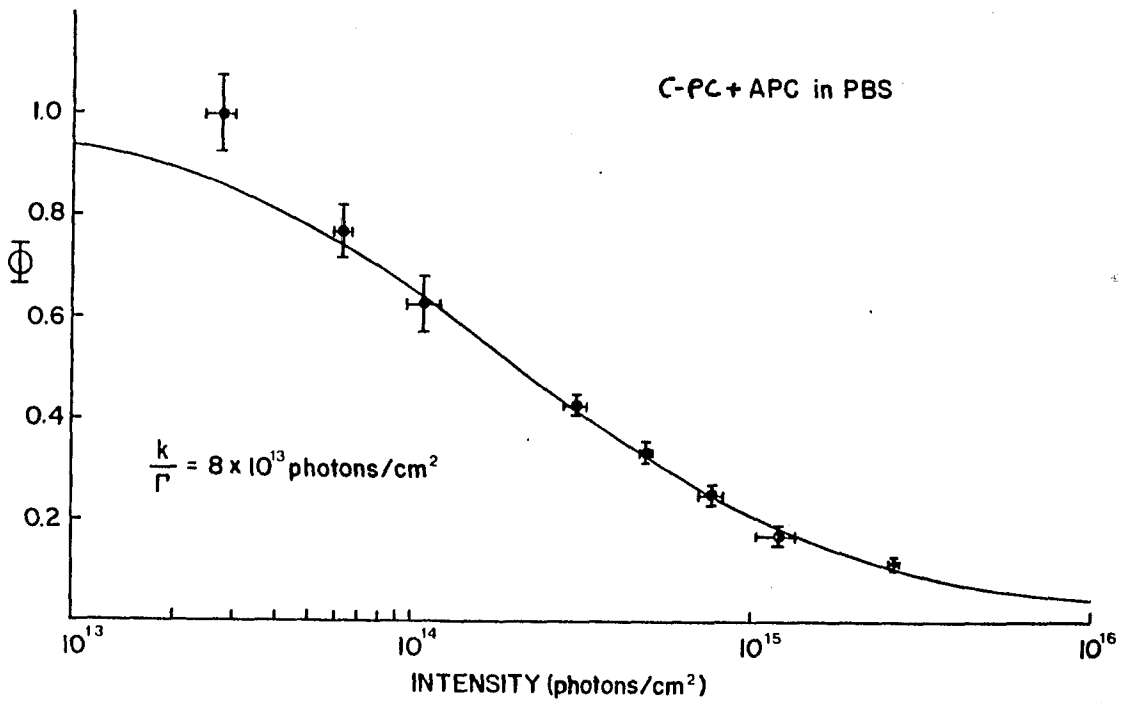

Fig 6.18 Relative Fluorescence Yield of C-PC+APC emission in PBS Versus Intensity.

Fluorescence Measurements in Phycobilisomes: Discussion

In the case of the intact phycobilisomes, the dramatic decrease in both the lifetime and quantum yield with intensity for the C-PC+APC emission component, as compared to the isolated case, is the result of the efficient transfer from PE which results in a higher effective absorption coefficient for APC in PBS at 530 nm than in the isolated APC case. In PBS's the stacked configuration of the C-PE and C-PC units gives rise to a higher local absorption and quenching relative to the unstacked units. The radial arrangements of the phycobilin units in PBS's causes a concentrated clustering of APC units at the core. The clustering decreases with increasing radial distance from the central APC units through C-PC and C-PE. This radial structure enhances singlet-singlet annihilation processes as well as energy transfers through the natural funneling, or directed migration of excitations from C-PE to C-PC and APC. At low intensity ($< 10^{14}$ photons/cm^2), the isolated components and the C-PE emission from PBS show little quenching, and $(k/\Gamma)_{APC/PBS} \sim 8 \times 10^{13}$ photons/cm^2, which is $\sim$ 100 times less than the estimated value for k/Γ for the isolated APC. This can be partly attributed to a higher effective absorption coefficient for APC in PBS's, since in PBS the relevant local absorption is that of C-PE. The relative local absorption of a C-PE unit is approximately 35 times

larger than that of a unit of APC. Thus there will be a higher singlet state population for APC in PBS as compared to isolated APC at a given excitation intensity at 530 nm. The difference between the estimated drop of $\sim$ 35 due to the contribution from the higher effective absorption and the observed decrease of $\sim$ 100 can be attributed to annihilation both within and among the C-PE and C-PC units in PBS, and the cumulative transfer from these units to the APC core.

The fluorescence decay of isolated C-PE in solution measured in this work was found to be exponential, with 1/e time of 1552$\pm$31 ps for pulse intensities $< 10^{14}$ photons/cm^2 and non-exponential with components: 1/e times, 130 ps and 1417 ps at higher intensities. In the PBS's, however, the C-PE fluorescence relaxation lifetime at pulse intensities $< 10^{14}$ photons/cm^2 was 31 $\pm$ 4 ps (Fig. 6.13), and was not dependent on the intensity of the excitation pulse. The measured short-lifetime, single-component process for the relaxation of the lowest excited singlet state of C-PE directly reflects the transfer of excitation energy from C-PE to C-PC in the PBS complex. This is supported by the measured risetime of C-PC+APC of 34 ps. A comparison of these findings with those of Searle et al., (1978) for PBS's isolated from P. cruentum, indicates that the fluorescence lifetime of phycoerythrin in phycobilisomes is indeed short and excitation intensity independent. The nearly four fold

difference between this measurement and those of Searle et al., (1978) is consistent with the idea of a greater efficiency of energy transfer in phycobilisomes of the blue green algae.

The drop in the fluorescence quantum yield for the C-PE emission from PBS's is comparable to that observed in the isolated phycobiliprotein C-PE, even though the relaxation rate k at low intensity is $\sim$ 30 times larger than in the isolated case. This can be explained by the higher singlet-singlet annihilation which, for the case of PBS's, occurs not only within a C-PE unit but among the several stacked C-PE units.

An estimate of the singlet-singlet annihilation coefficient for the case of C-PE in PBS's may be obtained by using the relation for the fluorescence yield at intensity I to the fluorescence yield at low intensities (Geacintov et al., 1977).

$$\frac{\phi(I)}{\phi(0)} = \frac{k}{\Gamma_I} \ln\left(1 + \frac{\Gamma_I}{k}\right) ,$$

where k is the inverse of the lifetime of fluorescence at low intensities and Γ is the singlet-singlet annihilation parameter related to the bimolecular rate constant for singlet-singlet annihilation, γ_{ss} through the local absorption coefficient, α, as $\Gamma = \gamma_{ss}\alpha/2$ (Campillo et al., 1976; Swenberg et al., 1976; Beddard et al., 1977;

Campillo et al., 1977; Geacintov et al., 1977; Mauzerall, 1978). This relation, plotted as a solid line in Fig. 6.4 satisfactorily fits the fluorescence yield data for the parameter $(k/\Gamma)_{PE} = 3\times10^{14}$ photons/cm^2. In PBS's from the fluorescence yield curve for C-PE in PBS's we obtain a value of,

$$\frac{k}{\Gamma} = 5.0 \times 10^{14} \text{ photons/cm}^2.$$

Using the experimentally measured value for k of 3.2×10^{10} sec^{-1} allows us to calculate the singlet-singlet annihilation parameter to be

$$\Gamma_{PE/PBS} = 6.4 \times 10^{-5} \text{cm}^2\text{sec}^{-1}.$$

This value is $\sim$ 30 times larger than in the isolated C-PE. The larger value for Γ_{PE} in the PBS as opposed to the isolated case can be attributed to increased contributions from both the effective local absorption coefficient and the singlet-singlet annihilation coefficient. Since C-PE in PBS's occurs in unit clusters consisting of 6 phycoerythrobilin units, the local absorption coefficient is,

$$\alpha_{PE/PBS} = 6\,\alpha_{PE} .$$

The singlet singlet annihilation coefficient, γ, may

be higher since the closer distances for the phycoerythrobilin units in the PBS's allows for a faster transfer of the excitation energy between the units as opposed to the isolated case.

As the C-PC component emission overlaps the component emission from APC in PBS's, a direct comparison between the fluorescence kinetics of the isolated phycobiliprotein C-PC in solution and its corresponding emission in PBS's is not possible. The measured lifetime for C-PC in solution is 2111±83 ps, which is in excellent agreement with previous reports for this biliprotein in the literature (Barber and Richards, 1977; Zilinskas et al., 1978).

A plot of the fluorescence quantum yield relationship for the parameter $(k/\Gamma)_{PC} = 5 \times 10^{14}$ photons/cm^2 obtained from the fluorescence quenching data for C-PC shown in Fig. 6.9 obtains a satisfactory fit of the experimental data.

The lifetime of the APC phycobiliprotein isolated by chromatography has been measured previously by Grabowski and Gantt (1978) who reported a value of 2.7±0.1 ns for

APC, and Wong, Zilinskas, Merkelo, and Govindjee (unpublished) who obtained 2.5±0.1 ns for all four forms of APC. The values of 1869±62 ps for the average lifetime for APC I, II, and III, and 2577±121 ps for APC B measured in this work are therefore taken to be in reasonable agreement with previous results. All the above lifetimes for APC are significantly shorter than the 4 ns for APC in the red alga, Porphyridium cruentum reported by Searle et al., (1978). It is not possible to speculate on the significance of this difference since the biochemical identity of the species containing the fluorescent chromophore was not ascertained in that work (Searle et al., 1978) and APC was extracted from a different alga.

In the case of the isolated phycobiliprotein APC, exciton annihilation may occur at a substantially higher intensity than was covered in this experiment. By extrapolating a fit to the ϕ vs I curve shown in Fig. 6.11a, the onset of quenching is estimated to occur at a value of $\frac{k}{\gamma} < 8 \times 10^{15}$ photons/cm^2. In PBS's the APC fluorescence risetime of 34 ps, which is taken as the time for the fluorescence to rise from 10% to 90% of its maximum value, is in good agreement with the fluorescence relaxation time measured for the PE emission.

The decay of APC fluorescence from PBS's is intensity dependent (Fig. 6.17 and 6.18), and therefore supportive of the interpretation that exciton annihilation in the PBS's occurs at the level of the allophycocyanins.

The C-PC+APC fluorescence emission from PBS's can be described by a dual exponential decay. Complete isolation of the C-PC emission component from that of APC in PBS's is not possible due to the overlap in the absorption and emission bands of these 2 components. Therefore, at low intensity ($< 10^{14}$ photons/cm^2), the fast component of 189 $\pm$ 20 ps can be due to the C-PC emission which is indicative of energy transfer from C-PC to APC.
As in the case of the C-PE emission we may obtain an estimate of the singlet-singlet annihilation parameter Γ_{APC}. From Fig. 6.18, it can be seen that,

$$\frac{k}{\Gamma_{APC/PBS}} = 8 \times 10^{13} \text{ photons/cm}^2.$$

Using k^{-1} = 1200 ps gives

$$\Gamma_{APC/PBS} = 1.04 \times 10^{-5} \text{ cm}^2 \text{ sec}^{-1}.$$

A comparison of the different fluorescence characteristics measured for the isolated phycobiliproteins as opposed to the case of intact phycobilisomes dramatically reveal the presence of energy transfer in the phycobilisome complex from C-PE → C-PC → APC. In addition, reports in the literature have shown much variation in the lifetime of C-PE fluorescence: 3.5$\pm$0.25 ns by Dale and Teale (1970), 3.1$\pm$0.1 ns by Barber and

Richards (1977), 2.6±0.2 ns for C-PE-I and 2.8±0.1 ns for C-PE-II by Grabowski and Gantt (1978), and 1.6±0.1 ns by Wong, Zilinskas, Merkelo, and Govindjee by the phase shift method (unpublished). The measurement reported here is in very good agreement with this latter measurement, and has helped to resolve this controversy.

Chapter 7. Energy Transfer Kinetics in the Carotenoid Accessory Pigment Complex of Photosynthetic Systems.

The most rewarding part of my thesis research was undoubtedly the investigation of the fluorescence from the yellowed leaves of the Norway maple. Over the last decade chlorophyll fluorescence from various photosynthetic systems has been investigated in order to obtain information on the energy transfer kinetics in the primary stages of the photosynthetic process. Although much interest has been expressed in the role of carotenoids in the primary energy transfer stages, little or no information has been obtained experimentally. The carotenoids form a major accessory pigment component which are present in nearly all photosynthetic organisms. Carotenoids consist of yellow-orange pigments which can be divided into two major groups, carotenes and carotenols (also known as xanthophylls). In higher green plants, both α, β, and δ carotene may be present, with β carotene forming the major component. Various forms of carotenols are found in higher green plants (e.g. lutein, violaxanthin and neoxanthin). The carotenoid absorption band spans the wavelength region from 380 to 510 nm.

The aim of this research has been to obtain an understanding of the energy transfer kinetics in the carotenoid accessory pigment system and to elucidate its

role in the overall energy transfer process. Since the fluorescence lifetime of chlorophyll emission from photosynthetic systems has been measured to be $\leq$ 10 ps (Yu et al., 1975, 1977; Campillo et al., 1976; Porter et al., 1977), it is generally accepted that carotenoid-chlorophyll energy transfer occurs within this time. In addition, no in vivo carotenoid fluorescence emission has been reported to date. However, it was not until this investigation of the autumnal yellow leaf from the Norway maple (Acer platenoides) that a more general possibility became apparent of approaching energy transfer kinetics from the point of view of a structural framework relating the physical arrangement of the accessory pigments on the photosynthetic membranes to their fluorescence kinetic properties.

In this study the emission kinetics from the carotenoids of the Norway maple leaf (Acer platenoides) and spinach leaf (spinacea oleracea) have been investigated as a function of excitation pulse intensity and wavelength of emission. The low temperature (90^{o} K) emission kinetics from the carotenoids of the yellow Norway maple as well as the effect of aging on a green spinach leaf have also been measured.

Experimental Methods:

The steady state fluorescence spectra was measured using 488 nm excitation from a 15 mW Argon ion laser, a Spex double spectrometer and RCA 7265 S-20 photomultiplier. The fluorescence signal was analyzed by a Princeton Applied Research (PAR) HR-8 lock-in amplifier (spectra uncorrected for instrumental response). The fluorescence kinetics were measured using a streak camera-optical multichannel analyzer system, previously described (Pellegrino et al., 1981). The spectral emission kinetics were analyzed with the use of Ditric cut-off filters (660 nm short pass) Corning 3-67, Optical Coatings Laboratory Cyan dichroic filter (600 nm cutoff) and narrow band filters. The low temperature (90^{o} K) kinetics for the yellow Norway maple leaf were measured by exciting a leaf inside a Nitrogen gas flow Dewar.

Experimental Results:

A. Yellow Norway Maple Leaf:

The steady state fluorescence emission from a yellow Norway maple leaf (Acer platenoides) is shown in Fig. 7.1. The important features of this spectrum are the absence of the prominent 685 nm emission from chlorophyll and the marked presence of an emission band spanning the wavelength region from 500 to 620 nm.

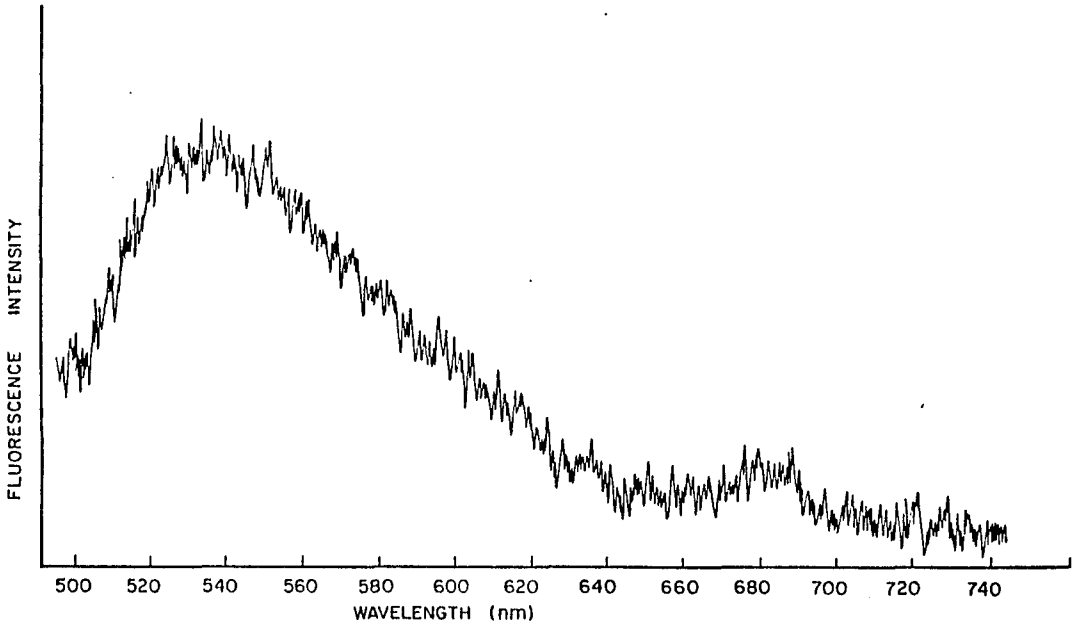

Fig. 7.1 Steady State Fluorescence Spectra from Yellow Maple Leaf at Room Temperature.

The low intensity (8×10^{13} photons/cm^2 per pulse) fluorescence lifetime from the same yellow leaf of the Norway maple was also measured using the picosecond streak camera apparatus. The region from 540 - 600 nm was isolated with the use of an Optical Coatings Laboratory (OCLI) cyan-dichroic filter and Corning 3-67 filter. A lifetime of 172 $\pm$ 41 ps was obtained. This lifetime is comparable to the decay time measured for spinach chloroplast (200 ps) in this intensity region (Yu et al., 1977, Geacintov et al., 1977). The kinetics measured for the yellow leaf of the Norway maple were characterized by a double exponential for excitation intensities greater than 5.7×10^{14} photons/cm^2 per pulse. At an average intensity of $5.7 \pm 0.5 \times 10^{14}$ photons/cm^2 per pulse (9 measurements), the long component decayed with a lifetime of 385 $\pm$ 38 ps and the fast component with 51 $\pm$ 7 ps with relative amplitudes of 0.39 $\pm$ 0.03 and 0.61 $\pm$ 0.03 for the long and short component respectively. As the intensity was increased to $1.44 \pm 0.14 \times 10^{15}$ photons/cm^2 per pulse both decay components remained essentially constant (369 $\pm$ 36 ps and 43 $\pm$ 6 ps with relative amplitudes of 0.34 $\pm$ 0.03 and 0.66 $\pm$ 0.03 for the long and short component respectively). A plot of the fluorescence lifetime and relative quantum yield as a function of excitation pulse intensity from the yellow Norway maple leaf is shown in Fig. 7.2 and 7.3 respectively. The intensity dependence of the fluorescence lifetime

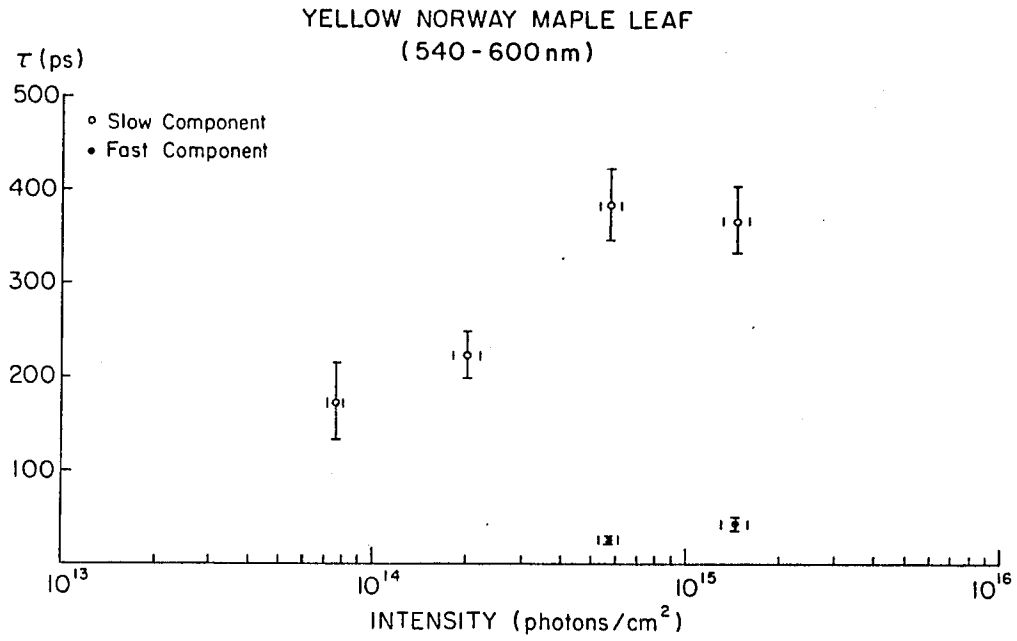

Fig. 7.2 Fluorescence Decay Time of Yellow Norway Maple Leaf Measured as a Function of Excitation Pulse Intensity.

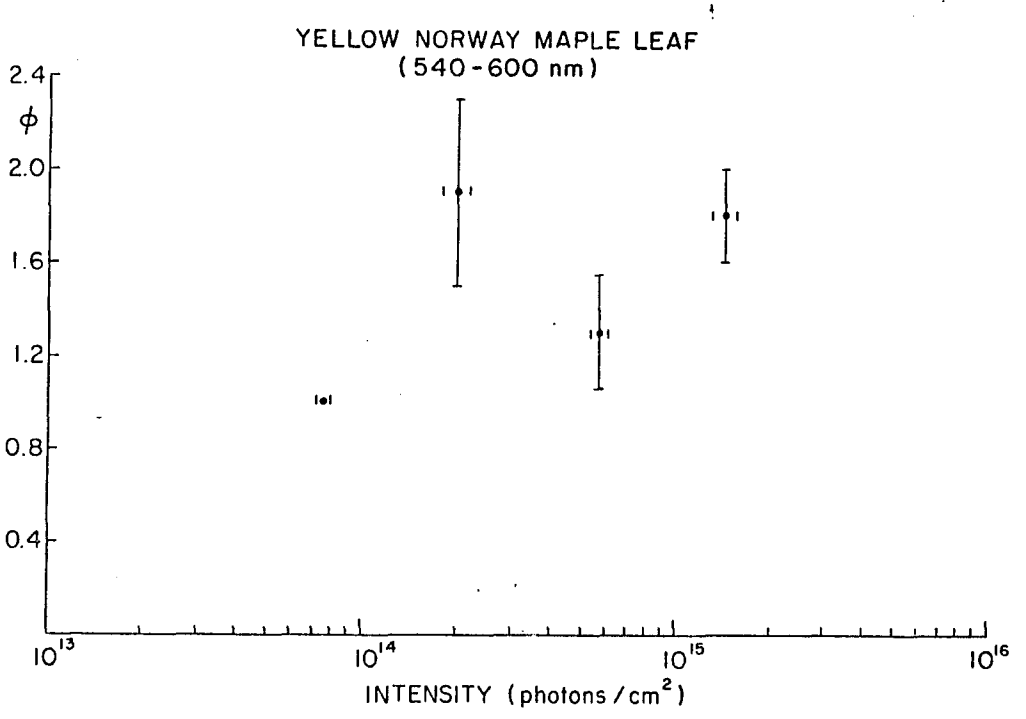

Fig. 7.3 Relative Fluorescence Quantum Yield from Yellow Norway Maple Leaf Measured as a Function of Excitation Pulse Intensity.

parallelled the intensity dependence measured for spinach chloroplast, spinach leaf and green Norway maple leaf (Chapter 8). However, the relative fluorescence quantum yield does not show the typical intensity quenching observed for green photosynthetic systems (spinach chloroplast preparation, spinach leaf, green Norway maple leaf, etc.).

Measurement of the fluorescence decay in the yellow Norway maple leaf, for wavelengths greater than 660 nm revealed that the emission could be adequately described as a double exponential throughout the intensity region investigated (1.3×10^{14} - 1.6×10^{15} photons/cm^2 per pulse) with a fast component of 35 ± 2 ps and a longer emission component of 243 ± 15 ps with relative amplitudes of 0.47 ± 0.03 and 0.53 ± 0.03 for the long and short component respectively. The fluorescence quantum yield again did not show the intensity dependence observed for fresh green spinach leaf or green Norway maple leaf.

Since the excitation in the yellow Norway maple leaf occurs directly in the peak of the absorption band for the carotenoid accessory pigment system, and the fluorescence emission emanates from the carotenoid system itself, a measurement of the fluorescence polarization in the carotenoid accessory pigment complex of the Norway maple leaf was made using the two-pulse excitation - optical delay technique described in detail in Chapter 9 (Pellegrino et al., 1981). Measurement without the

analyzer plate revealed a relative ratio for the two pulses of 0.97 $\pm$ 0.05. The fluorescence polarization intensity measured parallel to and perpendicular to the polarization direction of the incident pulse, $P_{\parallel}$ and $P_{\perp}$, were respectively measured by rotating the analyzer to the 0^{o} and 90^{o} position with respect to the polarization direction of the 530 nm excitation pulses. A measurement of 0.81 $\pm$ 0.1 was obtained for the ratio of the first pulse to the delayed pulse, indicating the lack of a significant degree of polarization in this system. Thus a fast and complete depolarization appears to take place in the carotenoid accessory pigment complex, with the depolarization occurring on a time scale which is faster than the resolution time of the detection system ($\sim$ 12 ps). This is consistent with the recent interpretation of singlet-singlet energy transfer time on the order of a picosecond as reported by Dallinger et al., (1981).

The low temperature (90^{o} K) fluorescence emission from a yellow Norway maple leaf was spectrally isolated by use of a Corning 3-67 filter ($\lambda \geq$ 560 nm). At a single pulse excitation intensity of 1.5 $\pm$ 0.32 x 10^{14} photons/cm^{2}, the fluorescence was observed to decay as a single exponential with a lifetime of 778 $\pm$ 84 ps. Isolating the low temperature emission with a Hoya R-72 filter ($\lambda \geq$ 720 nm) the fluorescence lifetime for wavelengths greater than 720 nm was also observed to decay as a single exponential with a lifetime of 632 $\pm$ 25 ps, at

an excitation intensity of 1.7×10^{15} photons/cm^2 per pulse. These measurements are consistent with the results of Yu et al., (1977), who reported a low temperature (90^{o} K) lifetime for spinach chloroplasts of 600 ps.

B. Fresh Green Spinach Leaf:

If the emission from the yellow leaf of the Norway maple is a true carotenoid system emission, then it must be assumed that some emission component from this system must also be present in the in-vivo fresh (green) system. In order to verify this hypothesis, the emission from a fresh green spinach leaf in the wavelength region below 660 nm was investigated with the use of a 660 nm short pass filter. In addition, it would appear that if the carotenoids are to be efficient energy transfer agents of the excitation energy absorbed, their fluorescence quantum yield must be necessarily low in order to ensure efficient transfer. This study revealed that the kinetics of the emission below 660 nm is practically identical to the emission emanating from the 685 nm component. However, the possibility of 685 nm fluorescence leakage through the 660 nm short pass filter was also a possible source of the observed signal. To resolve this problem, a Hoya R-66 filter with a 50 % transmission point at 660 nm and 75 % transmission from 670 - 2600 nm and 0 % transmission for wavelengths below 640 nm was added in front of the detector along with the 660 nm short pass filter. With this filter combination no fluorescence signal was

observed, thereby indicating that the detected signal did indeed arise from emission below 660 nm and not from leakage of the 685 nm fluorescence component. A comparison of the fluorescence decay measured for wavelengths in the region from 560 - 660 nm along with the fluorescence decay measured for all wavelengths beyond 560 nm is shown in Fig. 7.4 (I = 2×10^{15} photons/cm^2 per pulse). The fluorescence emission in the region from 560 - 660 nm decayed as a double exponential with a long component lifetime of 178 $\pm$ 34 ps and a short component of 23 $\pm$ 4 ps, with approximately equal amplitudes (Fig. 7.4a). The fluorescence emission for all wavelengths greater than 560 nm was also found to decay as a double exponential with nearly identical long (141 $\pm$ 4 ps) and short component (16 $\pm$ 2 ps) with approximately equal amplitudes (Fig. 7.4 b). Therefore, it appears that there is no significant difference between the fluorescence kinetics measured in these two wavelength regions, other than their quantum yield difference. Both measurements were obtained at an excitation intensity of

2×10^{15} photons/cm^2 per pulse in order to compare the fluorescence decay times under similar excitation conditions. Measurement of the fluorescence below 660 nm was not possible at lower excitation intensities. The relative fluorescence quantum yield from a green spinach leaf and green Norway maple leaf for the emission region spanning from 560 - 660 nm relative to the total emission

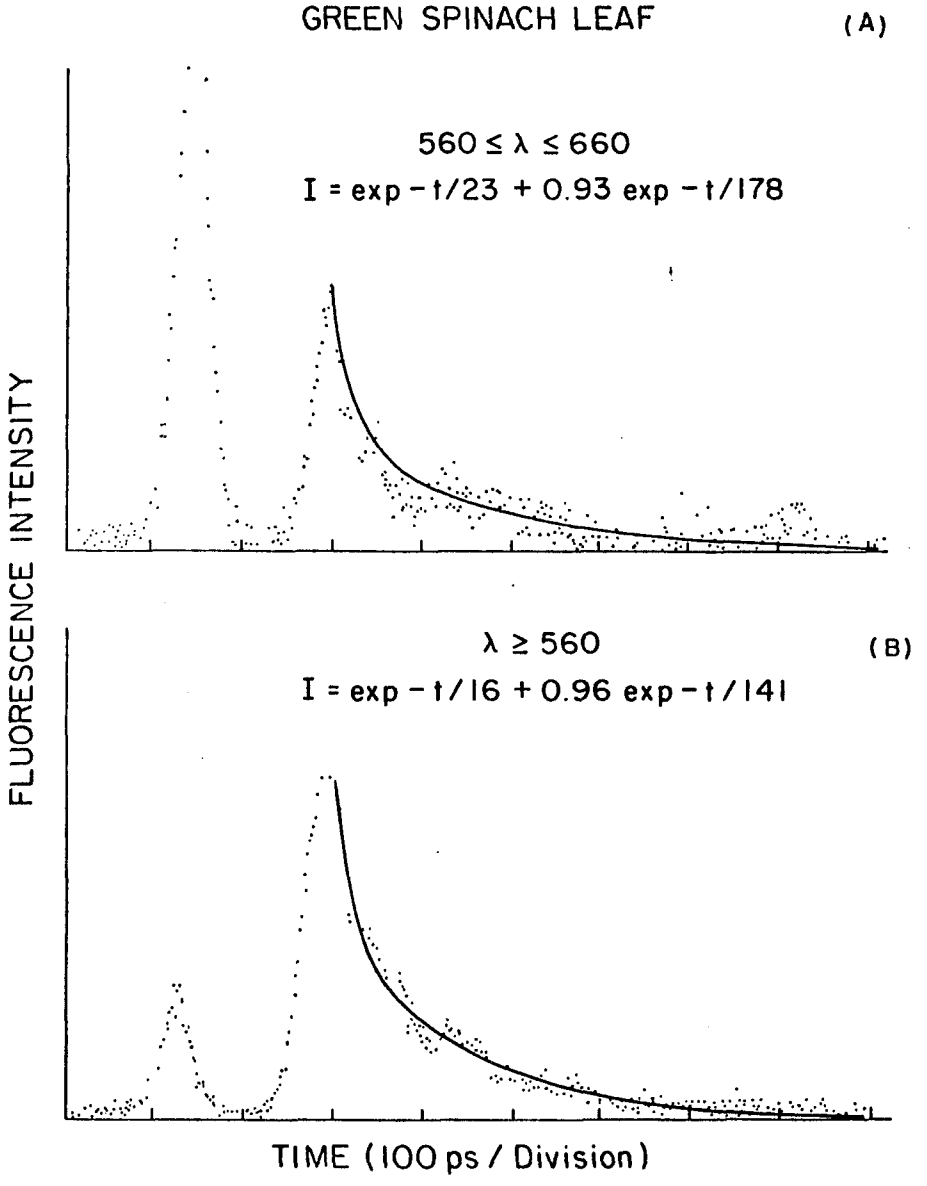

Fig. 7.4 Fluorescence Intensity Decay from a Fresh Green Spinach Leaf for (a) $560 \leq \lambda \leq 660$ nm; (b) $\lambda \geq 560$ nm.

for all wavelenghts greater than 560 nm was measured to be less than 1 %. It is important to note that this measurement was obtained at an excitation intensity of 2×10^{15} photons/cm^2 per pulse, in order to be able to measure the in vivo carotenoid emission. At this intensity the chlorophyll fluorescence is known to be highly quenched (by at least a factor of 5), so that the relative emission yield is probably much less than 1% (by at least a factor of 5). In addition, since the streak camera possesses an S-20 spectral response, it is less sensitive for wavelengths beyond 600 nm than for wavelenghts in the 500 - 600 nm region. Therefore it is expected that the yield measured below 660 nm is at least a factor of 5 lower than the 1 % measurement.

C. Yellow Norway Maple Leaf Preparation:

A preparation from the leaves of the yellow Norway maple directly analogous to the preparation previously reported for spinach chloroplasts (Chapter 5.5; Yu et al., 1977) was made with the following changes. The first supernatant was centrifuged at 10,000 RPM for 10 min, resuspended in 5 ml buffer and homogenized. The solution was placed in a 2 mm cuvette and frontally excited by a single 6 ps 530 nm pulse.

For wavelengths greater than 600 nm, a lifetime of 187 $\pm$ 41 ps was obtained at an excitation intensity of $8 \pm 0.3 \times 10^{14}$ photons/cm^2 per pulse. At an intensity of $2.1 - 0.2 \times 10^{15}$ photons/cm^2 per pulse the lifetime was

characterized by a double exponential decay with a a short component of 60 ± 6 ps and a long component of 487 ± 39 ps with relative amplitudes of 0.62 ± 0.03 for the short component and 0.38 ± 0.03 for the long component, respectively (7 measurements). These results closely parallel the general behaviour observed for the 685 nm emission component from fresh spinach chloroplasts at room temperature (200 ps for spinach chloroplasts at I 2 x 10^{14} photons/cm^2 per pulse: Yu et al., 1977; 50 ps for Chlorella at I~10^{15} photons/cm^2 per pulse: Campillo et al., 1976)

D. Yellow Norway Maple Carotenoid Extract:

A carotenoid solution in 90 % acetone was also prepared by the process of acetone extraction from the leaves of the yellow Norway maple. For wavelenghts of observation greater than 660 nm, no discernable fluorescence emission could be found. However, for wavelenghts above 560 nm, a dual exponential decay was obtained with a long component lifetime of 1810 ± 201 ps and a faster decay component of 114 ± 16 ps at an average excitation intensity of 1.5 ± 0.16 x 10^{15} photons/cm^2 per pulse with relative amplitudes of 0.40 ± 0.04 and 0.60 ± 0.04 for the long and short component respectively (8 measurements). Isolation of the carotenoids by use of paper chromatography on Whatman paper, and exciting the yellow band with 530 nm single pulse, a double exponential decay was also observed with a long component of

3633 ± 497 ps and a fast component of 57 ± 10 ps, with relative amplitudes of 0.85 ± 0.02 and 0.15 ± 0.02 respectively (3 measurements). These results indicate that, as in the case of chlorophyll in solution, the unimolecular decay rate for the carotenoid extract in solution is on the order of nanoseconds, while in the yellow or green plant (in vivo) it is on the order of a few hundred picoseconds, since in the former case (extract in solution) non-radiative energy decay routes and efficient energy transfer pathways have been effectively eliminated by disruption of the closely packed orderly arrangement of the pigments on the photosynthetic membrane.

E. Dessication Study of Green Spinach Leaf:

The fluorescence kinetics at low excitation intensity ($\sim 1 \times 10^{13}$ photons/cm^2 per pulse) in a green spinach leaf for $\lambda \geq$ 560 nm were measured as a function of time subsequent to the first initial measurement. These results are summarized as follows:

Time (hrs)	Decay Time (ps)	Excitation Intensity
0	256 ± 20	$1.4 \pm 0.2 \times 10^{13}$
16	225 ± 18	$1.3 \pm 0.1 \times 10^{13}$
40	308 ± 39 (0.4 ± .2)	$1.8 \pm 0.3 \times 10^{13}$
	84 ± 12 (0.6 ± .2)	

Physical dessication of the leaf is marked by the initial gradual loss of turgidity of the leaf (5 hrs exposure at room temperature). Subsequently, the leaf material becomes dried out and brittle (12 hours), becoming totally dry in a period of approximately 32 hours. From these measurements, the affect of aging, with the concomitant decrease in photosynthetic activity of the system therefore appears to have little or no affect on the fluorescence lifetime.

Discussion:

It is interesting to note that carotenoid fluorescence has not been previously observed. In particular, Campillo et al., (1975) have reported measurement of fluorescence from β carotene of $\leq$ 50 ps, although they later attributed this emission to the presence of impurities rather than true β carotene fluorescence emission. Since the pump excitation wavelength is in the peak absorption region of the carotenoid system, the possibility of a two photon absorption system must also be considered. However, two photon excitation is not a likely cause of fluorescence in photosynthetic systems since the two-photon energy at 530 nm would give rise to ionization states, and the in vivo generated ion concentration is non detectable (Breton et al., 1980).

Although chlorophyll has long been recognized to be the primary catalyst for photosynthetic activity, a general rule from which no exceptions are known (with the exclusion of mutant species, such as the carotenoidless mutant of Rhodopseudomonas spheroides R-26) is that all photosynthesizing cells possess an assortment of carotenoids. The presence of carotenoids together with chlorophylls in the photosynthetic apparatus is further highlighted by the close proximity of these two pigments in vivo. Goedheer (1972) inferred a close spatial relationship between the carotenoids and chlorophylls

in vivo from consideration of the assumed effective energy transfer existing between the carotenoids and Chl. a. In particular, β carotene is believed to be associated with the reaction center Chl. P-700 in the P-700-Chl. a light harvesting protein system, while a lutein/β carotene form is believed to be associated with the chlorophyll a/b protein complex of the LHC (Naqvi, 1980). Dallinger et al., (1981) have estimated the de-excitation lifetime of the singlet state of β carotene to be not greater than 1 ps from transmittance measurements and resonance enhanced picosecond Raman spectroscopy. From their results they have also inferred a very close association or near contiguity of these pigments in vivo.

A model is proposed to explain the kinetic measurements observed in the carotenoid accessory pigment complex of the yellow Norway maple and green spinach leaf reported in this study. Two lattices are postulated, a chlorophyll light harvesting lattice at an energy corresponding to 685 nm, and a carotenoid light harvesting lattice at higher energy corresponding to 380 to 510 nm. Both lattices are physically located on the thylokoid membrane in the chloroplast. The carotenoid lattice is a continuous lattice located in the lipid layer of the thylakoid membrane. The chlorophyll lattice on the other hand, occurs in unit clusters (PSU) on the surface of the thylakoid membrane. Traps (both photoactive and non-radiative) are uniformly spaced in the light

harvesting protein which forms the substrate of the carotenoid - chlorophyll a/b light harvesting complex. However, traps which are located in the region of a PSU, form physical associations with chlorophyll molecules and are classified as photoactive traps. Traps which occur in the protein complex and which are not located near a chlorophyll molecule form non-photoactive and non-radiative traps which can also act as quenchers of the excitation energy.

When the carotenoid lattice is excited, the excitation quickly transfers to the chlorophyll sub-lattice diffusing to the photoactive trap of the PSU associated with that chlorophyll molecule. For excitations which occur in the carotenoid super-lattice and which do not occur near the site of a PSU or chlorophyll molecule, the energy travels in the carotenoid super-lattice, diffusing until it is finally quenched at a non-radiative trap. Since the traps are uniformly spaced in the light harvesting protein complex, and since both the carotenoid and chlorophyll lattices possess similar inter chromophore separation, and relative alignment of donor and acceptor molecules, the trapping time in either the photoactive trapping case or the non-photoactive trapping case should be approximately the same (as is observed in the kinetic measurements).

The observed quenching of the fluorescence quantum yield for the case of the emission from the green spinach leaf or green Norway maple leaf (685 nm emission), is

interpreted in terms of exciton-exciton annihilation in the chlorophyll light harvesting complex in the localized domains of the PSU's. The lack of quenching in the case of the yellow Norway maple is consistent with the presence of a larger domain size for the excitation transfers occurring in the carotenoid super-lattice.

In summary, the quenching of the fluorescence lifetime in both the green Norway maple leaf, green spinach leaf and yellow Norway maple leaf is interpreted as indicative of the quenching from either photoactive traps in the former or non-photoactive (non-radiative) traps in the latter. The low temperature results in both systems are consistent with a decrease in excitation energy transfer arising from a lowering of the vibrational activation energy necessary for efficient transfer in either system.

The principal aspects of the proposed model are consistent with an energy transfer time from carotenoid to Chl. *a* of $\leq$ 10 ps and the observation of an energy transfer time of $\sim$ 200 ps in the non-chlorophyll containing carotenoid accessory pigment lattice. Furthermore, the close agreement between this rate and the normal fluorescence rate measured in various green photosynthetic systems is interpreted to be indicative of the properties of the light harvesting lattice.

This study therefore raises the question that the measured photosynthetic fluorescence kinetics to date are more likely indicative of the structural arrangement of

chromophores in their local environment rather than being necessarily representative of the photosynthetic state of the system in general, or the state of the reaction center traps in particular. The assumptions and conclusions of this model provide new avenues of investigation which can be used to better understand the primary energy transfer and trapping process.

Chapter. 8 Energy Transfer Kinetics in the Chlorophyll Light Harvesting Complex in Primary Photosynthesis.

The first picosecond time resolved measurement of the fluorescence decay time from a photosynthetic system was made by Seibert, Alfano and Shapiro on escarole chloroplasts in 1973. Later Yu et al., (1975a) also were able to associate the fast and slow emission component observesd in whole chloroplasts at room temperature with PS I and PS II, respectively. The results of measurements obtained on the energy transfer kinetics in higher green plant and algal photosystems during the course of the studies of this thesis will now be presented.

My first study in this investigation was performed with picosecond pulse train excitation, before the effects of exciton-exciton annihilation and long lived states such as from triplets and ions were understood. In order to eliminate the problem of exciton interactions a single pulse selection apparatus and streak camera detection system was set up in order to probe the time resolved fluorescence kinetics using single picosecond pulse excitation (Chapter 5).

8.1 Fluorescence Kinetics of Spinach Chloroplasts Measured With Picosecond Pulse Train Excitation and Optical Kerr Gate Detection System.

Picosecond time resolved fluorescence spectroscopy can provide invaluable information on the energy transfer processes that take place in the primary stages of photosynthesis. In particular, with the advent of mode-locked Nd:glass lasers the possibility of exciting a system on a picosecond time scale became available. The output of a Nd:glass laser consists of a train of approximately 100 pulses of typically 6 ps duration each, separated by the round trip time of the laser cavity, $\sim$ 5 ns. Detection of the fluorescence signal on a picosecond time scale is made possible by use of an optical Kerr gate actuated by the laser pulse itself or a streak camera-optical detection system.

Experimental Methods:

The wavelength and temperature dependence of the fluorescence kinetics from spinach chloroplasts were obtained using a train of 100 pulses of 6 ps duration each for excitation and a 10 ps resolution optical Kerr gate for detection. The average pulse intensity at 530 nm was 2×10^{14} photons /cm^2 (0.02 mJ/pulse). Chlorophyll concentrations were measured to be 40 ug/ml in a 1 cm long cuvette and 1 mg/ml in a 0.05 cm long cuvette.

Experimental Results:

At room temperature (300° K), the 730 nm fluorescence was observed to decay approximately as a single exponential with lifetime of 100 ps, while the 685 nm fluorescence decayed non-exponentially. A two component exponential decay was fitted to the 685 nm fluorescence decay with lifetimes of 56 and 220 ps and amplitudes of 1 and 1.2 respectively. In this study the fluorescence kinetics measured from a spinach leaf was found to be identical with the data obtained from the chloroplast preparation.

The room temperature and 90°K fluorescence kinetics at 685 $\pm$ 2.5 nm and 730 $\pm$ 2.5 nm are shown in Fig. 8.1.1. The fluorescence intensity measured at t=0 is indicative of the initial singlet state population. Both the t=0 and the time integrated fluorescence spectrum, obtained by uncrossing the polarizers in the Kerr gate setup, and normalized to 685 nm are shown in Fig. 8.1.2. The spectra were corrected for the spectral response of the RCA 7265 photomultiplier, 1-meter Jarrel-Ash spectrometer, Corning 1-75 and 3-67 filters, and Polaroid HN 22 polarizers. The same spectra corrected for self-absorption is shown in Fig. 8.1.3. The correction factors for self absorption were obtained by comparing the time integrated emission spectra of the samples used in the experiments, excited by a weak He-Ne laser, with the spectra of the same sample

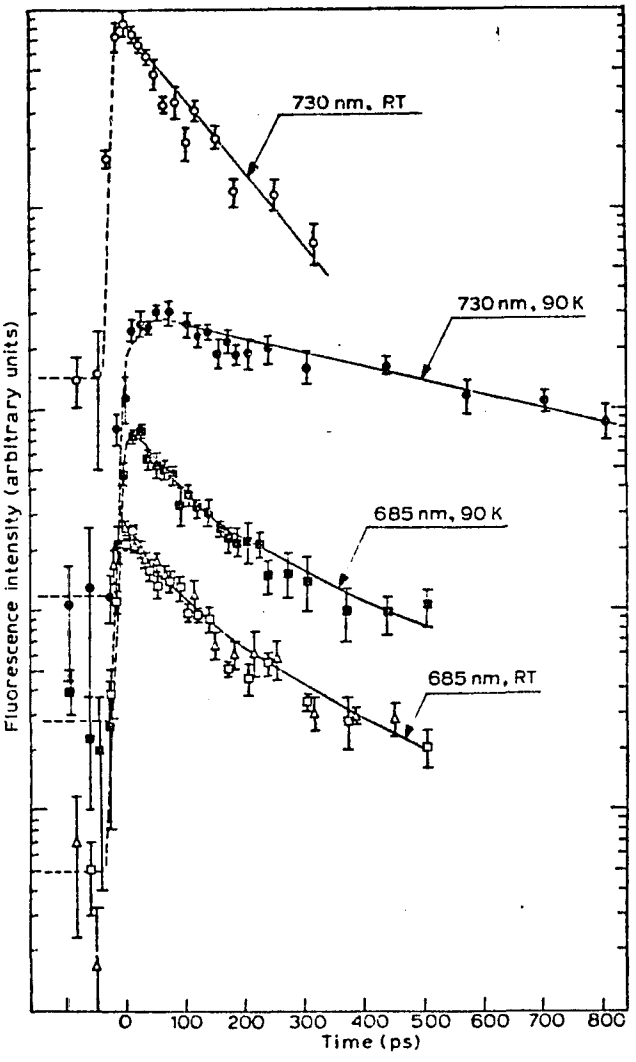

Fig. 8.1.1 Room Temperature and 90° K Fluorescence Kinetics in Spinach Chloroplasts at 685 and 730 nm.

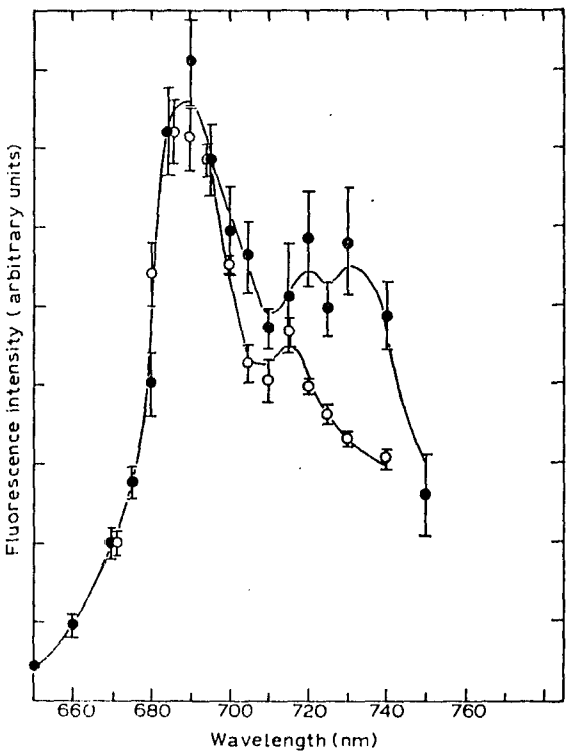

Fig. 8.1.? T=0 (●) and Time Integrated (o) Spectra of Spinach Chloroplasts.

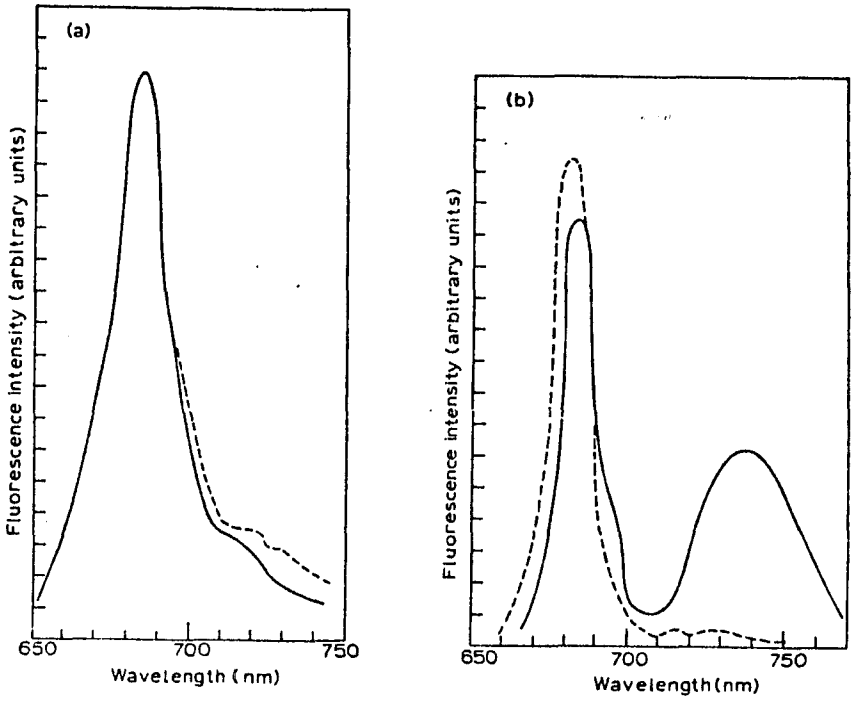

Fig. 8.1.3 T=0 (---) and Time Integrated (——) Spectra of Spinach Chloroplasts Corrected for Self Absorption at RT (a) and 90° K (b).

greatly diluted. The spectra indicates that for wavelengths greater than 700 nm, the fluorescence intensity measured relative to 685 nm is greater in the t=0 spectrum than in the time integrated spectrum. This observation indicates that at longer wavelengths ($\lambda \gtrsim$ 700 nm) the room temperature lifetime is shorter than that at 685 nm (as observed in the kinetic measurements). At 90^{o}K, the 730 nm lifetime increased to 600 ps from a value of 100 ps at room temperature. In this case the time integrated spectrum for wavelengths greater than 700 nm, measured relative to 685 nm, is greater than the t=0 spectrum, and the 730 nm component relative to 685 nm has increased by a factor of 2.5 from that measured at room temperature. These results are summarized in Table 8.1.

Since these measurements were carried out with pulse train excitation, the effect of such excitation mode as well as the intensity of excitation used on the state of the traps was investigated. This was done by measuring the fluorescence intensity from the sample versus the excitation intensity. This relationship was observed to be linear ($\pm$ 10%) throughout the pulse train of 100, 2 x 10^{14} photons/cm^{2} pulses. This indicates that either the fluorescence excited by each pulse is independent of prior pulse excitations, or that a steady state is achieved, after excitation by several pulses, which gives rise to a constant fluorescence yield.

However, measurements by Beddard et al., (1975) have

Table 8.1

Wavelength (nm)	Temperature (K)	Risetime (ps)	Lifetime and Amplitude (ps)		(relative)	
685	280	5	56	1	220	1.2
685	90	5	45	1	220	1
730	280	5	100	1		0
730	90	13±7	600	1		0
695	280	5		0	220	1
695	90	5		0	220	1

revealed that the fluorescence lifetime remains constant for a ten-fold change of excitation intensity, and Campillo et al.,(1976a) have also shown that under single pulse excitation the lifetime increases with decreasing excitation intensity. The measurement of the excitation yield versus incident excitation intensity is shown in Fig. 8.1.4. The fluorescence yield can be seen to decrease for excitation intensities $> 10^{14}$ photons/cm^2 per pulse. Similar findings have been obtained using a 7 ns, 377 nm pulse (Mauzerall, 1976) and a 20 ps 530 nm pulse (Campillo et al., 1976b). It is interesting to note that the fluorescence quenching using picosecond pulse train excitation is delayed by a ten fold factor of incident intensity compared to the single pulse quenching region. If the excitation intensity is increased by a hundred fold, the relative amplitude of the fast component increases by a factor of 3. If the excitation intensity is decreased by a factor of 3.5 the kinetics of the fast component are unchanged. The kinetics of the slow component are unchanged in both cases. This observed variation of the fast component, and independence of the slow component with intensity supports the analysis of the measurements in terms of a two component decay.

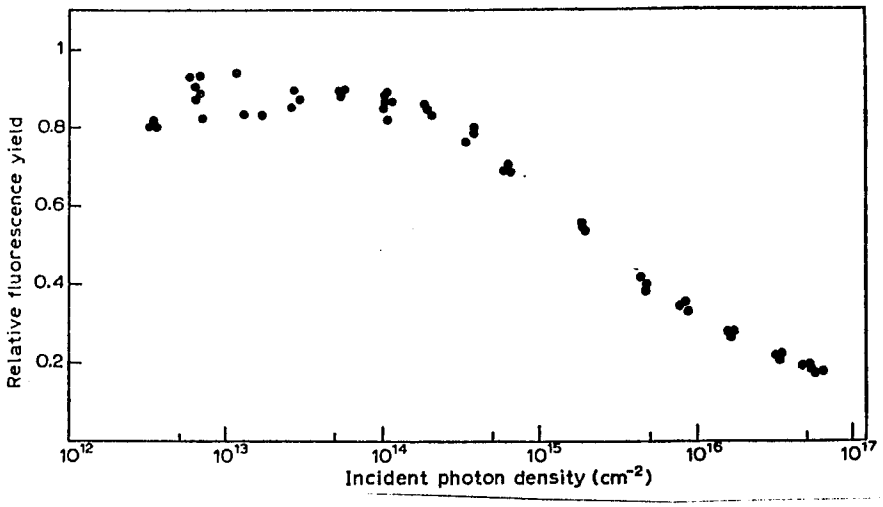

Fig. 8.1.4 Intensity Dependence of Fluorescence Quantum Yield of Spinach Chloroplasts Measured with Picosecond Pulse Train Excitation.

Discussion:

By comparing the results obtained here for whole chloroplasts (two component decay; 56 and 220 ps) with the fluorescence decay times for PS I (60 ps) and PS II (200ps) enriched preparations (Yu et al., 1975a,b) the association of the fast component with the PS I emission and the slow component with PS II emission is apparent. This association is further corroborated by the measurement in whole spinach chloroplasts (see Table 8.1) of 100 ps for the fluorescence decay at 730 nm, generally associated with PS I fluorescence, and 220 ps for the fluorescence decay at 695 nm, which is generally associated with PS II fluorescence.

These kinetic measurements are indicative of both a downhill energy transfer from 685 (or 695) nm to the reaction center trap, and an uphill energy transfer from 730 nm to the trap. At low temperature the transfer rate from the 730 nm level is reduced by the exponential factor $\exp(-\Delta E/kT)$ and the 730 nm lifetime becomes longer by a factor of 6. The estimated value for the location of the trap above the 730 nm level is therefore,

$$k_{300} = k_0 \exp(-\Delta E/k\ 300^{\circ}K)$$

$$k_{90K} = k_0 \exp(-\Delta E/k\ 90^{\circ}K)$$

$$\frac{k_{300}}{k_{90}} = \frac{\tilde{\tau}_{90}}{\tilde{\tau}_{300}}$$

$$= 6 = \exp -[\Delta E/k\ (1/300 - 1/90)]$$

$$\Delta E = k(\ln 6)\ (128.6\ ^{\circ}K)$$

$$\Delta E = 318 \pm 15 \times 10^{-23}\ J$$

$$\Delta E = 160 \pm 8\ cm^{-1}$$

This corresponds to a trap position of 722 $\pm$ 1 nm relative to the 730 nm level.

In the case of the 685 nm and 695 nm fluorescence, the downhill energy transfer should not be affected by a lowering of the temperature, and indeed the lifetime at these two wavelengths is observed to be independent of temperature. However, this interpretation for the energy level location of the trap applies only to the PS I case since the 730 nm fluorescence emission is predominantly from PS I. In fact such a trap state has been postulated for PS I by Kok (1956) as P-700 and by Butler (1961) as P-705.

8.2 Fluorescence From Intact Spinach Leaf:

An experimental problem which one often encounters in photosynthetic spectroscopy (and indeed in all experiments) is the proper preparation of the sample to be investigated in a way which does not affect the natural intrinsic characteristics to be measured. Addition of detergents and buffers sometimes prove to be indispensable in isolating particular components for investigation, yet they necessarily introduce the possibility of seriously affecting the outcome of the experiments. In particular, for spinach chloroplasts, the preparation of a chloroplast sample in an environment which most nearly approximates the natural *in vivo* conditions in the leaf is a serious one. Introducing agents foreign to that environment can alter the natural photosynthetic activity. Over the years various sample preparations have been proposed, basically consisting of sucrose buffers, which attempt to reproduce the natural chloroplast environment.

In the measurements performed in this research, the temporal decay characteristics of the fluorescence emission from both a whole spinach leaf with its stem immersed in water and chloroplast preparations prepared by the method described in Chapter 5.5 were found to be identical, within experimental error. The experiments included measurements using two different temporal resolution techniques. In the optical Kerr gate

measurements, light emanating from the end of a 1 cm long cuvette containing the chloroplast preparation (O.D.= 1 at 670 nm) or the back portion of the leaf was passed through the gate. In measurements using a streak camera, fluorescence from the surface of a 2mm cell containing the chloroplast preparation or the front surface of the leaf was collected into the streak camera, the sample being frontally excited. In both cases the intensity of excitation was $\sim 10^{14}$ photons/cm^2. No visible damage was observed to have occurred to the leaf from the laser excitation (laser pulse energy $\sim$ 10 uJ). These measurements have revealed the rather interesting result that the picosecond fluorescence kinetics may be directly investigated in the truly <u>in vivo</u> condition, namely the leaf, without the use of artificial environments present in preparations.

8.2.1 Fluorescence kinetics of spinach chloroplasts measured with single picosecond pulse excitation:

The results obtained using single pulse excitation at 530 nm confirmed the results previously obtained with picosecond laser pulse train excitation. The low intensity lifetime ($I \sim 1.4 \pm 0.2 \times 10^{13}$ photons/cm^2 per pulse) from a fresh green spinach leaf excited by a single 6 ps 530 nm pulse was found to decay as a single exponential with a lifetime of 256 $\pm$ 20 ps (4 measurements). This result is in good agreement with the most recent measurements using the photon counting technique by Sauer and Brewington, (1978), who obtained a lifetime of 0.20 ns in spinach chloroplasts.

The fluorescence kinetics were also measured as a function of excitation pulse intensity. As the intensity was increased, the fluorescence decay for excitation intensities $\geq 8 \pm 0.7 \times 10^{13}$ photons/cm^2 per pulse could best be described by a double exponential. The relative intensities of the two components at $1.75 \pm 0.3 \times 10^{14}$ photons/cm^2 per pulse were approximately equal for the long and short component (0.54 $\pm$ 0.05 and 0.46 $\pm$ 0.05 respectively). The decay time of the long component was measured to be 178 $\pm$ 12 ps while the decay time for the short component was found to be 58 $\pm$ 13 ps (4 measurements). The relative intensity of the long component declined to 0.31 $\pm$ 0.01 at an intensity of

$2.6 \pm 0.5 \times 10^{15}$ photons/cm^2 per pulse, while the lifetimes of both components remained relatively unchanged (151 $\pm$ 11 ps and 22 $\pm$ 5 ps for the long and short component, respectively for 4 measurements). This confirms the general behaviour observed in the picosecond pulse train excitation experiments, where a quenching of the fluorescence quantum yield along with a change of lifetime from single to double exponential is observed for excitation intensities greater than 10^{14} photons/cm^2 per pulse. The short and long component of the fluorescence decay are displayed as a function of single 530 nm excitation pulse intensity in Fig. 8.2.1.

The relative fluorescence quantum yield, which is taken as the fluorescence yield at intensity I normalized to the fluorescence yield at low intensity ($1.4 \pm 0.2 \times 10^{13}$ photons/cm^2 per pulse) is shown as a function of the intensity of a single 530 nm excitation pulse in Fig. 8.2.2. The quenching of the fluorescence quantum yield confirms the results previously obtained by Campillo et. al., (1976) and Breton and Geacintov (1976) in Chlorella and spinach chloroplasts, respectively. These results are also shown in Fig. 8.2.2.

A parallel study of the intensity dependence of the fluorescence quantum yield and lifetime for a fresh green Norway maple leaf (acer platenoides) was also undertaken for comparison with the results obtained in the green spinach leaf in order to establish a basis for comparison

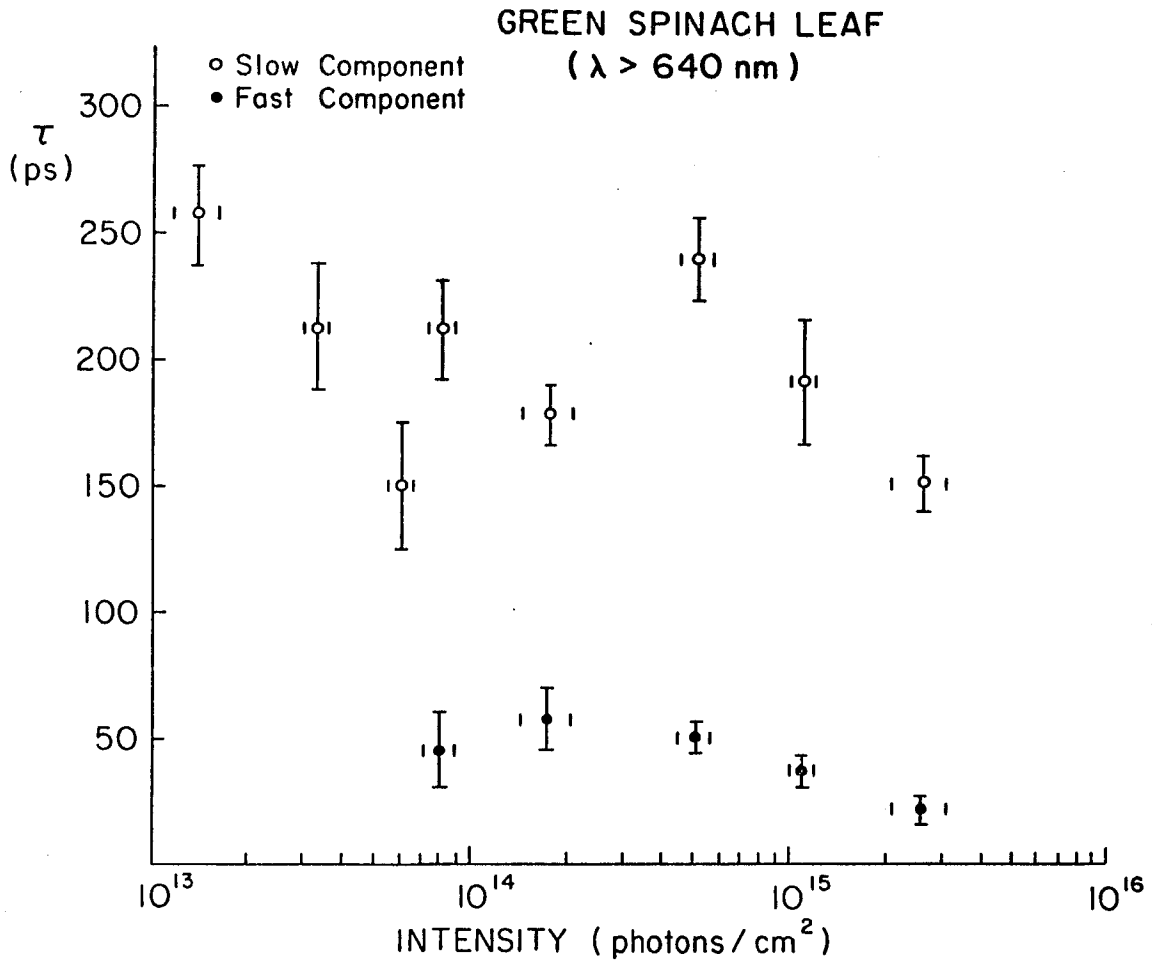

Fig. 8.2.1 Green Spinach Leaf Fluorescence Measured as a Function of Excitation Pulse Intensity.

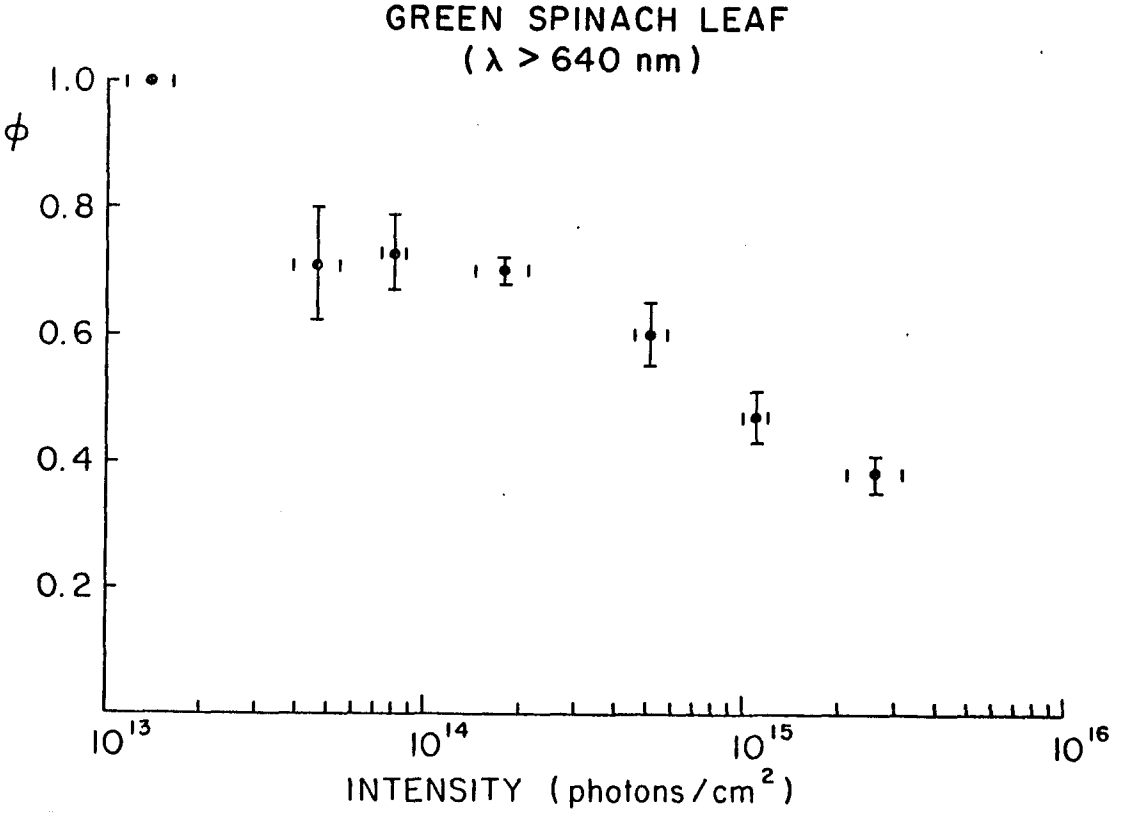

Fig. 8.2.2 Relative Fluorescence Quantum Yield from Green Spinach Leaf Measured as a Function Excitation Pulse Intensity.

of results obtained in the yellow and green Norway Maple with the results of previous investigations. Again, as in the case of the green spinach leaf, at low intensity ($1.3 \pm 0.1 \times 10^{13}$ photons/cm^2 per pulse), the fluorescence from the green Norway maple leaf decayed as a single exponential with a lifetime of 170 ± 6 ps (6 measurements). As the intensity was increased, the fluorescence quantum yield decreased and the lifetime was characterized by a double exponential behaviour for intensities greater than $7 \pm 0.6 \times 10^{13}$ photons/cm^2 per pulse. At an intensity of $6.9 \pm 0.6 \times 10^{13}$ photons/cm^2 per pulse, the decay was described by a double exponential with a long component of 205 ± 13 ps and a short component of 70 ± 8 ps (with relative amplitudes of 0.40 ± 0.05 and 0.58 ± 0.05 respectively). As the intensity was increased to $4.6 \pm 0.73 \times 10^{14}$ photons/cm^2 per pulse, the decay times for the long and short component remained relatively unchanged. At this intensity, the long component lifetime was measured to be 258 ± 24 ps and the short component lifetime 59 ± 3 ps, with relative amplitudes of 0.21 ± 0.02 and 0.8 ± 0.02 respectively. These results are summarized in Table 8.2.1. Therefore since only a slight change in the decay times of the two components were found over the intensity region investigated, the quenching of the fluorescence quantum yield is attributed to the relative shift in the amplitudes of the two components at higher intensity.

Table 8.2.1

Intensity	Decay Time (ps)	Amplitude (rel.)
$6.9 \pm 0.6 \times 10^{13}$	205 ± 13	0.40 ± 0.05
	70 ± 8	0.58 ± 0.05
$4.6 \pm 0.7 \times 10^{14}$	258 ± 24	0.21 ± 0.02
	59 ± 3	0.80 ± 0.02

A plot of the lifetime and relative fluorescence quantum yield as a function of the excitation pulse intensity is shown in Fig. 8.2.3 and 8.2.4 respectively. These results are interpreted in the singlet-singlet exciton annihilation model proposed by Swenberg et al., (1976).

The wavelength region greater than 720 nm was isolated by the use of a Hoya R-72 filter. In this region the lifetime at room temperature was measured to be 130 $\pm$ 3 ps (4 measurements) at an intensity of 5.2 $\pm$ 0.1 x 10^{13} photons/cm^2 per pulse. This result is consistent with the room temperature measurement of the decay time in spinach chloroplast preparation of 100 ps measured with the optical Kerr gate utilizing laser pulse train excitation at an intensity of $\sim$ 2 x 10^{14} photons/cm^2 per pulse (Chapter 8.1).

The wavelength dependence of the fluorescence lifetime from a fresh green spinach leaf is shown in Fig. 8.2.5. The fluorescence emission was spectrally isolated in 100 nm steps by use of narrow band filters (FWHM 100A) covering the spectral range from 680 -730 nm. The low optical transmission of these filters allowed for only two intensity regions to be investigated, at average excitation pulse intensities of 2.3 $\pm$ 0.1 x 10^{14} and 1.65 $\pm$ 0.1 x 10^{15} photons/cm^2 per pulse. The results of this investigation revealed that while the decay at 680 nm was characterized by a single exponential at both intensities, the decays measured for wavelengths greater

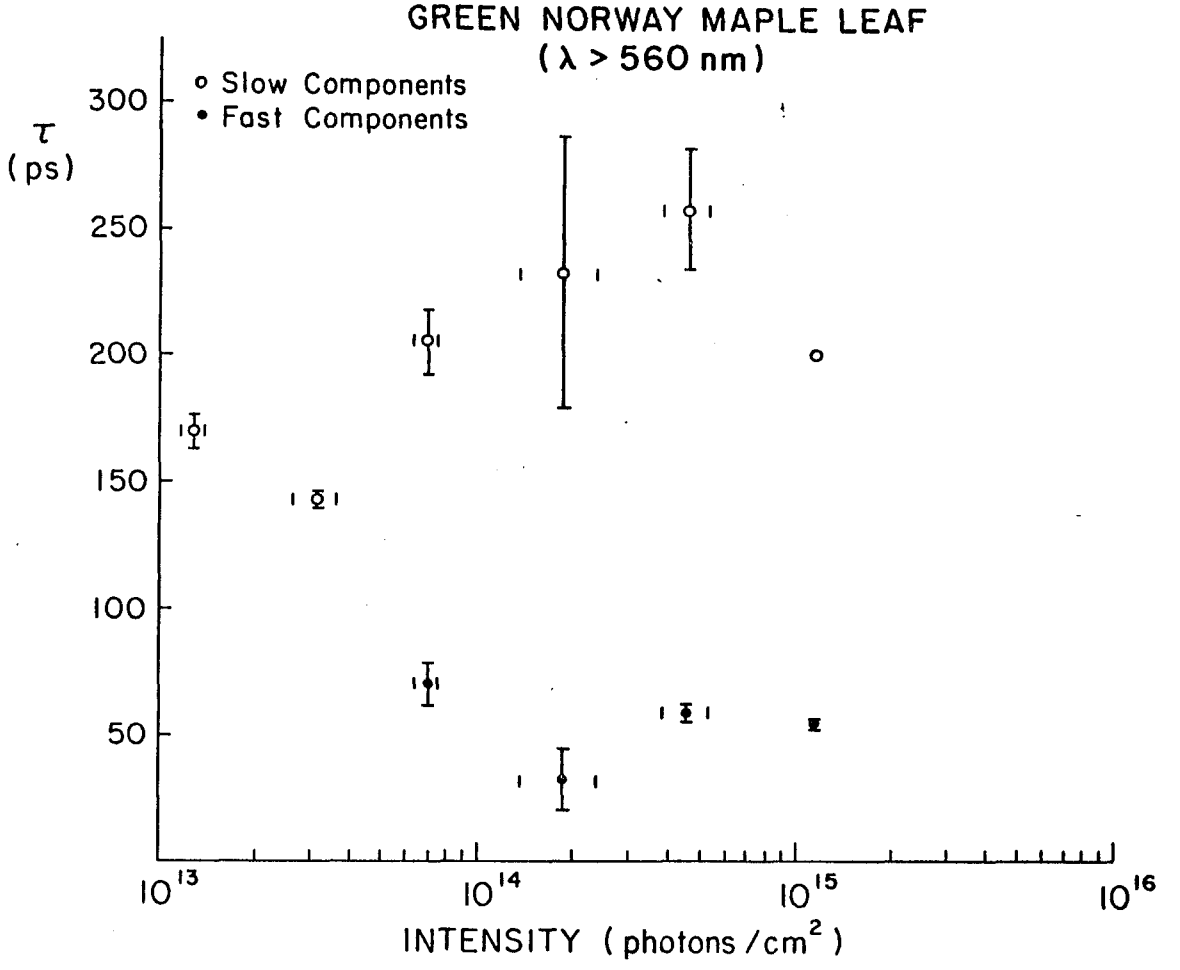

Fig. 8.2.3 Fluorescence Kinetics of Green Norway Maple Leaf Measured as a Function of Excitation Pulse Intensity.

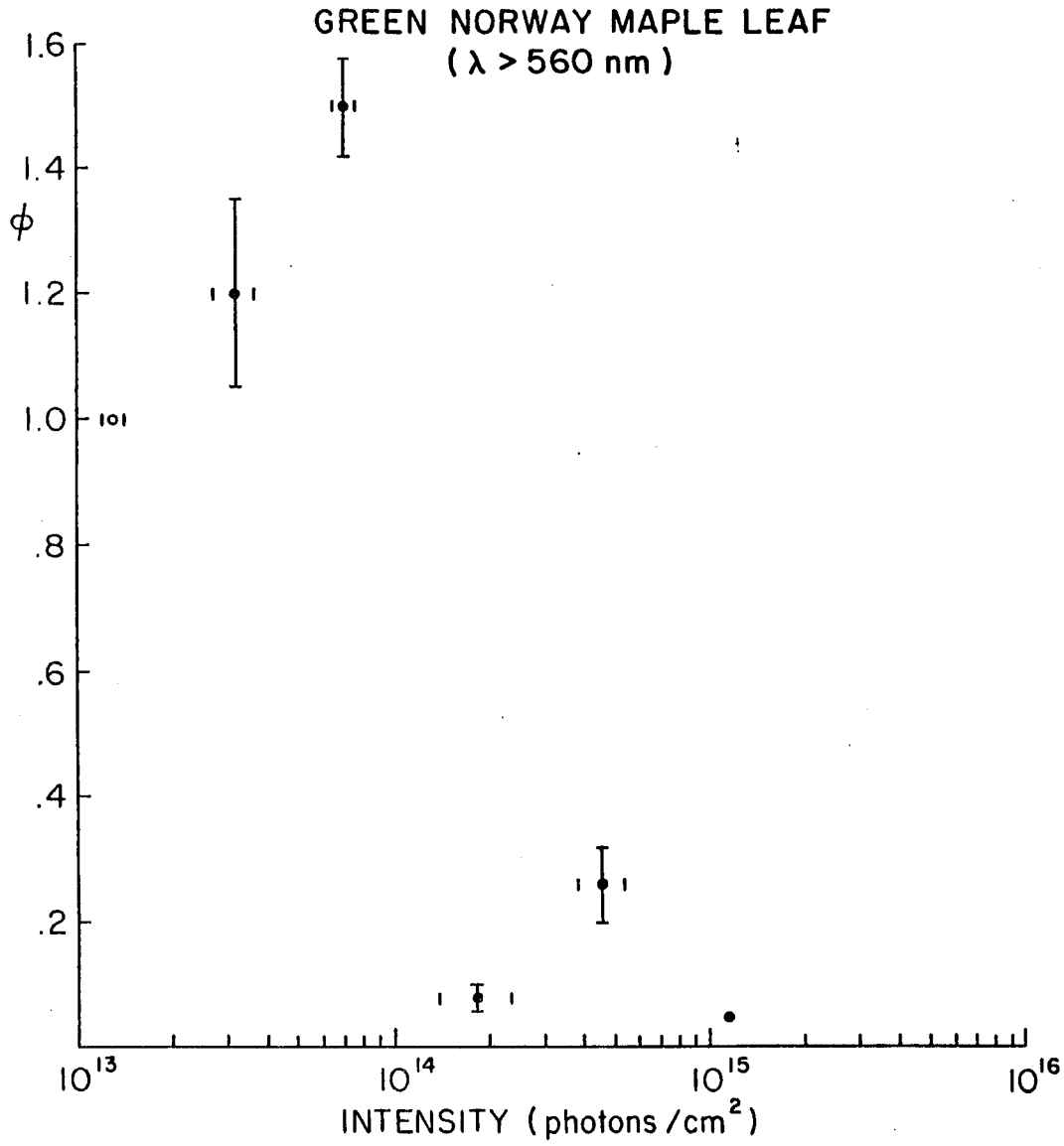

Fig. 8.2.4 Relative Fluorescence Quantum Yield from Green Norway Maple Leaf Measured as a Function of Excitation Pulse Intensity.

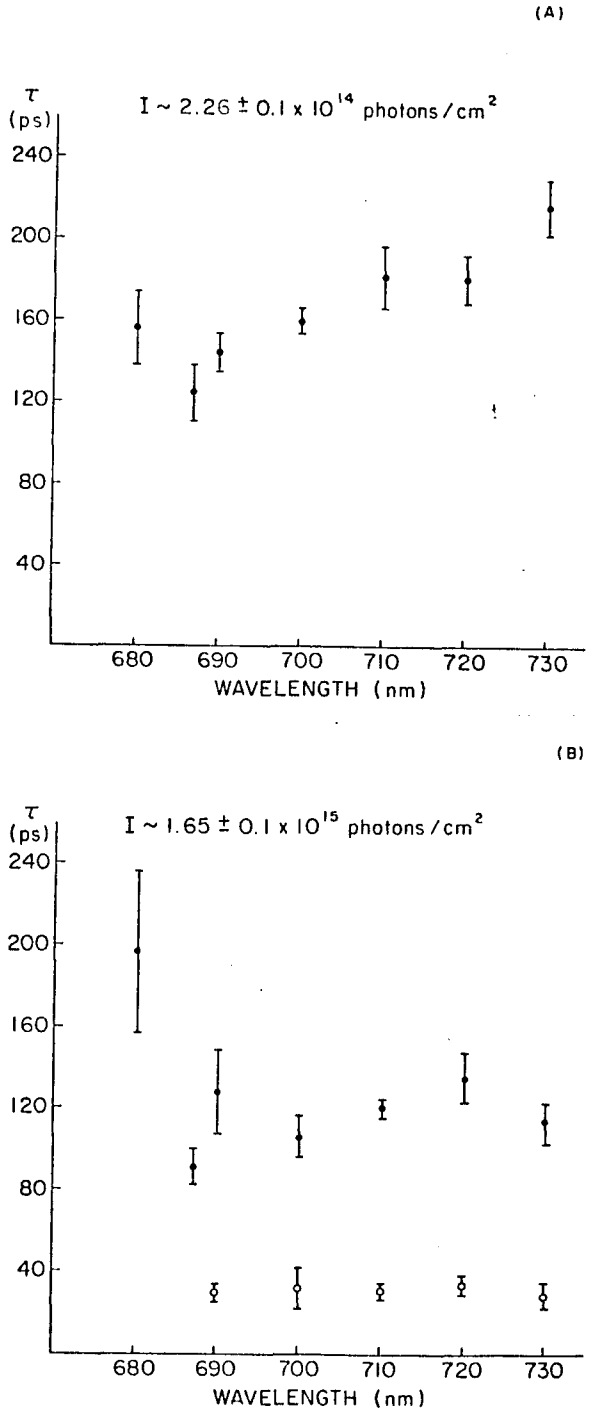

Fig. 8.2.5 Wavelength Dependence of Fluorescence Kinetics from Green Spinach Leaf Measured at (a) Medium ($2.26 \pm 0.1 \times 10^{14}$ photons/cm^2 per pulse) and (b) High Excitation Pulse Intensity ($1.65 \pm 0.1 \times 10^{15}$ photons/cm^2 per pulse).

than 680 nm (namely 690, 700, 710, 720 and 730) decayed as a single exponential only at the lower intensity region, possessing a two component decay with approximately equal amplitudes at the higher excitation intensity. This confirms the previous association of the 730 nm emission with the fast component of the fluorescence from spinach chloroplast preparation and PS I enriched preparations of spinach chloroplasts (Yu et. al., 1975, 1977).

This measurement confirms the previous observation of the intensity dependence of the 685 nm lifetime of spinach chloroplasts (Yu et al., 1977). In addition, the appearance of a second faster exponetial component for $\lambda \geq$ 690 nm at high intensity is consistent with the occurrence of exciton exciton annihilation at this intensity (Swenberg et al., 1976, Geacintov and Breton, 1977). However, the measurement of a 216 ps decay time for the 730 nm emission at room temperature is not consistent with the previous measurement of 100 ps obtained by Yu et al., (1977) for spinach chloroplasts at approximately the same intensity of excitation (2 x 10^{14} photons/cm^2 per pulse). Whether this discrepancy is due to the differences in samples investigated (spinach vs. Norway maple), physical state of the sample investigated (chloroplast preparation vs. leaf), or method of excitation (pulse train vs. single pulse) is not clear. However the 730 nm measurement for the Norway maple is also not consistent with the measurement

previously reported for the Norway maple leaf for all wavelengths $\lambda \gtrsim 720$ nm (130 $\pm$ 3 ps) at 5.2 $\pm$ 0.1 x 10^{13} photons/cm^2 per pulse. The possibility of a multi-component fluorescence emission in this wavelength region cannot be ruled out (Moya, 1979) and further detailed measurements at low intensity are needed in order to resolve the emission characteristics in this wavelength region.

8.2.2 Temperature Dependence of the Fluorescence Lifetime from Green Spinach Leaf Measured with Single Pulse Excitation:

The low temperature fluorescence lifetime (90^{o} K) from a green spinach leaf was measured with a 687 nm narrow band filter (FWHM 100 A) at an average single pulse excitation intensity of $5.5 \pm 0.5 \times 10^{14}$ photons/cm^2 per pulse. The decay was characterized by a single exponential behaviour with a lifetime of 227 $\pm$ 25 ps (10 measurements) in agreement with the results of Seibert et al., (1974) and Yu et al., (1975, 1977).

The low temperature intensity dependence of the lifetime for a green spinach leaf for wavelengths of observation greater than 720 nm is shown in Fig. 8.2.6, while the low temperature (90 ^{o} K) intensity dependence of the fluorescence quantum yield from the green spinach leaf is shown in Fig. 8.2.7. The results from two separate measurements are displayed in these figures. The low temperature quantum yield shows no clear intensity dependence. This is expected since at low temperature all of the photochemical traps have been closed and the excitonic domains are no longer photochemically active. For I $\leq$ 2 x 10^{13} photons/cm^2 per pulse the fluorescence decayed as a single exponential with a lifetime of 1348 $\pm$ 188 ps (7 measurements). For intensities greater than 7 x 10^{13} photons/cm^2 per

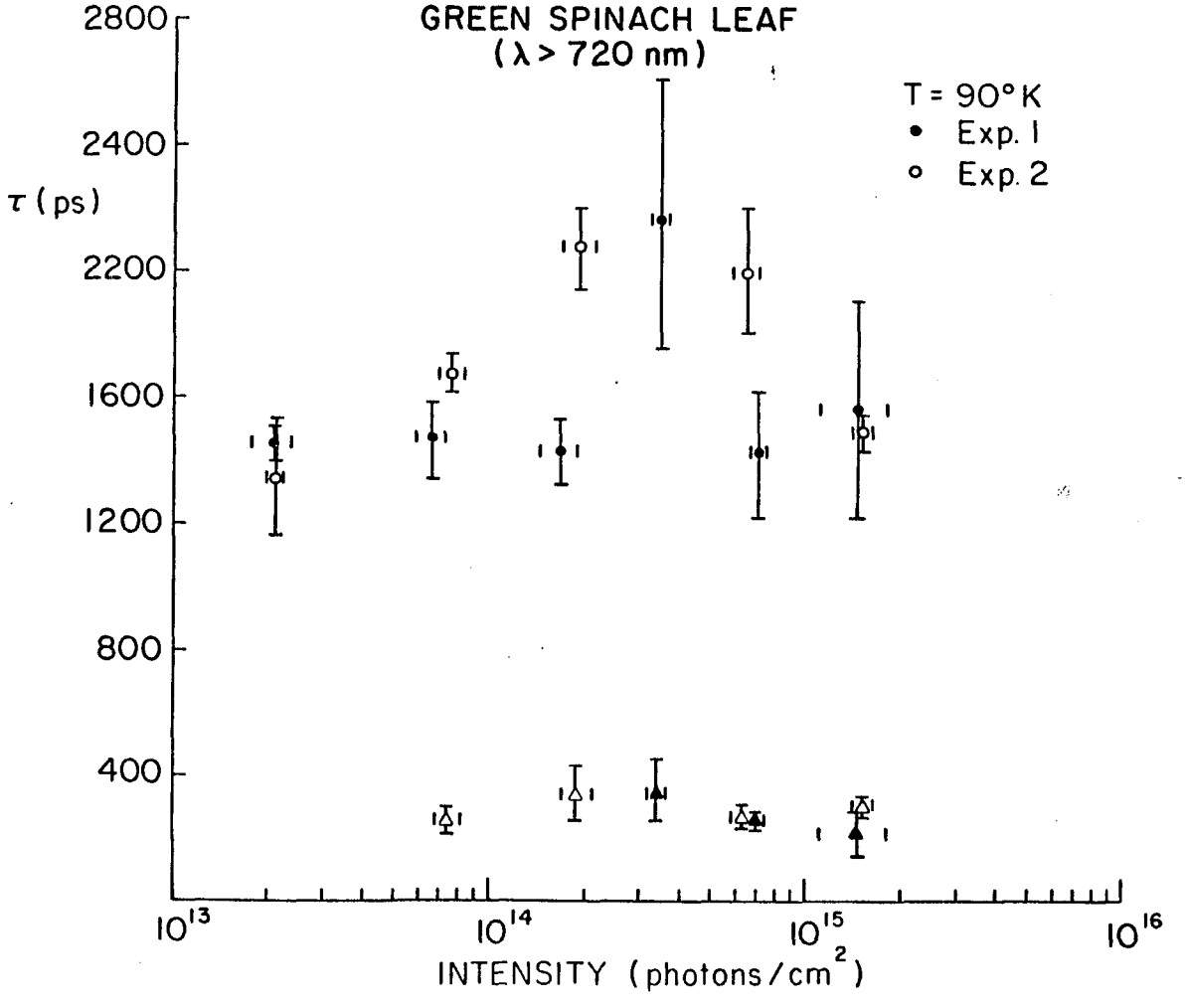

Fig. 8.2.6 Green Spinach Leaf Fluorescence Lifetime at 90° K ($\lambda \gtrsim 720$ nm) Measured as a Function of Excitation Pulse Intensity.

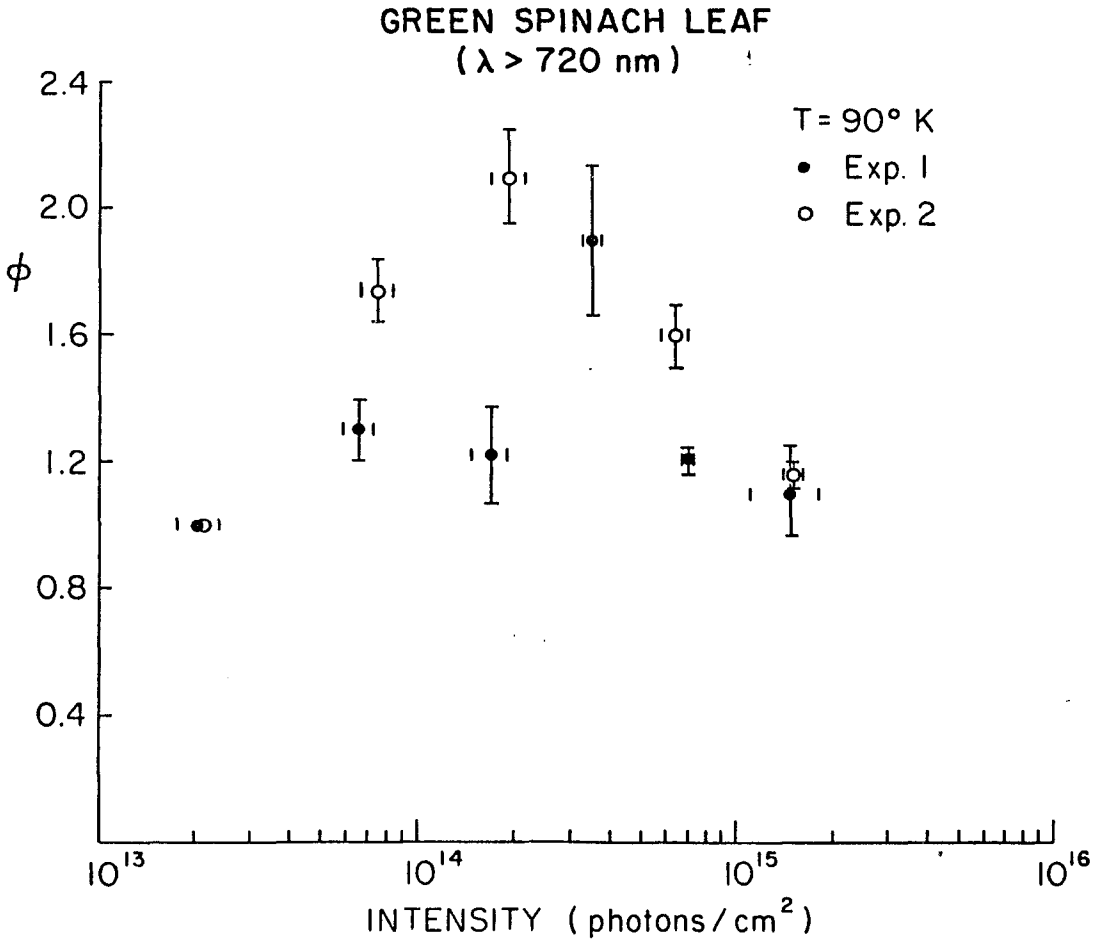

Fig. 8.2.7 Relative Fluorescence Quantum Yield from Green Spinach Leaf at 90 ^{o} K ($\lambda \geq$ 720 nm) Measured as a Function of Excitation Pulse Intensity.

pulse, the decay was characterized by a double exponential. At I = 7.4 $\pm$ 0.9 x 10^{13} photons/cm^2 per pulse (4 measurements) a long component of 1676 $\pm$ 61 ps and a short component of 248 $\pm$ 36 ps (with relative amplitudes of 0.75 $\pm$ 0.04 and 0.25 $\pm$ 0.04) were measured, respectively. The relative intensity of the long component decreased to 0.50 $\pm$ 0.08 at I = 1.5 $\pm$0.1 x 10^{15} photons/cm^2 per pulse (4 measurements) with the values of the long and short component decay time relatively unchanged (1488 $\pm$ 53 ps and 286 $\pm$ 34 ps respectively). These results indicate the presence of an exciton annihilation mechanism at the higher intensities, as in the case observed for the room temperature leaf results at high intensities. However, in this case the quenching of the fluorescence lifetime is not accompanied by a corresponding quenching of the fluorescence quantum yield since photochemical interaction-decay mechanisms have been inhibited.

A plot of the temperature dependence of the fluorescence lifetime for a green spinach leaf, for wavelengths of observation greater than 720 nm is shown in Fig. 8.2.8. This measurement was carried out at an average excitation pulse intensity of $\sim$ 1.4 x 10^{14} photons/cm^2 per pulse.

Assuming the presence of a photochemically active trap for PS I at a higher energy (e.g. P700 or P705) than the 730 nm accessory pigment (LHC of PS I), an estimate of the

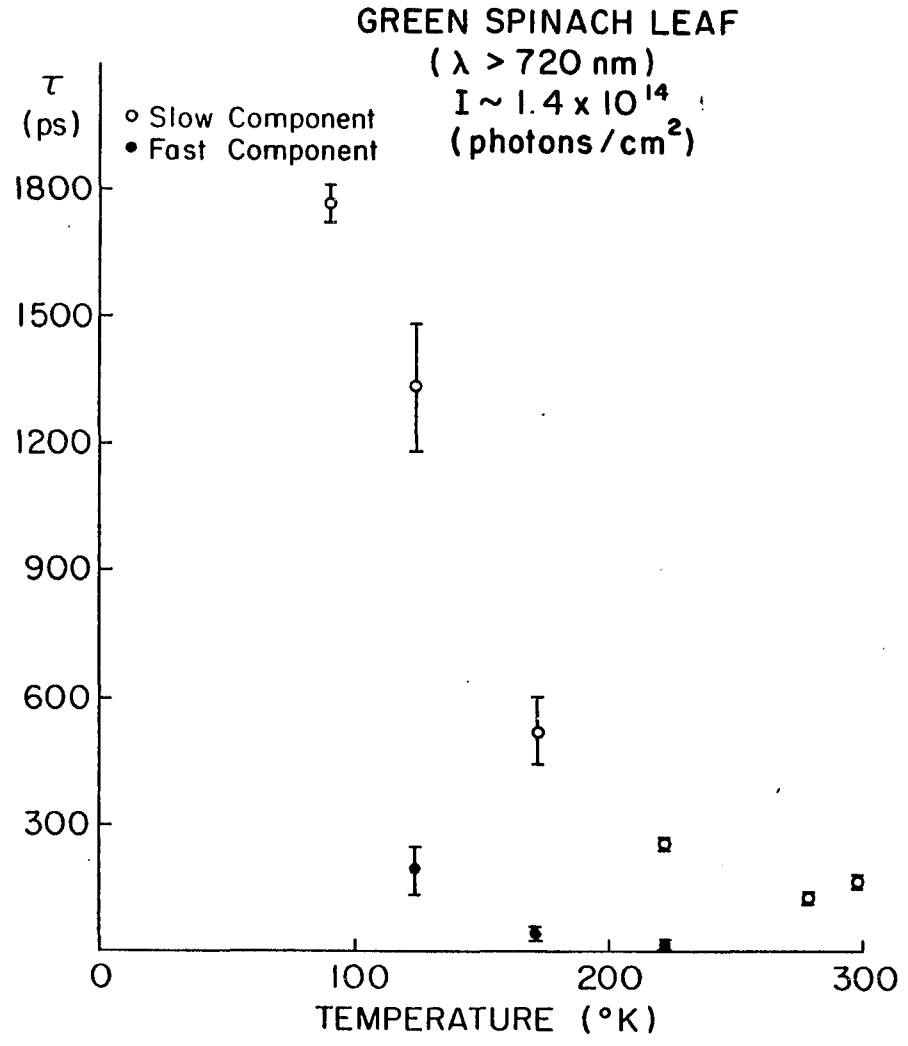

Fig. 8.2.8 Temperature Dependence of the Fluorescence Lifetime from Green Spinach Leaf ($\lambda \gtrsim 720$ nm)

location of the trap level may be obtained. If the trap level occurs at an energy difference of ΔE relative to the accessory pigment complex of PS I, then ΔE may be obtained by considering the trap to be inaccessible for temperatures differences of 300 - 90 ^{o} K or ΔT = 210 ^{o} K. The transfer probability at low temperature is therefore reduced by the Boltzman factor $\exp(-\Delta E/kT)$ and the lifetime increases from 165 ps to 1676 ps.

$$k_{300} = k_0 \exp(-\Delta E/k\ 300^{o}K)$$
$$k_{90} = k_0 \exp(-\Delta E/k\ 90^{o}K)$$

$$\frac{k_{300}}{k_{90}} = \frac{\tilde{\tau}_{90}}{\tilde{\tau}_{300}} = \frac{1763}{165}$$
$$= \exp -[\Delta E/k\ (1/300 - 1/90)]$$
$$\Delta E = k(\ln 10.68)\ (128.6\ ^{o}K)$$
$$\Delta E = 420 \pm 14 \times 10^{-23}\ J$$
$$\Delta E = 211 \pm 7\ cm^{-1}$$

This would place the location of the trap approximately 11 nm above the 730 nm level, or at 719 $\pm$ 0.5 nm.

This result (719 $\pm$ 0.5 nm) is in very good agreement with the previous estimate (722 $\pm$ 1 nm) of the trap location relative to the 730 nm level obtained from picosecond pulse train excitation of spinach chloroplasts using the optical Kerr gate detection system.

8.3 Picosecond Time Resolved Fluorescence Kinetics From Scenedesmus Obliquus Wild Type and Mutant 8 and 11.

The photosynthetic light harvesting process in higher green plants and algae begins with the absorption of photons in the accessory pigment complex which forms the antennae of PS I and PS II. The fluorescence kinetics from enriched PS I and PS II preparations of photosynthetic systems (Yu et al., 1975a) have been investigated in order to obtain specific information on the light harvesting apparatus in each photosystem, as well as interactions between the photosystems. The fluorescence lifetime in whole chloroplasts and PS I and PS II enriched preparations have revealed the presence of two fluorescence components, one at 685 nm which was attributed to PS II emission, and another at 730 nm which was attributed to emission from PS I (Seibert et al., 1974; Yu et al., 1975a, 1977a). In these studies the PS I and PS II traps were in an open state.

Over the years, several models have been proposed to explain energy transfer in the primary photosynthetic process. In particular, energy transfers may take place among the pigment molecules of an isolated photosystem. This is known as the "puddle" model. If the excitation is free to travel in the accessory pigment pool of many such photosynthetic units, such that the excitaton is capable of traveling to any trap in the entire system, then it is

known as the "lake" model (Robinson, 1967).

The alga Scenedesmus obliquus posesses both an active PS I and PS II. However, a mutant strain, Sc 8, posesses an inactive PS I trap while the strain Sc 11 posesses an inactive PS II trap (Weaver and Bishop, 1963). In this study the fluorescence rise and decay times of the alga Scenedesmus Obliquus, wild type and mutants 8 and 11 have been measured by picosecond time resolved fluorescence spectroscopy. Fluorescence kinetic information has been obtained which can be used to further clarify the association of the fluorescence components from PS I and PS II.

Experimental Methods:

Scenedesmus obliquus was grown heterotrophically in a darkened container in Bishop's media at 23 ^{o} C (Bishop, 1971). Subsequent to harvesting, the mutant 8 and 11 samples were resuspended in their growth media and tested for reversion back to the wild type form. A reliable method of determining whether reversion has occurred is to measure the delayed light emisson (this method was employed in order to verify the state of the sample subsequent to the experiment). Delayed emission was first discovered by Strehler and Arnold in 1951, and arises primarily from PS II. Bertsch et al., (1967) have shown that mutant 11 does not give rise to delayed light emission

(delayed light signal less than 1/250 of signal from WT) whereas the wild type strain gives rise to a fast decay and mutant 8 a slowly decaying delayed light emission.

Measurements were made in a 2 mm cell at O.D. 1.0 at 530 nm using single pulse excitation from a Nd:glass laser. The fluorescence signal was detected using a streak camera optical multichannel analyzer system previously described (Yu et al., 1977; Pellegrino et al., 1978,1981). Since the cells tended to settle, the sample cell was inverted 4 to 5 times every two shots (about every 2 minutes).

Experimental Results:

A typical fluorescence decay curve for the Scenedesmus obliquus wild type form is shown in Fig. 8.3.1, the decay was characterized by a single exponential with a lifetime of 181 ps. A typical fluorescence decay for Sc 8 is shown in Fig. 8.3.2, with a single exponential decay time of 364 ps, while a typical decay curve for Sc 11 is shown in Fig. 8.3.3 with decay time of 455 ps. These measurements were obtained at an intensity of $\sim 10^{14}$ photons/cm^2 per pulse. The fluorescence intensity in all three samples was found to decay as a single exponential, with an average lifetime of 222 $\pm$ 16 ps for the wild type form (10 measurements); 373 $\pm$ 27 ps for mutant 8 (10 measurements); and 483 $\pm$ 24 ps for mutant 11 (10 measurements). All of the risetimes were resolution

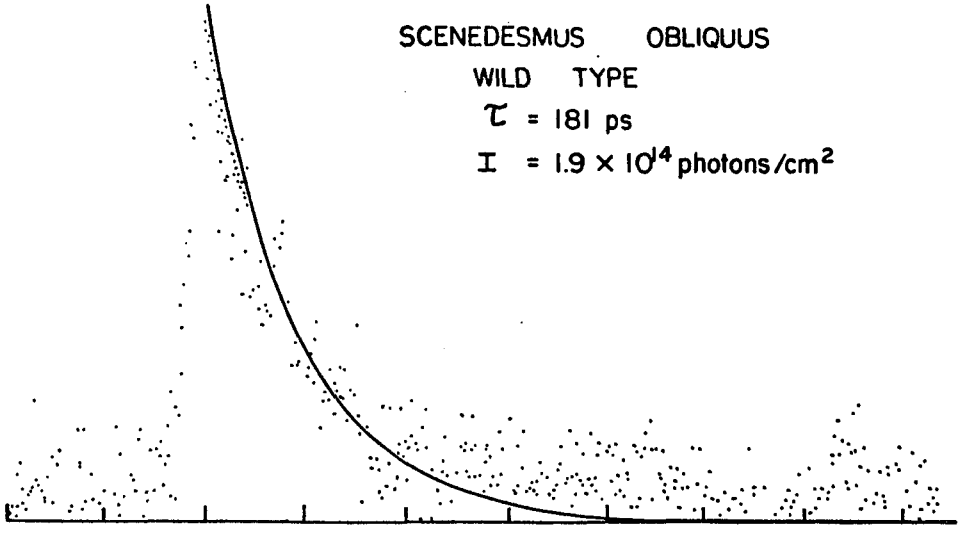

Fig. 8.3.1 Fluorescence Decay of Sc WT.

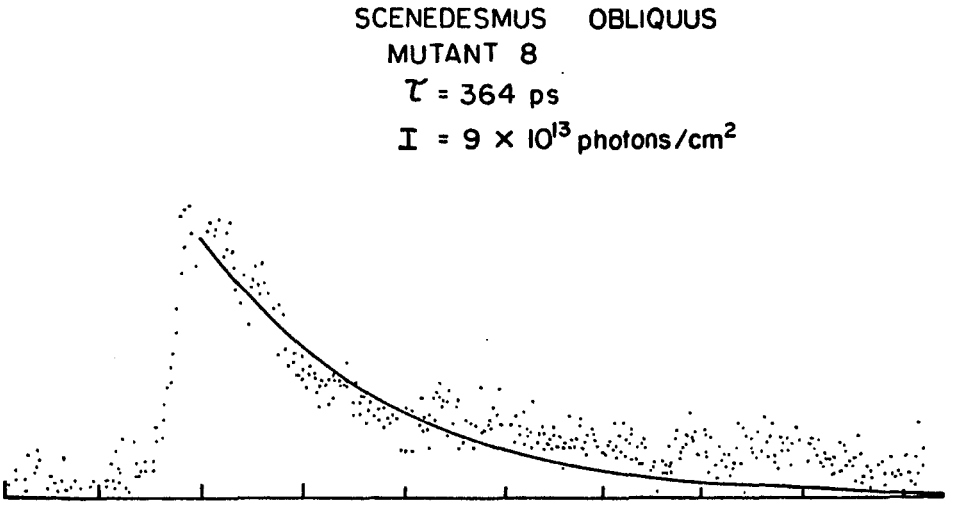

Fig. 8.3.2 Fluorescence Decay of Sc 8.

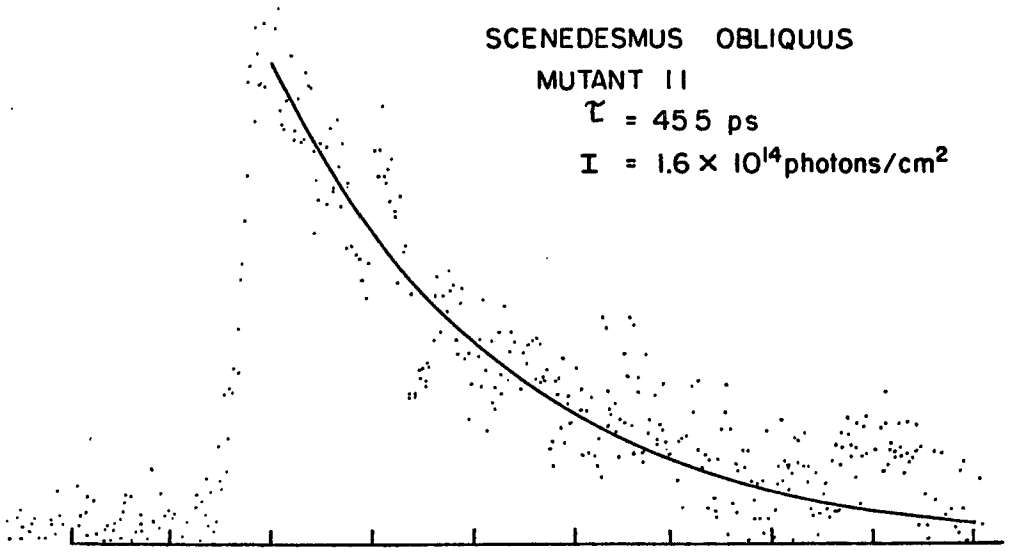

Fig. 8.3.3 Fluorescence Decay of Sc 11.

limited (less than 12 ps). These results are summarized below:

$$\tilde{\tau}_{WT} = 222 \pm 16 \text{ ps}$$

$$\tilde{\tau}_{M\ 8} = 373 \pm 27 \text{ ps}$$

$$\tilde{\tau}_{M\ 11} = 483 \pm 24 \text{ ps.}$$

Discussion:

The fluorescence from Scenedesmus obliquus Wild Type and mutant forms 8 and 11 should reflect the fluorescence kinetics of the light harvesting complex as well as the photoactive excitation energy trapping systems present in each sample. A simple model is proposed to explain the observed kinetic measurements. This model will be used to extract information from the measured relaxation rates.

The photosynthetic system is considered as a single connected physical unit with two independent traps, T_2 and T_1, representing P_{680} and P_{700} respectively (Fig. 8.3.4). The model considers that the energy transfer rate at any location in the system is determined by the local structural arrangement of pigment chromophores. Therefore when an excitation is generated by an absorbed photon, the energy transfer rate varies continuously as the excitation migrates toward T_1 or T_2. Outside the local neighborhood of T_1 and T_2 an effective migration rate k_2 is considered in the vicinity of T_2 and k_1 in the vicinity of T_1. Within the effective trapping zone of T_2 the rate is k_{2T}, while within the effective trapping zone of T_1 the rate is k_{1T}.

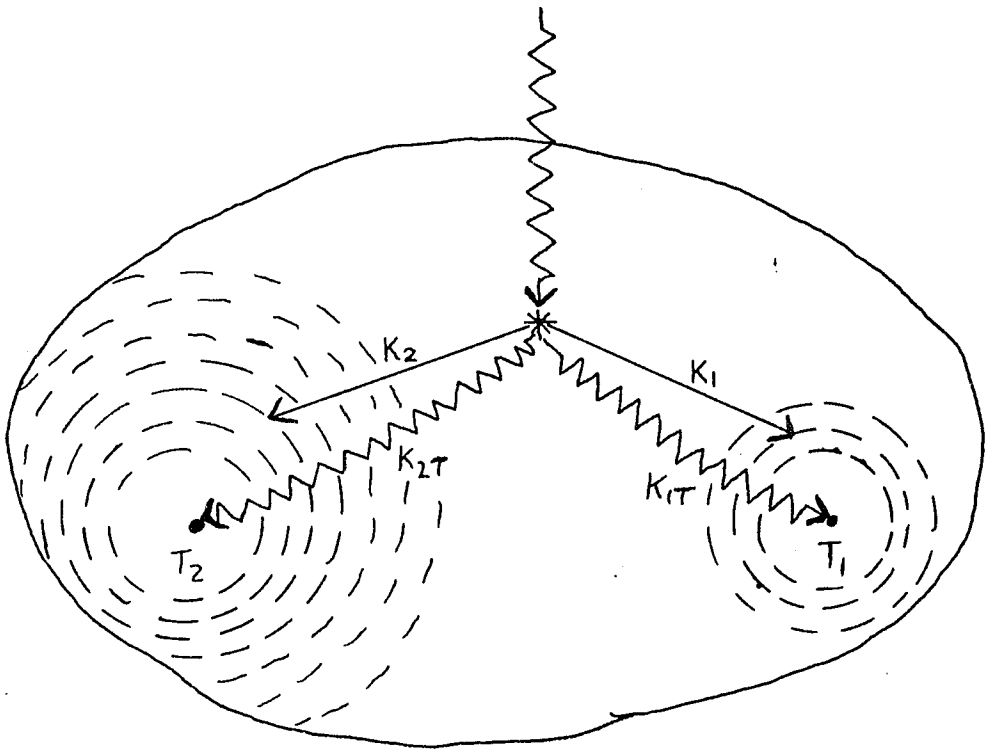

N = Number of excitations in the photosynthetic system.

k_2 = effective transfer rate in the neighborhood of trap T_2.

k_{2T} = effective transfer rate into trap T_2.

k_1 = effective transfer rate in the neighborhood of trap T_1.

k_{1T} = effective transfer rate into trap T_1.

Fig. 8.3.4 Proposed Model for Excitation Energy Transfer in the Photosynthetic System.

The temporal behaviour of the excited singlet state population in the Wild Type form is governed by the equation:

$$\frac{dN}{dt} = - (k_2 + k_{2T} + k_1 + k_{1T}) N \quad .$$

While for the mutant 8 form it is given by:

$$\frac{dN}{dt} = - (k_2 + k_{2T} + k_1) N \quad ,$$

and in mutant 11 by;

$$\frac{dN}{dt} = - (k_2 + k_{1T} + k_1) N \quad .$$

for $t > 0$.

The fluorescence decay rate for Sc WT, Sc 8 and Sc 11 are therefore given by:

$$k_{WT} = k_2 + k_{2T} + k_1 + k_{1T} \qquad (1)$$

$$k_{M\ 8} = k_2 + k_{2T} + k_1 \qquad (2)$$

$$k_{M\ 11} = k_2 + k_{1T} + k_1 \qquad (3)$$

respectively.

The measured fluorescence decay rates are:

$$k_{WT} = 4.5 \times 10^{9} \text{ sec}^{-1} \quad (4)$$

$$k_{M\ 8} = 2.68 \times 10^{9} \text{ sec}^{-1} \quad (5)$$

$$k_{M\ 11} = 2.07 \times 10^{9} \text{ sec}^{-1} \quad (6)$$

Considering equations (1) and (2), we find that,

$$k_{1T} = k_{WT} - k_{M\ 8} \ .$$

While from equation (1) and (3) we obtain,

$$k_{2T} = k_{WT} - k_{M\ 11} \ .$$

Using the above measured values the trapping times k_{1T}^{-1} and k_{2T}^{-1} are calculated to be,

$$k_{1T}^{-1} = 549 \text{ ps} \ ,$$

and

$$k_{2T}^{-1} = 412 \text{ ps} \ .$$

Using these values in equation (1) we obtain the effective transfer rate in the pigment complex as,

$$(k_1 + k_2)^{-1} = 4 \text{ ns.}$$

This effective energy migration time is the energy transfer time outside of the effective range of either T_1 or T_2. Since the observed decay times from most photosynthetic systems are $\leq$ 500 ps, these measurements suggest that the effective range of the traps is indeed large. Therefore, although the initial transfer rate may be slow, it quickly increases to the effective trapping rate of either T_2 or T_1 due to the physical structural arrangement of pigment molecules in the entire photosynthetic complex. This interpretation is consistent with the concept of a "lake" model.

Chapter 9. Fluorescence Kinetics and Polarization Anisotropy from Dyes, Pigments and Photosynthetic Systems.

This chapter is divided into three sub-sections covering the measurements obtained in 1) dyes 2) pigments and 3) photosynthetic systems.

The transfer of excitation energy to a specific trap in the PSU involves either a random walking of the excitation via weak resonance interactions or a strong transfer mechanism. For the case of homogeneous transfer, or transfer among like molecules, sensitized fluorescence is not available as a probe technique. However it is possible to follow the time dependence of the fluorescence polarization, which is directly indicative of intermolecular energy transfer. For a transfer probability time t, for transfer of the excitation energy from one neighboring molecule to another, the actual transfer time depends on the number of nearest neighbors. It is possible for the fluorescence to depolarize in a single transfer (1-2 ps) so that a complete depolarization from a well oriented sample of molecules is possible within a 10-12 ps resolution time element.

The observation of a small degree of polarization from Chl. a fluorescence indicates that the excitation diffuses via resonance transfer randomizing the initial polarization. A slightly higher degree of polarization at

725 nm which can be attributed to PS I has been observed (Rabinowitch and Govindjee, 1969; Knox, 1975). However, all of these polarization experiments were conducted using steady state excitation and observation techniques. It was Jablonski (see Bay and Pearlstein,1963) who first recognized the relatively greater benefits to be obtained through time dependent fluorescence depolarization measurements. Numerous time resolved fluorescence depolarization studies were subsequently undertaken.

Measurement of fluorescence depolarization kinetics allows a view into the intermolecular energy transfers. For homogeneous transfer, the parameter of sensitized fluorescence is not available for investigation as the molecular absorption and emission spectrum of the individual molecules are identical. However, when excited, such a molecular system reveals its energy transfer matrix through the depolarization of fluorescence. For energy transfers that are fast compared to the time of molecular rotation and vibration the excitation does not have a chance to depolarize, and strongly polarized emission is observed. Similarly for energy transfers that are slow compared to such internal molecular relaxation mechanisms, the molecule may reorient its transition dipole with respect to its neighbors through a collision or rotation giving rise to a fast and complete depolarization of its fluorescence within a few such transfers. Depending on the initial molecular

aggregation and orientation of the transition dipoles, the energy transfers will therefore be manifested by the depolarization kinetics. Such transfers are also indicative of the particular phase of the material.

Thus in particular, information on the angle between the absorption dipole and the incident polarization direction can be obtained by measuring the angular maximum of the t = 0 emission. The angle between the absorption and emission dipole can be similarly obtained by exciting parallel to the absorption dipole and again measuring the maximum of the t = 0 emission. The orientational distribution function of molecular dipoles $f(\theta)$ can be measured from the polarization anisotropy at t = 0, if one assumes that the absorption and emission dipoles are parallel. Measurement of the fluorescence lifetime and polarization anisotropy as a function of viscosity can also give valuable information on the phase state of the media.

9.1 Time Resolved Fluorescence Measurements in Dyes:

Dye molecules provide a particularly interesting means of exploring the energy decay mechanisms that take place subsequent to photoexcitation. The subnanosecond fluorescence kinetics and fluorescence polarization kinetics of the triphenylmethane dye malachite green were investigated in order to obtain information on the environmental effects on fluorescence polarization

kinetics and can provide a basis for the investigation of the fluorescence polarization from photosynthetic systems. Dye molecules in solution possess optical properties which are known to depend on many environmental factors (Pringsheim, 1949; Forster, 1951; Van Durren, 1963). The fluorescence yield and lifetime as well as the absorption and emission spectra can be readily affected by various parameters of the solvent such as the polarity, viscosity, pH, hydrogen bond donor or acceptor strength and temperature. In particular, the fluorescence yield of malachite green increases by orders of magnitude when the viscosity of the solvent is increased (Oster and Nishijima, 1956; Forster and Hoffman, 1971; Yu et al., 1977). The increase of the fluorescence yield and lifetime with increase in viscosity has been attributed to the inhibition of the rotational motion of the phenyl rings of the molecule in viscous media. The molecular structure of the dye malachite green is shown in Fig. 9.1.1. The structure is highlighted by the propeller like arrangement of the three phenyl rings about the central carbon atom.

In this study, the fluorescence lifetime and polarization anisotropy (R(t)) of malachite green were measured as a function of solvent viscosity in order to investigate the effect of environmental changes on the orientational order of dye molecules in solution.

Forster and Hoffman (1971) measured the quantum yields

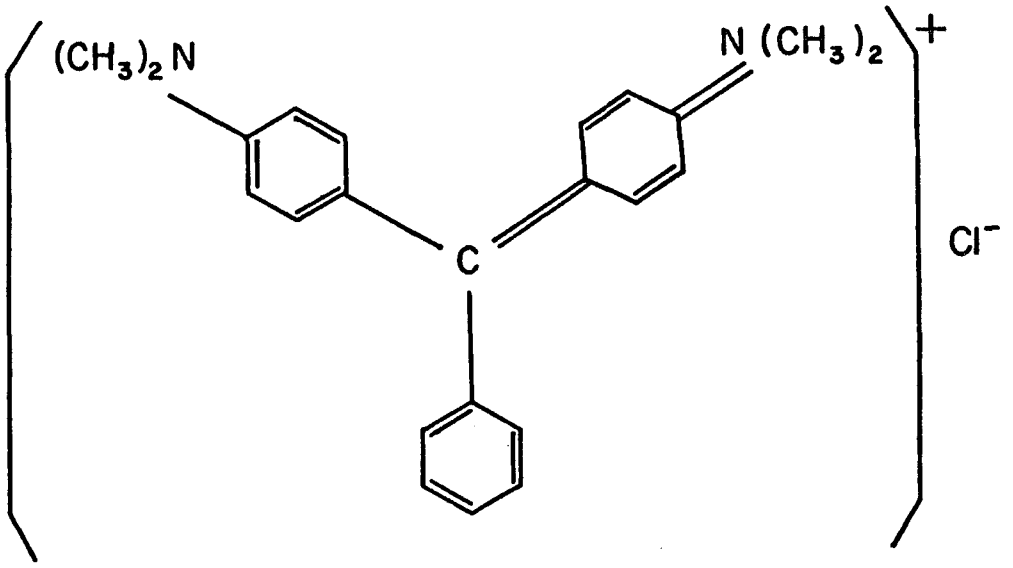

Fig. 9.1.1 Molecular Structure of Malachite Green.

of various triphenylmethane dyes in different solvents as a function of temperature. They found the quantum yield to vary with viscosity as $\eta^{2/3}$ for viscosity less than 200 poise(P). A model based on the rotational motion of the phenyl rings was proposed to explain the observed $\eta^{2/3}$ relationship. They additionally predicted a time dependence of $\exp(-bt^3/\eta^2)$ for the fluorescence relaxation. The recovery of the ground state population after excitation in this dye has also been measured by the method of time resolved absorption (Magde and Windsor, 1974). Ippen et al., (1976) have recently measured the absorption recovery of the ground state using a sub-picosecond dye laser. They have observed that the absorption recovery for malachite green behaves as a single exponential for $\eta < 1$ P. A second faster exponential component appeared for $\eta > 1$ P. The fast component was observed to behave closely to the $\eta^{2/3}$ relationship and was thus attributed to the fluorescence lifetime. The longer component was observed to follow more closely to $\eta^{1/2}$, and was suggested as the time for equilibration of the ground state manifold.

Using both an optical Kerr gate and streak camera, Yu et al., (1977) measured the fluorescence kinetics of malachite green over the viscosity range from 1 to 60 P, and obtained a dependence of the fluorescence lifetime on the solvent viscosity proportional to $\eta^{2/3}$. Despite the disadvantages of the Kerr gate and the more extensive

normalization used in that technique, both the Kerr gate data and the streak camera results were found to be in good agreement in that study. The measurements reported here are an extension of the work of Yu et al., (1977). In the present experiments, the lifetime of the first excited singlet state as well as the polarization effects have been studied as a function of the solvent viscosity from 6 to 60,000 P. The measured fluorescence kinetics were found to be single exponential decays, varying with viscosity as $\eta^{2/3}$ for $1 \leq \eta \leq 60$ P, $\eta^{1/2}$ for $\eta \geq 60$ P, and asymptotically approaching a constant value for $\eta > 1000$ P. In the present work, the polarization kinetics were also investigated as a function of the solvent viscosity in order to obtain information on the relationship between local molecular order and environmental changes.

Experimental Methods:

The fluorescence kinetics were measured with a streak camera optical multi channel analyzer detection system (Yu et al., 1977). The range of photon flux at the sample site was about 10^{14} to 10^{15} photons/cm^2 per pulse. A steady state fluorometer was used to measure the fluorescence spectra from the dye solution. The fluorometer was made from a light source, monochromator, light chopper, spectrometer with photomultiplier, and lock-in amplifier. The fluorescence from a thin sample cell (1-2 mm) was collected at 45° from the front

surface.

The chemicals malachite green (99% certified, Eastman Kodak) and anhydrous glycerol (J.T. Baker) were used without further purification. The concentration of malachite green was 5×10^{-4} M in a sample length of 5 or 2 mm. The viscosities of glycerol and glycerol water mixtures at various temperatures were obtained from standard tables (Sheely, 1932). A viscosity range of 1 to 60,000 P was covered in this experiment. The malachite green samples were placed in an optical Dewar, and the temperature of the sample was changed by flowing cooled nitrogen gas into the Dewar.

The fluorescence depolarization kinetics of malachite green were also measured as a function of solvent viscosity. In the polarization measurements, excitation was provided by two orthogonally polarized 5300 A, 6 ps laser pulses obtained from the single pulse at 5300 A by use of a beam splitter optical delay technique (Pellegrino et al., 1981) as shown in Fig. 9.1.2.

In the polarization measurements two orthogonally polarized 530 nm excitation pulses with approximately equal intensity and separated by one nanosecond delay were used to excite the sample. An analyzer (Polaroid HN 38) was placed between the sample and the streak camera, thus allowing for the simultaneous measurement of the fluorescence signal both parallel to and perpendicular to the incident polarization direction. The system was

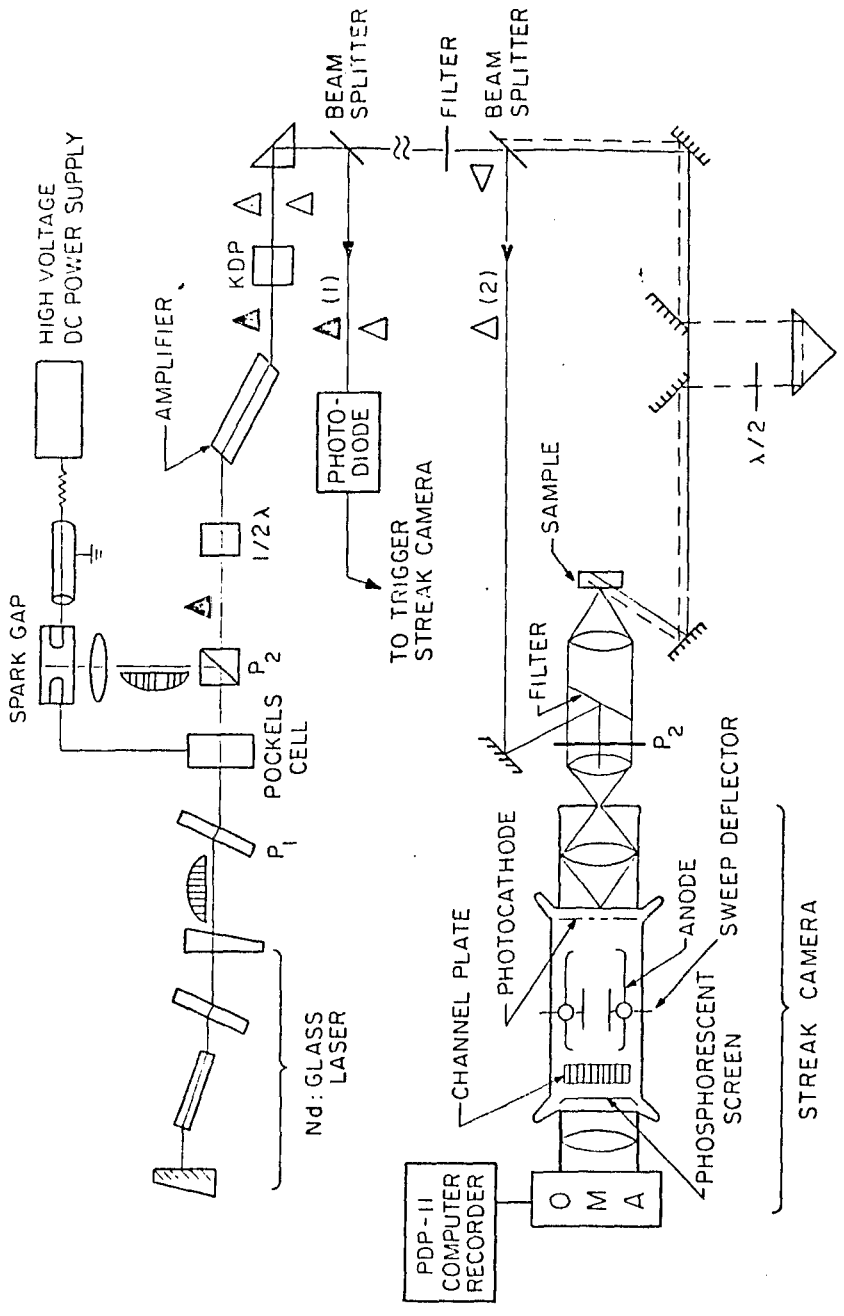

Fig. 9.1.2 Beam Splitter Optical Delay Technique Measurement of Fluorescence Polarization.

calibrated by equalizing the fluorescence emission from a $2x10^{-4}$ M solution of erythrosin in water excited by the two pulses with the analyzer removed. A viscosity range from 6.29 P to 60,000 P was covered in the polarization experiments, thereby providing overlap with the previous investigation of the fluorescence decay kinetics.

Experimental Results:

The fluorescent kinetics of malachite green in glycerol at room temperature measured by the streak camera and the Kerr gate are shown in Fig. 9.1.3a and b respectively. The decay of malachite green fluorescence is characterized by a single exponential. Fig. 9.1.4a shows the fluorescence decay of malachite green at room temperature and 6.29 P, measured with the two pulse excitation beam splitter optical delay technique of Fig. 9.1.2, with the analyzer removed from the front of the entrance slit of the streak camera. Fig. 9.1.4b shows the fluorescence polarization observed for malachite green at 6.29 P with the analyzer in place. The first decay profile is due to fluorescence measured parallel to the polarization direction of the incident pulse, with the second decay profile measuring the fluorescence component with polarization vector perpendicular to the polarization direction of the incident pulse. By rotating the analyzer 90^{o}, parallel to the polarization direction of the

second excitation pulse, the relative signals are reversed as expected (Fig. 9.1.4c).

Fig. 9.1.4 d shows the fluorescence polarization kinetics measured at 121 P. The marked increase of the fluorescence decay time clearly shows the effect of the increasing solvent viscosity on the local deexcitation of the molecule in solution. At each viscosity region investigated, at least 6 such measurements were obtained. The measured lifetimes are plotted in Fig. 9.1.5 as a function of solvent viscosity. The fluorescence polarization anisotropy at t=0 is plotted as a function of solvent viscosity in Fig. 9.1.6. The polarization anisotropy at t=0 for viscosities less than 1000 P is found to be 0.38 ± 0.01 in agreement with the expected theoretical value of 0.4 for a random arrangement of molecular dipoles in solution. However, for viscosities $\gtrsim$ 3000 P, the polarization anisotropy decreases to 0.11 ± 0.01.

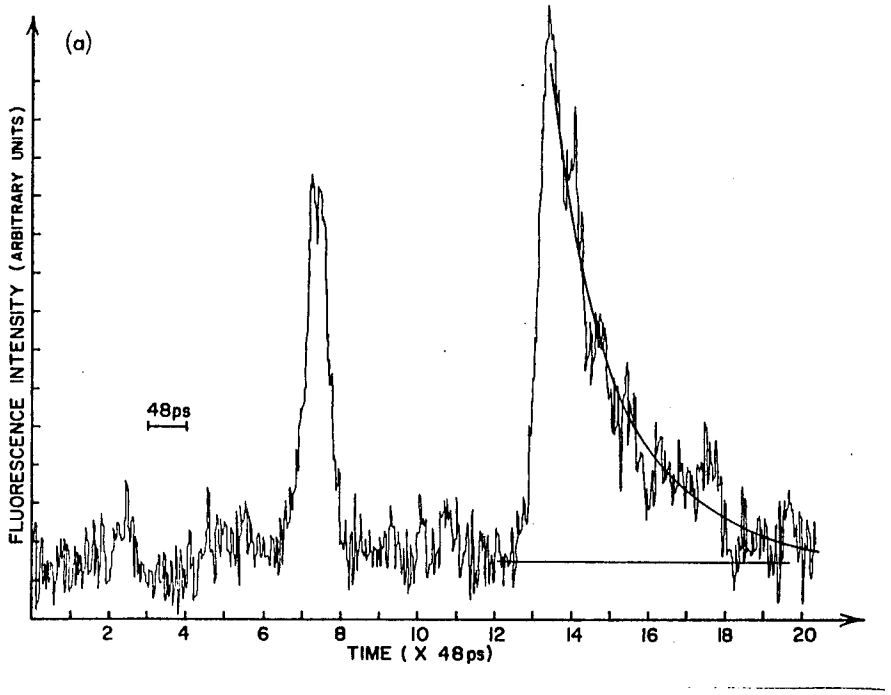

Fig. 9.1.3a Fluorescence Decay of Malachite Green in Glycerol Measured With Streak Camera.

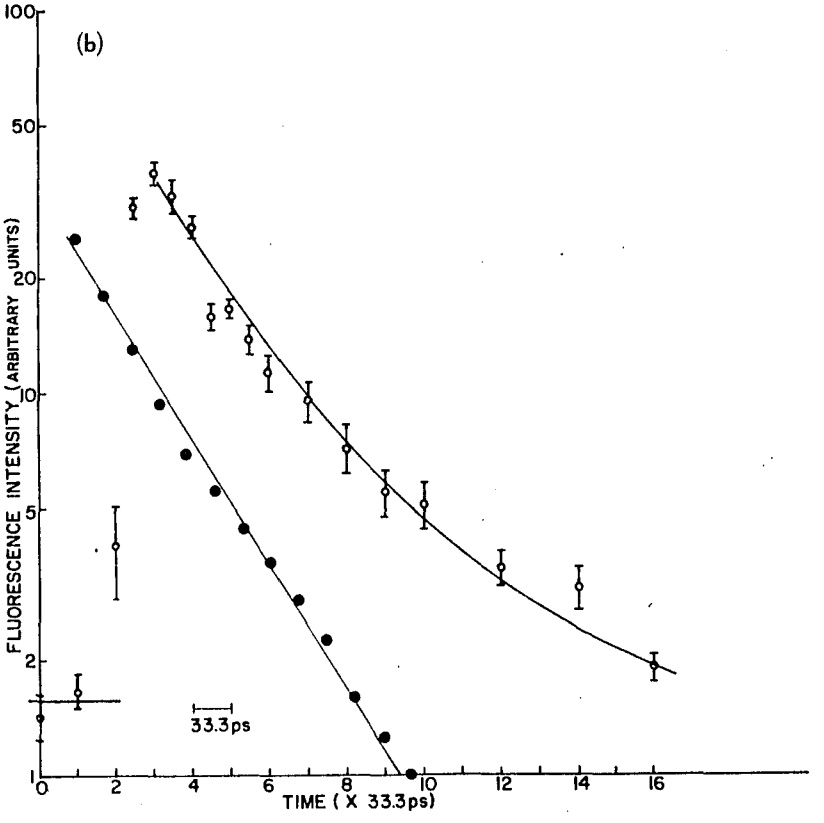

Fig. 9.1.3b Semilog Plot of Malachite Green Fluorescence as Measured with Streak Camera (●) and Kerr Gate (o).

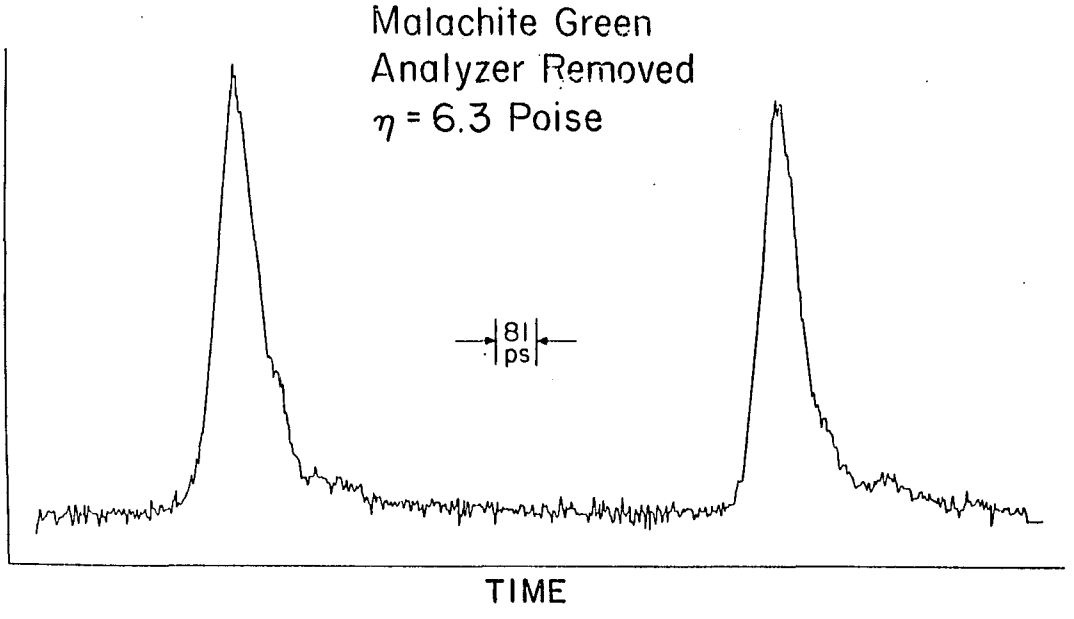

Fig. 9.1.4a Fluorescence Decay of Malachite Green at 6.29 P Measured Without Analyzer.

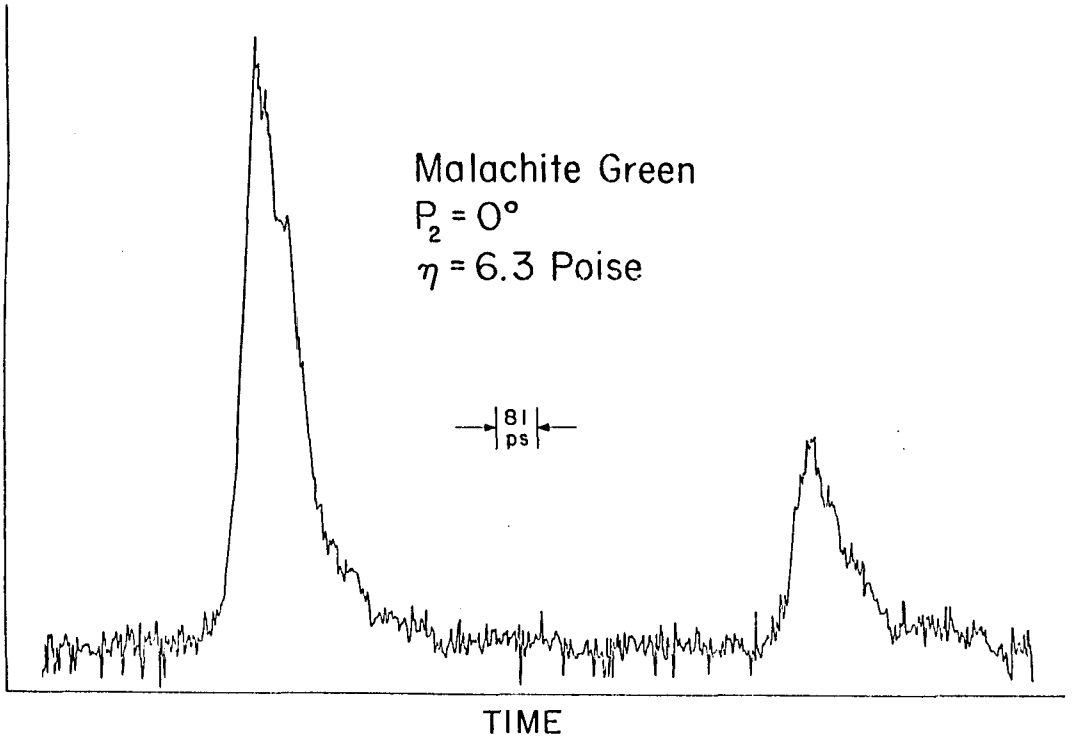

Fig. 9.1.4b Fluorescence Decay of Malachite Green at 6.29 P Measured With Analyzer in Place.

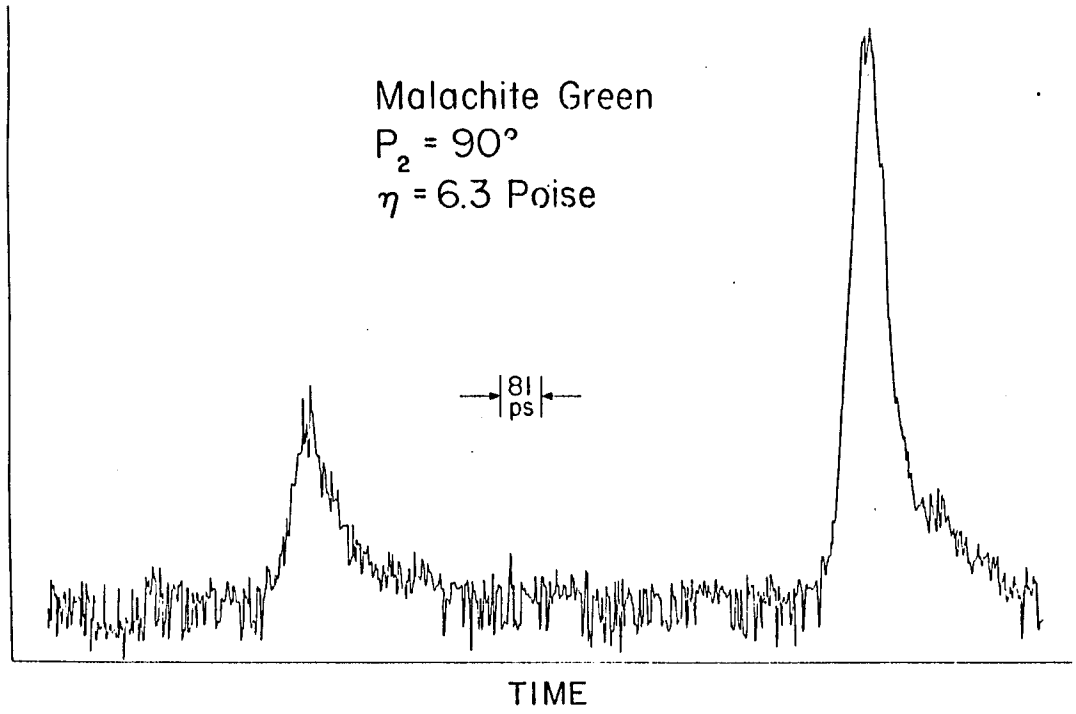

Fig. 9.1.4c Fluorescence Decay of Malachite Green Measured at 6.29 P With Analyzer Rotated 90°.

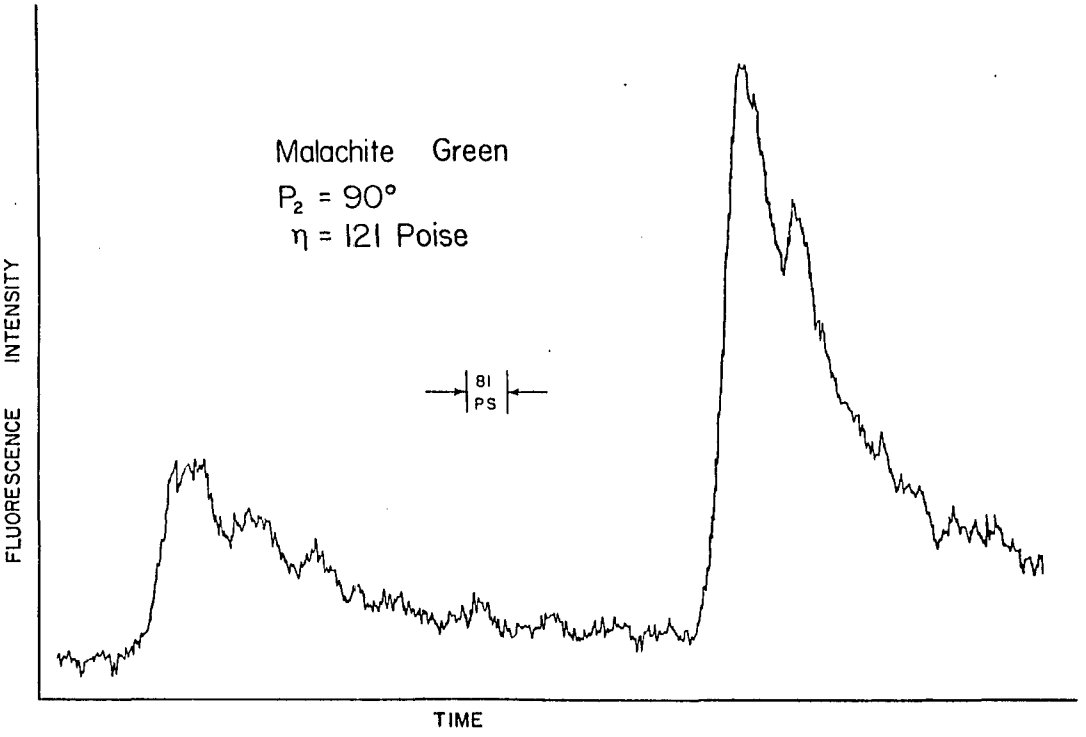

Fig. 9.1.4d Fluorescence Decay of Malachite Green Measured at 121 P.

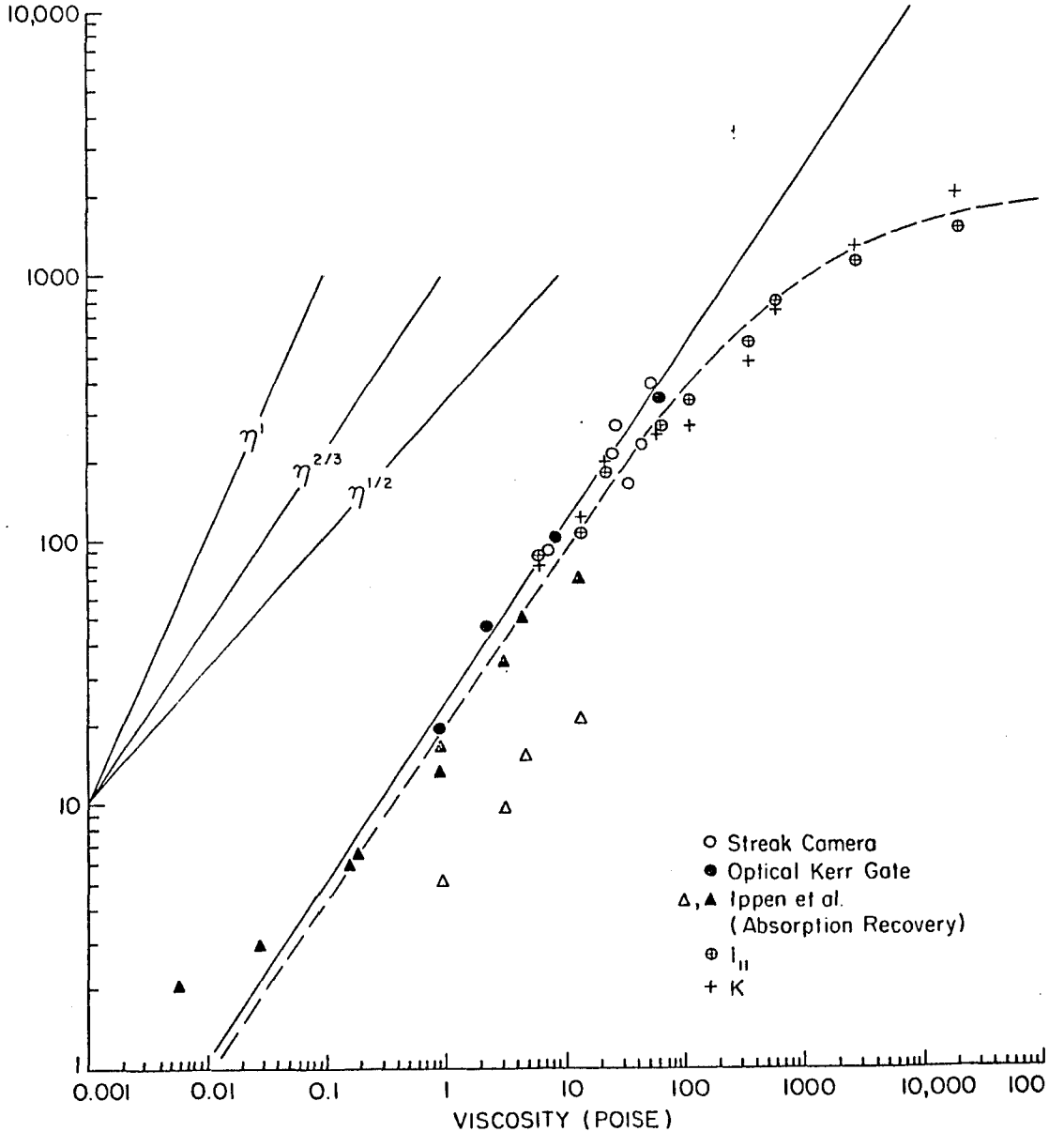

Fig. 9.1.5 Dependence of Fluorescence Lifetime of Malachite Green on Solvent Viscosity.

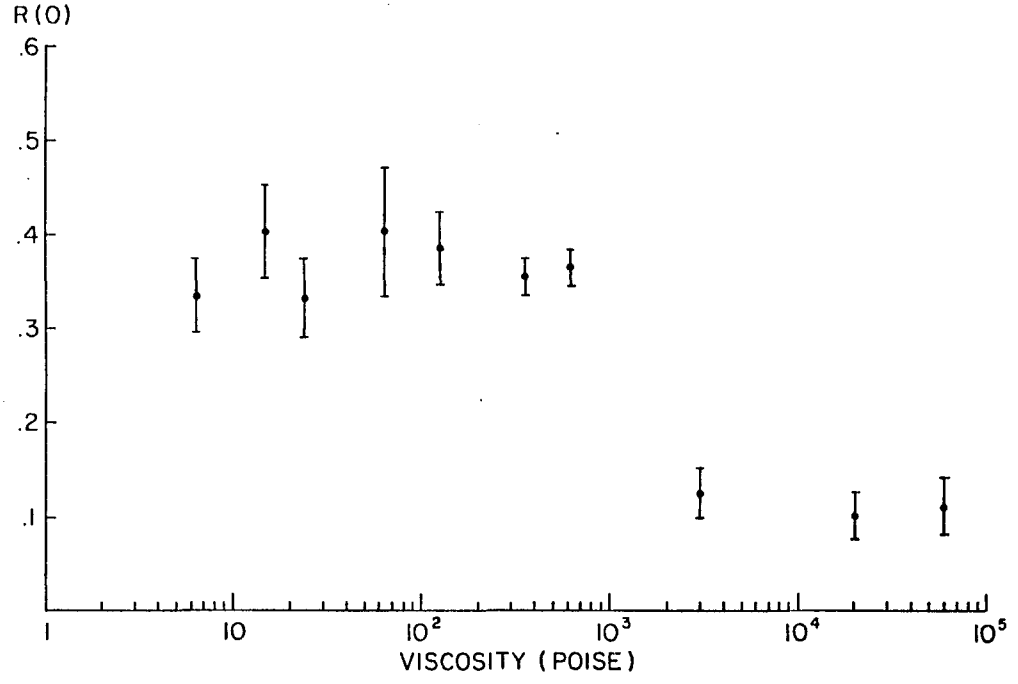

Fig. 9.1.6 T=0 Polarization Anisotropy of Malachite Green in Glycerol as a Function of Solvent Viscosity.

Discussion:

The dramatic increase in the fluorescence yield, fluorescence lifetime and rotational decay time with increasing solvent viscosity observed in these measurements is attributed to the inhibition of the rotational motion of the phenyl rings in viscous media. The temporal profile of the fluorescence at any given time measures the relative population of the first excited state at that time. Thus the measured rate of fluorescence decay is made up of the sum of the radiative ($S_1 \rightarrow S^*_o + h\nu$), nonradiative internal conversion ($S_1 \rightarrow S^*_o$), and inter-system crossing ($S_1 \rightarrow T_1$) rates. The radiative lifetimes of the dye molecules can be estimated from the absorption spectra and the 0-0 transition, and are essentially constant for the various solutions studied. In malachite green the intersystem crossing rate is small, as can be inferred from the observation of the fast and complete recovery of the absorption of the ground state in the experiment of Ippen et al., (1976). Therefore the observed variation of fluorescence lifetime in malachite green can be interpreted as the change of the internal conversion rate of the dye solution for varying viscosities.

The measured viscosity dependence of the fluorescence lifetime of malachite green in this measurement (Fig. 9.1.5) does not obey a simple viscosity dependence. For $1 \leq \eta \leq 60$ P, the fluorescence lifetime follows an

$\eta^{2/3}$ dependence, in agreement with the previous work of Yu et al., (1977) and with the fluorescence yield measurements of Forster and Hoffman (1971), who also theoretically predicted the $\eta^{2/3}$ viscosity dependence. However their predicted $\exp(-bt^3/\eta^2)$ time dependence was not confirmed in this experiment. For the viscosity range $60 \leq \eta \leq 1000$ P, the dependence can be best fit to $\eta^{1/2}$ viscosity dependence. As expected, for viscosities greater than 1000 P the lifetime approaches a constant value. Although attempts have been made to fit the viscosity dependence to $\eta^{2/3}$ and $\eta^{1/2}$, a more complicated viscosity dependence is indicated by the results of these measurements. Physically, a simple dependence of the fluorescence lifetime on the solvent viscosity should not be expected since the fluorescence lifetime must asymptotically approach the unimolecular decay rate as the rotational non-radiative deexcitations are frozen out. The fluorescence decay rate may be described by the relation;

$$k = k(\eta) + k(\infty)$$

where $k(\eta)$ is a viscosity dependent term which may be taken to be of the form $a\eta^{-2/3}$ for viscosities in the region of 1 to 60 P, and $k(\infty)$ is a viscosity independent term of the form $k(\infty) = k_{ST} + k_{NR} + k_R$. From the data presented in Fig. 9.1.5, a value of 5×10^8 sec^{-1}

can be estimated for $k(\infty)$ in the high viscosity region. In addition, $k(\eta)$ can be obtained in the low viscosity range as $5 \times 10^{10} \eta^{-2/3}$. This functional form for k can be fit to the data to within $\pm$ 10 %.

To this date, no satisfactory microscopic theory has been found to explain the functional form of the decay rate, the time-resolved fluorescence decay profile and steady state fluorescence quantum yield dependence on the viscosity. A detailed theoretical study of these effects is required in order to fully understand the relationship of the structural properties of dye molecules in solution with respect to solvent properties. Such a study is beyond the scope of the present work.

The absorption recovery times measured by Ippen et al., (1976) are also shown in Fig. 9.1.5 for completeness. It is interesting to note that the absorption recovery times of the slow component measured by Ippen et al., (1976) fall close to the measured fluorescence lifetime and the $\eta^{2/3}$ line. The fast component, however, measured to be less than 5 ps for viscosity $<$ 0.1 P, does not obey this relationship. Since the values of the slow component of the absorption recovery are found to be close to the values for the measured fluorescence lifetime for $\eta <$ 20 P, the observed slow component of the absorption recovery apparently manifests the internal conversion kinetics. The fast component may possibly reflect the time required for

non-radiative equilibration in the ground state manifold. In principle, the S_1 equilibration time is reflected in the fluorescence risetime. The risetimes measured in this experiment were resolution limited to $\leq$ 12 ps. Recently, the S_1 equilibration time for large dye molecules have been reported to be less than 0.2 ps, and independent of solvent properties. Therefore the ground state equilibration time can also be assumed to be of this order. The interpretation of the short component remains in doubt.

As a first approximation, the molecules of malachite green may be considered to be spheroidal. In the analysis of the viscosity dependence of the fluorescence polarization both a random distribution model, for the case of malachite green dye molecules in solution at low viscosity, and an oriented distribution model, for the case of malachite green dye molecules in solution in the high viscosity limit (where the molecular rotations have been essentially frozen) is considered.

When a linearly polarized pulse excites a distribution of molecules in solution a non-random distribution of excitation is achieved since molecules having their absorption dipole in the plane of polarization are preferentially excited. If such a molecule rotates or otherwise transfers its energy to another state or molecule prior to emission, the fluorescence will depolarize. If one considers the dye molecule to behave

as a spheroid in viscous media, two conditions arise. Either the molecule "sticks" to its viscous surrounding, or it "slips" in that surrounding. More specifically if the velocity vector of the solute and solvent are equal at their surfaces, then the solvent sticks to the solute and rotates with it. If on the other hand there is no tangential component of the stress tensor at the solute solvent interface, then the solute molecules can rotate freely and the slipping boundary condition is said to hold. The molecular symmetry as well as the polarity of the molecule with respect to its environment determines which condition applies. In addition, temperature can also affect the boundary conditions.

For a randomly oriented system of dipoles, the intensity of fluorescence observed through an analyzer set either parallel to or perpendicular to the incident polarization direction is obtained by applying a Green's function operator to the parallel and perpendicular components of the fluorescence decay relative to an initial random distribution of dipoles described in terms of the second Legendre polynomial. These components are:

$$I_{\parallel}(t) = (1/3 + 4/15 \langle P_2(e(0).e(t)) \rangle)\ u^2\ K(t)$$

$$I_{\perp}(t) = (1/3 - 2/15 \langle P_2(e(0).e(t)) \rangle)\ u^2\ K(t)$$

where P_2 is the second Legendre polynomial; e(0), e(t) are the directions of the transition dipole moment u at times 0 and t respectively; and K(t) describes the temporal behaviour of the fluorescence decay (Fleming et al., 1976).

An order parameter which characterizes the polarized fluorescence emission in terms of the intensity of fluorescence measured parallel to and perpendicular to the incident polarization direction ($I_{\parallel}$ (t) and $I_{\perp}$ (t) respectively), is R(t), the fluorescence polarization anisotropy defined by the following relation:

$$R(t) = \frac{I_{\parallel}(t) - I_{\perp}(t)}{I_{\parallel}(t) + 2I_{\perp}(t)} .$$

For a random distribution of spheroidal molecules in solution R(0) = 0.4, which agrees with the measured value for R(0) for viscosities less than 1000 P. If these molecules are now placed in a matrix or ordered array, the value of R(0) is expected to change as well as the form of $I_{\parallel}$ and $I_{\perp}$. The emission anisotropy at t=0 for an oriented molecular distribution, for the case where the absorption dipole is parallel to the unique symmetry axis of the system, is given by (Szabo, 1980):

$$R(0) = \frac{(2\langle P_2^2\rangle + \langle P_2\rangle)\, P_2(\cos\varphi)}{1 + 2\langle P_2\rangle}$$

where $\langle P_2\rangle$ is the expectation value of the second order Legendre polynomial for the distribution function $f(\theta)$, and is given by,

$$\langle P_2\rangle \equiv \langle P_2(\cos\theta)\rangle = \int_0^{\pi} \sin\theta\, d\theta\, f(\theta)\, P_2(\cos\theta)$$

and where θ is the angle between the long axis of the molecule and the major symmetry axis of the system, and φ is the angle between the absorption and emission dipole.

For a molecular distribution described by a distribution function of the form $f(\theta) = 3/2 \cos^2\theta$, $R(0) = 0.10 \pm 0.01$ (Pellegrino et al., 1981). For viscosities greater than 3000 P, the values for the polarization anisotropy were measured to be $R(0) = 0.11 \pm 0.01$. Since for $\eta \lesssim$ 1000 P, $R(0)$ was measured to be 0.38, an ordering of the malachite green molecules from a random distribution to an ordered molecular array appears to have taken place at $\eta \gtrsim$ 1000 P. This is consistent with the observed change in the lifetime dependence as a function of solvent viscosity in the 1000 P viscosity region where the rotational deexcitation mode appears to

have "frozen out".

At low viscosities the molecules are free to rotate in solution, so that no long range order can be established. As the viscosity increases, the rotational degree of freedom gradually decreases to a point where molecules may form local ordered clusters through covalent bond ligations or ionic interactions. This allows for a long range order to be established which manifests itself in the lower value of R(0) measured at high viscosity. However, the possibility that the decrease in R(0) with increasing viscosity arises solely from the freezing out of the individual molecular rotations and thereby being indicative of the molecular dipole polarization measurements alone (as opposed to a long range structural order effect) cannot be entirely ruled out. The dependence of the fluorescence lifetime and fluorescence polarization anisotropy on the viscosity of the solvent can therefore provide a measure of the orientational order of the molecules in relation to the viscosity of the solvent.

9.2 Fluorescence Depolarization of Anthocyanin Pigments:

A system that is very closely related to that of dye molecules in solution may be found in the case of the anthocyanin pigments which occur naturally in flowers. The anthocyanins provide an interesting contrast to the case of accessory pigments found in photosynthetic systems. While photosynthetic accessory pigments are generally always found on a protein substructure which is generally part of a highly structured matrix, the anthocyanin pigments are ligated to proteins which can move inside vacuoles and are thus closer to the case of a dye in solution.

Anthocyanin pigments are found in the petals and leaves of flowers, and the skins of fruits. These pigments are responsible for their varied coloration which also serves to attract birds and insects for plant pollination and seed dispersal. These measurements provide the first *in vivo* and *in vitro* picosecond fluorescence kinetics and polarization measurements of anthocyanin pigments from flowers. Information on the orientational distribution of these chromophores in the *in vivo* molecular environment can be obtained by measurements of the fluorescence polarization anisotropy. A non-random orientational order of the anthocyanin pigments in their naturally occurring vacuoles is indicated by comparison of the *in vivo* and *in vitro* initial values of the

fluorescence polarization anisotropy. Evidence for fluorescence quenching was also found in the in vivo samples.

The polarization measurements were obtained with the beam splitter optical delay technique shown in Fig. 9.1.2 previously described. The kinetics of the fluorescence emission beyond 550 nm were isolated by use of a Corning 3-67 filter which is present in front of the streak camera in all of the streak camera measurements utilizing 530 nm excitation.

Samples of Streptocarpus holstii and Anthurium andreanum were obtained from the Bronx Botanical Gardens of New York. An anthocyanin extract was prepared by placing the flower petals in a methanol solution titrated to pH 0.3 with concentrated HCL. The low pH was used to maintain a reducing environment which stabilized the anthocyanins. This was necessary since anthocyanins become oxidized and break down at higher pH concentrations (Jurd, 1972). At this pH the integrity of the purple color of the Streptocarpus anthocyanins as well as the red color of the Anthurium anthocyanins were maintained. Fluorescence from anthocyanin extracts were measured in a 2 mm optical cell at room temperature. The intact flower petals were mounted on a flat piece of aluminum and a portion of the sample, selected for homogeneity of color and physical appearance such as uniformity of texture and the absence of structural folds, was illuminated.

Absorption spectra of the anthocyanin extracts were measured with a G.C.A. McPherson spectrophotometer. The spectra showed an absorption maximum at 533 nm for both extracts. These results are consistent with those obtained by Song et al., (1972) for cyanidin and pelargonidin extracts.

The time resolved polarized fluorescence emission measured parallel and perpendicular to the incident polarization direction is shown in Fig. 9.2.1 for the Streptocarpus flower, and Fig. 9.2.2 for the Streptocarpus extract. Measurements of the fluorescence decay kinetics and polarization anisotropy at t=0 are displayed in Table 9.2.1. All results are reported as the average and mean standard deviation of the specified number of measurements. The fluorescence lifetime for the Streptocarpus extract was 128 $\pm$ 33 ps (15 measurements), while for the flower it was 59 $\pm$ 13 ps (20 measurements). The fluorescence lifetime for the Anthurium extract was 18 $\pm$ 8 ps (5 measurements), while for the flower it was 10 $\pm$ 3 ps (7 measurements).

The shorter lifetimes measured in the in vivo condition as compared to the in vitro case may be indicative of concentration quenching in the flowers. Although the values for the pigment concentrations in flowers have not yet been established, these concentrations must be greater than any which can be possibly obtained in vitro. From the observed lifetime

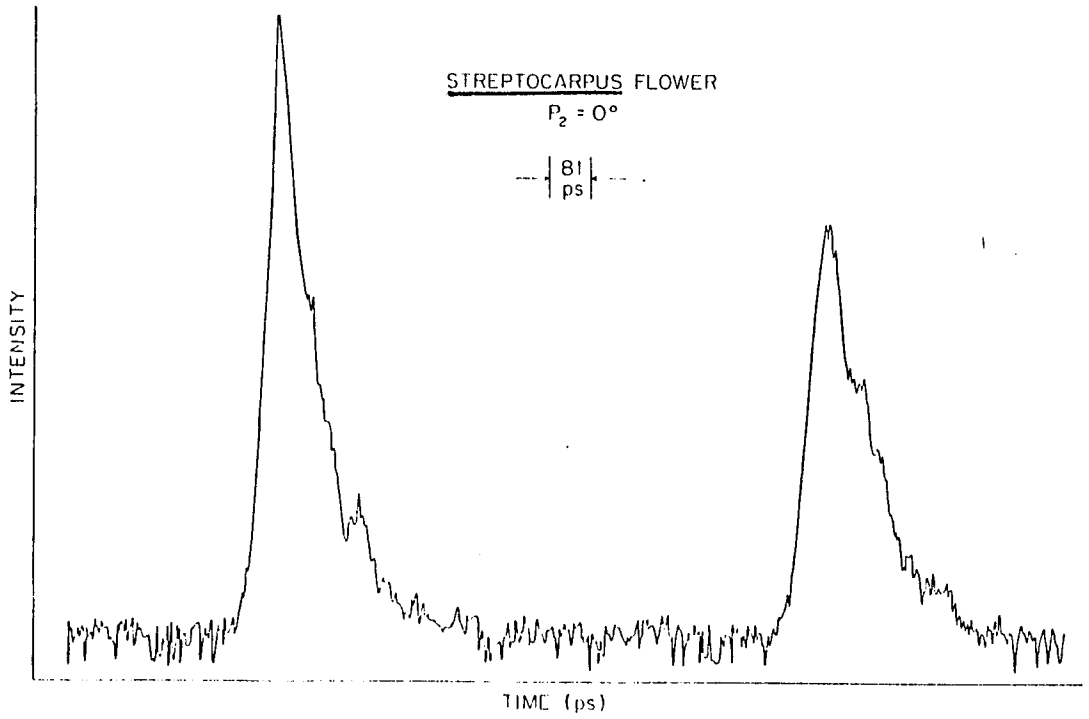

Fig. 9.2.1 Time Resolved Fluorescence Depolarization of Streptocarpus Flower.

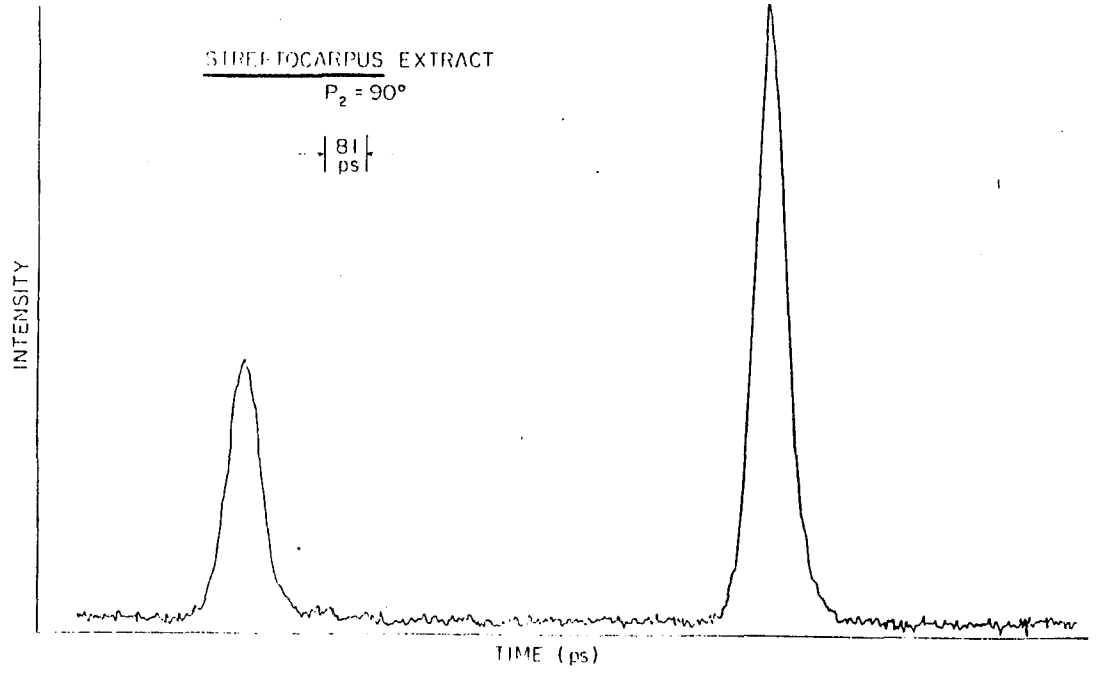

Fig. 9.2.2 Time Resolved Fluorescence Depolarization of Streptocarpus Extract.

Table 9.2.1

SAMPLE	FLUORESCENCE LIFETIME (ps)	POLARIZATION ANISOTROPY
Streptocarpus Flower	59 ± 13	0.13 ± 0.05
Streptocarpus Extract	128 ± 33	0.31 ± 0.03
Anthurium Flower	10 ± 3	———
Anthurium Extract	18 ± 8	0.35 ± 0.16

changes *in vivo* and *in vitro*, the quenching rate is estimated to be 9×10^9 sec^{-1} for the *Streptocarpus* flower and 4×10^{10} sec^{-1} for the *Anthurium* flower.

The fluorescence polarization anisotropy, R(t) ,at t=0 (i.e. within the resolution time of the apparatus) was obtained from the polarized fluorescence intensity peaks. R(0) for the *Streptocarpus* extract was 0.31 ± 0.03 (14 measurements) and 0.35 ± 0.16 (5 measurements) for the *Anthurium* extract. *In vivo*, however, the measured value of R(0) for the *Streptocarpus* flower was 0.13 ± 0.05 (7 measurements). Polarization measurements in the *Anthurium andreanum* flower were not possible due to its weaker fluorescence emission. It is apparent that the *in vivo* lifetime is faster than that in solution.

The fluorescence polarization anisotropy, R(t), is an experimentally accessible parameter which characterizes the polarized fluorescence emission in terms of the intensity of fluorescence measured parallel to and perpendicular to the incident polarization direction ($I_{\parallel}$ (t) and $I_{\perp}$ (t) respectively):

$$R(t) = \frac{I_{\parallel}(t) - I_{\perp}(t)}{I_{\parallel}(t) + 2I_{\perp}(t)} .$$

The orientational order of molecules in their local environment can be obtained in steady state polarized fluorescence measurements only through knowledge of both

the fluorescence decay time and correlation time for rotational diffusion. Time dependent fluorescence polarization measurements however, allow the measurement of the fluorescence polarization anisotropy which in turn directly determines the orientational distribution of molecules. The emission anisotropy at t=0 for an oriented molecular distribution, for the case where the absorption dipole is parallel to the unique symmetry axis of the system, is given by (Szabo, 1980):

$$R(0) = \frac{(2\langle P_2^2\rangle + \langle P_2\rangle)\, P_2(\cos\varphi)}{1 + 2\langle P_2\rangle}$$

where $\langle P_2\rangle$ is the expectation value of the second order Legendre polynomial for the distribution function $f(\theta)$, and is given by,

$$\langle P_2\rangle \equiv \langle P_2(\cos\theta)\rangle = \int_0^{\pi} \sin\theta\, d\theta\, f(\theta)\, P_2(\cos\theta)$$

where 0 is the angle between the long axis of the molecule and the major symmetry axis of the system, and φ is the angle between the absorption and emission dipole.

The calculated values of R(0) for two different orientational distribution functions are presented in Table 9.2.2. For Streptocarpus, the in vitro measured

Table 9.2.2

ORIENTATIONAL DISTRIBUTION f(Θ)	R (0)
1/2	0.4
$3/2 \cos^2 (\Theta)$	0.1039

value for R(0) was 0.31 $\pm$ 0.03, which is in fair agreement with the theoretical value of R(0)= 0.4 for a random distribution. The *in vivo* measured value of R(0)= 0.13 therefore indicates that the alignment of these pigment molecules in their vacuoles is non-random. As a model for the orientational order of the pigment molecules in their vacuoles we can take a normalized orientational distribution function. In particular, by taking $f(\theta) = 3/2 \cos^2\theta$, a calculated value of 0.1039 is obtained for the emission anisotropy. This agrees quite well with the measured value of 0.13.

Thus the kinetic measurements in the *in vivo* *Streptocarpus* flower present evidence for a strong non-radiative decay which can arise from either concentration quenching, molecular orientational order (which can increase the energy transfer efficiency among the pigments to a non radiative trap), or some specific *in vivo* interaction with protein or other molecules. Evidence is also found for orientational order of the anthocyanin pigment molecules in their vacuoles. The highly polarized emission is clear evidence of the local molecular order. Further research is needed to establish the exact morphological order of these pigment molecules *in vivo*.

9.3 Polarization Measurements in Photosynthetic Pigment Systems

At the concentrations present in the PSU ($\sim$ .16 M) chlorophyll molecules are essentially locked in and are not free to rotate. This arrangement gives rise to the possibility of a structural order of molecular dipoles which can be manifested in time resolved fluorescence polarization measurements. As reported in Chapters 7 and 8, no discernable polarization was found either in the carotenoid accessory pigment complex of the yellow Norway maple or the green spinach leaf within the resolution of the experimental apparatus (for completeness it should also be noted that a preliminary polarization measurement was also performed in the phycobiliprotein C-PE, with similar findings). These results are expected since although the pigment molecules may possess a preferential alignment on the stromal lamellae in the chloroplast, the chloroplasts themselves are generally randomly oriented in suspension so that any polarization signal is effectively either very weak or completely randomized. When a system is excited by polarized light, the molecular dipole component along the direction of polarization of the incident light is preferentially excited, so that even for a randomly oriented group of polarized molecular dipoles, a non-zero polarization is expected. Depolarization of the fluorescence emission may arise from various sources.

Rotational motion of the molecule subsequent to excitation can cause the dephasing of the fluorescence emission. This occurs on a time scale of $\sim$ 5 to 500 ps. Energy transfer from donor to acceptor accessory pigments can also dephase the fluorescence emission on a time scale consisting of a few transitions (e.g. 1 - 10 ps). In addition, depolarization can also occur within the molecule itself through vibrational or electronic dephasing, on a time scale of 10^{-15} to 10^{-12} sec.

Using a sample with a preferential alignment of chloroplasts allows the possibility of increasing the polarized fluorescence emission. A sample which provides such an orderly arrangement of chloroplasts within its cell body is the alga Nitella (Fig. 9.3.1). In this study the polarized fluorescence kinetics from Nitella have been investigated in order to obtain information on the energy transfer time and associated depolarization kinetics from the accessory pigment pool to the chlorophyll light harvesting system.

The alga Nitella is generally found in fresh water ponds and lakes, it basically consists of a cylindrical unit cell with a vacuole along the inner cell body parallel to the cylindrical (z-axis) of the cell. The cells grow in extended chains of individual unit cells attached to each other at the cylinder top and bottom. Nitella cells were chosen according to age by selecting the fifth cell along

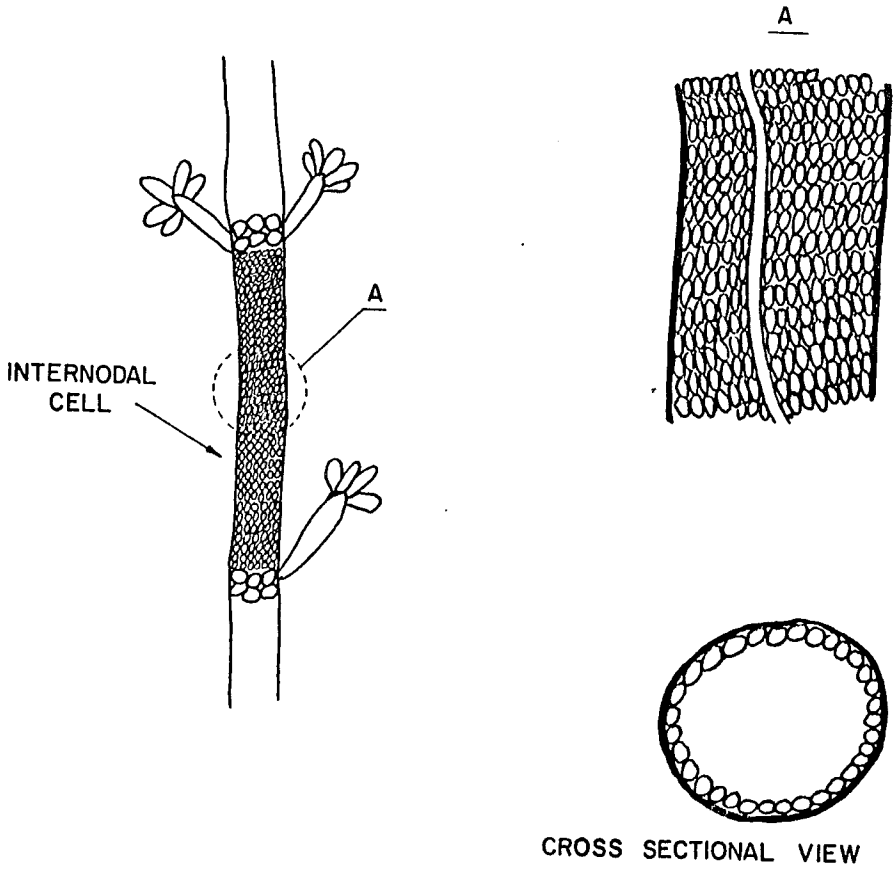

Fig. 9.3.1 Nitella cell.

the chain. Microscopic examination of the cylindrical Nitella cells reveal that the chloroplasts of Nitella are generally prolate and are arranged with their long axis parallel to the cylindrical symmetry (z) axis of the cell. This would appear to favor a preferential alignment of the grana also along the z-axis of the cell. Since the chlorophyll molecules are closely packed on the grana lamellae in their photosynthetic clusters, a preferential alignment of the chlorophyll molecules with respect to the z-axis of the cell is thus also expected. Energy transfer in the photosynthetic unit is very sensitive to the mutual orientation of chlorophyll accessory pigment molecules. Van Nostrand (1972) has found that the bulk of in vivo chlorophyll is oriented with its red transition moment parallel to the plane of the lamellae. The orientaion of the carotene transition dipoles were also found to be parallel to the lamellae plane. This orientation of pigment dipoles should give rise to a high degree of polarized fluorescence emission, when the system is excited by polarized light.

Steady state polarization measurements in Nitella utilizing a 1 mW He:Ne laser excitation source with lock-in amplifier detection system (Chapter 8) revealed a polarization value of 1-6 %, in agreement with the low values of in vivo polarization previously reported by Arnold and Meek, (1956) and Mar and Govindjee, (1972). Recently, Geacintov et al., (1974) have measured the

fluorescence polarization ratio ($I_{\parallel} / I_{\perp}$) from Chlorella (1.2-1.9), Scenedesmus obliquus (1.2-1.25) and spinach chloroplast preparation (1.4-1.5) by aligning the chlorophyll dipoles in a high magnetic field (10-13 KG).

Using 530 nm, 6 ps, single laser pulse excitation, the intensity of the fluorescence from Nitella (aligned with its cylindrical symmetry axis perpendicular to the plane of the table) both parallel to and perpendicular to the incident polarization direction was individually measured. The relative amplitudes of the polarized fluorescence emission measured parallel to the incident polarization direction (measurement of t=0 height normalized to the excitation pulse intensity) was found to be 1.0 $\pm$ 0.08 (6 measurements), while the polarized fluorescence intensity measured perpendicular to the incident polarization direction was found to be 0.96 $\pm$ 0.08 (6 measurements). These measurements were obtained at an excitation pulse intensity of $\sim 2 \times 10^{15}$ photons/cm^2 per pulse. Therefore no significant difference in the polarization of the two components was observed within the resolution time of the streak camera -OMA detection system (~12 ps). The possibility of equally polarized components due to a polarization emission at 45 ^{o} relative to the incident polarization direction was eliminated by rotating the analyzer and measuring the emission at 45 ^{o} relative to the incident polarization direction, with a result of 1.04 $\pm$ 0.09.

Therefore the fluorescence emission from Nitella is completely depolarized within the resolution time of the experimental system (~12 ps). Measurement of the polarization from a spinach chloroplast preparation also revealed no statistically significant difference between the fluorescence intensity measured parallel to and perpendicular to the incident polarization direction, yielding $P_{\parallel} / P_{\perp} = 1.01 \pm 0.02$ (8 measurements).

The decay time of the polarized fluorescence emission from Nitella, measured at very low intensity ($\sim 4 \times 10^{13}$ photons/cm^2 per pulse) obtained a value of 326 $\pm$ 27 ps (13 measurements) for $P_{\parallel}$, the fluorescence emission measured parallel to the incident polarization direction, and 305 $\pm$ 21 ps for $P_{\perp}$ (9 measurements), the fluorescence emission measured perpendicular to the incident polarization direction. Thus the low intensity ($I \sim 4 \times 10^{13}$ photons/cm^2 per pulse) polarized fluorescence emission, as reported above, was found to decay as a single exponential with a lifetime of ~300 ps. The fluorescence lifetime at higher excitation intensities was found to be non-exponential. The lifetime at $I \sim 1.5 \pm 0.3 \times 10^{14}$ photons/cm^2 per pulse was characterized by a double exponential decay with a slow emission component of 277 $\pm$ 21 ps and a fast emission component of 38 $\pm$ 8 ps with relative amplitudes of 0.42 $\pm$ 0.04 and 0.57 $\pm$ 0.04 for the slow and fast component, respectively (6 measurements). At $I \sim 1.9 \pm 0.5 \times 10^{15}$ photons/cm^2 per

pulse, the slow emission component decreased to 157 ± 11 ps while the fast emission component was relatively unchanged (32 ± 8 ps). The relative amplitudes at this intensity were 0.44 ± 0.02 and 0.56 ± 0.02 for the slow and fast component, respectively (3 measurements).

The room temperature emission was also spectrally isolated with the use of narrow band filters (FWHM 100 A) at high excitation intensity. The emission at 687 nm was found to decay as a single exponential with a lifetime of 85 ± 9 ps at an excitation intensity of $3.2 \pm 0.3 \times 10^{15}$ photons/cm^2 per pulse (10 measurements), while the emission component at 730 nm decayed as a single exponential with a lifetime of 59 ± 9 ps at an excitation intensity of $2.7 \pm 0.4 \times 10^{15}$ photons/cm^2 per pulse (6 measurements). Exciton-exciton interactions at this intensity is the most likely reason for the short lifetime measurements at these wavelengths. These particular spectral kinetic measurements are therefore used only as an estimate of the emission lifetimes at these wavelengths. Measurement of time resolved spectra at lower intensities was not possible in this alga due to the low chloroplast concentration in the samples. The lower fluorescence signal obtained for the alga Nitella as compared to either the leaf or spinach chloroplast preparations can be attributed to the greater inter-chloroplast separation in Nitella, as opposed to either the leaf or chloroplast preparation. In addition,

the emission from Nitella is due to a cell thickness comprising at most 2-3 whole chloroplasts (the cell has a cylindrical wall and an inner vacuole structural arrangement) as opposed to the more highly concentrated chloroplast arrangement in the leaf or chloroplast preparation.

Since excitation of even a randomly aligned system of dipoles with linearly polarized light should give rise to polarized fluorescence emission, the measurement of a completely depolarized signal from a sample possessing an oriented distribution of molecular dipoles indicates a rapid dephasing time that is either comparable to or faster than the resolution of the detection system. For Nitella, this depolarization may occur either in the carotenoid accessory pigment complex or in the associated Chl.a/Chl.b light harvesting complex. Dallinger et al., (1981) have estimated that the singlet-singlet energy transfer time in the carotenoid complex can indeed occur in $\leq$ 1 ps. Therefore, with 530 nm excitation the fluorescence emission from Nitella is found to completely depolarize extremely rapidly, within the resolution time of the detection apparatus ($\sim$12 ps), and therefore occurrs within the very first few excitation energy transfers that take place in the accessory pigment complex of the photosynthetic light harvesting system.

Chapter 10. Summary and Future Directions

This work has been concerned with the study of the primary energy transfer kinetics occurring in various photosynthetic pigments and photosynthetic systems. The goal of this research has been to obtain a better understanding of the energy migration in the photonsynthetic light harvesting system as it travels to the photochemically active reaction center traps.

The fluorescence kinetics from various photosynthetic systems were investigated, including a study of:

A) Isolated phycobiliproteins and intact phycobilisomes from the blue-green alga Nostoc sp.

B) The carotenoid light harvesting system from Norway maple (Acer platenoides).

C) The photosynthetic systems of spinach chloroplasts, whole spinach leaf and the alga Scenedesmus obliquus wild type and Sc 8 and Sc 11.

D) The dye malachite green in glycerol, the anthocyanin pigments from flowers and the alga Nitella.

The following is a summary of the research work accomplished in this thesis.

A). Both the isolated phycobiliproteins and the intact phycobilisomes of the blue-green alga Nostoc sp. were studied. The results of these investigations revealed that:

i) Energy transfer in the phycobilisomes can be directly followed through measurement of the fluorescence rise and decay kinetics of the constituent accessory pigments.

ii) The fluorescence from the C-PE emission from PBS was found to decay as a single exponential throughout the intensity region investigated with a lifetime of 31 $\pm$ 4 ps, while the corresponding rise of the C-PC+APC emission from PBS's was found to be 34 $\pm$ 13 ps, consistent with energy transfer from C-PE to C-PC.

iii) The component fluorescence yields were found to decrease with increasing excitation intensity, indicative of the occurrence of exciton annihilation in this system. In particular, a dramatic fluorescence quenching was observed for the APC emission in PBS's as opposed to the measurement for the isolated APC in solution. This is attributed to the higher effective absorption resulting from the efficient energy transfer in the phycobilisomes.

B). The carotenoid accessory pigment complex from autumnal yellow Norway maple leaves and a green spinach leaf were studied in order to better understand energy transfer in the primary light harvesting complex. The results of this study revealed the following new information.

i) The fluorescence kinetics from a green spinach leaf at room temperature below 660 nm was found to decay nearly identically to the emission at 685 nm.

ii) As the leaf aged, the decay rate was relatively unaffected, implying that the affect of the photosynthetic state of the traps on the fluorescence emission from the system is a relatively minor one.

iii) Studies of the carotenoid light harvesting system in the yellow Norway maple revealed that the fluorescence from the carotenoid component shows the same characteristics observed in the fluorescence emission from the chlorophyll component:

a) in vivo (lifetime 200 ps)

b) in preparation (lifetime 220 ps)

c) in solution (lifetime 1800 ps)

d) at low temperature, $\lambda \gtrsim 720$ nm (lifetime 630 ps)

These results have been interpreted in terms of a model which considers the fluorescence decay from the photosynthetic system as representative of energy transfer on a light harvesting lattice consisting of the photosynthetic pigments, and which is not necessarily

affected by the state of the reaction center traps.

C) The fluorescence kinetics from a green spinach leaf were measured at low intensities ($\sim 10^{13}$ photons/cm^2) with single pulse excitation, and found to be consistent with the previous results obtained using pulse train excitation. This result led to a deeper investigation of energy transfer in the LHC itself. Intensity dependence studies in both a green Norway maple leaf and a green spinach leaf were carried out and revealed a drop in the fluoresence quantum yield for excitation intensities 7×10^{13} photons/cm^2 both at room temperature and at 90°K. The results of these measurements have been interpreted in terms of the exciton-exciton annihilation mechanism which was found to be present in all of the photosynthetic systems investigated. Indeed the study of exciton annihilation effects have presently become the subject of intense investigation in their own right. However, while exciton transport phenomenon can and has been used to probe the primary energy transfer mechanism, it has mostly proven to be a foil or mask for the true energy transfer kinetics.

In summary the results of the single pulse investigation of the primary energy transfer kinetics in the various photosynthetic systems have revealed the following:

i) In all of the photosynthetic systems investigated (either in preparation form or the truly in vivo leaf), the fluorescence decay kinetics at an intensity of exccitation of $\sim 10^{14}$ photons/cm^2 per pulse can be described as a single exponential with a decay time of 200-300 ps.

ii) The 680-690 nm fluorescence kinetics decays as a single exponential at both room temperature and 90K under both single pulse and pulse train excitation.

iii) The 730 nm fluorescence kinetics at 90^{o}K is approximately six times longer than at room temperature.

The affect of the photoactive state of the trap on the energy transfer kinetics in the photosynthetic system was investigated in the alga Scenedesmus obliquus, where the Sc WT possesses both an active PSI and PSII reaction center trap while the Sc 8 form possesses on inactive PSI trap and the Sc 11 an inactive PSII trap. It was observed that Sc WT decayed faster than either Sc 8 or Sc 11. The difference in the observed decay rates are interpreted in terms of the presence of a larger effective domain size for excitations in either the Sc 8 or Sc 11 case, as well as the effect of increased forward (Sc 11) and reverse (Sc 8) spillover rates in the case where the mutants possess an inactive trap for PS II or PS I, respectively.

D). A study of the fluorescence polarization kinetics and polarization anisotropy from photosynthetic and non-photosynthetic pigment systems was conducted in order to elucidate the transfer of excitation energy among molecules from sensitizer to fluorescing specie. In vivo polarization measurements in the alga Nitella revealed a fast and complete depolarization of the absorbed light energy within the resolution time of the experimental detection system ($\leq$ 12 ps). In addition fluorescence polarization measurements of anthocyanin pigments in vivo and in vitro have provided evidence for the presence of preferred orientation of these non-photosynthetic pigments in their local environments.

The fluorescence kinetics and polarization anisotropy of the dye malachite green were investigated as a function of solvent viscosity. The results of this study revealed that the malachite green dye molecules in solution undergo a phase transition at $\sim$ 1000P which is manifested in both the fluorescence decay and polarization anisotropy.

This thesis has shown that the picosecond time resolved fluorescence kinetics from the primary energy transfers in photosynthetic systems is $\sim$300 ps at low intensity. This is consistent with the latest findings obtained using conventional time resolution techniques by Sauer and Brewington (1978), and is also consistent with the earlier measurements of Hervo et al., (1975). More

importantly, my investigations have shown that the fluorescence kinetics from the carotenoid accessory pigment system reveal an underlying basic relationship between the structural arrangement of the accessory pigments on the photosynthetic membrane and their energy transfer properties. This association is interpreted in terms of a new model of energy transfer in the accessory pigment-chlorophyll a/b light harvesting complex. In the case where the chlorophyll light harvesting system is not present (i.e. yellow Norway maple) excitations travel in the carotenoid lattice until they are quenched at a non-radiative trap site. The decay time (~300 ps) being determined by the energy transfer time to the trap. In the case where the chlorophyll light harvesting system is present, the carotenoid molecules efficiently transfer the excitations to the chlorophyll lattice. The decay time (300 ps) now being determined by the energy transfer time in the chlorophyll lattice to either an open or closed reaction center trap. Since the two lattices are closely interwoven, one would expect the decay times to be comparable, as observed.

Future Directions:

The results of the investigations conducted in this research have provided new information and insights into the direction of future studies. In particular, continued investigation of the LHC should include studies of

Rhodopseudomonas spheroides, where the strain R-26 contains no carotenoids, as well as isolated LHC preparations from spinach chloroplasts. Additional information may also be obtained from preparations of various special LHC systems with known relative concentrations of Chl. a, Chl. b and carotenoid molecules (e.g. PS II and PS I preparations from spinach chloroplasts) in order to obtain information of the relative role of these pigments with reference to energy transfer on the light harvesting lattice.

An obvious extention of the Scenedesmus study includes the preparation of PS I and PSII particles from Sc WT , Sc 8 and Sc 11, thereby further isolating the various energy transfer rates. In the case of the phycobilisomes, a study of the various energy transfer rates in the intact alga Nostoc sp. are needed in order to complete the study of the energy transfer from the in vivo phycobilisome accessory pigment system to the associated light harvesting chlorophyll.

The results of the polarization studies conducted in Malachite green have provided a novel approach to the investigation of possible phase transitions through the simultaneous measurement of the fluorescence decay rates and fluorescence polarization anisotropy, and it is hoped that these studies will be repeated in similar molecular systems. The measurement of the temporal evolution of the fluorescence polarization from photosynthetic pigments

in vivo can provide detailed information on the properties of the light harvesting lattice which will become available with the development of faster temporal resolution techniques.

In conclusion, it is hoped that this investigation has provided new insight into the workings of the primary energy transfer processes in photosynthesis and will stimulate further research toward the complete understanding of this all important process.

References

Alfano, R.R. and Ockman, N., J. Optical Soc. of Am. 58, No. 1 90-95 (1968).

Alfano, R.R. GTE Technical Report, TR 72-2301 (1972).

Alfano, R.R., and Shapiro, S.L., Scientific American 228, 43 (1973).

Arnold, W., and Meek, E.S., Arch. Biochem. Biophys. 60, 82 (1956).

Arnold, W., J. Phys. Chem. 69, No. 3, 788-791 (1965).

Arnold, S., Alfano, R.R., Pope, M., Yu, W., Ho, P., Tharrats, T., and Swenberg, C.E., J. Chem. Phys. 64, 5104 (1976).

Arnold, W. Proc. Natl. Acad. Sci. 73, 4502-5 (1977)

Arnon, D.I., Knoff, D.B., McSwain, B.D., Chain, R.K. and Tsujimoto, H.Y., Photochem. Photobiol. 14, 397 (1971).

Arntzen, C.J., and Briantais, J.M., "Chloroplast Structure and Function" in Bioenergetics of Photosynthesis, ed. Govindjee, Academic Press, New York (1975).

Arntzen, C.J. and Ditto, C.L., Biochim. Biophys. Acta 449, 259-274 (1976).

Avron, M., Anal. Biochem. 2, 535 (1961).

Bailey, E.A., and Rollefson, G.K. J. Chem. Phys. 21, 1315 (1953)

Barber, J. in The Intact Chloroplast ed. J. Barber Elsevier Scientific, Amsterdam, The Netherlands (1976).

Barber, D.J.W. and Richards, J.T., Photochem. Photobiol. 25, 565-569 (1977).

Barber, J., "Biophys. of Photosynthesis" in Primary Processes of Photosynthesis, ed. J. Barber Elsevier North-Holland Biomedical Press, Amsterdam (1977).

Barber, J., "Biophysics of Photosynthesis" Rep. Prog., Vol. 41, Great Britain, (1978).

Barber, J., Searle, G.F.W., and Tredwell, C.J., Biochim. Biophys. Acta 501, 174-182 (1978).

Bay, Z., and Pearlstein, R.M., Proc. Natl. Acad. Sci. 50, 1071-8 (1963).

Beddard, G.S., Porter, G. and Tredwell, C.J. Nature 258, 166-168 (1975).

Beddard, G.S., and Porter, G. Nature 260, 366-7 (1976).

Beddard, G.S. and Porter, G., Biochim. Biophys. Acta 462, 63-72 (1977).

Beddard, G.S., Fleming, G.R., Porter, G., Searle, G.F.W. and Synowiec, J.A., Biochim. Biophys. Acta 545, 165-174 (1979).

Bennett, A. and Bogorad, L., Biochemistry 10, 3625-3634 (1971).

Berns, D.F., in Subunits in Biological Systems, eds. S.N. Timasheff, G.D. Fasman eds. Part A, Chap. 3, Marcel Dekker, N.Y. 105-148 (1971).

Bertsch, W., Azzi, J.R., Davidson, J.B., Biochim. Biophys. Acta 143, 129-143 (1967).

Bishop, N., in Methods in Enzymology, ed. A., San Pietro, Vol. 23, Part A, 130-142 (1971).

Blackman, F.F., Ann. Botany 19, 281-295 (1905).

Bloembergen, N., in Nonlinear Optics, Cambridge, 1964.

Borisov, A. Yu, Godik, V.I. Bioenergetics 3, 211 (1972a).

Borisov, A. Yu, Godik, V.I. Bioenergetics 3, 515 (1972b).

Borisov, A. Yu, and Il'ina, M.D. Biochim. Biophys. Acta 305, 3 64-37 (1973).

Boxer, S.G. and Closs, G.L., J. Am. Chem. Soc. 98, 5406-5408 (1976).

Bradley, D.J., Higgins, J.F., and Key, M.H., Appl. Phys. Lett. 16,53 (1970).

Bradley, D.J., Liddy, B., and Sleat, W.E., Opt. Comm. 2, 391 (1971).

Breton, J., and Roux, E. in Lasers in Physical Chemistry and Biophysics ed. J. Joussot-Dubien, Elsevier, Amsterdam, 379-388 (1975).

Breton, J. and Geacintov, N.E., FEBS Lett. 69, 86 (1976).

Breton, J., Geacintov, N.E. and Swenberg, C.E., Biochim. Biophys. Acta 548, 616-635 (1980).

Breton, J. and Geacintov, N.E., Biochim. Biophys. Acta 594, 1-34 (1980)

Briantais, J.M., Govindjee and Merkelo, H., Photosynthetica 6, 133-41 (1972).

Brody, S.S., and Rabinowitch, E. Science 125, 555 (1957).

Bryant, D.A., Guglielmi, G., Tandeaude, N., Marsac, G., Astets, A.M., and Cohen-Bazire, G., Arch. Microbiol. 123, 113-127 (1979).

Butler, W.L., Arch. Biochem. Biophys. 93, 413-422 (1961).

Butler, W.L., Proc. Nat. Acad. Sci., U.S. 69, 3420 (1972).

Butler, W.L. and Kitajima, M., Biochim. Biophys. Acta 386, 72-85 (1975).

Butler, W.L., Brookhaven Symp. Biol. 28, 338-44 (1977).

Butler, W.L. and Strasser, R.J., in Proceedings of the Fourth International Congress in Photosynthesis eds. D.O. Hall, J. Coombs and T.W. Goodwin, The Biomedical Society, London, 11-20 (1978).

Butler, W.L., Ann. Rev. Plant Physiol. 29, 345-378 (1978).

Butler, W.L., Tredwell, C.J., Malkin, R. and Barber, J., Biochim. Biophys. Acta 545, 309-315 (1979).

Campillo, A.J., Hyer, R.C., Kollman, V.H., Shapiro, S.L., Sutphin, H.D., Biochim. Biophys. Acta, 387, 533 (1975).

Campillo, A.J., Kollman, V.H., and Shapiro, S.L. Science 193, 227-229 (1976a).

Campillo, A.J., Shapiro, S.L., Kollman, V.H., Winn., V.R. and Hyer, R.C., Biophys. J. 16, 93-97 (1976b).

Campillo, A.J. and Shapiro, S.L., "Picosecond Relaxation Measurements in Biology" in Topics in Applied Physics: Ultrashort Light Pulses: Picosecond Techniques and Applications ed. S.L. Shapiro, Springer-Verlag, New York (1977).

Campillo, A.J., Hyer, R.C., Monger, T.G., Parsons, W.W. and Shapiro, S.L. Proc. Nat. Acad. Sci. USA, 74 1997-2001 (1977a).

Campillo, A.J., Shapiro, S.L., Geacintov, N.E. and Swenberg, C.E., FEBS Lett. 83, 316-320 (1977b).

Campillo, A.J. and Shapiro, S.L., Photochem. Photobiol. 28, 975-989 (1978).

Cho, F., and Govindjee, Biochim. Biophys. Acta 216, 139 (1970).

Clayton, R.K., in Molecular Physics in Photosynthesis Ginn (Blaisdell), Boston, Mass. (1965).

Clayton, R.K., in Light and Living Matter Vol. 2: The Biological Part, McGraw Hill, New York (1971).

Cohen-Bazire, G., Beguin, S., Rimon, S., Glazer, A.N., and Brown, D.M., Arch. Microbiol. 111, 225-238 (1977).

Colbow, K., Biochim. Biophys. Acta 314, 320-7 (1973).

Cramer, W.A., and Butler, W.L., Biochim. Biophys. Acta 143, 332 (1967).

Dale, R.E. and Teale, F.W.J., Photochem. Photobiol. 12, 99-117 (1970).

Dallinger, R.F., Woodruff, W.H. and Rodgers, M.A.J., Photochem. Photobiol., 33, (1981).

DeMaria, A.J., Electronics 112, Sept. (1968).

DeMaria, A.J., Glenn, W.H., Brienza, M.J. and Mack, M.E., Proc. IEEE, 57, 2 (1969).

Dimitrievsky, U., Ermolaev, V. and Terenin, A., Dokl. Akad. Nauk. S.S.S.R. (Transl.) 114, 468 (1957).

Doring, G., Bailey, J.L., Kreutz, W., and Witt, H.T., Naturwissenshaften 55, 220 (1968).

Doring, G., Renger, G., Vater, J., and Witt, H.T., Z. Naturforsch. B24, 1139 (1969).

Doring, G., Stiehl, H.H. and Witt, H.T., Z. Naturforsch. B22, 639-644 (1967).

Doring, G. and Witt, H.T. Proc. Int. Congr. Photosynthesis Res. 2nd 1, 39 (1972).

Duguay, M., and Hansen, J., Appl. Phys. Lett., 15, 192 (1969).

Duguay, M.A. and Mittick, T.T., Appl. Optics 10, 2162 (1972).

Dutton, H.J., Manning, W.M., and Duggan, B.B., J. Phys. Chem. 47, 308 (1943).

Duysens, L.N.M., Ph.D. Thesis, Univ. of Utrecht, The Netherlands (1952).

Duysens, L.N.M., and Sweers, H.E., in Studies on Microalgae and Photosynthethic Bacteria, ed. J. Ashida 353, Univ. of Tokyo Press, Tokyo (1963).

Emerson, R., and Arnold, W., J. Gen. Physiol. 15, 391 (1932a)

Emerson, R., and Arnold, W., J. Gen. Physiol. 16, 191 (1932b).

Erixon, K., and Butler, W.L., Biochim. Biophys. Acta 234, 381 (1971).

Fleming, G.R., Morris, J.M., and Robinson, G.W., Chem. Phys. 17, 91-100 (1976)

Fong, F.K. and Koester, V.J., Biochim. Biophys. Acta 423, 52-64 (1976).

Fong, F.K. and Galloway, L., J. Am. Chem. Soc. 100, 3594-3596 (1978).

Forster, T., Ann. Physik 2, 55 (1948).

Forster, T., in Fluorescence Organischer Verbindugen Vandenhoeck and Ruprecht, Gottingen, (1951).

Forster, T., "Delocalized Excitation and Excitation Transfer", in Modern Quantum Chemistry, Part III: Action of Light and Organic Molecules, ed. O. Sinanoglu, 93-137, Academic Press, New York (1965).

Forster, T. and G. Hoffman, Z. Phys. Chem. N.F. 75, 63 (1971).

Fowler, V.J., and Schlafer, J., Proc. IEEE, 54, 1437 (1966).

Franken, P.A., Hill, A.E., Peters, C.W., and Weinreich, G. Phys. Rev. Lett. 7, 118-119 (1961).

French, C.S., and Young, V.M.K., J. Gen. Physiol. 35, 873 (1952).

Gaffron, H., and Wohl, K., Naturwissenschaften 24, 81 (1936a).

Gaffron, H., and Wohl, K., Naturwissenschaften 24, 103 (1936b).

Galloway, L., Matthews, T.G., Lytle, F.E., and Fong, F.K., J. Am. Chem. Soc. (1979).

Gantt, E. and Lipschultz, C.A., Biochim. Biophys. Acta 292, 858-861 (1973).

Gantt, E., Bioscience 25, 781-788 (1975).

Geacintov, N.E., Pope, M., and Vogel, F., Phys. Rev. Lett. 22, 593 (1969).

Geacintov, N.E. Van Nostrand, F. and Becker, J.F., Biochim. Biophys. Acta 347, 443-463 (1974).

Geacintov, N.E. and Breton, J., Biophys. J. 18, 1-15 (1977).

Geacintov, N.E., Breton, J., Swenberg, C.E., and Paillotin, G., Photochem. Photobiol. 26, 619-638 (1977a).

Geacintov, N.E., Breton, J., Swenberg, C., Campillo, A.J., Hyer, R.C. and Shapiro, S.L. Biochim, Biophys. Acta 461, 306-312 (1977b).

Geacintov, N.E. and Breton, J., Biochim. Biophys. Acta, Rev. of Bioenergetics (1980).

Giordmaine, J.A., Phys. Rev. Lett. 8, 19 (1962).

Giordmaine, J.A., Rentzepis, P.M., Shapiro, S.L. and Wecht, K.W., Appl. Phys. Lett. 11, 216 (1967).

Glazer, A.N. and Hixson, C.S., J. of Biol. Chem. 250, 5487-5495 (1975).

Glazer, A.N., Photochem. Photobiol. Rev. 1, 71-115 (1976).

Glazer, A.N., Arch. Microbiol. 123, 113-118 (1979).

Goedheer, J.H.C., Ann. Rev. Plant Physiol. 23, 87 (1972).

Govindjee and Yang, L., J. Gen. Physiol. 49, 763-780 (1966).

Govindjee and Briantais, J.M., Fed. Eur. Biochem. Soc. Lett. 19, 278 (1972).

Govindjee and Mohanty, P., in Biology and Taxonomy of Blue-Green Algae, ed. T.V. Desikachary, Univ. of Madras, Madras, India (1972).

Govindjee and R. Govindjee, "Introduction to Photosynthesis" in Bioenergetics of Photosynthesis, ed. Govindjee, Academic Press, New York (1975).

Govindjee, Photochem. Photobiol. 28, 935-935 (1978).

Grabowski, J. and Gantt, E., Photochem. Photobiol. 28, 39-47 (1978).

Gray, B.H. and Gantt, E., Photochem. Photobiol. 21, 121-128 (1975).

Hall, D.O., Trends in Biochem. Sci. 2, 99-101 (1977).

Harnwell, G.P., and Livingood, J.J., in Experimental Atomic Physics, International Series in Physics, McGraw Hill, New York, 101-102, (1961).

Harris, L., Porter, G., Synoweic, J.A., Tredwell, C.J., and Barber, J. Biochim. Biophys. Acta 449, 329-39 (1976).

Hellwarth, R.W., in Lasers, ed. A.K. Levine, 253, Marcel Dekker, Inc., New York (1966).

Hellwarth, R.W., Phys. Rev., 163, 205 (1967).

Hemenger, R.P., Pearlstein, R.M., Lakatos-Lindberg, K.J., J. Math. Phys. 13, 1056 (1972).

Hervo, G., Paillotin, G. and Thiery, J., J. Chem. Phys. 72, 761-766 (1975).

Hill, R. and Bendall, F., Nature 186, 136 (1960).

Hiyama, T. and Ke, B., Arch. Biochem. Biophys. 147, 99 (1971).

Ho, P.P., and Alfano, R.R., J. Chem. Phys. 67, 1004 (1977).

Hoch, G., and Knox, R.S., "Primary Processes in Photosynthesis", in Photophysiology ed. A. Giese, Vol. 3, 225-251, Academic Press, New York (1968).

Ingram, L.O. and Van Baolen, C., J. Bacteriol. 102, 784-789 (1970).

Ippen, E.P., Shank, C.V., and Bergman, A., Chem. Phys. Lett. 38, 611 (1976).

Izawa, S., and Good, N.E., Plant Physiol. 41, 544 (1966).

Javan, A., Bennett, Jr. W.R., and Herriott, D.R., Phys. Rev. Letters 6, 106 (1961).

Jurd, L., In The Chemistry of Plant Pigments, ed. C.O. Chichester, 123-142. Academic Press, New York, London (1972).

Klauder, J.R., Duguay, M.A., Giordmaine, J.A., and Shapiro, S.L., Applied Phys. Lett. 13, No. 5, 174-176 (1968).

Knox, R.S., J. Theor. Biol. 21, 244-259 (1968).

Knox, R.S., "Excitation Energy Transfer and Migration: Theoretical Considerations" in Bioenergetics of Photosynthesis, ed. Govindjee, Academic Press, New York (1975).

Knox, R.S., in Bioenergetics of Photosynthesis ed. Govindjee, Academic Press, New York, 183-219 (1975).

Knox, R.S., "Photosynthetic Efficiency and Exciton Transfer and Trapping" in Primary Processes of Photosynthesis, ed. J. Barber, Elsevier North-Holland Biomedical Press, Amsterdam (1977).

Kobayashi, T., Degenkolb, E.O., Bersohn, R., Rentzepis, P.M., MacColl, R. and Berns, D.S., Biochemistry 18, 5073-5078 (1979).

Kok, B., Biochim. Biophys. Acta 22, 399-401 (1956).

Kollman, V.H., Shapiro, S.L., Campillo, A.J. Biochem. Biophys. Res. Comm. 63, 917 (1975).

Kopelman, R. in Radiationless Processes ed. F.K. Fong, Springer Verlag 297-347 (1976a)

Kopelman, R., J. Physical Chem. 80, No. 20, 2191-2195 (1976b)

Kopelman, R., J. Lum. 12, 775 (1976c).

Lavorel, J., and Joliot, P., Biophys. J. 12, 815 (1972).

Lavorel, J., in Bioenergetics of Photosynthesis ed. Govindjee, Academic Press, New York, 223-317 (1975).

Magde, D. and Windsor, M.W., Chem. Phys. Lett. 24, 144 (1974).

Maiman, T.H., Nature 187, 493 (1960).

Malkin, S., and Kok, B., Biochim. Biophys. Acta. 126, 413 (1966).

Malkin, S., in Primary Processes of Photosynthesis, Vol. 2 Topics in Photosynthesis ed. J. Barber, Elsevier, Amsterdam, 349-431 (1977).

Mar, T., and Govindjee, Proc. Int. Congr. Photosynthesis Res. 2nd 1, 271 (1972).

Mathis, P., Butler, W.L. and Satoh, K., Photochem. Photobiol. 30, 603-614 (1979).

Mauzerall, D., Proc. Nat. Acad. Sci., U.S. 69, 1358 (1972).

Mauzerall, D., J. Phys. Chem. 80, 2306-2309 (1976).

Mauzerall, D., Biophys. J. 16, 87-92 (1976).

Mauzerall, D., Photochem. and Photobiol. 28, 991-998 (1978).

McEwen, C.R., Analy. Biochem. 20, 114-149 (1967).

Melissinos, A.C., in Experiments in Modern Physics, Academic Press, New York 65-80, (1966).

Merkelo, H., Hartmann, S.R., Mar, T., Singhal, G.S. and Govindjee, Science 164, 301 (1969).

Montroll, E.W., J. Math. Phys. 10, 753-765 (1969).

Mourou, G., and Knox, R. Appl. Phys. Lett. 36, 492(1980)

Moya, I., Biochim. Biophys. Acta 358, 214-227 (1974).

Moya, I., Govindjee, Vernotte, C., and Briantais, J.M. FEBS Lett. 75, 13-18 (1977).

Moya, I., Ph.D Thesis, University of Paris-Sud, France (1979).

Muller, A., Lumry, R., and Kokubun, H., Rev. Sci. Instr. 36, 1214 (1965).

Muller, A., Lumry, R., Walker, M.S., Photochem. Photobiol. 9, 113 (1969).

Munday and Govindjee, Biophys. J. 9, 1 (1969).

Murakami, S. and Packer, L., Arch. Biochem. Biophys. 146, 337 (1971).

Murakami, S., Torres-Pereira, J., and Packer, L. in Bioenergetics of Photosynthesis ed. Govindjee, Academic Press, New York, 607 (1975).

Murty, N.R., and Rabinowitch, E., Biophys. J. 5, 655-661 (1965).

Nakashima, N. and Yoshihara, K., J. Chem. Phys. 73, 3553-3559 (1980).

Naqvi, K.R., Photochem. Photobiol. 31, 523-524 (1980).

Nicholson, W.J. and Fortoul, J.L. Biochim. Biophys. Acta 143, 577-582 (1967).

Oster, G. and Nishijima, Y., J. Am. Chem. Soc. 78, 1581 (1956).

Owyoung, A., Ph.D. Thesis, California Institute Tech. (1972).

Paillotin, G., Swenberg, C.E., Breton, J., and Geacintov, N.E. Biophys. J. 25, 513-534 (1979a).

Paillotin, G. and Swenberg, C.E. in Chlorophyll Organization and Energy Transfer in Photosynthesis, Ciba Foundation Symposium 61 Elsevier, North Holland, Amsterdam, 201-209 (1979b).

Papageorgiou, G., in Bioenergetics of Photosynthesis ed. Govindjee, Academic Press, New York, 319-371 (1975)

Park, R.B., and Biggers, J. Science 144, 1009 (1964).

Paschenko, V.Z., Protasov, S.P., Rubin, A.B., Timofeev, K.N., Zamazova, L.M., Rubin, L.B. Biochim. Biophys. Acta 408, 145 (1975).

Pearlstein, R.M., Brookhaven Symp. Biol. 19, 8 (1967).

Pearlstein, R.M., J. Chem. Phys. 56, 2431 (1972).

Pellegrino, F., Yu, W., and Alfano, R.R., Photochem. Photobiol. 28, 1007-1012 (1978).

Pellegrino, F., and Alfano, R.R. in Multichannel Image Detectors ed. Yair Talmi ACS Symposium Series 102, American Chem. Soc. (1979)

Pellegrino, F., Wong, D., Alfano, R.R. and Zininskas, B.A., Photochem. Photobiol. (1981) (accepted for publication).

Porter, G. and Archer, M.D., Interdisciplinary Sci. Rev. 1, 119-43 (1976).

Porter, G., Synowiec, J.A. and Tredwell, C.J., Biochim, Biophys. Acta 459, 329-336 (1977).

Pringshein, P., in Fluorescence and Phosphorescence, Interscience, New York, (1949).

Rabinowitch, E., Disc. Faraday Soc. 27, 161 (1959).

Rabinowitch, E., and Govindjee in Photosynthesis, John Wiley and Sons, New York (1969).

Rahman, T.S. and Knox, R.S., Phys. Stat. Sol. 58, 715 (1973).

Robinson, G.W., Brookhaven Symp. Biol. 19, 16 (1967).

Ruben, S., Randall, M., Kamen, M.D., and Hyde, J.L., J. Amer. Chem. Soc. 63, 877 (1941).

Rusckowski, M. and Zilinskas, B.A., Plant Physiol. 65, 392-396 (1980).

Sauer, K. In Bioenergetics of Photosynthesis ed. Govindjee, Academic Press, New York, 115-181 (1975).

Sauer, K., Acher, S., Mathis, P., and VanBest, J.A., in Bioenergetics of Membranes, ed. L. Packer, G. Papogeorgiou and A. Trebst 351-359, Elsevier North-Holland Biomedical Press, Amsterdam (1977)

Sauer, K. and Brewington, G.T., in Proceedings of the Fourth International Congress on Photosynthesis ed. D.O. Hall, J. Coombs and T.W. Goodwin, The Biochemical Society, London, 409-421 (1978).

Schawlow, A.L., in Advances in Quantum Electronics, ed. J.R. Singer, Columbia University Press, New York (1961).

Schiller, N.H., Tsuchiya, Y., Inuzuka, E., Suzuki, Y., Kinoshita, K., Kamiya, K., Iida, H., and Alfano, R.R., Optical Spectra June 1980.

Searle, G.F.W., Barber, J., Harris, L., Porter, G. and Tredwell, C.J. Biochim. Biophys. Acta 459, 390-401 (1977).

Searle, G.F.W., Barber, J., Porter, G., and Tredwell, C.J., Biochim. Biophys. Acta 501, 246-256 (1978).

Searle, G.F.W., Tredwell, C.J., Barber, J. and Porter, G., Biochim. Biophys. Acta 545, 496-507 (1979).

Seibert, M., Alfano, R.R. and Shapiro, S.L., Biochim. Biophys. Acta 292, 493 (1973).

Seibert, M. and Alfano, R.R., Biophys. J. 14, 269 (1974).

Shante, V.K., and Kirkpatrick, S., Adv. Phys. 20, 325 (1971).

Shapiro, S.L. and Broida, H.P., Phys. Rev. 154, 129 (1967).

Shapiro, S.L., Kollman, V.H., Campillo, A.J., FEBS Lett. 54, 358 (1975).

Sheely, M.L., Ind. Eng. Chem. 24, 1060 (1932).

Shelev, M. Ya., Richardson, M.C., and Alcock, A.J., Appl. Phys. Lett. 18, 354 (1971).

Shimizu, F., and Stoicheff, B.P., IEEE, QE-5, 544 (1969).

Shipman, L.L., Cotton, T.M., Norris, J.R., and Katz, J.J., Proc. Natl. Acad. Sci. USA 73, 1791-1794 (1976).

Siegelman, H.W. and Firer, E.M., Biochemistry 3, 418-423 (1964).

Singhal, S.S., and Rabinowitch, E., Biophys. J. 9, 586-591 (1969).

Smith, P.W., Proc. IEEE, 58, 1342 (1970).

Song, P.S., Moore, T.A., Sun, M. in The Chemistry of Plant Pigments, ed. C. O. Chichister, 33-74, Academic Press, New York, London (1972).

Strehler, B., and Arnold, W., J. Gen. Physiol. 34, 809-20 (1951).

Swenberg, C.E. and Stack, W.T., Chem. Phys. Lett. 2, 327 (1968).

Swenberg, C.E., Geacintov, N.E., and Pope, M. Biophys. J. 16, 1447-1452 (1976)

Swenberg, C.E., Dominijanno, R., and Geacintov, N.E., Photochem. Photobiol. 24, 601 (1976).

Szabo, A., J. Chem. Phys. 72, 4620-4626, (1980).

Szent-Gyorgyi, A., Sicence 93, 609-611 (1941).

Teale, F.W.J. and Dale, R.E., Biochem. J. 116, 161-169 (1970).

Thomas, J.B., Minnaert, K., and Elbers, P.F. Acta Bot. Neerl. 5, 315-21 (1956).

Thornber, J.P., Ann. Rev. Plant Physiol. 26, 127 (1975).

Tomita, G. and Rabinowitch, E., Biophys. J. 2, 483-499 (1962).

Trosper, T., Park, R.B., and Sauer, K. Photochem. Photobiol. 7, 451-69 (1968).

Troxler, R.F., Greenwald, L.S. and Zilinskas, B.A., J. Biol. Chem. (1980).

Tumerman, L.A., Borisova, O.F. and Rubin, A.B., Biophys. (Transl) 723-728 (1961).

Tumerman, L.A. and Sorokin, E.M., Molec. Biol. 1, 628-38 (1967).

Van Niel, C.B., Cold Spring Harbor Symp. Quant. Biol. 3, 138 (1935).

Van Durren, B.L., Chem. Rev. 63, 325 (1963).

Van Nostrand Jr., F.W., Ph.D Thesis (N.Y.U.), University Microfilms, Ann Arbor, Michigan (1972).

Vernon L.P. and Seely G.R. , in The Chlorophylls, Academic Press, New York (1966).

Wasielewski, M.R., Studier, M.H., and Katz, J.J., Proc. Natl. Acad. Sci. USA 73, 4282-4286 (1976).

Weaver, E.C. and Bishop, N.I., Science 140, 1095 (1963).

Williams, W.P., in Primary Processes of Photosynthesis ed. J. Barber, Elsevier Scientific, Amsterdam, The Netherlands 99-147 (1977).

White, R.M., and Enderby, C.E., Proc. IEEE 51, 214 (1963).

Wong, D., Govindjee, and Jursenec, P., Photochem. Photobiol. 28, 963-974 (1978).

Wong, D., Pellegrino, F., Alfano, R.R. and Zilinskas, B.A., Photochem. Photobiol. (1981) (accepted for publication).

Yariv, A., in Quantum Electronics, John Wiley and Sons, New York (1975).

Yu, W., Ho, P.P., Alfano, R.R., Seibert, M. Biochim. Biophys. Acta 387, 159-164, (1975a).

Yu, W., and Alfano, R.R., Bull. Am. Phys. Soc. 20, 336 (1975b).

Yu, W., Pellegrino, F., and Alfano, R.R., Biochim. Biophys. Acta 460, 171-181 (1977a).

Yu, W., Pellegrino, F., Grant, M., and Alfano, R.R., J. Chem. Phys. 67, 1766-1773 (1977b).

Zavoiskii, E.K., and Fanchenko, S.D., Sovietski Physitchiskii Doklady 1, 285 (1956).

Zilinskas, B.A., Zimmerman, B.K. and Gantt, E., Photochem. Photobiol. 27, 587-595 (1978).

Zilinskas, B.A., Greenwald, L.S., Bailey, C.L. and Kahn, P.C., Biochim. Biophys. Acta 592, 257-263 (1980).